F

N73-26796

CR 120969

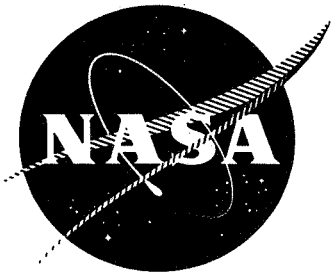

FINAL REPORT

PRELIMINARY DESIGN STUDY OF QUIET INTEGRAL FAN LIFT ENGINES FOR VTOL TRANSPORT APPLICATIONS IN THE 1980'S

By

G.R. Rabone
E. Paulson

GENERAL ELECTRIC COMPANY

Prepared for

NATIONAL AERONAUTICS AND SPACE ADMINISTRATION

NASA Lewis Research Center
Contract NAS3-14404
R. Roelke, Contract Manager

1. Report No.	2. Government Accession No.	3. Recipient's Catalog No.
CR120969		

4. Title and Subtitle	5. Report Date
Final Report Preliminary Design Study of Quiet Integral Fan Lift Engines for VTOL Transport Applications in the 1980's	June 1973
	6. Performing Organization Code
7. Author(s)	8. Performing Organization Report No.
G.R. Rabone and E. Paulson	
	10. Work Unit No.
9. Performing Organization Name and Address	
General Electric Company Cincinnati, Ohio/Lynn, Massachusetts	11. Contract or Grant No. NAS3-14404
	13. Type of Report and Period Covered Contractor Report
12. Sponsoring Agency Name and Address	
National Aeronautics and Space Administration Washington, D.C. 20546	14. Sponsoring Agency Code

15. Supplementary Notes

Contract Manager, R. Roelke
NASA Research Center, Cleveland, Ohio 44135

16. Abstract

Preliminary designs of three integral lift fan engines suitable for commercial certification in the 80's were completed. Emphasis was placed on low cost, simplicity, low noise, low emissions, minimum weight, and design features meeting all commercial standards for fire safety and containment.

17. Key Words (Suggested by Author(s))	18. Distribution Statement
	NASA Distribution

19. Security Classif. (of this report)	20. Security Classif. (of this page)	21. No. of Pages	22. Price*
Unclassified	Unclassified	280	-

* For sale by the National Technical Information Service, Springfield, Virginia 22151

TABLE OF CONTENTS

TABLE OF CONTENTS (Continued)

TABLE OF CONTENTS (Concluded)

LIST OF TABLES

LIST OF TABLES (Concluded)

LIST OF ILLUSTRATIONS

LIST OF ILLUSTRATIONS (Continued)

LIST OF ILLUSTRATIONS (Continued)

LIST OF ILLUSTRATIONS (Continued)

LIST OF ILLUSTRATIONS (Continued)

LIST OF ILLUSTRATIONS (Concluded)

SUMMARY

Preliminary design studies were conducted for three low noise integral lift fan engines consistent with commerical certification in 1980's.

Important engine characteristics are summarized in the following table. Weights indicated include all commercially required features of fire safety and containment.

Engine	ILF1A1	ILF2A1	ILF2A2
Bypass Ratio	12.6	11.6	11.7
F_N Flat Rated to 90° F	12,500	12,500	12,500
Noise Rating Point, 90° F	10,000	10,000	10,000
Fan Tip Diameter - in.	57.1	60	60
Engine Max. Diameter - in.	69.8	74	74
Overall Length - in.	43.5	50.6	54.5
Length/Diameter	0.62	0.68	0.74
Overall Weight (with Treatment) lb.	1050	1140	1250
Overall Weight (without Treatment) lb.	980	1070	1170
Lift/Weight Ratio, 90° Day	11.9	10.9	10
Volume - $ft.^3$	96	126	136
Lift/Volume - $lb/ft.^3$	130	99	92
Frontal Area - $ft.^2$	21	26	28
Lift/Frontal Area $lb/ft.^2$	595	480	445
PNdB @ 500' Sideline, 12 @ 10,000 lb.	96	95	95
SFC	0.36	0.36	0.36
Fan P/P	1.25	1.20	1.20
Overall P/P	10	7	7
Fan Tip Speed	1180	1060	855
Turbine Inlet Temperature ° F	2500	2000	2000

Of paramount importance was low noise and this was reflected in every facet of the study; cycle selection, weight and envelope. The design rationale for attaining this noise level along with assumptions and uncertainties involved is described in the body of the report.

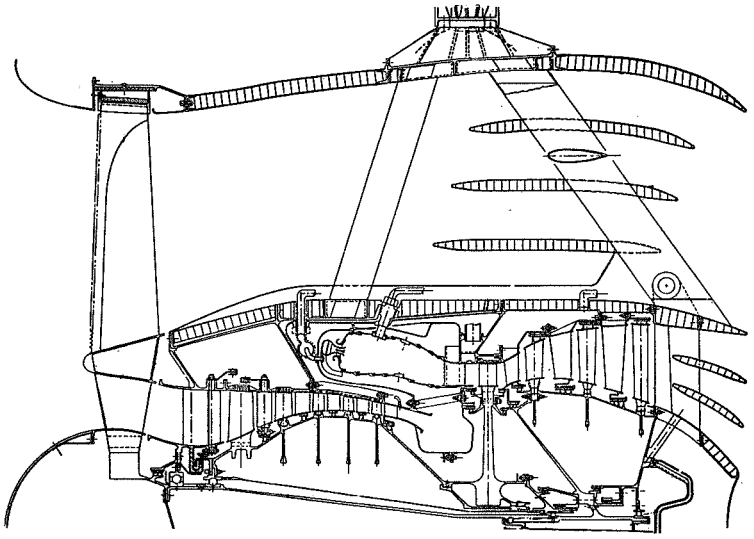

ILF1A1 Features

Fan Pressure Ratio	1.25
Bypass	12.6
Fan Tip Speed	1180'/sec
Turbine Inlet	2500° F

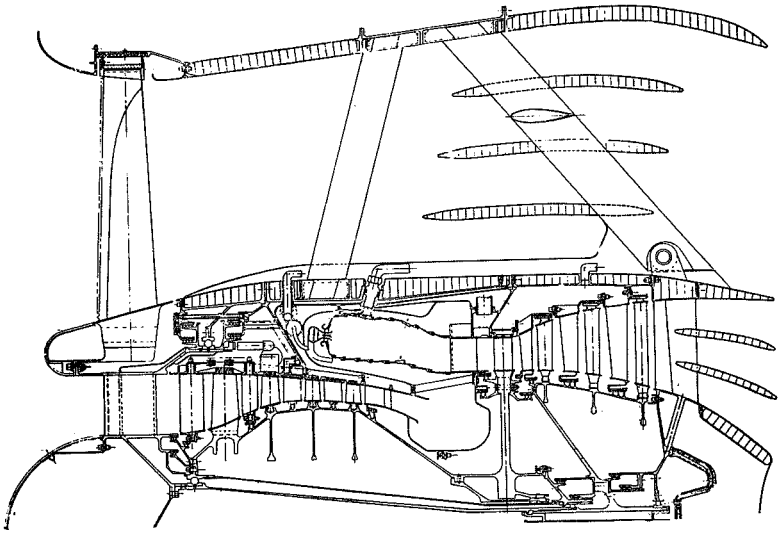

ILF2A1 Features

Fan Pressure Ratio	1.20
Bypass	11.6
Fan Tip Speed	1060'/sec
Turbine Inlet	2000° F

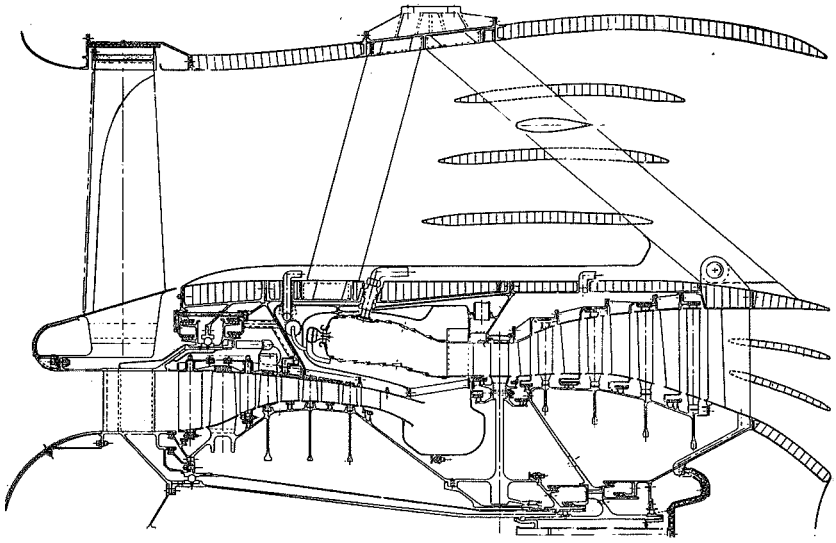

ILF2A2 Features

Fan Pressure Ratio	1.2
Bypass	11.6
Fan Tip Speed	855'/sec
Turbine Inlet	2000° F

The cycles for the three preliminary designs were selected based on the results of a parametric study of the noise, weight, and performance characteristics of more than forty candidate designs. A simple weight merit factor based upon an assumed VTOL mission was utilized as an overall measure of envelope, weight, and performance effects and compared with the noise levels for each cycle.

Component aerodynamic and mechanical designs were completed for each component, using materials and technology consistent with the 1980 time period. Emphasis was placed on achieving a compact design with a small number of stages which in turn allowed a simple rotor and structural arrangement. Engine system layouts were completed in the final phase of the effort and engine off design performance estimates completed for a range of operating conditions. Weight analysis based on the layouts and component designs indicate that lift to weight ratios of from 10-12 will result from the selected cycles. This level of thrust to weight ratio is a consequence of the very low engine noise requirement (about 84 PNdB for one engine at 500' sideline and 10,000 lb. thrust on a 90° day).

The payoff in use of advanced technology is reflected in the favorable size, weight and volume of the engines, particularly the 2500° F T_4 ILF1A1. Weight and size characteristics result from the application of advanced composite materials in the fan, compressor, and duct; use of a compact 7:1 4-stage or 10:1 5-stage compressor; a high space rate reverse liner flow combustor located over the compressor; and a very highly-loaded 3-stage fan turbine with an OGV system.

Considering the application of these concepts, several component areas stood out with regard to need for substantial future development. The most prominent of these are:

- Techniques for fan and core source noise reduction and suppression
- Installation aerodynamics for compatible airframe/engine design
- Composite blade, shroud, and dovetail design and construction

- 5-stage, 10:1 P/P core compressor
- Low emission reverse liner flow combustor with 2500° F T_4
- Very highly loaded fan turbine
- All electronic fuel controls

INTRODUCTION

Recognition has been increasing concerning the need for safe, quiet, and economical air transportation between city centers of from 200 to 500 mile distance. A V/STOL commerical transport having a passenger capacity of from 100 to 150 appears to have the potential of contributing to meeting this need in combination with other air and surface systems in the 1985 time frame.

NASA Ames and NASA Lewis are sponsoring industry studies on both near term V/STOL research vehicles and potential 1985 commercial transports. The present work of this report is concerned with providing preliminary designs of several integral fan lift engines to NASA Lewis which in turn provide insights into required future developments. Data provided include: component characteristics, engine performance, engine design characteristics, noise estimates, and engine weight and envelope.

The work was divided into three phases: A cycle parametric study to select the cycles for further study, preliminary component designs for the selected cycles, and engine system layouts with noise and weight estimates. The effort was completed over a fourteen-month period starting on June 24, 1970 and ending on August 31, 1971.

TASK I

GENERAL ENGINE DESIGN REQUIREMENTS

Initial Design Requirements as set forth in the statement of work are as follows:

1. Maximum sideline noise at 500' of 95 PNdB for one engine.
2. 10,000 lb. F_N for 90° day.
3. 30 second contingency rating at 11,000 lb. F_N.
4. 0.3 second response time for 10% F_N increase above 60% thrust.
5. Hot part TBO at service maturity of 10,000 cycles.
6. Cold part life 5000 hours at service maturity.
7. Capability for vectoring 15° forward and 45° aft.
8. No visible smoke.
9. FAA tentative airworthiness standards for V/STOL.

Additional design requirements imposed by the nature of the application were low cost, simplicity, and low weight, consistent with other requirements.

OBJECTIVES

The objectives of Task I were to survey a wide range of cycle parameters and determine their effect on overall engine envelope size, weight, performance, noise characteristics, and on a simple weight merit factor reflecting a combination of weight, size, and performance. From these results a recommendation will be made as to the two or three cycles to be selected for more detailed design during Tasks II and III.

CYCLE PARAMETRIC STUDY

A split flow fan configuration was chosen for the baseline case. See Figures 1 and 2. Both geared and direct drive configurations were evaluated in Task I. Baseline cycles were selected, about which parameters were systematically varied. The Task I baseline cycles which were selected were:

Non Geared		Geared
1.4	Fan Pressure Ratio	1.3
10	Overall Pressure Ratio	10
2500	Turbine Inlet Temperature ° F	2500
1.3	V_8/V_{28}, Extraction Ratio	1.3
1200		----
(1165 $U_T/\sqrt{\theta}$)	Fan Tip Speed 90° F	1069 (1035 $U_T/\sqrt{\theta}$)
8.8	β, Bypass Ratio	12.4

Components selected for the baseline non-geared configuration included a high tip-speed split flow fan. A high tip-speed axial flow compressor, a high space rate carbureting combustor, a single-stage high pressure turbine, a highly-loaded low pressure turbine, short duct with acoustics splitters, and a truncated core nozzle. The components for the geared design are the same except for a lower tip-speed fan and a more moderate low pressure turbine loading. These characteristics being consistent with the fan and low-pressure turbine speed mismatch made possible with the use of the reduction gearing. The choice of a highly-loaded fan turbine was dictated by a desire for a short engine, and the realization of the relative unimportance of SFC for an engine used only a few minutes of every mission.

Specific characteristics of components assumed in Task I were:

Fan

- Integrated OGV and frame
- Unshrouded Graphite/Polyimide composite blade
- Reduced velocity parameter = const.
- Radius ratio $\geq$ 0.37
- 1.4 tip solidity
- $W\sqrt{\theta}/\delta A$ = 41.3
- 20% stall margin
- ηp a function of corrected tip speed (Figure 3)

Compressor

- Axial flow
- Constant hub diameter
- Stage 1 corrected tip speed 1450 ft/sec.
- Inlet radius ratio = 0.65
- $\eta\rho = 0.89$
- $W\sqrt{\theta}/\delta A = 40$
- Advanced Ti Blade Material, except for S9 and S10 (A286)
- Advanced Ni Disc Material
- 18% stall margin
- Stator casing FWD-Al
  AFT-Ti (Steel for 15/1 P/P)

P/P	No. Stages	No. Variable Stages	M_{exit}
5	5	2 + IGV	0.292
5	6	2 + IGV	0.286
10	8	3 + IGV	0.288
15	10	4 + IGV	0.250

Combustor

- Carbureting
- Reverse flow
- Dump diffuser
- High space rate
- No visible smoke
- Advanced Ni sheet material
- Machined ring liner
- Δ P/P dry loss = 0.08

- $\eta B = 0.985$
- 70'/sec. reference velocity
- Pattern factor - 0.2
- H/L = 2.5

High Pressure Turbine

- Axial flow
- Single stage
- $\eta T = 0.89$
- $W_{coolant} = f\ (T_4\ \&\ T_3)$, Table I and II
- Loading $(JG\Delta H/2U_p^2) \approx 1.0$
- Advanced Ni based blade material
- Advanced Ni based disc material

Low Pressure Turbine

Non-Geared

- Axial flow
- Stages as required
- $\eta t = f$ (loading) $JG\Delta H/2U_p^2$

  0.89 1.7

  0.85 2.5
- $W_{coolant} = f\ (T_{54}\ \&\ T_3)$ Table I & II
- OGV $\Delta P/P = 0.02 - 0.03$
- Swirl = 20° - 40°
- Exit radius ratio $\geq$ 0.55

Geared

- Axial flow
- 2 Stage
- Loading 1-1.3
- $W_{coolant} = f\ (T_{54}\ \&\ T_3)$ Table I &
- OGV $\Delta P/P$ - 0.02
- Swirl = 20°
- Exit radius $\geq$ 0.55

Frames and Ducts

- Containment allowance in weight
- Integral turbine frame/OGV
- Duct treatment integral with structure
- Duct length = engine length

- Aluminum and composite fan frame
- Separated flow
- $\Delta P/P$ fan duct = 0.02
- $\Delta P/P$ core duct = 0.01
- Fan and core nozzle C_v = 0.99
- Truncated core nozzle
- Trunnions on outer ring

Bearings

- Max. Dn = 3.2×10^6 for large front bearing
- Ausformed M-40 Material

Controls and Accessories

- Bleed driven accessories
- Impingement air starting
- Swiveling engine vectoring
- Fuel/Oil heat exchanger (geared fan)

Gearing

- Gear Loss - 0.005
- Maximum 5 sun gears
- K Factor = 600
- Minimum pinion pitch diameter = 3.5 inches
- Minimum ring pitch diameter
- Steel gears, shafts and bearings
- Root stress = 45,000 lb./in.^{2}
- Other components Ti consistent with 1975 demonstrator
- Double herringbone, toothwidth $\leq$ pitch diameter

- Life-compatible with 35,000 cycles and 5000 hr.
- Oil-fuel cooler designed for 1% heat rejection

The actual cycle parameters were varied over the range of values given below.

Non-Geared		Geared
1.2 - 1.5	Fan Pressure Ratio	1.2 - 1.4
5.0 - 15.0	Cycle Pressure Ratio	5.0 - 15.0
1.1 - 1.5	V_8/V_{28} Extraction	1.1 - 1.5
1850 - 2800	T_4° F	1850 - 2800
1100 - 1600	Corrected Fan Tip Speed	900 - 1400

The relation between fan loading levels selected and corrected tip speed is shown on Figure 4.

In all cases, cycle was balanced to calculate required airflow for the specified 10,000 lb. thrust level on a 90° F day at sea level static conditions with a 0.99 ram recovery. No bleed or power extraction were applied outside of the engine.

Typical results of the cycle calculations are shown on Figures 5 and 6 for the geared and non-geared fans respectively for 1.3 V_8/V_{28}. Trends of SFC and bypass ratio (essentially core size) with fan pressure, turbine inlet temperature, and overall pressure ratio are as expected with core size and SFC improving with increased turbine inlet temperature. Pushing core pressure ratio much past 10/1 has limited beneficial effect.

Figures 7, 8, and 9 demonstrated the effect of core pressure ratio and fan pressure ratio and total airflow (or frontal area). The effect of core pressure ratio on total airflow is second order relative to fan pressure ratio, which is expected.

COMPONENT SIZING AND WEIGHTS

Sizing

From the more than 300 design point cycles calculated 22 non-geared and 20 geared configurations were selected for use in studying trends and derivatives

about the selected baseline cases. Parameters were systematically varied one at a time to evaluate effect of tip speed, fan pressure ratio, V_8/V_{28}, overall pressure ratio, and turbine inlet temperature, on noise, weight, performance and merit factor.

Actual sizing of components was deliberately kept consistent by a systematic procedure which used fixed values of fan and compressor specific flow and fixed relationship between core compressor tip diameter and high pressure turbine pitch diameter. Fan inlet radius ratio and low pressure turbine exit radius ratio were not allowed to fall below 0.36 and 0.55 respectfully. Reduction gear size was postulated as a function of speed reduction ratio. Low pressure turbine loading for the non-geared cases was allowed to vary slightly to achieve an integral number of stages, using a last stage loading less than average to limit exit swirl. Case IA of Table III was undertaken to evaluate the effect of using a very high fan turbine loading.

Results of the sizing procedure, and the cases selected for additional evaluation are shown on Tables III and IV and Figures 10 and 11.

Parametric Weights

The parametric weights for the cases listed on Table IV and Figure 11 were generated by making preliminary designs of the baseline engine's components, and then applying scale factors to correct for size. This procedure was used to produce a large number of weight estimates being consistent among themselves, but with reduced absolute accuracy in line with the objectives of the parametric portion of the study.

(Weight/Base Weight)	$(\text{Diameter/Base Diameter})^C$
Component	Exponent "C"
Rotors	2.80
Stators	2.60
Combustor	2.20
Structures	1.75
Ducting	2.20
Bearings & Seals	2.30
Drives	2.00
Augmentor	2.00
C&A	1.80
Nozzle	2.50

The results of the procedure described above are shown on Tables V and VI.

WEIGHT FACTOR DEVELOPMENT

In order not to limit comparisons among candidate cycles to characteristics of the isoltated engine, a simple mission weight (merit) factor was evolved with the objective of generating a number which would be a more realistic evaluation of an "installed" propulsion system.

This weight factor is the summation of five weight elements as listed below:

- Engine weight
- Fuel used in lift
- POD weight per lift engine
- Acoustic treatment weight
- Incremental cruise fuel

The base mission and airplane assumptions were as follows:

- 10 x 10,000 lb. lift engines with gimbaled vectoring
- 2 x 24,000 lb. vectorable cruise engines
- Lift engine installed in two engine pods (See Figure 12)
- Airplane TOGW = 109,500 lbs.
- Wing area = 841 $ft.^2$
- Cd = 0.03
- Cruise @ Mo = 0.75 20,000 ft.
- 500 NM range
- 2 minutes at 80% F_N in lift/mission
- 4 minutes at idle/mission

Basic engine weight is as calculated.

Fuel used by lift engine per mission is calculated by the cycle performance SFC and the assumed time in lift and at idle.

POD weight per engine is calculated from the total number of square feet of sheet metal, including an allowance for inlet and exhaust doors, required to cover a five-engine pod with gimbaled engines. A weight of 2.7 lb/ft^2 was assumed. The total weight calculated is then divided by five to be consistent with the single engine basis of the weight factor.

The weight of duct and inlet acoustic treatment is included as calculated. The weight of the acoustic treatment is consistent with the noise data presented in the acoustic section.

The incremental cruise fuel calculated is intended to be a measure of how the physical size of the lift engine pod affects the fuel used by the cruise engines during the cruise portion of the mission. An incremental pod drag is calculated for the five-engine pod, and this drag is corrected into an equivalent fuel weight per lift engine.

$$\text{pod drag} = \gamma \; 1/2 \; \gamma \; M_o^2 \; P_o \; A_{wet} \; C_{d_f}, C_R, F_F$$

Where: $\gamma = 1.4$

M_o = cruise Mach no.
P_o = ambient static pressure
A_{wet} = pod wetted total area
C_{d_f} = 0.002 Friction Drag Coefficient
C_R = 1.05 Roughness Factor
$F_F = 1.60/(L/D)^3 + 0.0025(L/D)$ Pressure Drag Form Factor
L/D = pod Fineness Ratio

In addition to the baseline mission described above, alternate missions and alternate airplanes were evaluated in order to determine the sensitivity weight factor to assumed mission and aircraft.

Alternate Missions

- 1 minute in lift, 4 minutes in lift
- 200 and 800 NM range
- Max. TOGW (STOL) M_o = 0.8 3500', 200 NM range

Alternate Airplane (STOL)

- 4 × 10,000 lb. lift engines
- 2 × 21,000 lb. cruise engines
- 0.75 20,000' 500 NM
- 0.80 35,000' 2000 NM

ACOUSTIC STUDY

Considering the importance of the noise aspects of the study, great care was taken to apply consistent methods of evaluation to all engines. Unsuppressed noise predictions were based on the following assumptions.

- Vertical Engine Axis
- Angles from Inlet $\leq$ 90° not pertinent
- Aircraft out of Ground Effect (less attenuation with distance)
- Fan Noise - Analytical/Empirical
- Jet Noise - SAE Extrapolated for Jet Velocities less than 1000'/sec
- No Relative Velocity Effect on Jet Noise
- Turbine Noise - Empirical
- 500' Sideline as Defined in Figure 13

Suppressed noise estimates were made assuming that advances in acoustic technology between the present time and the 1980's time period would provide an additional Δ5 PNdB fan source noise reduction. This Δ5 PNdB source reduction is identified where it is used. Several possibilities currently present themselves which appear to have potential; serrated leading edge rotor or stator, casing treatment for boundary layer and control, leaned outlet guide vanes, and slotted rotor blades. Several of these are currently under investigation in other NASA sponsored programs.

In cases where turbine suppression is called for, this is provided by application of suppression material to the inner and outer turbine exit flowpath.

For purposes of the acoustic parametric study, fan duct suppression capability was reduced to a simple empirically derived relation between L/H, H/λ, and duct transmission loss. These relationships are described and illustrated on Figure 14.

An important constituent of overall noise is that of the forward radiated fan noise which is heard in the aft quadrant. For the Task I parametric study, Figure 15 was developed, based upon experimental data available at the time. Inlet radiated noise in the rear quadrant is assumed to be 10 PNdB less than the exhaust radiated noise. Thus at 110° from the inlet, if the exhaust noise (unsuppressed) is 100 PNdB the inlet radiated noise at that angle is 90 PNdB. This inlet noise level then stays constant as the exhaust is suppressed.

Since application of suppression material is only effective in reducing turbo-machinery noise, duct and core jet noise are very important constituents in the overall noise characteristics of the engine. The effect of jet noise "floor" is illustrated on Figure 16. As more and more fan suppression is added, the closer the total noise approaches the jet noise. The significence here is, that beyond a point, providing additional duct treatment is decreasingly effective in reducing overall noise. As this jet noise "floor" is approached, the only way to lower system noise is by additional reduction in duct and core exit velocity. Duct exit velocity is essentially a function of only fan pressure ratio, while core exit velocity is primarily a function of turbine energy extraction level, and a secondary function of turbine inlet temperature. The cycles finally selected for detailed preliminary design in Task II and III heavily reflect the strong effect of jet noise on overall engine noise.

Figure 17 is an illustration of the effect of fan pressure ratio on the relationship between fan noise, jet noise, and turbine noise, for a non-geared engine. Unsuppressed fan noise is given as a band here to reflect a range of tip speeds as indicated as well as the uncertainty involved in the absence of a specific aerodynamic blade design (aside from an assumed 2 chord rotor-stator spacing). The jet noise floor problem at fan pressure ratio of 1.5 is very clear. Any amount of rotor noise suppression will not

allow more than a total noise reduction of more than about 5 PNdB below the unsuppressed fan level. At fan pressure ratio of 1.2, however, the 20 PNdB difference between the jet noise floor and the unsuppressed fan noise indicates that duct suppression material will be very effective in the reduction of overall system noise. Turbine turbomachinery noise will require increased suppression at low fan pressure ratios because the lower tip speeds implied draw the turbine blade passing frequency into a more heavily weighted spectrum region of the PNdB estimates. For a geared engine, turbine turbomachinery noise adds in very little because of the high turbine speed made possible by the reduction gearing in the low pressure system.

As previously discussed, cycle extraction has an effect on overall engine noise. This effect for an engine with fan pressure ratio of 1.4, 2500° F T_4, and an overall pressure ratio of 10/1 is shown in Figure 18. The results shown in the figure require that extraction be set as low as possible, consistent with reasonable turbine exit design parameters of diffuser design, and exit guide vane loading level.

The effect of turbine inlet temperature and overall pressure ratio is shown for fan pressure ratio of 1.4 on Figure 19. For moderate levels of extraction, a wide latitude can be allowed in the selection of cycle parameters (other than fan pressure ratio) without affecting noise appreciably.

It is generally realized that in normal operation of a VTOL airplane, requirements for excess power for control and for engine-out operation dictate that normal thrust during takeoff will probably be in the range of 80% of maximum thrust. For this reason, the data on Figure 20 were generated. It is clear from this figure that the operational mode of the engines during VTOL has a strong effect on overall noise. In the case evaluated, up to 10 PNdB overall reduction is obtained by operating the engine at 80% of its maximum thrust rating. In this Figure, and in those which follow the floor shown represents the sum of the jet and turbine noise constituents.

Figure 21 presents the effect of fan suppression, and jet plus turbine noise floor on overall noise level. The geared engine requires three exhaust splitters in the fan duct to achieve suppression comparable to that achieved on the non-geared engine with two splitters because of the shorter duct and resulting reduced L/H. See Figures 1, 2, and 14. The important conclusion to be drawn from this chart, along with Figure 16, is that to obtain the full benefit of low fan pressure (1.2) on overall noise, considerable turbine treatment may be required to reduce the jet plus turbine floor of the non-geared configuration to the level of the geared configuration. At the higher fan pressure ratio of 1.3, it can be seen from Figure 22 that the noise of the geared and non-geared configurations are comparable.

Another important parameter to be considered was the effect of number of fan blades on overall noise. As shown on Figure 23, increasing the number of blades from 40 to 70 can reduce overall noise from 1 to 5 PNdB depending on the degrees of suppression supplied. As is shown in the figure, however, the higher frequencies of the increased number of blade configuration reduce the effectiveness of a fixed number of splitters due to a reduction in the H/λ parameters. A configuration with a high number of blades may thus require an additional splitter to achieve maximum potential noise reduction.

Figures 24, and 25 are summary charts for overall noise as a function of the 100% F_N fan pressure for both geared and non-geared engines. Figure 24 indicates that the target of less than 100 PNdB can be achieved by a geared engine with a fan pressure ratio of less than approximately 1.33, provided three duct splitters are used, or two duct splitters with the $\Delta 5$ PNdB source reduction as previously described. Figure 25 indicates approximately the same range of fan pressure ratio to obtain the less than 100 PNdB target using two splitters for a non-geared engine. In order to achieve a level of 95 PNdB, the geared fan pressure ratio would have to be reduced to 1.25, and non-geared approximately to the same level, but with increased turbine suppression and utilization of the $\Delta 5$ PNdB source reduction assumption. The additional point shown on Figure 25 marked T_4 = 1850° F, P/P core = 7, is an additional indication that cycle changes at constant V_8/V_{28} do not have significant effect on the overall noise characteristics of the engine.

RESULTS

As discussed in the weight factor section, baseline cases were selected for both geared and non-geared cycles. Excursions were made with one variable at a time from the established base in order to determine its effect on engine weight and merit factor. The two baseline engine cycles are repeated below for convenience.

Non-Geared		Geared
1.4	Fan Pressure Ratio	1.3
10	Overall Pressure Ratio	10
2500	Turbine Inlet Temp. ° F	2500
1.3	V_8/V_{28} Extraction Ratio	1.3
1165	Fan Corrected Tip Speed	1035
8.8	Bypass Ratio	12.4

Since fan pressure ratio is the prime independent variable, it is important to show what effect this parameter has on several merit factor elements as well as the basic engine weight constituents.

The second order importance of engine SFC as affected by fan pressure ratio selection is clearly illustrated by Figure 26. The engine SFC (@ 10,000 F_N, T_0 = 90° F) is strongly dependent on fan pressure ratio as would be expected, but the total fuel used in a typical mission is only a fraction of the engine weight. This result is valid for both the non-geared and geared engines operating over the range of tip speeds previously selected (See Figure 4). Basic engine SFC was not a factor in the selection of a design fan pressure ratio.

The effect of pod size on incremental aircraft drag as reflected in Δ cruise fuel used is shown on Figure 27. For both geared and non-geared engines, engine diameter affects incremental cruise fuel to a minor degree. The geared engine is lower in all cases because of the shorter engine obtained by use of a two-stage turbine with reduction gearing. This smaller engine results in decreased pod surface area, and therefore less pod drag.

The effect of fan pressure ratio on fan tip diameter is shown on Figure 28. While having a relatively small effect on Δ cruise fuel, engine diameter and length are shown on Figure 29 to have a very major impact on engine pod weight. The design of the pod structural elements, skin, and inlet and exhaust doors and actuation systems are going to be very strongly affected by engine volume. A nominal value of 2.7 lbs/ft^2 of surface area was used in this study. The effect of fan pressure ratio on pod size is most clearly illustrated by Figure 12. Geared fan pod weight is less than non-geared for the same fan pressure ratio because of reduced pod depth brought about by the shorter geared engine. A conclusion here would be that if low fan pressure ratio were selected for purposes of, say, very low noise, every approach must be exhausted to achieve minimum engine length to minimize engine volume.

Figures 30 and 31 illustrate the contribution of non-geared and geared engine component weights to the total engine weights as a function of fan pressure ratio. Examination of these curves indicates that for the range of pressure ratio covered as excursions from the baseline cases, that engine weight is relatively constant due to the counter acting effects of weight changes in the low and high pressure spools, where a lighter fan is offset by a larger size core engine. It must be remembered that all of these data thusfar discussed have been generated at a constant turbine inlet temperature 2500° F.

Total weight factor constituents that is, engine, pod and fuel weight for both baseline engines are shown on Figure 32, as a function of fan pressure ratio for the moderate tip speed schedule. The top band on the geared curve labeled third (3rd) splitter is shown to achieve equal noise suppression. The third splitter is required because of the shortness of the geared engine duct. Engine weight and pod weight are clearly the areas of interest in improving overall weight factor. The weight factor elements of Δ cruise fuel, lift fuel, and acoustic treatment will not yield substantial reductions. In terms of overall total weight factor, optimum fan pressure ratio appears to be between 1.35 and 1.45 for the non-geared engine, and between 1.3 and 1.4 for the geared engine.

The effect of varying fan tip speed is shown on Figures 33 and 34 for non-geared and geared engines respectively. For a non-geared, higher tip speeds increase basic engine weight, but result in fewer low pressure turbine stages, making a shorter engine with its saving in pod weight. This trend becomes increasingly apparent at the lowest fan pressure (1.3) investigated. In the case of the geared engine, of course this is not the case, since we are dealing with a constant number of low pressure turbine stages. At the lowest pressure ratio investigated (1.2) however, gear size and weight begin to have an effect on engine weight and fan diameter because of the increased size and weight of the reduction gear (see Figure 2) needed to achieve the required speed ratio between the low pressure turbine and fan spool. Constituents for these graphs are shown on Figures 35 and 36. The solid dots on these figures and those which follow indicate the location of the baseline cycle point within the matrix of data. The data point on Figure 36 labeled LPT Ψ_p = 2.0 just below the baseline case indicated the advantage to be obtained from use of a more highly loaded low pressure turbine than the nominal value of $\simeq$ 1.7. The use of this more highly loaded turbine resulted in reducing the number of stages from 4 to 3. The resulting lighter and shorter engine yields the indicated improvement in weight factor, and points toward a probable direction of increased benefit for the direct drive approach.

It would be expected that turbine inlet temperature would have a major impact on total weight factor due to a higher turbine inlet temperature resulting in a smaller lighter core engine, up to the point where the need for excessive cooling air reduces any advantage in further increasing temperature. Figures 37 and 38 show the effect of turbine inlet temperature and overall cycle pressure ratio on total weight (merit) factor for non-geared and geared engines. Strong trends indicate that for a non-geared engine advantages of increased T_4 still existing beyond 2500° F and cycle pressure ratio beyond 10/1, a choice of T_4 and cycle pressure ratio in the non-geared system may well be dictated by considerations of simplicity inherent in a moderate T_4 and a small number of compressor stages. In the case of the

geared fan, little advantage in overall weight factor is obtained above 2400° F and overall pressure ratio of 10/1 because of increasing gear weight and relatively constant engine length. Comparison of the two curves will indicate that the non-geared engine has greater potential for better weight factor than the geared engine.

The final engine parameter which was investigated was V_8/V_{28}, extraction ratio. Figure 39 indicates that small variations around the baseline value yield a predictable trend. In any event, extraction level will very likely, in the final analysis, be established by acoustic requirements (see Figure 18).

In order to assure that the results were not biased unduly by the mission assumptions, the weight factors of the baseline engines were generated using the alternate missions and alternate airplanes described in the weight factor section. The results of the analysis are described on Figures 40, 41, 42 and 43. Examination of these curves indicate that the range of the primary design parameter to be selected (fan pressure ratio) is not at all affected by these different mission assumptions.

Figures 44 and 45 are summary charts showing cross hatched areas having the potential to meet the stated noise requirements. As can be seen on the charts, the best engine meeting the noise requirements appears to be a non-geared design with a fan pressure ratio of 1.3 to 1.35 and a turbine inlet temperature of 2500 to 2700° F. In the case of the geared design, it is not competitive with a non-geared engine except when the non-geared engine is designed for low turbine inlet temperatures. Geared engine designs were dropped from further consideration at this point for the following reasons:

- no noise advantage over direct drive
- higher development risk than direct drive due to advanced technology gearing required.

Consideration was thereby narrowed to two regions:

Low T_4		Moderate T_4
1800-2000	T_4° F	2500-2600
1.2-1.25	Fan Pressure Ratio	1.25-1.3
6-8	Core Pressure Ratio	10
1.2-1.3	V_8/V_{28}	1.2-1.3
1000-1200	$U_T/\sqrt{\theta}$	1100-1400
3	No. Fan Turbine Stages	3-4
∿ 95	PNdB @ 10,000 lb.	∿ 98
∿ 90	PNdB @ 8,000 lb.	∿ 95
∿ 2	LPT ψ_P	2-2.5

The selection of higher turbine loading than originally selected for the parametric study is supported by several reasons: The lower performance associated with the higher turbine loading (2 to 2.5 as compared with 1.7) does not have an important effect on overall weight factor since lift fuel used is a relatively small fraction of the total weight factor. The realization that compactness and simplicity demand as few turbine stages as possible. This effect is shown on Figure 46 where increased loading can result in a saving of 1 to 2 stages. These savings are reflected in Figures 47 and 48 which show the bare engine weight and total weight factor advantages which are available to two typical cycles in the region of continued interest. Finally, NASA sponsored work in the area of highly loaded fan turbines was moving forward with sufficient momentum to assure that the risks with this design approach would not be undue for an engine of the 1983-1985 time period. Desire for compactness also led to the recommendation of a more advanced compressor having higher loading, tip speed and axial velocity.

REVISED ENGINE REQUIREMENTS

Continuing review of engine noise requirements in light of evolving objectives for CTOL, STOL, and VTOL aircraft combined with considerations of probable life engine operational procedures led, at this point, to revised design requirements, particularly in the area of noise. The new requirements are listed below, with the original listed as reference.

Original		Revised
10,000 lb.	Maximum thrust 90° day	12,500 lb.
-	Noise Rating thrust	10,000 lb.
< 95 for 1 engine @ 10,000 lb.	500' sideline PNdB	< 100 for 12 engines @ 10,000 lb.
11,000 lb.	Engine out emergency	13,000 lb.

The effect of the revised noise requirements is very substantial since the equivalent single engine noise target is now approximately 88 relative to an original requirement of 95. In addition, it was required to better the < 100 target by as wide a margin as possible, hopefully in the range of 4 or 5 PNdB.

ADDITIONAL RESULTS

Noise data were recomputed using the revised engine size and noise rating point criteria. Noise constituents as a function of fan pressure ratio are shown on Figure 49. The fan jet noise was computed by two methods, both of which are shown. The SAE prediction is based on the standard SAE method with a linear log-log extrapolation below 1000 feet/sec.

The modified fan jet method is based on cold jet noise data supplied by NASA - Lewis. These data indicate that actual noise will be in the range 3 to 4 PNdB lower than that computed by the extrapolation of the standard SAE method. Note that for the data shown here the fan requires two splitters plus 5 PNdB source noise reduction while the turbine requires 2 splitters. Total noise generated is shown on Figure 50 for two levels of fan suppression. With the use of two splitters the objective level cannot be met at any fan pressure ratio within the range of the investigation. Three splitters plus Δ5 PNdB source reduction are required to achieve < 100 PNdB. A fan design pressure ratio of 1.3 is as high as it is possible to set without exceeding the 100 PNdB limit, and this with no margin. Reducing fan design pressure ratio down to 1.2 results in a noise of about 95 PNdB. Noise requirements have thus established a maximum design fan pressure ratio of 1.3.

Engine bare weight and engine weight factors are shown on Figures 51* and 52* for the cycles of interest. Results are generally similar to those using

* Results shown here are for engine having 25 percent more thrust than engine described up to and including Figure 45.

the original design requirements, the 1.3 fan pressure ratio design with the highest T_4 yields the lowest bare engine weight and the best total weight factor. For the low T_4 designs, very little difference exists in the factors between fan pressure ratio of 1.2 and 1.25. The trend for both, however, indicates that increasing T_4 results in substantial improvements in both weight and weight factor. With these data available, the stage is thus set for selection of the specific engines for use in the component (Task II) and engine layout (Task III) phases of the preliminary design study.

RECOMMENDATIONS FOR TASKS II/III

From the outset of the deliberations on engine selection it was clear that two main branches might be profitably investigated. One approach just meeting the noise requirements with the lowest engine weight and best total weight factor, and another meeting the noise requirements with a wide margin, with not as attractive a weight, but having a low turbine inlet temperature and an uncooled fan turbine. Implicit in this approach is that the lower temperature engine with the lower noise represents a lower risk design, particularly with regard to noise. The turbine inlet temperature selected for the lightweight engine is not, however, considered to be an item of risk since current commerical transport engines operate in this range, and the lift engine is planned for use in the 1980's.

The lightweight engine recommended was as follows:

- bypass ratio 12.6
- fan pressure ratio 1.25
- fan corrected tip speed 1180
- overall pressure ratio 10/1
- turbine inlet temperature 2500° F
- No. HP turbine stages 1
- No. LP turbine stages 3
- average LP turbine loading 2.5
- extraction V_8/V_{28} 1.3

In this case, the 1.25 fan pressure ratio was selected to provide a small noise margin relative to the maximum value of 1.3 (see Figure 50).

The more conservative engine recommended was as follows:

- bypass ratio 11.6
- fan pressure ratio 1.2
- fan corrected tip speed 1060
- overall pressure ratio 7
- turbine inlet temperature 2000° F
- No. HP turbine stages 1
- No. LP turbine stages 3
- average LP turbine loading 2.0
- extraction V_8/V_{28} 1.3

The method of selection of level of turbine inlet temperature is shown on Figure 53. A turbine inlet temperature of near 2000° F is as far as it is possible to go without needing to begin cooling the low pressure system.

In order to more thoroughly investigate the potential of tip speeds below 1000 feet/second, which some investigators believe will produce substantial noise reduction, it was recommended that a third design be undertaken, essentially a modification of the low T_4 approach.

- bypass ratio 11.6
- fan pressure ratio 1.2
- fan corrected tip speed 855
- overall pressure ratio 7
- turbine inlet temperature 2000° F
- No. HP turbine stages 1
- No. LP turbine stages 4
- average LP turbine loading 2.2
- extraction V_8/V_{28} 1.3

Tip speed of this third engine was set with regard to achieving a subsonic relative tip velocity at the noise rating point, and limiting the number of fan turbine stages to 4 with average loading less than 2.5. Objective fan design stall margin is to be the same.

These three designs were mutually recommended and approved for the Task II and Task III work of component design and engine layout, detailed acoustic and performance evaluation, and engine weights.

TASK II

SELECTED ENGINE CHARACTERISTICS

Component Parameters

The following component design parameters were established for Task II.

Engine	ILF1A1	ILF2A1	ILF2A2
Flat Rated Thrust to 90° F	12,500	12,500	12,500
Bypass Ratio	12.6	11.6	11.6
Fan Pressure Ratio/$U_T\sqrt{\theta}$	1.25/1180	1.2/1060	1.2/855
Fan Bypass Corrected Airflow	590	656	656
Fan Stall Margin	18%	18%	18%
Number of Compressor Stages	5	4	4
Core Pressure Ratio/$U_T/\sqrt{\theta}$	10/1390	7/1410	7/1430
Core Corrected Airflow	44.9	54.4	54.4
Core Stall Margin	18%	18%	18%
T_4 ° F 90° Day	2500	2000	2000
Number HP Turbine Stages	1	1	1
Number LP Turbine Stages	3	3	4

Margins

Turbine inlet temperature margin is established at 110° F for ILF2A1 and ILF2A2 and 135° F for ILF1A1. A three percent fuel flow margin is applied everywhere.

The general arrangement of the components will be consistent with 0.65 inlet radius ratio compressor and split flow fan shown on Figure 54.

MATERIALS SELECTION

Selection Criteria

The materials and processes selected for the ILF engine are state-of-the-art materials for many components since cost is a major design criteria. However, some component requirements dictated the use of more advanced materials to meet the equally important design criteria of weight. An all important consideration is reliability and the method of attaining this reliability with the materials and processes chosen is a part of the following materials selection discussion.

Light materials, aluminum, titanium, and composites are specified for the fan, fan frame, fan duct, compressor spool and forward compressor case and blading. Advanced high strength nickel base allows are used in the turbine rotor to reduce weight. All sound suppression panels are lightweight honeycomb structures combined with light weight cases to become structural members of the engine.

Major engine parts and their material, coating (where applicable), specification and material form are shown on Table VII.

Advanced alloys assumed for use represent byproducts of the continuing efforts by General Electric to develop materials and processes to meet the requirements for future engine programs.

Material Forecasts

The practice of forecasting structural materials for aircraft engines that would be available during the following four to five year time period was begun in 1961.

These forecasts were made as materials data curves and were first used in preliminary design of the GE4 engine for the supersonic transport. These forecasts, or goals, then developed into major materials programs at General Electric and led to the timely introduction of new, advanced materials. An example of the success General Electric has experienced with this approach is shown below:

Original Designation	Generalized Goal for '67-'70 Availability	Alloy Now Available
X1600	Sheet, 1600-1800F Stronger than Hastelloy X	HS188
X1800	Sheet, 50F R41, 1600-1800 F	René 63
X1900	Forged Bucket 50F Udimet 700 Forged	René 85
X2000	Sheet, 1800-2200F Applications	TDNichrome
Ni70XD	Discs, 800-1200F, Stronger than IN718	René 95
Ni69XB	Cast Buckets, 50F U700 Cast	René 80
Ti900X	Discs/Blades, 2X strength of Ti 6-2-4-2	Ti 562 1S

1972 - 1975 Forecast Goals

Generalized goals for 1972-1975 materials used in the present preliminary designs are shown below:

Original Designation	Generalized Goals	Year Available
Ni72XB	Ni alloy for blades and vanes improved over René 80 - now called René 120 - in production scale up phase.	1972
Ti72XD	Ti alloy for blades and discs, higher tensile and fatigue over Ti 6-4. Now called René 17.	1972
Ti75XD	Ti alloy for high strength discs.	1975
Ni76XB	Disc alloy with higher strength over René 95	1975
Gr/Pi72XB	A 450° F graphite/epoxy laminate for blades, vanes and frames.	1972

Additional Considerations

The proper selection of materials for a design evolves from studies involving tradeoffs among diverse requirements including common strength design criteria such as 0.2% yield strength and 0.2% plastic creep strength, effects of environment (oxidation, hot corrosion, and erosion) and factors governing

cyclic life such as low and high cycle fatigue strengths; ductility, and resistance to crack propagation. All of these criteria are factored into cost and weight evaluations for material selections. Influence is also felt from other factors such as producibility, maintainability and reliability.

Sufficient knowledge about the scatter of design (property) data must be available so that statistical minumums may be established. These minimum property levels must be integrated with material specifications. The necessary confidence level in these design data comes from carefully controlled testing of specimens machined from components (forgings, castings or sheet) that have experienced representative material and processing histories.

Representative Stress Levels

Typical critical stress levels applied to the preliminary designs of the components are shown below:

Fan

Disc	-	Average Tangential - 25,000 lb/in.^{2}
Blade	-	Root - 8500
Shroud	-	(Graphite/Epoxy Portion) - 50,000

Compressor Rotor

Stage	Bore	Rim	Blade Root
1	90,000	75,000	9,000
2	115,000	75,000	15,000
3	135,000	75,000	10,000
4	135,000	75,000	9,000
5	135,000	75,000	7,000

HPT Rotor

195,000	55,000	30,000

LPT Rotor

Stage	Bore	Rim	Blade Root
1	80,000	65,000	5,000
2	80,000	65,000	7,000
3	80,000	70,000	10,000
4	80,000	70,000	10,000

Fan Shaft

6_s 60,000 lb/in.^{2}

Combustor Outer Casing

40,000 lb/in.^{2}

FAN AND COMPRESSOR DESIGN

Preliminary mission and cycle performance analyses specified the pressure ratio and flow of the fan and compressor components for the ILF1A1 and ILF2A1. Fan tip speeds were determined through cycle, acoustic and low pressure turbine design requirements. With these parameters fixed as a starting point, the fan and compressor flowpath and blading were designed which are most attractive in the total engine flowpath configurations.

The ILF2A2 fan is proposed to demonstrate a noise reduction associated with reducing fan tip speed while maintaining performance. Fan pressure ratio and flow are to be the same as ILF2A1 and the compressor will be the same as in the ILF2A1. Tip speed and flowpath configurations are to be determined which best complement the total engine configuration.

Experience with distortion levels and general engine operating requirements indicates that 18 percent constant speed stall margin will be sufficient for both the fan and compressor components. Inlet distortion levels are expected to be greater than in a conventional application since the engine will be installed vertically resulting in inlet crossflows during transition. Engine vectoring, however, will tend to reduce the cross flow effects and inlet distortions toward typical subsonic engine levels such that the engines will run stably with continued thrust.

Since cycle analysis indicated little overspeed requirement, the design specific flow for both fan and compressor were made high to minimize machine size. The specific flow values selected are 42.5 lb/sec-ft^2 and 40.0 lb/sec-ft^2 for fan and compressor, respectively. These specific flow levels are consistent with General Electric experience to yield good component efficiencies.

Parametric studies were then made to determine the best component configuration consistent with aerodynamic, acoustic and engine configuration requirements. The design objectives that have been established are summarized below.

Fan Aerodynamic Design

The fan design requirements for this study are very similar to the first stage of the TF39, an existing developed fan stage, designed for a pressure ratio of 1.25 and a tip speed of 1100 ft/sec. Significant design parameters of the VTOL fans and the TF39 stage are compared in Table VIII. This similarity in design performance allows the use of the TF39 first stage data as a base for determining the stall pressure rise and design point efficiency of VTOL fans.

Stall test results for stage 1 of the TF39 fan define the peak pressure rise that can be achieved at that speed, aspect ratio, and solidity. A stall correlation procedure developed by General Electric, which relates solidity, aspect ratio and vector diagrams, permits the designer to predict the peak pressure rise capability of a new design by relating to the demonstrated performance of a similar existing machine. This correlation, therefore, can be used to make tradeoffs in speed and aspect ratio for example, for a required stall margin.

The above procedure was applied to Fans ILF1A1 and ILF2A1 to relate rotor aspect ratio against stall margin for a given speed. Results of the study are shown in Figure 55. Blade and vane aspect ratios were selected to keep essentially a constant blade to vane ratio of 0.5 with rotor and OGV pitchline solidities held constant. The study shows that ILF1A1 and ILF2A1 fans will have 18% or greater constant speed stall margin at rotor aspect ratios of 3.9 and 3.2, respectively.

A similar parametric study was conducted for the ILF2A2 fan with exception of tip speed being a variable, not a fixed parameter. The results of the study (see Figure 56) were used in conjunction with aeromechanical, acoustical, and low pressure turbine requirements to set the tip speed at 855 ft/sec and rotor aspect ratio at 2.9.

The final flowpath and vector diagrams were determined with the Compressor Axisymmetric Flow Determination program described in NASA CR5458. Since this study is a preliminary design, details of the design were simplified where end results are not critical to the objective for this study. In the axisymmetric analysis, only blade row edge stations and several free space stations between the rotor and outlet guide vane were assigned. Similarly the outlet guide vane was treated as a radical vane although it will be tilted axially and circumferentially for acoustical reasons in the final design. Experience with other tilted designs show that average blade loadings will not be significantly changed.

Cross sections of the ILF1A1, ILF2A1, and ILF2A2 flow paths are shown in Figures 57, 58, and 59, respectively. The fan consists of the blade above the flow splitter. Spacing of the outlet guide vane was made on acoustic considerations requiring minimum 2 blade chords at the tip and 1 blade chord at the hub. Annulus area distributions are identical with the peak pressure rise predictions. Axisymmetric calculations do not consider the strong viscous and three dimensional flow effects on an explicit basis. They are handled in part through assessment of an effective area coefficient which is distributed uniformly over the annulus. Based on fan design experience the coefficient values used are 0.98 at the rotor inlet, 0.96 at rotor discharge and OGV inlet, and 0.95 at OGV. The vector diagrams for the ILF1A1, ILF2A1 and ILF2A2 fans are summarized in Tables IX, X, XI, respectively.

Examination of the blade and vane loadings indicate that a higher design pressure ratio could be achieved at these tip speeds which were set by low pressure turbine and/or acoustic requirements. As a result the fan rotor hub is capable of delivering the average fan pressure ratio. For preliminary design purposes, it was assumed that the radial total pressure profile was constant at stage discharge. A final design may possibly incorporate some radial pressure gradient to redistruibute blade loadings. The loss coefficients are in general agreement with the NASA correlations with modifications based on experience and their level is consistent with the objective overall efficiency.

Fan performance maps for ILF1A1, ILF2A1, and ILF2A2 are based on the TF39 stage 1 measured performance. The estimated performance maps are shown in

Figures 60, 61, and 62 for ILF1A1, ILF2A1, and ILF2A2, respectively. Design efficiencies are estimated based on the TF39 first stage fan. Relative to the TF39, efficiency differences due to lower OGV loadings, tip speed, higher specific flow, tip shroud, rotor OGV free space, and sound treatment were accounted for. The sum of these differences result in design efficiencies of 87.0% for ILF1A1, 87.6% for ILF2A1, and 88.2% for ILF2A2.

Design of the blading elements was performed along axisymmetric stream surfaces using the projection recommended in Vol. 85, Series D, ASME Transactions. This projection cuts the blades along axisymmetric surfaces but views the cut sections along the blade axis (blade axis for these designs is a radial line). The incidence and deviation angles are defined in this "cascade projection" and are called cascade angles.

Blading is selected based on the inlet Mach number of the streamline sections. If the inlet Mach number is about 0.9 and above, the airfoil will have special meanline to minimize the shock Mach number but have sufficient throat area margin to pass the flow. Thus, the tip sections of the rotors will be special airfoils while the inner sections may be double circular arc. For the outlet guide vanes, the inlet Mach number is sufficiently low ($\lesssim$ 0.8) and the 65 series thickness on a circular arc mean line will be used.

Incidences selected for the rotor tip region are estimated to yield the correct flow alignment with the suction surface. All other incidences are based on low speed cascade data. Trailing edge angles are set using Carter's deviation rule. When changes in radius and axial velocity are present along a streamline, the deviation angle is based on the camber of an equivalent two-dimensional cascade having the same circulation. Occasionally, an empirical adjustment X_f, is used to provide an adjustment on Carter's deviation, based on experience. Incidence, total deviation, and X_f distributions of both rotors and stators are shown in Tables IX, X, and XI.

Supercharger Aerodynamic Design

The core supercharging stage of all the engines is the hub section of the fan rotor below the flow splitter. It is, therefore, also a structural load carrying member. Because of the inherent low wheel speed it has low energy

input capability. The fan tip speed and core flow requirements of each engine set the supercharger wheel speed and weight flow.

In setting the pressure ratio of the supercharger, prime consideration was given to the induced crossflow and pressure distortion at the inlet. Significant to the high pressure system is the close coupling between the supercharger and compressor. Stability of this system will be set by the compressor which contributes over 90% of the pressure rise. Therefore, a supercharger that does not amplify the inlet distortion, which could significantly degrade the compressor stall margin, and reduces the inlet radial velocity components is of prime importance. To prevent the present inlet distortion amplification across the supercharger, the design work coefficient was limited and a stall margin exceeding the compressor stall margin was set. Based on General Electric experience with high flow coefficient stages which have shown low pressure recovery capability, the work coefficient was limited to 2.0 at the hub.

Resultant supercharger stage design pressure ratios are 1.048 for ILF1A1 and ILF2A1, and 1.029 for ILF2A2. These are based on the hub work coefficient of 2.0 and radially constant total pressure profile at stage discharge. The estimated overall adiabatic design efficiency of 83.6% for all three superchargers is in good agreement with the NASA loss coefficient correlations.

For preliminary design purposes, the off design performance estimate was limited to an operating line. A reasonable assumption was made that the overall adiabatic efficiency would be constant down to 50% speed. Preliminary cycle calculations provided an estimate of flowspeed and the assumption of constant deviation angle led to the estimated operating line performance. Supercharger performance for ILF1A1 and ILF2A1 is shown in Figure 63. The same performance is applicable since their average wheel speed is nearly equal. ILF2A2 supercharger performance is show in Figure 64.

ILF2A1 and ILF2A2 have identical core compressors and therefore, identical supercharger flowpaths. The flowpaths for ILF1A1, ILF2A1 and ILF2A2 are shown in Figures 65 and 66. In both cases the flowpath is a result of the core rotor one geometry and the minimum hub requirements through the fan rotor that were set by mechanical considerations. The O.D. wall through the supercharger is

merely a forward extension of the tip radius of the compressor. The hub geometry, however, is a gradual transition from the hub slope of the compressor first stage to a zero slope, zero curvature condition at the supercharger rotor leading edge. Spacing between the supercharger rotor and stator was determined through mechanical requirements of the rotating flow splitter.

The final vector diagrams of the supercharge stage were determined with the compressor Axisymmetric Flow Determination program previously described. Here again, details of the design were simplified where end results are not critical to the overall objectives of the study. For this reason, only rotor leading and trailing edge and stator trailing edge stations were assigned in the axisymmetric analysis. Effective area coefficients used in the analysis were 0.990 and 0.985 at rotor leading and trailing edges respectively and 0.980 at stator exit and core inlet stations.

The core compressors for ILF1A1 and ILF2A1 specify 10 degrees of swirl, in the direction of rotation, into rotor one. This provision, and the counter-rotation of the low pressure and high pressure spools, requires the supercharger stator to turn past axial by the swirl value of 10 degrees.

The loss coefficient for the supercharger rotor and stator are in general agreement with the Mach numbers, blade loadings and overall efficiency as tabulated in the vector diagram summaries for ILF1A1, ILF2A1, and ILF2A2 in Tables IX, X and X1, respectively.

The supercharger rotor and stator blading elements were designed using the projection described in the Blading section of the Fan Design portion of this report. The inlet Mach number levels are sufficiently below the 0.9 limit such that double circular arc meanlines with 65 series thickness distribution can be used for both rotors and stators. Incidence, total deviation and X-Factor distribution estimates as described in the Fan Design section are given in Tables IX, X and X1.

Fan and Supercharger Mechanical Design

The fan/supercharger combination used in these engines are a departure from conventional designs. The outer portion, the fan part, consists of tip shrouded composites (Epoxy - Graphite) blades, dovetailed into the supporting wheel. The supercharger is a 17-7 PH casting with a lesser number of blades

than the fan. This arrangment allows adequate length chords on the supercharger without excessive root solidity as would be the case in a conventional blade row with a radius ratio of ≈0.2.

This arrangement results in a light weight small diameter fan which is extremely important to this design.

Requirements

- 115% max. rated speed for 5 minutes
- 101% max. rated speed, transients
- Capable of continuous operation at max. rated speed and temperature.
- Blading shall have 2500 hours life.
- Blading shall be capable of enduring 40,000 low cycle fatigue cyles. (Major speed fluctuations such as start-stop, or idle to power setting).
- The composite blades shall be individually removable.
- The leading edges of the blade shall be suitably clad to prevent FOD.
- The reduced velocity parameter shall be sufficiently low to prevent damaging torsional response.
- Provide a sufficiently sturdy supercharger (HUB) to withstand torsional and gyro loads.
- Provisions for anti-icing.
- Low weight
- Low cost

Approach

Lift engines differ in many respects from cruise engines. Two items of these differences, weight and cost, assume unusually large factors in the design selections. The assumed certification date of 1980's also influences the design selections, since time for developing new concepts is available.

Several different fan and supercharger designs were considered, bearing in mind the foregoing limitations and requirements. The composite blades with tip

shrouds were selected after considering the following:

- Unshrouded solid Ti
- Unshrouded hollow Ti
- Mid span shrouded solid Ti
- Tip shrouded solid Ti

The cast 17-7 PH supercharger was selected after considering cast aluminum and fabricated steel. The overall differences were not great and it is possible that some of the developmental aluminum alloys may make cast or fabricated aluminum superchargers the logical choice.

The fan stators provide one leg of the triangular main frame thereby minimizing weight, complexity and cost. Al-5052 was chosen for this part; however, composite Graphite-Epoxy was considered and could possibly be used.

The following comparison of graphite/epoxy and titanium bladed fan rotors will give a quantative understanding of some of the pros and cons of the suggested construction.

	G/E	Ti
Impact (Energy Basis)	1	27.5
Weight	1	1.4
Cost	1	1

The ability to absorb impact loading was determined on a strain energy basis, and indicates a potential serious problem which will require considerable development. The weight comparison is favorable to the G/E bladed fan and there is potential for further weight reduction by disc wrapping or alternate types of blade anchorage. The cost of blades at the present time appears to be roughly equal and here again alternate methods of manufacture offer possible reductions in composite costs.

Considerable development is indicated before the use of G/E blades can achieve their full potential. However, they do definitely offer the possibility of lower weight and cost. Developmental work on this subject is being actively pursued now at General Electric.

Design

Composite bladed fans can be made in several ways; continuous detachable shrouding, continuous integral shrouding (if individual blade removal is not required), integral individual tip shrouds, and mid-span shrouds (with a spar type blade).

The configuration chosen is shown in Figures 67 and 68 and has a continuous tip shroud which provides slots for the blade tips and means for locking the blades and shrouds together. The outer portion of the shroud is a continuous graphite/epoxy wrapping which is the load carrying element. The retainer that locks the shroud tips and the inner shroud to the outer portion is an aluminum alloy part. The inner shroud, providing the blade tip anchorage slots is supported by the outer portion through the retainer. The inner shroud is designed to be made up of chopped fiber.

The blades themselves are laminated composites, the graphite fibers oriented to give the best combination of longitudinal and transverse properties for the application. The bases of the blades are formed into axial dovetails as shown.

The leading edge cladding is bonded to the blade and includes serrations for inlet noise reduction.

The "disc" is a generally rectangular titanium alloy section giving maximum axial stiffness to resist a two/rev deflection.

The fan hub has 24 hollow, inclined struts of airfoil shape. This member transmits the fan torque and carries the gyro moment. The hub can be either fabricated or of cast steel.

The containment of a failed fan blade is provided by a retainer built into the outer casing. This retainer is made of AMS 304L and is two chord lengths wide. The thickness of the containment is a function of the blade kinetic energy but because the G/E is expected to lack the penetration of metal, the thickness has been assumed to be less than that required by a metal blade of the same energy.

The containment configuration is shown in Figure 68.

Provisions for anti-icing the various parts of the fan system are as follows:

- Bellmouth

  Warm air ducted from the cruise engine to the bellmouth manifold

- Fan Blade

  Past experience has shown that no protection is needed.

- Splitter Nose

  A covering of 1/8" RTV silicone rubber compound has been applied to this surface.

- Fan Hub

  This part is automatically anti-iced by the return lube oil that passes through it.

- Bullet Nose

  This part is also coated with RTV.

Compressor Aerodynamic Design

Design of the compressor for these VSTOL engines requires an advancement in the state of the art since a minimum number of stages is desired. These machines will have high blade loading at high tip speed as a result. Feasibility of these machines is projected to the 1980+ time period wherein today's promising advanced technology may be substantiated and its application developed in multistage compressors.

An area of advanced technology, which offers a potential significant improvement in compressor design, is casing treatment. Single stage tests performed at NASA, General Electric, and elsewhere have shown significant gains in constant speed stall margin. It is reasonable to assume that casing treatment will provide a stall margin improvement in a multistage environment. The core compressor designs of these engines include a casing treatment application over each rotor tip. It is assumed that a stall margin improvement of 5% will be

obtained. The application of this improvement is applied through designing the compressor at 13% constant speed stall margin in place of the 18% margin. Benefits of this improvement will come through tradeoffs on lower tip speeds, fewer stages, higher blade aspect ratio and/or lower solidity.

Flowpath Design

Parametric studies employing the analytical capability of relating stage peak pressure rise capability of known compressors correlated with prime design parameters such as vector diagram, aspect ratio and solidity were made to first determine the number of stages and tip speed range of prime interest. These initial studies indicated that a five stage compressor was feasible for ILF1A1 and a four stage compressor for ILF2A1. Final parametric studies were then made to determine the effect of flowpath radial variation and inlet radius ratio changes. These results are shown in Figures 69 and 70 for the ILF1A1 and ILF2A1, respectively.

Calculated results show that a constant tip radius flowpath with a low inlet radius ratio was most desirable in terms of efficiency, tip speed and size. For the type of engine application without fan supercharging, physical rim speed does not become a problem in the rear stages. Also the low cycle pressure ratio does not result in high exit radius ratios or small rear stage blade heights. Therefore, the constant tip type of flowpath is acceptable. Consideration of the total engine configuration resulted in a 0.65 inlet radius ratio selection.

The final compressor design is slightly modified relative to the parametric result. Reductions on the tip radius were made to obtain additional area convergence across some blade rows and the rear stages were dropped radially for engine configuration requirements. In addition, the supercharger pressure delivery into the compressor was accounted for. The final compressor design parameters are shown in Figures 69 and 70. It is shown that an increase in tip speed was required because the reduction in tip speed as a result of the supercharging did not offset the increase in tip speed due to decreasing the tip radii.

Final vector diagrams and flowpath configurations were determined with the axisymmetric analysis of NASA CR5458. For the preliminary design approach. only trailing edge stations were defined except for the first rotor leading edge.

Consistent with design experience, effective area coefficient values employed are 0.99 at the supercharger inlet, 0.980 at the first rotor inlet and 0.92 at compressor discharge. The variation of the coefficient through the machine is essentially linear. Schematics of the flowpaths are shown in Figures 65 and 66 for the ILF1A1, and ILF2A1 compressors, respectively. Vector diagrams summaries at tip, pitch and hub are given in Tables XII and XIII for the ILF1A1 and ILF2A1 compressors, respectively.

Radial total pressure profiles were assumed to be constant radially at stage discharge and blade element loss coefficients are in general agreement with NASA correlations. The stage pressure ratios, area convergence across each row, aspect ratios and solidities are consistent with the stage peak pressure rise analysis.

The primary design parameters for the final compressor designs are summarized in Tables XIV, XV and XVI for the ILF1A1, ILF2A1 and ILF2A2, respectively. Overall objective adiabatic efficiencies were derived from current design and test experience and includes factors such as rotor inlet Mach number, blade loading and tip clearances. Predicted performance maps are shown in Figures 71 and 72 for the ILF1A1 and ILF2A1 compressors, respectively.

Good part speed stall margin is considered essential for these engines. For both compressors, the inlet guide vane (or supercharger stator) and first stator must be variable to ensure proper stage matching for good part speed stall margin. This assessment is based on General Electric experience through correlation of density and axial velocity ratios across a fixed block of stages. Variable stator schedule requirements have been established for a true position system. If subsequent mission evaluations require a fully variable stator system could be added. A typical system of this type would have stators closed up to about 50% speed and opened approximately linearly to nominal position at 90 to 95% speed.

Casing Treatment

Single stage component tests have shown that increases in stall margin have been achieved through the use of casing treatment over the rotor tip as reported in NASA CR82862. As a general statement, some of these treatment

configurations have shown no appreciable change in peak efficiency. One of the most promising treatments is the circumferential groove configuration shown schematically in Figure 73. Stall margin improvements over a radial casing configuration for two different stages reported in NASA CR82862 are shown in Table XVII. Stall margin improvement results for the two different stages are quite different and the reason for the difference is not understood. Analysis of the test results indicated that the increase in stall margin was obtained essentially through a flow roll back without a change in peak pressure coefficient. The data in Table XVII shows that a minimum of 3% in constant speed stall margin was achieved. Thus, it is assumed for this study that casing treatment will improve the stall margin for a stage by 3%.

Application of casing treatment in a multistage environment over each stage would possibly permit the stage or group of stages initiating stall to roll back without an increase in pressure rise. The remaining stages would then be permitted to approach their peak pressure coefficient through the additional flow roll back. An assumed 2% additional compressor stall margin seems reasonable for the additional pressure rise for the remaining stages. Therefore, a constant speed stall margin improvement of 5% for casing treatment was selected for these compressors.

Blading

Compressor rotor and stator blading elements were designed using the projection described in the blading section of the Fan Design portion of this report. Based on the inlet Mach number levels, airfoil section selections were made as indicated on Tables XII and XIII. Incidence, total deviation and X values are also summarized on Tables XII and XIII.

Compressor Mechanical Design

The compressor mechanical designs, five stage for the ILF1A1 and four stages for the ILF2A1 and ILF2A2 are essentially the same for all of the engines studied.

The rotor discs, spacers and steel shafts are fabricated into a single component. This eliminates flanging which costs weight, assembly time and manufacturing cost as well as providing a very stable structure.

The first stage blades are graphic-epoxy while the balance are Ti 6-4. All dovetails are circumferential except the first stage which is axial. The proven single hook dovetail is used in all cases.

The forward end of the rotor is mounted on a differential bearing which runs on the low speed fan shaft. The aft end is supported on the high pressure turbine through a curvic coupling. The seal teeth are integral parts of the spacers and the aft cone.

The stator case is split longitudinally and circumferentially, the forward part being made of cast 224 T6 aluminum alloy. The aft portion is made of 17-4 PH. Casing treatment is provided for each blade row.

The IGV's and the first row of the stator vanes are variable to assist in off design operation. All stator vanes are tip shrouded and provide the static part of the interstage seals. The vanes are fastened to the case by conventional "T" slots.

The OGV's and diffuser are integral and bolt to the aft compressor flange. Design features are summarized below:

- inertia welded rotor
- low aspect ratio, long chord blades
- circumferential dovetails
- individually replaceable blades and vanes
- split casing
- two rows of variable stators
- casing treatment

A material and stress summary of the ILF1A1 compressor is shown below:

Stage No.	Blade Material	Vane Material	Disc & Spacer Material	Blade Hub Stress Levels
1	G/E	G/E	Ti 77XD	9.6 KSI
2	Ti 6-4	Al,224 T6	Ti 77XD	16.0 KSI
3	Ti 6-4	Inco 718	Ti 77XD	10.4 KSI
4	Ti 6-4	Inco 718	Ti 77XD	9.1 KSI
5	Ti 6-4	Inco 718	Ti 77XD	7.2 KSI

Average metal temperatures are shown on Figure 74.

COMBUSTOR DESIGN

The reversed flow combustor arrangement was chosen since it allowed a shorter more compact engine. This arrangement provides for a large, ~30% cross flow of cooling air through the HP nozzle thereby insuring adequate cooling under all conditions of operation.

Requirements

- Minimum contribution to the engine length
- 0.2 pattern factor
- Dual fuel system
- High space rate for minimum volume
- No visible smoke (to meet FAA emission requirements)
- Dual ignition
- Life

Per installation	1250 hr
Total	2500 hr

Combustor Aerodynamics Design

The combustion system for the engines is a highly loaded, reverse flow, carbureting design. This configuration provides a very short, compact combustion system that is ideally matched to the overall configuration.

Airflow leaving the core engine compressor enters a short, slightly curved diffuser with an area ratio of 1.4 which recovers about one half of the compressor discharge velocity head. This flow is then dumped into an annular plenum chamber which feeds air in the reverse direction to the dome and inner liner shell of the combustor and to the outer shell through the first stage nozzle vanes of the turbine. About 30% of the total flow passes radially through the turbine vanes where it is used to convectively cool the vanes and is then passed through a small diffuser at the tip of each vane. These diffusers reduce the velocity head down to about one percent of the total pressure before the flow

is dumped into the outer plenum region. An additional four percent of the total flow enters the vanes at the root section and is used to film cool the outer surfaces of the vanes.

Airflow moving forward along the inner and outer combustor liner walls is used for liner cooling and for secondary dilution air. The secondary dilution air is used to dilute the hot primary combustion gases down to the required turbine inlet temperature. About 42% of the total flow enters the dome region from the inner annulus. This flow is used to burn the fuel in the primary combustion zone of the burner.

For this design about 10% of the total airflow is mixed with the fuel flow in annular pre-mixing chamber upstream of the dome. Additional comustion air enters the dome through annular slots located on the inner and outer sides of the pre-mixer. The strong cross-flow results in intimate mixing of the fuel and air in the primary combustor region of the burner, which helps to achieve good flame stability and efficient combustion.

Air for the pre-mixer is picked up by a set of 20 separate ram scoops that are evenly spaced around the dome of the combustion system. Fuel is then injected into alternate air scoops from a set of 10 fuel tubes that project into the sides of the scoops. Ignition of the fuel-air mixture is achieved with either of two electrical spark ignitors that project through the upstream end of the outer combustor liner from the outer casing of the core engine.

Combustor gas flowpaths are shown on Figures 75 and 76. Important design features are summarized below:

	ILF1A1	ILF2A1 & ILF2A2
Space Rate - (Btu/hr)/atm. $ft.^3$	12.5×10^6	12.5×10^6
Length/Height Ratio	2.5	2.7
Temperature Rise	1866°	1460°
No. of Nozzles	20	20
Pattern Factor	0.2	0.2
Δ P/P	0.07	0.07

	ILF1A1	ILF2A1 & ILF2A2
η_B	0.9875	0.9875
Reference Velocity	66 FPS	83FPS
Compressor Exit Mach No.	0.35	0.35
Diffuser Dump Mach No.	0.25	0.25
Liner Material	Hast X	Hast X
Inner Shell Material	Inco 624	Inco 625
Outer Shell Material	Inco 718	Inco 718

Fire Safety

The basic fire safety design is inherently a low risk arrangement. The remote controls and accessories are packaged in a fire proof container. The double walled fuel manifold and nozzles are mounted inside of the fire proof combustor outer casing and the stator actuator liners have double walls.

One of the considerations in conventional turbine engines is to make provisions for draining out unburned fuel left in the engine from a false start. This engine automatically drains through the turbine and out the exhaust nozzle leaving no dangerous pockets of fuel.

The fuel manifold shown (Figures 75 and 76) is a double walled arrangement located inside of the fire proof outer combustion casing. The manifold can be a single ring with one lead-in tube or split into 180° segments with two lead-in tubes. This makes a simple arrangement in which the mid-space can be safely vented overboard at the aft end of the fan duct. An alternative method would be to have an external manifold which would not require double walling but would require piercing the combustor casing for every fuel tube. Both methods have their advantages; however, the former seems the simplest at the present time.

The stator actuators are operated by fuel line pressure and are double walled in the conventional manner.

The non-engine mounted elements, air turbine, fuel pump, lube and scavenge

pump, alternator, controls, air cooler and tank, are mounted in the nacelle in a separate fire proof enclosure.

Engine Emissions

It is recognized that missile smoke is not the only area which requires treatment. A detailed study of methods to reduce CO_2, NO_x, and trace metals emissions from the ILF engines has been sponsored by NASA and is now underway. The results of this study, and the changes in combustor design required to meet various levels of emissions will be reported in the NAS 14406 final report, due early in 1972.

TURBINE DESIGN

HP Turbine Aerodynamic Design

The core turbines designed in this program have the following aerodynamic design requirements:

Core Turbine Design Requirements

Cycle	ILF1A1	ILF2A1 and ILF2A2
$\Delta h/T_4$	0.0526	0.0475
P_4/P_5	2.665	2.368
$N/\sqrt{T_4}$	324.8	337.4
$W\sqrt{T_4}/P_4$	16.28	27.71
$GJ\Delta h/2\ U\ P^2$	0.71	0.57
W_c/W_{2c}%	5.7	2.3
η net	87.0	88.6
Exit Mach No.	0.5	0.5

The turbines are all single stage designs with their tip diameters set relative to the compressor diameter and an exit area size for 0.5 Mach No. Turbine performance was estimated based on General Electric Company's experimental performance with similar tubines. Free vortex calculations were made to determine the preliminary vector diagram. A summary of the vector diagram data is given in Table XVIII.

The turbines are lightly loaded with fairly high reaction and near zero leaving swirl. A blading summary of the turbines is shown below. Turbine flowpaths are shown on Figures 77 and 78.

Core Turbine Blade Summary

Cycle	ILF1A1	ILF2A1 and ILF2A2
No. Nozzles	62	48
No. Blades	112	76
Rotor Pitchline Axial Width (in.)	1.05	1.2

Fan Drive Turbine Aerodynamic Design

The fan drive turbines have the following aerodynamic design requirements:

Fan Drive Turbine Design Requirements

Cycle	ILF1A1	ILF2A1	ILF2A2
No. of Stages	3	3	4
$\Delta h/T_5 4$	0.0556	0.0468	0.0468
P_{T54}/P_{T55}	2.99	2.39	2.40
$N/\sqrt{T_{54}}$	103.38	94.70	74.39
$W\sqrt{T_{54}}/P_{54}$	42.44	62.23	62.23
$GJ\Delta h/2\varepsilon U_p 2$	2.54	2.04	2.23
η	83.8	86.6	86.5
Exit Mach No.	0.42	0.415	0.416

The turbine flowpaths were designed to be close-coupled with the core turbines (i.e., no transition passage between turbines) and have overall aerodynamic work coefficients of 2 to 2.5. The exit areas behind the turbines were set for 0.4 Mach number. Turbine performance was estimated based on an extrapolation of General Electric Company's experience. Some of the turbine blading characteristics are summarized in Table XIX.

In all cases, the energy was set on the last stage to give a prescribed swirl level with ten percent hub reaction. The swirl level was selected based on the outlet guide vane design requirements, and the reactions level was selected to eliminate diffusion across the rotor. The remaining energy was split relatively evenly among the initial stages to keep all the blade row leaving Mach numbers about the same level. All calculations performed for these studies were free vortex. A summary of the vector diagram data for all engines is shown in tables, XX, XXI and XXII.

Data given in NASA SP-36, "Aerodynamic Design of Axial Flow Compressors," was used to determine the performance characteristics of the outlet guide vane system. As shown in Figure 79, the minimum expected pressure loss corresponds to a D-factor of about 0.5. This value is higher than the D-factor usually assumed for compressor blade design, but the problem of compressor stall does not apply to these outlet guide vane designs. That is, the maximum turning and Mach number requirements occur at the design point and tend to be less at other operating conditions.

Outlet Guide Vane

A summary of the outlet guide vane designs is shown in the following table.

Outlet Guide Vane Design Summary

Cycle	ILF1A1	ILF2A1	ILF2A2
Inlet Angle $_{P}^{(o)}$	38.8	36.7	31.6
Exit Angle $_{P}^{(o)}$	0	0	0
No.	128	140	86
Solidity	1.8	1.75	1.14
D-Factor	0.51	0.49	0.475
Pressure Loss $\Delta P/P$	0.024	0.021	0.012
Pitchline Axial Width (in.)	0.95	0.95	0.95

Turbine flowpaths are shown on Figures 80, 81 and 82.

Turbine Cooling Design

Table XXIII shows the cooling design requirements for the high pressure turbine vanes and blades. The design gas temperatures were calculated for the design T_4 value shown (including margin) and include effects of combustor discharge temperature profiles, coolant dilution and relative velocity effects. The metal temperatures were selected based on life considerations discussed separately in this report. The coolant temperature was calculated based on compressor discharge conditions, from whence the air is extracted, and includes allowance for heat pick-up prior to entering the cooled airfoils and the effect of expansion in the cooling air inducers for the blade coolant. The cooling effectiveness have been calculated based on the gas temperature, coolant temperature and metal temperature, and are shown in Table XXIII.

The vanes are cooled mainly by convection of the combustor outer liner coolant and dilution air which passes through the vanes. It is necessary to bleed some air out through the vane trailing edges to cool the extremity, in addition, the ILF1A1 vane requires some additional film cooling.

The relatively low effectiveness required for the ILF2A1 blade allows use of a simple convection system, whereas the higher effectiveness required by the ILF1A1 blade makes necessary a combination of convection and film cooling.

The cooling flow rates as a % of W_{2_c} were estimated using a General Electric Company correlation which includes effects of cooling type, effectiveness, gas side, a heat transfer coefficient, airfoil surface area and number of airfoils.

The cooling design requirements, cooling effectiveness and cooling flows for the low pressure turbines are shown in Table XXIV. The ILF1A1 LP turbine is cooled by third stage compressor air. Convection cooling is used for all three cooled blade rows. The ILF2A1 LP turbine does not require cooling; however, some air passes through the second vane as seal blockage air.

Cooled Turbine Performance

The calculated effect of turbine cooling and leakage air on turbine performance is show in Table XXV for the ILF1A1 and Table XXVI for the ILF2A1. The tabulation shows the assumed clean aerodynamic efficiency, the location at which the cycle calculation assumed the coolant returned to the flowpath and the net effect on turbine efficiency. The net effects include mixing losses,

coolant pumping energy, and available expansion energy of the coolant from entrance to the charging station.

High Pressure Turbine Mechnical Design

The close coupled reverse flow combustor results in some departures in high pressure turbine design, particulaly in the stator area. Briefly the features of this turbine are:

Part	Material	Feature
Vanes	MM509	Thru flow of ~30% of core engine flow.
Blades	Ni 76XB	Film cooled blade
Wheel	Ni 75XD	Thermally isolated
Shroud	R-120	Transpiration cooled
Impingement starter	Hast-X	Integral

Requirements

Life per installation 1250 hr. (20,000~)

Total 2500 hr. (40,000~)

	Turbine Inlet Temperature		
	ILF1A1	ILF2A1	ILF2A2
Max. Continous, ° F	2500	2000	2000
Max. Emergency, ° F	2585	2063	2063

115% emergency N for 5 minutes, normal continuous T_4

No goose neck between nozzle and rotor

Stator

The HPT stator includes the following items:

- Nozzle
- Impingement starter
- Impingement starter manifold
- Mid support cone
- HPT tip shroud

The HPT nozzle departs from the usual design practice in that it provides cold air passages for about 30% of the combustion requirements. This large quantity of cooling air plus the 4% which is bled out of the trailing edges of the vanes provides ample cooling for this member. Under max T_4 conditions the metal temperature is limited to less than 1950° F. The discharge side of the passages form diffusers which drop the cooling air velocity at that point of 0.2 Mach number.

The impingement starter is an integral part of nozzle - midframe assembly. The manifold and jet nozzle extend 360° around the outer wall of the HPT flow path providing the minimum bending moment to the buckets during the starting cycle.

The mid support core extends from the manifold to the inner surface of the fan duct and includes the turbine shroud support. This arrangement insures close alignment of the HPT stator and rotor parts.

The HPT shroud is transpiration cooled and located from the shroud support. The short connection through the turbine rear frame insures good rotor tip clearance control.

Rotor

The single stage HPT together with the compressor make up a two bearing rotor. The connection between the compressor and the turbine is a curvic coupling fastened by a single tubular bolt which provides for minimum assembly and disassembly time. The rear stub shaft is flanged to the aft side of the wheel insuring low stress in the bolting area.

The buckets are hollow with double hook case type dovetails. They are cooled by air that enters through a single passage in the shank and discharges thru 0.005-inch diameter holes.

The running elements of the seals are ribbeted to the HPT wheel. Thus the diameter of the seal teeth is set by the wheel itself, insuring a minimum seal clearance extension. The seal member themselves are so contained that even a full length axial crack will not cause catastrophic failure.

The cooling air for the buckets and the blockage air for the seals is supplied from the compressor discharge through an inducer. This arrangement allows minimum cooling air temperature and the path effectively provides a wheel rim thermal barrier.

Key information on cooling, leakage, and materials is given below:

Cooling Flow (Percentages of W_{2c})

	ILF1A1	ILF2A1	ILF2A2
Blade	3.1	1.1	1.1
Shroud	0.5	0.2	0.2
Nozzle	30	30	30

Leakage (Seals)

	ILF1A1	ILF2A1	ILF2A2
Nozzle-Rotor	2.25	1.7	1.7
Rotor-LPT Stator	0.8	0.7	0.7

Material

Nozzle	Hastelloy X
Seals	MM509
Blade	Ni 76XD
Disc	Ni 75XD
Stub Shaft	In 718

Metal Temperature	ILF1A1	ILF2A1	ILF2A2
Nozzle ° F	1850	1700	1700
Blade ° F	1610	1610	1600

A typical disc stress curve is shown on Figure 83.

Low Pressure Turbine Mechanical Design

The low pressure turbines for the ILF1A1, ILF2A1, and ILF2A2 are similar in that the integral disc-spacer combination is overhung from a single conical

web. The fan, shaft and LPT comprise a single two-bearing rotor which also supports the two heavy high pressure rotors. The ILF1A1 and ILF2A1 have three stage turbines and the ILF2A2 has a fourth stage.

Requirements

The requirements for the LPT are very similar to those of the HPT. They are:

- 120% design N for 5 minutes
- Continuous operation at max. rated temperature
- Life

  Per installation - 1250 hr
  Total - 2500

- Cycles

  Per installation - 20,000

  Total - 40,000

- Inlet to coincide with HPT exit
- Exit diameter not to exceed combustor OD

Stator

The stator consists of three (four in the case of the ILF2A2) vane rows which hold together to form the shell, the stator vane assembly and the inter stage seals. This design has the advantage over conventional arrangements in low weight and no distortion due to longitudinal joints.

The ILF1A1 requires 3.95% cooling to the 1st stage nozzle and 1% to the 2nd stage nozzle.

The ILF2A1 requires essentially no cooling. However, 1.3% blockage air is required for the HP-LP seal and this air is ducted through the 1st stage nozzle.

The cavity is not really cooled but it is purged with the leakage air from the HP-LP seal and the No. 3 and No. 4 bearing sump seals.

The vanes and their outer and inner bands and extensions are considered here to be integral castings. These could be made as a single 360° unit or as

segments later welded. The static part of the inner seals are supported from the inner shroud band. The seal surface itself is made up of small-cell honeycomb.

Rotor

The disc and spacers of the last two stages(last three in the ILF2A2) are fabricated into a single unit. The spacers also have the seal teeth as integral parts. The first stage has a conventional disc which is flanged to the support cone and the aft rotor down.

The integrally shrouded blades are anchored by one hook axial dovetail. The first stage in all three designs uses a post type of anchorage allowing for bolt insertion in the root area. The method of through bolting does not result in the usual stress concentration of a conventional bolt hole.

The ILF1A1 requires 1.25% cooling air which passes through an inducer mounted on the inner seal of the 1st stage stator. The ILF2A1 and ILF2A2 do not require cooling, as previously stated.

Shaft and Coupling

The fan shaft is conical in shape to provide the maximum rigidity between the fan rotor and the LPT rotors. The covering also provides for the raising of the oil from the aft sump to the No. 1 and 2 bearings in the forward part of the engine.

The aft end of the shaft is splined in the conventional manner to the LPT stub shaft. Two locating lands are provided, one on either side of the coupling teeth.

Summary characteristics of the designs follow:

Cooling Flows (percent W_{2c})

	ILF1A1	ILF2A1	ILF2A2
Blade (1st)	1.25	None	None
Shroud(1st)	0.2	0.2	0.2
(2nd)	0.1	0.1	0.1
Nozzle (1st)	3.95	None	None
(2nd)	1.0	None	None

Leakage (Seals)

	ILF1A1	ILF2A1	ILF2A2
Nozzle - 1st R.	0.9	0.6	0.6
Nozzle - 1st R.	0.9	0.6	0.6
1st - 2nd	0.45	0.45	0.45
2nd - 3rd	0.3	0.30	0.30

Material

Nozzles and Casings	All
1	R120
2	R120
3	R120
4 (For ILF2A2)	R120
Seals	Hast. X Honeycomb
Blades	
1	Ni 76XB
2	R120
3	R77
4 (For ILF2A2)	R77
Disc and Spacers	Ni 75XD
Stub Shaft and Cone	IN718

FRAMES DESIGN

The ILF engines have two frames, the main frame Figure 84 that supports the whole unit and the turbine rear frame Figure 85 that links the main frame inner ring and the rear bearing supports.

Frame requirements are summarized below:

Main frame provides:

- Proper number of vanes and spacing of OGV's of fan
- Pads for Gimbal trunnions
- Rigid light weight structure covecting outer shell and core engine
- Service line ducts
- Support for exit splitters
- Life - 5000 hr.

Rear Turbine Frame provides:

- LPT - OGV support
- Service struts
- Support for rear bearing

Main Frame

The main frame supports the entire engine and provides for the mounting of the two trunnions. It consists of an outer ring connected to an inner ring by the fan OGV's and to the turbine rear frame by hollow struts. The OGV's, struts and inner ring form a truss through which the engine thrust and reaction is transmitted.

Both the inner and outer rings are fabricated (bonded) structures to which the OGV's are bonded. The aft struts are bonded to the outer ring hub pinned to bosses provided on the turbine rear frame.

Differential expansion between the inner ring and the outer is provided for by leaving the OGV's and the struts 15° from radial and by pinning the strut-rear frame joints.

Two trunnion bases or pads are an integral part of the outer ring. The prime function of these pads is to spread the load from the mount to the outer ring. The design is shown in Figure 86 and may be either a fabrication or a casting. One trunnion will be ball mounted and the other will have a roller mount to allow for differential expansion.

The principal load on that part will be from the engine thrust, as "G" and "gyro" are small.

Rear Frame

The turbine rear frame utilizes both OGV's and struts to connect the outer ring to the inner. The six large struts provide for hub passages and anchorage supports as seen in Figures 85. The main struts are also bossed to accommodate the two exhaust nozzle suppressor rings.

Main features of the frame design are:

Main Frame	Turbine Rear Frame
• OGV - Solid Al 6061	• Six Struts
• 6 rear struts hollow 321SS	• Lube and scavenge lines ducted through struts
• Pinned core joints	• INCO 625 material
• Trunnion pads on outer ring	• OGV No. ILF1A1/ILF2A2/ILF2A2 140/128/86

DUCT AND NOZZLE AERODYNAMIC DESIGN

Fan Duct

Because of the low fan pressure ratios involved in the designs, the fan duct from the OGV to the exit is almost constant area, except for contouring required to account for the blockage of the acoustic splitters and rear fan frame. Friction losses in the fan duct are calculated in the standard manner with the friction coefficient increased to account for the effect of the surface holes in the acoustic treatment material. Pressure drag and interference drag losses from the struts, splitters and their intersections are estimated based on Horner's "Aerodynamic Drag" as well as experience gained from evaluation of existing similar systems. Duct velocity and flow coefficients are based on recent large scale test experience.

At an operating condition where the reference duct Mach number is 0.5, losses are as follows:

	$\Delta P/P_T$
Friction	0.0097
Pressure drag of struts and splitters	0.0040
Interference drag of struts and splitters	0.0013
Total	0.015

In actual practice, since the loss is a function of duct Mach number, the computer deck representation is given as:

$$\frac{P}{P_T} = (1/2\gamma\, M^2_{duct}\, \frac{P}{P_T})\ K$$

The value of K is calculated to match the loss at the design point chosen.

The duct velocity coefficient, C_{V28} and duct flow coefficient C_{F28} have been established at 0.995 and 0.975, respectively.

Core Duct

As in the case of the fan duct, the core duct is essentially a constant area passage from the turbine exit guide vanes to the exit of the nozzle. This low Mach number (~0.4) results from the relatively high extraction from the core,

required to achieve low jet core noise.

For the match point Mach number of 0.4, the losses are as follows:

	$\Delta P/P_T$
Friction	0.005
Pressure drag of acoustic splitters	0.00002
Interference drag of OGV/ acoustic splitters	0.00032
Total	0.005

Representation of the loss in the performance is in the same manner as for the fan duct.

The core velocity coefficient, C_{V8} and core flow coefficient C_{F8} have been established at 0.995 and 0.084* respectively. No additional loss is expected from the blunt core base because of the direction of the core and fan exit flow toward the engine centerline. This effect has been experimentally verified during previous direct lift engine programs.

Duct flowpaths are shown on Figures 87, 88, and 89. Core exhaust flowpaths are shown on Figures 90 and 91.

Duct and Nozzle Mechanical Design

The duct, nozzle and suppression surfaces are integrated into the overall engine structure utilizing parts of the frame shells and like structural elements. The suppression elements in the fan duct are generally 1 inch deep with the exception of the splitters which are 3/4 inch.

Requirements are as follows:

- Minimum weight
- Corrosion resistant
- No retention of water or liquids
- High rigidity for weight
- Capable of being cleaned of deposited oil, fuel and dirt

* 0.084 flow coefficient is due to very low value of P_{T8}/P_o.

- In the case of the core engine discharge - high temperature
- Life - 5000 hr.
  80,000 cycles
- Low cost
- Resistant to deterioration under buffeting and high sound intensity

The outer duct must provide sound suppression material for its full length, support the face tip seal, and form the outer surface for the fan nozzle. The aluminum honeycomb structure selected meets this criteria as well as the general requirements listed previously. The panel material was made up of 1/4 inch cells, 1 inch deep with 0.020 inch outer and inner walls.

The cells were vented to adjacent cells such that water would drain from one to the next and at the same time provide a multiphase type of suppressor.

The cell walls, which are 0.0025 inch thick will be protected from corrosion by a non-metallic coating.

The inner wall of the fan duct takes advantage of the substantial frame and support members as one wall of the suppressor member, thus external loading is no problem.

The suppressors or nozzle for the gas generator are made of IN718 to stand the exhaust gas temperature. The basic construction is similar to that of the low temperature outer duct. Figures 92 identifies the material and location of the panels.

VECTORING SYSTEM DESIGN

The requirements for vectoring thrust have been initially established at 15° forward and 45° aft. Although it is recognized that the ultimate values depend on a specific design for an air vehicle, and well defined transition trajectories, these are considered to be representative.

Two candidate systems were considered for conceptual design in a six engine pod; louvered vectoring, and engine gimbaling. In the former system, the engine is fixed in the pod in a vertical position and thrust vectoring is achieved by movement of cascaded louvers in the jet efflux. Some experience with devices of this type has been obtained during the XV5A program. In the latter system, vectoring is achieved by swivelling the entire engine through the required angles. In this system, a longer pod results from the required clearance required by the rotating engines.

A conceptual design of the two systems yielded the following results for engines installed in a six engine pod of conventional construction.

	Gimbaled	Louvered
Total Pod Volume	base	-5.5%
Pod Frontal Area	base	+20%
Pod Planform Area	base	-25%
Pod Side Area	base	-5%
Pod Surface Area	base	-14%
Pod life thrust	base	-2%
Pod thrust/weight ratio	base	+3%

The louvered system provides a smaller volume pod, shorter, but with greater depth to accommodate storage of the vector louvers. The louvers also cause about a 2% thrust penalty relative to a gimbaled system.

The overall pod thrust/weight ratio difference of 3% is not considered to be significant within the depth and accuracy of the analysis.

Some qualitative factors affecting the selection of a system are:

	Gimbaled	Louvered
Simplicity	greater	less
Number of parts	fewer	greater
Crossflow characteristics	better	worse
Actuation forces	lower	higher
Air starting	easier	more difficult

Based on these two comparisons, a gimbaled vectoring system was selected for preliminary design use. As previously stated, relative to the design thrust vector range requirements, it is recognized that selection of a vectoring system is very closely connected to the air vehicle configuration, and the ultimate design may evolve to gimbaled, louvered, clamshell, or some other design not presently in hand. The point is that the engine can be designed to be compatible with any installation configuration, recognizing that some may require more work and complexity than others.

Figure 93 and 94 illustrate the concept of the gimbaled vectoring system. The engines are mounted between two beams on bearing supports and are driven by hydraulic actuators mounted on the beams. Engines are connected to each other by synchronizing rods tied to the end of the actuator arms so that all engines have the same vector angle. This system also provides a degree of redundancy in the event of actuator failure. A cross-section of the bearing and mounting system is shown on Figure 95. One bearing is a roller type and the other of the ball type to allow for diametral growth. The support system is arranged for rapidly dismounting the engine from its supports.

BEARINGS, SEALS, AND LUBE SYSTEM DESIGN

Lubrication System

The lubrication system of the Integral Lift Fan contains the following sub-systems:

- Oil Supply Sub-System
- Oil Scavenge Sub-System
- Oil Seal Pressurization Sub-System
- Sump Vent Sub-System

A dry sump is used, as in all other General Electric jet engines. Oil is pressure fed to each engine component which requires lubrication and/or cooling and is removed from the sump areas by scavenge pumps. The bulk of the system oil supply is thereby retained in the oil tank. The lubrication system schematic diagram is shown in Figure 96.

Oil Supply Sub-System

The oil supply sub-system consists of the oil tank, which serves as the main resevoir of oil in the system, the oil supply pump, oil supply filter, and oil supply nozzles. Oil is supplied to the inlet of the supply pump from the oil tank. Oil under pressure is then routed through the supply filter and distributed to the engine by the oil supply nozzles.

Oil supply pressure to the engine shall be limited during cold starts in order to avoid draining excess power from the accessory drive system. A static leak check valve prevents leakage from the oil tank into the engine during periods of engine shutdown. An oil supply pressure tap is located downstream of the static leak check valve. The pressure tap indicates oil pressure across the oil supply nozzles hence will be sensitive to oil temperature and flow rate. Abrupt changes in oil supply pressure will be indicative of broken nozzles, plugged nozzles, loss of oil or other system malfunctions. The oil supply pump is protected from contamination by an inlet screen.

Oil Scavenge Sub-Systems

The oil scavenge sub-system consists of the scavenge pumps, and oil cooler and scavenge oil derator.

Each major area of the engine is scavenged by a separate pumping element. The combined flow is then routed through the oil cooler and back to the oil tank via the scavenge oil derator which reconditions the oil for re-use by the engine.

Each pumping element is protected from contamination, particles too large to pass through the element without causing damage, by an inlet screen. Each scavenge inlet screen contains a magnetic chip detector to collect ferrous particles which may indicate failure of a main shaft bearing.

Seal Pressurization Air Sub-System

Main shaft oil seals require pressurization air in order to cause air to flow across the seals into the sumps at all operating conditions. If air is allowed to flow out of the sump through an oil seal, some oil is carried with it. This oil leakage must be eliminated in order to prevent excess oil consumption and seal coking. Pressurization air is extracted from the compressor and routed to the various engine oil seals.

Vent Sub-System

Each area of the engine, which requires pressurization of oil seals, is vented to remove the air which enters the sumps through the oil seals. This also allows the sump internal pressure to remain low enough to prevent reverse air flow out through the oil seals during a rapid power reduction. The engine is vented radially inward through the low pressure shaft and routed forward and out to the fan discharge cavity.

Lube System Components

A description of the major lube system components is as follows:

Oil Tank

The oil tank functions to:

- Store engine lubricating oil
- Supply oil to the engine over the range of altitude requirements.

- Provide for removal of air from the scavenge air/oil mixture.
- Provide space to accommodate system fluid volume changes.

The scavenge system of the engine will result in a derated scavenge oil flow being returned to the tank. Air removal will be accomplished by a static centrifugal derator. The scavenge air/oil mixture enters the scavenge return chamber in a tangential direction at relatively low velocity. The mixture then passes through the vortex generator which accelerates the mixture and discharges it in a swirling motion of the walls of the vortex tube. Centrifugal force holds the oil on the walls of the tube and the lighter air forms a vortex in the center of the tube. Air is vented out of the top of the assembly and oil is discharged into the oil tank and is ready for reuse.

The oil tank size of 1.8 gallons is determined by adding the following volumes:

Unusable Oil

This is the quantity of oil required to provide fluid with air entrainment of less than 10 percent by volume. This volume is a function of system mechanization derator configuration, flow rates through the tank, attitude requirements and tank shape. This volume shall be approximately 0.25 gallon.

Usable Oil

Usable oil shall be approximately 1.25 gallons and is determined by adding the following allowances:

Mission oil capacity - That volume allowed for engine consumption during the required mission. Mission capacity of 1.0 gallon is provided.

Gulping volume - Previous experience has shown a difference between non-operating full level and full level when the engine is at max power. This difference is defined as gulping volume. An allowance of 0.25 gallon is provided in the tank.

Expansion Volume

Expansion volume shall be 20% of the usable and unusable volume. This volume allows for foam and thermal expansion of the oil, and provides space to keep the tank vent clear over the range of engine attitudes.

Lube and Scavenge Pump

The lube and scavenge pump is driven by the accessory drive system and consists of one positive displacement lube system element and two positive displacement scavenge elements. Each element is protected with a removable non-bypassing inlet screen. The installed inlet screens will prevent entrance of any particle greater than 0.037-inch x 0.037-inch have have an effective flow area of 4 time the cross sectional area of the element inlet port. The scavenge element inlet screens shall also include magnetic chip collectors. A cold start bypass check valve shall be provided to limit oil supply pressure during cold starts. The valve shall be located downstream of the lube supply filter and shall relieve to the inlet of a scavenge pump.

Lube and scavenge pump sizes shall be as follows:

		Oil Flow	Inlet Pressure
a.	Lube supply	6.0 gpm	12 - 14 psig
b.	Forward scavenge	6.0 gpm	12 - 14 psig
c.	Aft scavenge	6.0 gpm	12 - 14 psig

Lube Supply Filter

The lube supply filter serves to protect the lube supply nozzles from containment as well as remove system generated contamination such that system cleanliness is maintained at an acceptable level. The filter shall be a non-bypassing full flow type with a filtration level of 46 microns nominal. An automatic service shut off provision shall be incorporated into the unit to prevent system drainage while the filter is being serviced. The pressure differential across the filter shall not exceed 10 psi for a new or newly cleaned filter with full flow, 6 $\pm$ 0.25 gpm, of oil at 80 to 100° F.

Static Leak Check Valve

A static leak check valve shall be provided to prevent leakage from the oil tank into the engine during periods of engine shutdown. The check valve shall have a minimum cracking pressure of 5 psi. The valve shall be capable of passing full oil flow of 6 gmp with a pressure drop not exceeding 10 psi at 80 to 100° F.

Oil Cooler

The oil cooler shall be capable of transferring the engine lube system heat rejection to the engine fuel. The oil slide of the cooler shall be capable of withstanding a transient pressure of 1,000 psi. A temperature or viscosity sensitive control valve shall be provided which will bypass oil back to the oil tank during cold starting and hence aid engine oil warmup. The cooler shall be capable of heat rejection as follows:

Oil in Flow ppm	Temp. ° F	Fuel in Flow ppm	Temp. ° F	Heat Rejection Btu/min
45	240	80	200	1,850

Oil Supply Temperature Tap

An oil supply pressure tap shall be provided to indicate pressure differential across the lube nozzles. The oil pressure shall be 45 $\pm$ 10 psi with an oil flow of 6 gpm at 150° F.

Main Shaft Bearings

Considerable attention has been paid to the design of the main shaft bearings. Detail calculations utilizing the RECAP computer analysis method and other analytical techniques have been made to determine fatigue life and proper lubrication.

The fatigue life of the bearing was determined from a detailed load analysis taking into account the bearing capacity and the detailed geometry of the bearing. This information was applied to an advanced digital computer program and the life was determined. The results were modified by a factor of 5 for M50 material.

The following table shows the bearing life for the Integral Lift Fan engines.

Position	Material	Bore mm	DN	Capacity lb.	Life Hours
L. P. Thrust	Ausformed M50	545	2.6	16,180	15,416
H. P. Thrust	Ausformed M50	165*	1.98	11,362	15,930
Intershaft	M50	60	0.75	5,353	23,775
L. P. Roller	M50	60	0.25	5,353	87,800

* Counter rotating.

Critical Speeds

The rotor assemblies of these engines are close-coupled-rigidly mounted designs. The link between the No. 1 bearing and the No. 4 bearings is further stiffened by the truss type main frame. Preliminary estimates indicate criticals well above 120% max. design speeds.

Seals

Labyrinth seals are used throughout the Integral Life Fan engines. Labyrinth seals were selected because of the large diameter and high surface speed of the seal adjacent to the thrust bearings. This type of seal has been used extensively and successfully on the J47, TF39 and CF6 engines. The low flight speed and altitude where the Integral Lift Fan engines will be used assumes cool air for seal pressurization without the hazard of oil coking. Labyrinth seals have provided dependable wear free systems when used with adequately vented sumps.

CONTROLS AND ACCESSORIES DESIGN

Introduction

The control system selected for the Integral Lift Fan utilizes the most advanced components and logic presently available consistent with engine requirements. An air turbine driven fuel pump was selected as the fuel supply to eliminate the need for a radial driveshaft and gearbox; and all required

computation is done electronically with fuel at pump discharge pressure providing the hydraulic power.

Major Assumptions

- Fuel pump sized for 4500 pph normal steady state flow at ΔP of 450 psid. Additional flow requirements (stator, pump servo, cold day and transient thrust, and accel flows) bring this total to 7500 pph.
- Oil heat exhanger required.
- Ignition power and logic supplied by the cruise engine.
- Air impingement starting.
- All air and fuel piping assumed to be AMS 321 for purposes of weight estimates.
- Electronic computer and cables located in an environment which never exceeds 200° F.
- Air turbine supplied by cruise engine or APM during start and accel to idle.

System Description

As can be seen from the schematic in Figure 97, the control system consists of an air turbine driven fuel pump and alternator, an electronic computer, various air and fuel valves, and engine sensors.

The air turbine is driven by cruise engine CDP or APM air during lift engine starting and acceleration to idle; at idle, the shutoff valve is closed and lift engine CDP air is used. Check valves are located, as shown in each supply line to prevent reverse flow from cruise engine CDP to lift engine CDP or vice versa.

The quantity of air supplied to the air turbine is controlled by an air valve which is positioned by a fuel driven actuator. The fuel actuator is

positioned by a torque motor servo valve which ports pump discharge pressure to the appropriate side of the actuator piston. Controlling the airflow in this manner allows fuel pump speed to be controlled.

The fuel pump is a positive displacement vane pump. Therefore, by controlling pump speed, fuel flow is actually being controlled. A pressurizing valve is located at the pump discharge to minimize fuel pressure variation so that the torque motor servo valves operate with small pressure gain changes.

A second solenoid valve is mounted on the pump package to position the lift engine variable stators. This valve operates as does the previous one, fluid is ported to the head side or rod side of the stator actuators depending upon the direction of desired stator motion.

The alternator, which is located on the opposite side of the air turbine from the pump, provides electrical power for the electronic computer and also provides a pump speed signal for control use.

The electronic computer provides the speed governing, core speed limiting and maximum fuel scheduling logic based upon the indicated sensor inputs and the power level position.

An Oil/Fuel Heat Exchanger capable of removing 2460 Btu/min is required. Based upon an 8 gpm oil flow with a 350° F maximum temperature and 4500 pph fuel flow with an inlet temperature of 120° F, an 8 lb. heat exchanger is required. The dimensions are 2.5 inches diameter by 10 inches length.

The control block diagram is shown in Figure 98. The power lever demands corrected fan speed through the throttle schedule. A speed error signal is then formed by subcontracting actual corrected speed which is computed using outputs from the T_2 and N_f sensors. This fan speed error then enters the proportional plus integral governor which sets the fuel demand. The fuel flow feedback is subtracted from the fuel demand, and this error signal is basically the torque motor current drive of the servo valve. The servo valve flow positions the fuel actuator which positions the air valve which, in turn, sets pump speed. As mentioned earlier, pump speed is almost exactly proportional to fuel flow. Pump leakage distorts this proportionality only slightly.

Overrides on corrected fan speed error are provided to limit core speed. This operates by decreasing the error signal as the limit is approached and thereby decreasing fuel demand. A further override on W_f demand is provided by the acceleration schedule, which protects the engine against stall. This schedule is a typical W_f/P_{S3} limit except that T_{2C} (compressor inlet temperatue) is calculated from corrected fan speed instead of sensed, as is usually done.

The stator schedule is two position, the position depending upon core speed. An error is generated as in the fuel loop and a solenoid valve drives the stator actuator.

Component Description

Air Turbine

The air turbine is a single-stage axial flow device with a blade center-line diameter of 4.75 inches. The blade height is 0.21 inches and there are 31 blades. The air supply line is 1.25 inches diameter. A graph of the airflow required is shown in Figure 99, also shown there are the speed and torque requirements.

Fuel Pump

The fuel pump is a constant displacement vane pump which is also used as the metering valve by varying its speed. Its maximum speed capability is 8000 rpm and its flow capability is 21 gpm. Pump displacement is 0.6 cubic inch/rev. It appears that a reasonable pressure rise is 450 psid. The inlet fuel line size is 1.1 inches and the discharge is 0.5 inches. A fuel filter is not used in the fuel system since none of the components are dirt sensitive.

Alternator

The alternator package is 2.7 x 4.4 inches diameter. The diameter is slightly larger than normal since the drive speed is less than one third normal. The alternator provides a pump speed signal and power to the electronic control. It has been assumed that ignition power and logic are supplied by the cruise engine.

Pump-Turbine-Alternator Package

A cross-sectional drawing of this concept as applied to the Integral Lift Fan is shown in Figure 100.

Electronic Computer

The electronic computer will probably utilize analog devices with digital three dimensional schedules. The box which houses the electronics is 9.5 x 8.0 x 3.5 inches; it has been EMC (electron-magnetic compatibility) protected according to Military Standard procedures. The P_{S3} sensor is also located inside the electrical box and pressure piped to it. The electrical loads are single armor shielded flexible cables with teflon covering. Redundant leads are provided for power, T_2, N_c, N_f, and both torque motor servo valve demand currents. It has been assumed that the control is located in an ambient that never exceeds 200° F.

Torque Motor Servo Valve

This is a two-stage valve - the first stage is a jet pipe and the second is a four-way valve. Operationally, the jet pipe is rotated by the torque motor current, the more the current the more the rotational. This positions the second stage which ports high pressure supply fluid to the proper side of the load actuator.

Air Valve

This valve is basically a plug-type valve which is capable of completely shutting off the flow (except for leakage). At its largest diameter, it is 1.375 inches in diameter.

Air Valve Actuator

This fuel actuator is attached to the air valve so that positioning the actuator positions the valve. This actuator has a piston diameter of 1.0 inch and a stroke of 0.75 inch.

Air Check Valve

This valve is a typical butterfly type check valve which allows flow in one direction only.

Compressor Discharge Pressure Sensor

The P_{S3} sensor is a strain gage type requiring electrical excitation. The sensor is about 1.0 inch in diameter by 1.8 inches long excluding the pressure fitting and the electrical connector.

Core Speed Sensor

This sensor is an eddy current device which mounts on the casing at the compressor blade tip. As the blade passes, it completes an electrical circuit and current flows. In this manner, the number of blades passing can be counted. The sensor requires electrical excitation.

Fan Speed Sensor

This sensor is a magnetic sensor mounted in the bearing sump. It senses the passing of a notch on an area of rotating fan structure.

Engine Inlet Temperature Sensor

This is a resistance temperature device (RTD); its electrical resistance changes with temperature, providing T_2 indication to the control. A drawing of this component has been previously supplied.

Pressurizing Valve

This valve is a normally closed single-piston fuel valve which maintains pump discharge pressure above a design point value. Previous engines have set this pressure at 200 psi. The purpose of the valve is to maintain servo pressure under low flow conditions.

Stator Actuators

These actuators are double acting linear hydraulic actuators which position the stators. Fuel is used as the hydraulic fluid. The actuator piping consists of head, rod, and drain lines 0.25 inches in diameter.

Fuel Manifold and Valves

The fuel manifold is an 0.375 inch diameter tube. The fuel manifold valves serve the function of maintaining a full manifold and providing even flow distribution to each burner cup. There are 20 valves, each 1.0 inch in diameter and 2.25 inches long.

Ignition System

The system is completely redundant, using two exciters, two high voltage leads and two igniters. Input 115 Volt, 400 Hertz power supplied by the airframe through two separate cables.

Each exciter, lead, igniter combination would supply the following spark parameters:

Output spark energy (Lead and igniter attached)	-	1.0 Joule Min.
Output Peak Watts	-	100,000 min.
Output Spark Duration	-	30 microseconds min.
Output Spark Current	-	1500 amps min.
Output Spark Rate Per Second	-	2.0 $\pm$ .5 at 115 V 400 Hz

Packaging

All controls, plus the dual ignition exciters and engine oil tank are remotely mounted in a fireproof steel case. A schematic of this arrangement is shown on Figure 101. The dimensions of this case are 22-1/2 x 7 x 11 inches. It is constructed of a .050-inch, 321 stainless steel material.

Turbine Inlet Temperature

At the outset of the design, use of a T_4 pyrometer had been planned for use as a control input and as a cockpit instrument readout. The pyrometer has been removed from the system since the engine overates with no bleed or horsepower extraction and over a relatively small flight envelope. Because of this, the primary control input, fan speed, is very tightly tied to turbine inlet temperature, and no control input of an independent temperature input is required. Of course, no cockpit readout is available, it is questioned how the pilot could monitor the large number of instruments which go with 8 to 12 lift-engines. If it is subsequently determined that cockpit readout is absolutely required, a thermocouple harness can be added somewhere in the low pressure turbine system with the attendant weight and cost penalty.

Low Idle Emissions

While the basic carbureting combustor provides good low visible smoke characteristics at takeoff power, some consideration was given to the problem of idle emissions. A detailed study of methods of achieving reduced emissions in integral lift engines is currently underway in NAS 14406 Task IV, but for purposes of the present design a system was selected for using every other fuel nozzle during idle operation. This is achieved by replacing the spring in alternate valves with one having a larger spring rate. The low emission idle point would open the valves with the light spring, and as speed is increased to the "flight idle" point, the second set of valves would open. This scheme would involve no additional hardware and, very likely, negligible switching transients.

TASK III

ENGINE SERVICE REQUIREMENTS

Commercial Aircraft Requirements

Engines are designed to meet all existing FAR airworthiness standards, Parts 25 and Parts 33 with advisory circulars. The following features assure meeting commerical standards.

Fire Safety

- Controls remote mounted in fireproof steel case.
- Fireproof steel case around combustion section.
- Shrouded fuel manifold in fire zones.
- Automatic drain for combustion system.

Containment

- 2 tip chord lengths of AMS 3041 material
- Continuous tip shroud

Ignition System

- Dual ignitors
- Dual leads
- Dual ignition exciters

Postulated VTOL Mission

45.0 minutes total duration including; 37.5 minutes climb cruise and descent conventional flight mode (83.3%), and 7.5 minutes VTOL combined with ground operation (16.7%).

VTOL and ground operation:

Start-up taxi and checks	3.5 minutes (46.7%)
Takeoff	1.0 minutes (13.3%)
Landing	3.0 minutes (40.0%)
Total	7.5 minutes (100%)

Engine Service Life

Ultimate Life - The engine total useful life shall be 5000 engine operating hours achieved in 30,000 aircraft hours over ten years. The engine will encounter 80,000 stop-start cycles during its ten years of service.

Stationary Components

	Service Life per Installation		Total Service Life	
	Hrs.	Cycles	Hrs.	Cycles
Casings	5000	80,000	5000	80,000
Frames	5000	80,000	5000	80,000
Combustor	1250	20,000	2500	40,000
HPT Vanes	1250	20,000	2500	40,000
LPT Vanes	1250	20,000	2500	40,000
Suppression Panels	5000	80,000	5000	80,000

Rotating Components

	Service Life per Installation		Total Service Life	
	Hrs.	Cycles	Hrs.	Cycles
Fan Blades	2500	40,000	5000	80,000
Fan Disc, Spacers & Shafts	3000	48,000	5000	---
Comp. Blades	2500	40,000	5000	---
Comp. Disc, Spacers & Shaft	3000	48,000	5000	---
HPT Blades	1250	20,000	2500	40,000
HPT, Disc Spacers & Shafts	3000	48,000	5000	80,000
Main Bearings	1500	24,000	3000	40,000
Seals	2500	40,000	5000	80,000

Controls & Accessories Components

Service Life per Installation		Total Service Life	
Hrs.	Cycles	Hrs.	Cycles
1250	40,000	5000	80,000

Note:

Heavy maintenance check scheduled every 1000 hr. (6000 flight hours)

1. Inspect and/or replace main bearings.
2. Repair and/or replace combustor.
3. Repair and/or replace HPT.

Design Life Objectives

	Cold Parts	Hot Parts
Service Life per Installation, engine hours	2500	1250
Stop-Start cycles per Installation	40,000	10,000
Total Service Life, Engine hours	5000	2500
Stop-Start Cycles Total	80,000	20,000

Duty Cycle

START-UP, TAXI, & CHECK OUT

Time = 2330 hours = 46.7% of engine total service life

Level of Vehicle control applied	Max.	Neutral	Min.
Time - hours of engine total service life	466	1398	466
% of engine total service life (The engine total service life in 5000 hrs.)	9.35	28.0	9.35
Thrust - lbs.	11900	9500	7030
% of design thrust	95	76	56

Vertical Landing

Time - 2000 hours = 46.7% of engine total service life

Level of Vehicle control applied	Max.	Neutral	Min.
Time - hours of engine total service life	400	1200	400
% of engine total service life	8	24	8
Thrust - lbs.	11,900	9500	7030
% of design thrust	95	76	56

Vertical Takeoff - Normal Operation

Time = 665 hours = 13.3% of engine total service life

Level of Vehicle control applied	Max.	Neutral	Min.
Time - hours of engine total service life	133	399	133
% of engine total service life	2.66	7.95	2.66
Thrust - lbs.	12,500	10,000	7500
% of design thrust	100	80	60

Vertical Takeoff - One Engine Out

Time = 5 hours = 0.1% of engine total service life

Level of Vehicle control applied	Max.	Neutral	Min.
Time - hours of engine total service life	5	0	0
% of engine total service life	0.1	0	0
Thrust - lbs.	13,000	11,600	10,200
% of design thrust	102	---	---

Climb Cruise & Descent

Engine inoperative but there may be some rotation of engine.

Time = 25,000 hours of aircraft operation

Maneuver Loads

A. Definitions

1. Inertia Load Factors (g's)

Aircraft linear accelerations develop inertia forces acting at the fan center of mass and also each component center of mass, and are reacted by respective support structure. Magnitudes of the maneuver loads are in g's or number of 32.18 feet per second^2 units. Forces developed should be computed using maximum weight; i.e., target weights plus contingencies.

2. Gyroscopic Precession Rates

These are angular velocity displacements of the rotor axis producing rotor inertia torque loading which is reacted by a couple force through the bearings and fan mount structure.

3. Angular Acceleration Factors

These angular accelerations apply to the fan mass system and produce inertia torque loading which is reacted by a couple force through the bearings and fan mount structure.

B. Low Cycle and Thermal Fatigue

The engine shall be capable of a minimum of 80,000 start-stop cycles (see Life requirements).

C. Application of Load Requirements

Three basic levels of maneuver requirements are to be used in the engine design. In each case, they shall be applied in accordance with the duty cycle and rotor speed table previously referenced. In other words, where life criteria are involved in such design factors as creep, fatigue, and stress rupture, the loads shall be determined and pro-rated according to the rotor speed and percent life defined.

1. Steady Maneuver

Figure 102 defines maneuver requirements which should be considered as continuously applied. These levels are sufficient to account for all normal

engine powered flight except landing. Figure 103 defines the special case of vertical landing and shall be considered applied at the rate of one each 0.1 hour of operation for a duration of five seconds each occurrence. The unpowered flight maneuver requirements are defined in Figure 104.

2. Frequent Maneuver

Figure 105 maneuver requirements shall be considered to occur at the rate of once each hour for a duration of 15 seconds each occurrence. Goodman diagrams used in determination of alternating stress limits shall be based on 10^7 cycles (high cycle fatigue design criteria).

3. Infrequent Maneuver

Figure 106 defines maneuver requirements which shall be considered to occur at the rate of once each 100 hours for the duration of 15 seconds each occurrance. Goodman diagrams used in determining alternating stress limits for this maneuver requirement shall be based on 10^5 cycles. Nominal rotating-to-static part clearances shall be based on this maneuver requirement. Nominal clearance is based on assembly stack-up with probability theory applied. It is not the worst combination of parts. Objective nominal clearance at this maneuver condition shall be zero unless limited by Ultimate Maneuver Requirements.

4. Ultimate Maneuver

The engine shall be designed to withstand an ultimate procession velocity of 2 radians per second in roll and 1 radian per second in pitch in combination with a vertical and side load factor of $\pm$ without rupture, burst or other catastrophic failure.

The frequency of occurrance will be one in the life of the fan and no accumulated time or cycles shall be considered. Negative clearance (rotor-stator rubbing interference), yield and other permanent deformation shall be permitted, providing the fan shall be capable of operating (with impaired performance) up to 90% rpm for at least 30 seconds with the Steady Maneuver Requirement envelope. the fan shall then be removed from service for repair or salvage.

The degree to which this maneuver requirement is factored into the determination of nominal rotating-static part clearance cannot be precisely defined. As a guide, the following are permissible:

- Complete destruction of air seals including physical loss of rotating and static components thereof.
- Loss of portions or damage to turbine airfoils.
- Zero nominal clearance between bucket airfoil leading edge and nozzle trailing edge.

Other Engine Service Considerations

Climatic and Environmental Conditions

The engine is to be designed to operate at the following temperatures and altitudes:

Temperature	-65 to -130° F
Altitude	0 to 10,000 feet

Vibration

Loading resulting from vibrations, when combined with operating maneuver loads, shall not exceed the maximum maneuver loading.

Anti-Icing

The engine shall meet the requirements of FAR Part 33 and FAR Part 25. The engine shall meet this requirement without use of special in-flight operating procedures.

Rotor Speeds

FAA certification requirements require a five (5) minute demonstration at 115% of the maximum rated speed at maximum rated temperature.

ACOUSTIC DESIGN CONSIDERATIONS

Component Analysis

Task I had been directed towards comparison of cycle variations and the definition of engine components which were critical to the overall noise. From

Task I, the critical components were defined as the fan and turbine turbomachinery noise along with the basic jet noise floor produced by the fan and turbin exhaust. Once the specific engine cycles and corresponding fan pressure ratios were selected, the acoustic analysis was directed to evaluating these component designs.

To achieve the acoustic objectives, the components were designed to have minimum noise at the source then supplemented with extensive acoustic treatment to suppress noise after it is generated. The following reviews the prediction technique, the component acoustic features, and the acoustic treatment design for the three selected cycles: (1) 1.25 fan P/P, (2) 1.20 fan P/P, and (3) 1.2 fan P/P with fan tip speed below 900 ft/sec.

Component Prediction Technique

The integral lift fans have several component noise sources which must be evaluated to obtain the total engine noise. Each of these components or noise sources were evaluated separately during the detailed design and individual noise spectra defined which were then added together to arrive at the total noise spectrum. As component suppression methods were defined, the suppression levels were applied to the particular spectra affected as a function of frequency. These modified spectra were then summed to obtain the suppressed engine noise levels.

As with any prediction method there is a degree of uncertainty involved in the estimated noise levels. General Electric has found the prediction technique used for this program to be a good simulation of high bypass ratio turbofan noise. Generally comparisons of measured and predicted PNdB levels using this program have been within a $\pm$ dB band of accuracy. The following summarizes the methods for predicting the noise constituents:

Fan

This is a major noise source in the ILF and is made up of a pure tone at the blade passing frequency and broadband noise. The pure tone level is predicted analytically from the physical and aerodynamic fan characteristics

and is based on the interaction of the fan rotor wakes with the outlet guide vanes. Directivity patterns for the pure tone are based on full scale measured levels.

The broadband noise is based on full scale measurements correlated with rotor tip relative Mach number for level and tip physical Mach number for directivity.

The effect of crossflow on the fan generated noise was not included in the acoustic analysis since it was assumed the aircraft to be moving vertically with no forward motion. These crossflow effects become significant as inlet performance deteriorates and inlet turbulence increases. Increases in noise on the order of 5 dB have been measured in wind tunnel tests of fans. these effects, however, should be evaluated on the basis of aircraft noise footprints using the aircraft operating characteristics.

Fan Jet

NASA large scale fan and GE scale model cold jet data were used to define a level of overall sound pressure level as a function of jet velocity. This curve was approximately 5 dB below the corresponding SAE jet noise line extrapolated to velocities below 1000 ft/sec. The SAE flight spectrum shape was used along with GE cold jet directivity indices to define the noise at each angle. As with the fan noise, no crossflow effects were included although measured noise from jets in crossflow have indicated spectral and level variations. These types of effects should be evaluated in accordance with aircraft operating characteristics for the particular engine installation being considered.

Turbine Jet

The SAE jet noise curves were extrapolated to velocities below 1000 ft/sec for the hot turbine jet predictions. As with the cold fan jet, the SAE spectrum and GE directivity indices were used to define the noise at each angle. Cross-flow effects were not included in the prediction.

Turbine

A pure tone level is defined using the same type rotor-stator interaction as used in the fan noise analysis. The directivity indices are based on full scale engine data. The associated broadband noise was also estimated from full scale engine data.

Component Acoustic Features

The Task I results had shown the jet floor to be dependent upon the extraction ratio, turbine jet velocity/fan jet velocity. This ratio was established on acoustic terms to keep the jet floor approximately 10 PNdB below the objective noise level of the total system. With this amount of difference the jet noise floor will add very little to the total noise.

The noise generated by both the 1.2 and 1.25 fan pressure ratio configurations were designed with large spacing between the rotor and OGV which decreases the fan puretone or blade passing frequency. Tip speed was set primarily on the basis of aerodynamic considerations since acoustically tip speed has a balancing effect of fan noise for constant fan geometry. If tip speed decreases, the broadband generated noise goes down while the puretone noise increases. The opposite occurs as tip speed increases. As a result of one noise source increasing while the other decreases, the PNdB is expected to stay in a very narrow band over a range of tip speeds on the order of $\pm$ 10%. As will be seen for the low tip speed ILF2A2 configuration, changes in balde number and spacing resulting from the reduction in tip speed were critical.

One of the prime variables in the deisgn was rotor blade number. Acoustically, it would be desirable to use as large a number of blades as possible to keep the fan noise in the high frequency range beyond the heavily weighted portion of the PNdB spectrum. The mechanical system design considerations, however, even with use of a tip shroud, resulted in relatively low blade numbers which put the fan blade passing frequency in the weighted region (3150 kc). This was not a major problem for the integral lift fan, however, since a sufficient length was available in the fan exhaust duct to suppress the fan noise significantly.

For the selected number of rotor blades, the number of outlet guide vanes was chosen to provide a ratio of 2.0, 1.67 and 1.95 for the ILF1A1, ILF2A1 and ILF2A2 respectively. This combination of rotor and OGV blade numbers is consistent with minimizing the noise generated by the rotor OGV interaction.

Serrated leading edges have shown promise as an effective means of reducing inlet radiated fan noise. For the integral lift fan designs, it is important to utilize this type of rotor blade design to reduce the inlet radiated noise seen in the aft quadrant. As discussed in the Task I analysis, the inlet noise is assumed to be 10 dB less than the exhaust noise in the aft quadrant. As the exhaust noise is reduced by large spacing, OGV number and acoustic splitters, the inlet noise must also be reduced to keep it below or at the same level as the exhaust radiated noise. For the study, it was assumed the serrated leading edge would provide 4 dB inlet noise reduction. Serrated leading edge designs are still being evaluated, however, and a specific design will be deferred until more research, both empirical and analytical, has been completed.

Acoustic design criteria for the turbine were limited to keeping the blade passing frequency as high as possible. This was achieved by using the maximum number of blades on each stage that was mechanically acceptable. By putting the turbine blade passing frequency as high as possible, it kept the PNdB weighting effect to a minimum. the resulting turbine noise was still a major contribution to the overall noise and required acoustically treated splitters to reduce it to an acceptable level.

Reducing the 1.2 fan pressure ratio design tip speed for the ILF2A2 affected the acoustic characteristics in several ways. Primarily, the unsuppressed fan noise increased as a result of increased blade loading with the lower tip speed. The rotor blade number decreased from 48 to 36 due to mechanical design criteria which with constant solidity increased the rotor chord length. Since the rotor chord was longer, the spacing between rotor and OGV decreased which also increased the fan noise. A benefit was obtained at the lower tip speed/blade number combination since

the pure tone moved to a lower frequency with lower PNdB weighting. This was offset by the factors increasing noise, however, and the net result was 2.6 PNdB higher unsuppressed fan noise.

Turbine noise for the ILF2A2 increased slightly, 1.3 PNdB due to lower tip speed or rpm which shifted the turbine noise to a lower more heavily weighted portion of the spectrum. The number of stages and blades also changed with associated changes in the noise generated. With the same turbine exhaust splitter design, the suppressed turbine level was also 1.3 PNdB higher but this did not seriously affect the total engine suppressed noise level.

With the jet noise remaining constant, since the low tip speed and high tip speed core cycles are essentially identical with the lower tip speed configuration, the overall noise decreased slightly by 0.8 PNdB.

Acoustic Treatment Design

Both the fan and turbine required acoustically treated splitters to reduce the noise to the objective levels. Each component was evaluated unsuppressed and a spectrum defined which contained both the broadband and puretone noise. The splitter number and length were then selected and a suppression spectrum calculated and applied to the component spectra. The suppressed spectra were then combined with the other noise sources to determine the overall noise. The splitter thickness was set at 3/4 inches for the fan duct in order to obtain sufficiency band width for large suppression levels. These splitters were particularly effective in reducing the fan noise since the fan noise and max. PNdB weighting coincided. For cases where the max. noise and max. PNdB weighting area are separated, the band width must be wide enough to cover both areas.

For the ILF2A2 the fan suppression due to duct splitters increased by 2 dB as a result of the lower frequency fan noise. This is seen on Figure 14 where the lower values of H/λ provide more suppression. The turbine exhaust splitters were set at 1/2-inch thickness due to the high frequency turbine noise to be suppressed. Since the turbine noise affects only a narrow portion of the spectrum, the suppressors band width obtainable with 1/2-inch splitter was adequate.

The fan and turbine exhaust splitters designs are described on Table XXVII. These designs are based on calculated suppression spectra as well as estimated unsuppressed spectra. In a design and build study, it would be desirable to test different splitter designs with regard to covering, thickness and flow effects. The assumed basic values of thickness and length should be sufficiently accurate to allow tuning of the design to achieve the desired suppression.

ENGINE ACOUSTIC ANALYSIS

Objectives

Total system noise was evaluated at the following conditions:

- 12 engines
- 80% thrust at T/O (10,000 lbs.)
- 90° F Day
- 500 ft. sideline

These conditions are referred to as the "Noise Rating Point" (NRP). As a result of the revised requirements given at the end of Task I (See page 23); the following new objectives were established:

Fan Design P/P	NRP Level
1.20	95
1.25	98

After the engine design was established, the total noise was predicted using an advanced 3 dimensional computer program which evaluates vertical takeoff from the ground or runway, and predicts the noise at any point on the ground. For all the noise estimates presented, the takeoff is vertical with no movement down the runway.

Figures 107, 108 and 109 show the PNdB versus takeoff altitude for the ILF1A1, ILF2A1 and ILF2A2 respectively. Altitude represents the vertical distance at the point of lift-off, i.e., no movement down the runway.

VTO Profiles

The 1.2 fan pressure ratio configurations are essentially at the objective level of 95 PNdB. The 1.25 fan pressure ratio configuration is below the objective level of 98 PNdB. This configuration could also meet 95 PNdB by lengthening the fan exhaust duct splitters by 3 inches and introducing more inlet suppression, about 2 PNdB.

Each configuration noise level peaks at about 280 ft. altitude which corresponds to an acoustic angle between the source and maximum sideline noise at the noise measuring point of approximately 120° as shown on Figure 13.

Figure 110 shows PNdB levels for the ILF1A1, ILF2A1, and ILF2A2 as a function of thrust. The Noise Rating Point conditions were used with the exception of varying engine power setting. Note that there are cross-over points for the three designs. These occur as the spectra change with decreasing rpm or thrust and the splitter suppression effectivenss changes. The maximum noise for each configuration is approximately 5 PNdB higher than the NRP level. Thus, at max. control condition, the aircraft could possibly be designed to be under 100 PNdB, assuming all configurations could meet the 95 PNdB level after installation design effects are included.

Constituent Levels

Table XXVIII lists the noise constituents for each cycle configuration. As a result of keeping the extraction ratio V_8/V_{28} as low as possible, the fan and core jet noise levels are essentially balanced. With exhaust splitters, the turbine noise has also been reduced to a level consistent with the jet noise. The sum of the jet and turbine noise represents the floor or minimum noise obtainable for the cycles selected. The fan noise has been reduced to the point that the floor is adding approximately 1.5 to 3.0 PNdB to the overall noise. As the fan is suppressed further, this adder will increase thus decreasing the effectiveness of the fan suppression. Note that it is possible for the sum of the two noise sources to increase more than 3 PNdB which is the ideal increase for two equal noise sources. This is a result of adding the spectra for each source thus changing the overall spectrum shape which after being weighted for PNdB could give more than 3 PNdB increase.

Constituents Suppression

Suppression was applied to both the inlet and exhaust sides of the fan. This is shown graphically in Figures 111, 112, and 113 along with the jet plus turbine noise floor and the resulting total noise.

On the exhaust side of the fan, the basic noise generated was assumed reduced by 5 PNdB due to advanced source reduction techniques. This is the same assumption utilized and discussed in Task I. Exhaust duct splitters were then used to bring the aft radiated noise to point A on Figures 111, 112, and 113.

As discussed previously, the inlet noise was assumed to be 10 dB below the exhaust noise. Next, the 5 PNdB source reduction was assumed to affect the inlet as well as exhaust radiated noise. Since serrated leading edges on rotor blades had been found to be effective in reducing inlet noise, they were included in the design and brought the inlet radiated noise level to point B^1 on Figures 111, 112, and 113. Further inlet noise reduction was assumed to bring the level to point B which is equal to the radiated noise, point A. This reduction will be the result of installation design studies where inlet doors, vanes, etc., will be acoustically treated to obtain the desired suppression. Figure 114 shows the level of inlet suppression that will be required depending on the other assumptions made for inlet noise reduction. The arrows on Figure 114 represents the assumed levels of inlet reduction of Figures 111, 112 and 113. The range of variation in each assumption is shown by the cross-hatched areas. Examples of the use of this figure are given below.

If serrated blades provide 5 PNdB reduction, advanced source reduction 5 PNdB and the assumed split between exhaust and inlet radiated noise is increased to 15 PNdB then no inlet treatment will be required. If serrations provide only 3 PNdB reduction, advanced source reduction 2 PNdB and the assumed difference remains at 10 PNdB then as much as 9 PNdB reduction will be required from inlet treatment.

ENGINE PERFORMANCE CHARACTERISTICS

Computer Representation

Tapes were generated for the three engines using the standard General Electric cycle system. Complete fan, compressor, and turbine maps are represented, while combustor, ducts, struts, and nozzles are described in equation or curve form. A customer format lists the following parameters:

ID	Identification Point Number
ALT	Altitude - feet
M_o	Flight Mach No.
VOKNOT	Flight Velocity Knots
P_o	Ambient Pressure psia
T_o	Ambient Temperature ° R
ETAR	Ram Recovery
P_2	Fan Face Total Pressure psia
T_2	Fan Face Total Temperature ° R
ALPHA	Thrust Vector Angle Relative to Vertical (+ is aft)
W_o	Total Inlet Airflow lb/sec
WFAN	Fan Duct Inlet Airflow lb/sec
BETA	Bypass Ratio
PCNFK	Fan Corrected % rpm
FGV	Vertical Gross Thrust Component - lbs.
FGH	Horizontal Gross Thrust Component - lbs.
FG	Resultant Gross Thrust - lbs.
FD	Ram Drag (W_oV_o/g) lbs.
PCNF	Fan % rpm
V_8	Core Duct Exit Velocity ft/sec
V_{28}	Fan Duct Exit Velocity ft/sec

F_N	Net Thrust lb. (arbitrarily defined as $T_g - F_D$)
WFM	Fuel Flow lb/hr
SFC	Specific Fuel Consumption lb/hr/lb (arbitrarily defined as WFM/F_N

The above parameters are those commonly used by airframe companies during preliminary design work and do not represent any departure from past practice except for the definitions of net thrust and specific fuel consumption as noted above. A three percent margin is used in WFM and SFC at all conditions.

At flight speeds other than zero, with an engine having vectored thrust capability there arises the question of what is considered inlet drag and what is considered ram drag and additive drag. The present definitions used here allow the inlet designer to apply any bookkeeping system he desires in converting gross thrust to net propulsive effort.

Typical Results - Uninstalled

Uninstalled performance is shown in Figures 115, 116, and 117. No bleed or customer power extraction (none are available) are used and ram recovery is set equal to 1.0. Figure 115 presents uninstalled thrust as a function of corrected fan speed at sea level static conditions on a 90° F day.

These engines are flat rated to 90° F for the maximum thrust rating of 12,500 lbs. This means that the 12,500 lb. rating can be reached on days up to 90° F without exceeding the turbine inlet design temperature. When operated at ambient temperatures less than 90° F, a substantial reduction in turbine inlet temperature results. This effect of T_0 on T_4 is shown on Figure 116. The difference between standard day and 90° F day turbine inlet temperature is about 150° F.

Uninstalled specific fuel consumption is shown as a function of uninstalled net thrust on Figure 117. The similarity between the engines is not intentional, but a result of the combinations of fan pressure ratio, turbine inlet temperature, and core pressure ratio that were chosen for the design.

Fan speed/flow characteristics for the engines are shown on Figure 118.

The performance data presented are valid over the desired range of 80% to 150% of the engine design thrust of 12,500 lbs. Scaling effects over this span are judged to be negligible relative to performance.

INSTALLATION AERODYNAMICS AND ENGINE STABILITY

Configuration Selection

The desire to investigate potential installation aerodynamic and crossflow effects necessitated the establishment of engine inlet distortion and recovery objectives against which to evaluate engine performance. This work is intended only to show typical effects of an assumed installation having the assigned characteristics, which are reasonable based on the limited information available for this type of installation. As an actual design evolves during airframe/engine integration in an actual development program, substantial testing, static, wind tunnel, and full scale would be required to assure an adequate design.

The assumed configuration has the following features:

- 6 engine pod
- Gimbaled engine (-15° through +45°)
- Synchronized vector angle
- 120°/second slew rate on vectoring
- Hydraulic actuation
- Upper and lower double hinged doors
- Engine inlet bellmouth radius varies (radius/fan tip diameter 0.15 - 0.2)

Three views of the pod incorporating these features are shown on Figure 119. Inlet and exhaust doors in the open, closed, and transition modes are shown on Figure 120. Details of the inlet and exhaust doors are shown in Figures 121 and 122. Figure 123 shows a typical airplane using an installation concept of this type.

Inlet Characteristics

Inlet recovery and distortion parameter objectives for the worst engine in the pod (usually the first or last) are presented as a function of inlet velocity ratio (freestream velocity/fan inlet velocity) and engine vector angle. Figure 124 shows inlet recovery, P_{T2}/P_{T0}; while Figure 125 shows distortion parameter, $(P_{Tmax.} - P_{Tmin.})/P_{Tavg}$. Reference lines on both of these curves show extremes which might be encountered over a wide range of engine power settings at the maximum envelope velocity of 200 knots. The effect of power setting on crossflow velocity ratio is further explored on Figure 126. Inspection of these figures will reveal that at normal takeoff power settings inlet recovery and distortion should pose no serious problem.

Method of Distortion Representation

The distortion effects described above manifest themselves in changes in fan and compressor stall margin, airflow, and adiabatic efficiency. Scale factors for these changes are generated for use in modifying the fan and compressor map characteristics as shown on Figure 127. Crosswind distortion effect curves used in generating "installed" performance data are shown on Figures 128 and 129.

Effect on Performance

Uninstalled performance is generated with a ram recovery of 1.0, and no distortion effect superimposed on the basic component maps. Installed data is generated with ram recovery from Figure 124 and fan and compressor map modifiers generated by the procedure as described above. No customer bleed or power extraction is included in either case since the engine has no provision for these.

A simple way to obtain an insight into potential installation effects is to compare installed and uninstalled performance along a typical takeoff trajectory. A typical trajectory is postulated on Figures 130 and 131. This trajectory is based in part on the experiences of Dornier in operating

the DO.31 VTOL airplane. Power setting, altitude, thrust vector angle, and forward speed are presented as a function of distance from liftoff point. The trajectory chosen happens to be a minimum fuel trajectory, and it is recognized that a minimum noise trajectory may be different, but effect on performance should still be informative.

Four points are selected from along the trajectory, and % thrust is converted into fan corrected speed, the primary control input.

Corrected fan speed PCNFK	Altitude feet ALT	Thrust vector angle	Airspeed V_o	Distance from T/O
90%	0	+10°	0	0
90%	80	+37°	60 Kt	350 ft.
80%	100	+45°	80 Kt	650 ft.
65%	190	+45°	120 Kt	1500 ft.

Effect on gross resultant thrust, fan stall margin, and total corrected airflow are shown on Figures 132, 133, and 134 respectively. For the assumptions made, the installation effects, based on available information, do not seem to impose undue restraints on the engine design. This conclusion is reinforced by experience which has been obtained during the XV5A and DO.31 flight test programs. This is not to say, as previously discussed, that installation design and engine/aircraft integration are going to be simple. Substantial development component and systems testing are going to be required to achieve a satisfactory installation. The results of the present investigation indicate only that this should not present a barrier problem, but requires development of fan and compressor with adequate stall margin and distortion tolerance.

TRANSIENTS AND STARTING CHARACTERISTICS

Starting

Since the engine has bleed driven accessories and no requirement for customer power extraction, there is no engine gearbox and drive available for use with a conventional starter. The selected starting system is of

the air impingement type. A manifold above and between the high pressure turbine nozzle and rotor is pressurized with air which is directed through a series of small slot type nozzles toward the blades. The torque thus produced is sufficient to accelerate the engine to self sustaining fire speed providing sufficient air is available. Based on experience with this type of starter on one GEJ85 model, it is estimated that to achieve the following sequence of events, 1.5 lb/sec of starter air at 50 psia and 350° F would be required to bring the engine up to idle in 30 to 35 seconds.

% Core Speed	
15%	Fire
40%	Cutout
55%	Idle

Start time per engine could be cut to 20 to 25 seconds with an increase in starter air quantity to about 2.5 lb/sec. The starter air required could be supplied by either APU or from bleed from any cruise engines aboard the air vehicle.

The 55% idle core speed used in the starting time study was arbitrarily chosen as being representative. Actual idle speed will be determined in practice with an air vehicle designer, and will be a balance among several requirements:

- Idle Emissions - A low idle speed makes the treatment of idle emissions more difficult.
- Idle Thrust - A low idle thrust is probably desirable both in the air and on the ground so that starting the lift engines does not substantially alter the aircraft trim.
- Acceleration Time - Obviously rapid thrust response from idle to max. can be obtained if initial idle is high.

Engine Transient Response

Consideration was given to the thrust response characteristics of these engines. The statement of work required a 10% thrust increase within 0.3 seconds at fan corrected speeds above 60%. A limited study using an existing

dynamic model of a two-spool turbofan engine indicated the following thrust increase could be achieved within the 0.3 second time interval by a throttle burst from the indicated fan speed:

% Fan Speed	% Thrust Increase in 0.3 seconds
60	16
70	15
80	13
90	11

It should be cautioned that the 0.3 second is not a time constant in the usual sense, but a total elapsed time during a throttle burst. Engine time constants are expected to be approximately 0.16 to 0.2 seconds over a range of power settings. Additional work to more accurately and completely define the thrust response characteristic has been authorized by NASA and will be reported in the NAS 14406 final report.

As in many other system parameters, it is recognized that the airframe/propulsion system integration and overall air vehicle configuration will have a very strong effect on engine thrust response requirements. The present work is only a brief look to achieve some understanding of present capability and potential.

RESULTS

Engine Size, Weight, and Noise

Engine characteristics estimated in this study are summarized in the following table.

Engine	ILF1A1	ILF2A1	ILF2A2
Fn Flat Rated to 90° F	12,500	12,500	12,500
Fan Tip Diameter - in	57.1	60	60
Engine Max. Diameter - in.	69.8	74	74
Overall Length - in.	43.5	50.6	54.5
Overall Weight (with Treatment as shown in Fig.92) lb.	1050	1140	1250
Overall Weight (without Treament) lb.	980	1070	1170
Thrust/Weight Ratio, 90 ° Day	11.9	10.9	10
Volume - $ft.^3$	96	126	136
Frontal Area - $ft.^2$	21	26	28
PNdB @ 500' Sideline, 12 @ 10,000 lb. (assumes installation inlet noise suppression, see Figures 111, 112, 113)	96*	95	95
SFC	0.36	0.36	0.36

*Could be reduced to 95 with additional treatment (Δ 3" splitter length).

Engine cycle parameters are given below:

Engine	ILF1A1	ILF2A1	ILF2A2
Fan Pressure Ratio	1.25	1.20	1.20
Fan Tip Speed, Corrected	1180	1060	855
Hub Supercharger Pressure Ratio	1.048	1.048	1.029
Overall Pressure Ratio	10	7	7

T_4 - ° F	2500	2000	2000
V_8/V_{28}	1.3	1.3	1.3
Bypass Ratio	12.6	11.6	11.7

Engine Scale Factors

$$\text{Size} \sim (\text{Diameter/Base Diameter}) = (\text{Thrust/Base Thrust})^{1/2}$$

$$\text{Weight} \sim (\text{Weight/Base Weight}) = (\text{Thrust/Base Thrust})^{1.25}$$

DISCUSSION OF RESULTS

Noise Characteristics - Effect on Weight and Size

A major result of this study was the establishment of the compromises required to meet the stringent noise requirements. Most affected were engine weight and engine diameter. Many advanced technology features were applied with the aim of reducing the impact on weight and size; a shrouded graphite/epoxy fan, composite compressor blades and acoustic panels, a short highly loaded compressor using casing treatment, a reverse flow combustor, and a highly loaded fan turbine. The achievement of a thrust to weight ratio of twelve is encouraging in light of the following.

Results are based on a preliminary design of all components and includes a development weight adder. Thrust to weight ratio is quoted on a 90° F day. A substantial acoustic treatment weight is included.

On a basis of more typical comparison, no development adder, no acoustic treatment, and on a standard day non-flat rated thrust to weight ratio would be in the range of 14-1/2. This is a respectable figure for an engine with a design fan pressure ratio of 1.25, a level dictated by consideration of the need for low jet noise.

Engine Performance

Results of the Task I parametric study indicated that, primarily because of the short mission use, basic engine SFC was relatively unimportant as a measure of successful design. Emphasis was therefore placed on achieving adequate stall margin, compactness, simplicity, fewer parts, ease of assembly, and

potential low manufacturing cost. The high tip speed compressor and highly loaded fan turbine were two instances where performance was traded for engine volume. A reduced level of high pressure turbine cooling effectiveness requiring increased cooling air for the ILF1A1 was accepted to achieve a simpler and lower cost bucket design.

Fan Tip Speed Effect

The primary purpose of completing the preliminary design on the ILF2A2 was to achieve a comparison in terms of weight, noise performance, and size relative to the ILF2A1. The only difference in these two 1.2 fan pressure designs being that the ILF2A2 has a 25% lower fan tip speed and an additional low pressure turbine stage due to the reduced wheel speed. The results of the study based on standard General Electric procedures indicate that the lower speed fan has negligible noise advantage while suffering an increase in engine length, engine weight, and in number of parts.

Installation Aerodynamics

The results of the installation study indicated that engine-airframe integration will be an important part of any air vehicle development program. Basic technology data covering installation characteristics of turbofan lift engines are very limited. Design requirements relative to transient response and stall margin must be postulated for the present since they are dependent on operating method and takeoff trajectory selection. In the case of takeoff trajectory alone; this may be a function of required noise ground contour. A new field of installation aerodynamics and engine stability analysis requires extensive analytical and experimental investigation.

Commercial Design Features

Most lift engine designs completed in the past have been for military applications with reduced life requirements, no noise or emission limits, no containment requirements, and have different needs relative to fire safety, reliability, and simplicity. An important result of the present designs was to determine the effect of strict adherence to FAR Part 25 and Part 33 requirements on a commercial turbofan lift engine. Fire safety requirements were met with use of automatic drains, fireproof cases, and shrouding of fuel and hydraulic lines in fire

zones. Reliability requirements were met by use of dual ignition leads, exciters, and igniters. Fan blade containment was provided to prevent damage to adjacent structures by providing for complete containment of a failed blade.

Additional safety in this regard is obtained by use of a continuous tip shroud. Reduced exhaust emissions will be achieved through detailed design of the combustor. The overall results presented reflect consideration of all these commercial design requirements plus a recognition for the need of simplicity and the use of a few parts as possible.

CONCLUSIONS AND RECOMMENDATIONS

The insights gained and the experience derived through the preliminary design completed on the three commercial direct lift turbofan engines lead to the following major conclusions:

- A noise level of 95 PNdB at 500' sideline for 12 engines operating at 10,000 lb. thrust each is projected although there are uncertainties which require further exploration.
- Commercial design requirements of fire safety, containment, and reliability can be met by proper attention to these needs during preliminary and detailed component design. A lift to weight ratio of 12/1 based on the 12,500 lb. maximum rating is projected for a lift turbofan engine meeting these requirements in the early to mid 1980's.
- A short relatively simplet compact engine having a small number of parts can be designed using a reverse liner flow combustor combined with an advanced compressor and highly loaded fan turbine.

Another valuable aspect of the current work is the identification of areas of technology in which voids exits, and therefore appear to have potential for development of new knowledge and improved design techniques.

- Source noise reduction techniques in the 1.2 to 1.25 fan pressure ratio range.
- Treatment of combustor and turbine noise.

- Degree of compressor and fan inlet radiated noise heard in the rear quadrant.
- Effect of crossflow velocity on fan and jet noise.
- Effect of trajectory on ground noise contours including reflection effects.

Additional design studies in several areas suggest themselves as being of future importance to air craft system characteristics.

- Engine emission study (initial work being accomplished under NAS14406).
- Manufacturing cost reduction and value engineering design effort under (NAS14406).
- Evaluation of louvered vectoring and alternate inlet design concepts.
- More detailed study of operational requirements relative to engine aircraft control integration, ground and air starting, and engine transient operation.

The preliminary designs underlined the needs for analytical and experimental development work in several component areas:

- Techniques for fan and primary source noise reduction and suppression
- Installation aerodynamics for compatible airframe/engine design
- Composite blade, shroud, and dovetail design and construction
- 5 stage, 10:1 p/p core compressor
- Low emission reverse liner flow combustor with 2500° F T_4
- Very highly loaded fan turbine
- All electronic fuel controls

SYMBOLS

Latin

A	Flow area, $ft.^2$
A_w	wetted area - $ft.^2$
ALT	Altitude, ft.
ALPHA	Thrust vector angle, ° relative to vertical (+ is aft)
BETA	Bypass ratio
C_f	Friction drag coefficient
c	Chord, in
C_F	Nozzle flow coefficient
C_z	Axial velocity, ft./sec.
C_v	Nozzle velocity coefficient
C_d	Drag coefficient
D	diameter, in
D_f,D.F.	Diffusion factor
ETAR	Ram recovery
FGV	Vertical gross thrust component - lb.
FGH	Horizontal gross thrust component - lb.
FG	Resultant gross thrust - lb.
F_F	Pressure drag factor
F_D	Ram drag (W_o V_o/g) - lb.
F_N	Net thrust, lb. (arbitrarily defined as FG - FD)
g	Gravitational constant
H	Height, in
h	Enthalpy, Btu/lb.
i	Incidence angle, deg.

Latin

ID	Identification number
ILE, ILF	Integral lift fan engine
J	Mechanical equivalent of heat
L	Length, in
M	Mach no.
M_o	Flight Mach no.
M_R	Relative Mach no.
N	Number of stages, and rotor speed, rpm
NRP	Noise Rating Point
P	Pressure, psia
P_o	Ambient pressure, psia
P_2	Fan face total pressure, psia
PCNG	Fan % rpm
PCNFK	Fan % corrected rpm
PNdB	Perceived noise, decibels
R	Radius, in
R_x	Reaction
SFC	Specific fuel consumption $\frac{lb/hr}{lb}$ (arbitrarily defined as $\frac{WFM)}{F_N}$
SOL	Solidity
T	Temperature, ° R
T_o	Ambient temperature, ° R
T_2	Fan face total temperature, ° R
t	Thickness, in
t_m	Maximum thickness, in
t_e	Trailing edge thickness,in

Latin

U	Wheel speed, ft/sec
V_o	Flight velocity, ft/sec
V_8	Core duct exit velocity, ft/sec
V_{28}	Fan duct exit velocity, ft/sec
VOKNOT	Flight velocity, knots
W	Weight flow, lb/sec
W_o	Total inlet airflow, lb/sec
WFAN	Fan duct inlet airflow, lb/sec
WFM	Fuel Flow, lb/hr
X_f	Deviation correction factor, deg.

Greek

α_1	Absolute inlet air angle, deg.
β_1	Relative inlet air angle, deg.
β_2	Relative discharge air angle, deg.
β_m	Stagger angle, deg.
γ	Specific heat ratio
Γ	Swirl angle
Δ	Incremental change
δ	Deviation angle, deg. and inlet pressure correction
η_{ad}	Adiabatic efficiency
η_p	Polytropic efficiency
λ	Wave length
ω	loss coefficient

Greek

ρ	Camber
Σ	Sum of
σ	Solidity
θ	Inlet temperature correction
Ψ	Turbine loading

Subscripts

1	blade row inlet
2	blade row exit and inlet station
C	compressor
EX	exit
F	fan
H	hub
P	pitch
R	relative
T	tip
o	ambient
4	high pressure turbine rotor inlet
8	core nozzle throat
54	low pressure turbine inlet
55	low pressure turbine exit
28	fan nozzle throat

Superscripts

$\overline{\text{bar}}$	average
prime'	compressor inlet

Table I. Turbine Cooling Technology.

T_{Bulk} = 1650° F
(Using Simplest Method)

T_4 ° F	Technology	High Pressure Turbine	Low Pressure Turbine
2800	Adv. Impingement Film	Vane and Rotor	Stage 1 and Stage 2
2500	Impingement - T/E Holes	Vane and Rotor	1st Stage Only
2200	Convection - T/E Holes	Vane and Rotor	1st Stage Vane Only
1850	Convection	Vane Only	None

Table II. Turbine Cooling Summary.

(Percentages of Core Compressor Flow)

	High Pressure Turbine			Low Pressure Turbine				
T_4 ° F	Leakage	Vane	Blade	Leakage	Vane	Blade 1	Vane 2	Blade 2
2800								
P/P 5	1.8	1.8	1.8	3.0	1.4	1.3	1.0	0.6
7	1.8	2.0	2.0	3.0	1.3	1.2	0.8	0
10	1.8	2.2	2.2	3.0	1.2	1.1	0.6	0
15	1.8	2.6	2.6	3.0	1.0	0.9	0	0
2500								
P/P 5	1.8	2.0	2.0	3.0	1.6	1.6	0	0
7	1.8	2.5	2.5	3.0	1.2	1.2	0	0
10	1.8	3.0	3.0	3.0	1.0	0	0	0
15	1.8	3.5	3.5	3.0	0.5	0	0	0
2200								
P/P 5	1.8	1.4	1.4	3.0	0.8	0	0	0
7	1.8	1.6	1.6	3.0	0.5	0	0	0
10	1.8	1.9	1.9	3.0	0	0	0	0
15	1.8	2.3	2.3	3.0	0	0	0	0
1850								
P/P 5	1.8	1.0	0	3.0	0	0	0	0
7	1.8	1.0	0	3.0	0	0	0	0
10	1.8	1.0	0	3.0	0	0	0	0
15	1.8	1.0	0	3.0	0	0	0	0

Table III. Summary Results Of Initial Sizing (Non-Geared).

Cycle				Fan							LP Turbine			HP Turbine			Diameter	
						Diameter		Blade Chord										
						Tip	Hub	Tip	Pitch	Hub								
Case	T4° F	V_8/V_{28}	P/P	P/P	U_T ft/sec	inches		inches			Number of Stages	Avg. ψp^*	N1 rpm	Number of Stages	ψp^*	N_2 rpm	D28 inches	D28 inches
1	2500	1.3	10	1.4	1200	46.09	21.82	4.61	3.55	3.30	4	1.68	5973	1	0.963	17692	44.20	27.19
1A	↓	↓	↓	1.4	1200	46.09	21.82	4.61	3.55	3.30	3	2.0	5973	↓	↓	17692	45.31	29.04
4				1.3	1122	48.98	20.80	4.81	3.70	3.44	7	1.64	5220			18683	47.61	24.21
5				1.3	1312	48.98	20.80	5.62	4.33	4.02	5	1.68	6139			18683	47.61	24.21
6				1.4	1492	46.09	21.82	5.73	4.41	4.10	3	1.70	7426			17642	43.09	25.32
7				1.5	1409	44.05	22.65	4.94	3.81	3.54	3	1.50	7330			16871	40.50	26.29
8	↓			1.5	1652	44.05	22.65	5.80	4.46	4.15	2	1.37	8594			16871	42.29	28.96
9	1850			1.4	1200	46.91	27.00	4.11	3.17	2.94	2	1.40	5863			13751	45.03	29.80
10	2200					46.23	23.56	4.44	3.42	3.18	3	1.59	5948			16107	44.38	28.30
11	2800	↓				45.80	20.31	4.73	3.64	3.38	5	1.70	6005			19220	44.65	27.37
12	2500	1.1				46.42	21.71	4.68	3.60	3.34	4	1.70	5924			17749	45.95	28.05
13	↓	1.5	↓			45.65	21.98	4.53	3.49	3.24	4	1.70	6024			17482	43.09	25.87
14		1.3	5			46.46	23.78	4.45	3.43	3.18	4	1.63	5920			15935	44.60	28.50
15		↓	7			46.23	22.62	4.55	3.50	3.25	4	1.70	5949			16899	44.18	27.40
16	↓		15			46.01	21.62	4.63	3.56	3.31	4	1.70	5977			17833	43.16	25.38
18	1850		5			47.12	28.11	3.98	3.07	2.85	2	1.41	5837			13133	45.82	32.29
19	2800	↓	15	↓	↓	45.70	19.85	4.76	3.66	3.40	5	1.70	6018		↓	19769	44.21	26.50
20	1850	1.3	7	1.2	1069	54.60	24.19	5.02	3.87	3.59	4	1.62	4487		0.734	15615	57.56	27.98
21	1850	1.3	7	1.3	1122	49.75	25.87	4.41	3.40	3.16	3	1.34	5768		0.734	14443	49.06	29.47
22	1850	1.3	7	1.3	1312	49.75	25.87	5.16	3.97	3.69	2	1.47	6043	↓	0.734	14443	49.06	29.47

* Turbine Work Coefficient (Pitch Line) = $\psi p = gJ\Delta H/2Up^2$

Table IV. Summary Results of Initial Sizing (Geared Configuration).

Cycle				Fan								LP Turbine		HP Turbine				
						Diameter		Blade Chord				Gear Ratio-N3/N1					Diameter	
						Tip	Hub	Tip	Pitch	Hub							DT	DR
Case	T4° F	V_8/V_{28}	P/P	P/P	U_T ft/sec	inches		inches			N1 rpm	1 Stage $\psi p^* = 1.0$	2 Stage $\psi p^* = 1.3$	Number of Stages	ψp^*	N2 rpm	inches	
1	2500	1.3	10	1.3	1069	49.67	22.11	4.56	3.51	3.26	4932	3.68	3.23	1	0.963	19131	18.69	15.09
2	↓	↓	↓	1.2	874	55.19	22.41	4.28	3.30	3.06	3030	5.53	4.85	↓	0.963	20703	17.27	13.94
3				1.4	1200	46.37	22.20	4.62	3.56	3.30	5931	2.91	2.56		0.963	18055	19.80	15.99
4				1.2	989	51.18	22.41	4.85	3.73	3.47	4107	4.89	4.29		0.963	20703	17.27	13.99
5				1.3	1205	49.67	22.11	5.14	3.96	3.67	5560	3.27	2.87		0.963	19131	18.89	15.09
6				1.4	1360	46.37	22.20	5.23	4.03	3.74	6722	2.57	2.25		0.963	18055	19.80	15.99
7				1.3	971	49.67	22.11	4.14	3.19	2.96	4480	4.06	3.56		0.963	19131	18.69	15.09
8		↓		1.4	1069	46.37	22.20	4.11	3.17	2.94	5284	3.27	2.87		0.963	18055	19.80	15.99
9		1.1		1.3	1069	50.00	22.11	4.60	3.54	3.29	4899	2.81	2.46		0.963	19217	18.61	15.02
10		1.5	↓	1.3	1069	49.32	22.10	4.51	3.48	3.23	4968	3.58	3.14		0.963	19024	18.82	15.19
11	↓	1.3	5	1.2	874	54.97	22.67	4.25	3.27	3.04	3644	4.95	4.34		0.963	18778	16.88	10.35
12	2800		10	1.2	874	55.42	22.33	4.31	3.32	3.08	3614	6.58	5.77		0.969	22546	15.80	12.86
13	1850		↓	1.3	1069	49.11	24.08	4.30	3.31	3.08	4988	2.23	1.96		0.926	14932	24.21	19.07
14	2200			1.3	1069	49.38	22.63	4.47	3.45	3.20	4961	3.06	2.68		0.939	17471	20.55	16.45
15	2800			1.3	1069	49.87	21.79	4.61	3.55	3.30	4912	4.21	3.69		0.969	20830	17.10	13.92
16	2500		5	1.3	1069	49.52	22.71	4.49	3.45	3.21	4997	3.70	3.25		0.963	17343	18.27	11.21
17	↓		7	1.3	1069	49.61	22.33	4.53	3.49	3.24	4938	3.60	3.16		0.963	18356	18.22	13.28
18			15	1.3	1069	49.69	22.06	4.57	3.52	3.26	4930	3.64	3.19		0.963	19318	20.18	17.45
19	2800		15	1.3	1069	49.93	21.73	4.62	3.56	3.31	4907	4.47	3.92		0.963	21396	18.14	15.83
20	1850	↓	5	1.3	1069	49.03	24.57	4.24	3.27	3.03	4996	2.24	1.96	↓	0.963	14315	21.87	12.93

* Turbine Work Coefficient = $\psi p = gJ\Delta H/2Up^2$

Table V. Non- Geared Reversed Flow Combustor.

Case No.	1	1A	4	5	6	7	8	9	10	11	12	13	14	15	16	18	19	20	21	22
Fan Blade & Disk	53	53	64	79	74	54	73	42	50	55	54	51	50	52	53	41	55	80	54	68
Fan Hub	13	13	13	14	15	14	16	16	14	12	13	13	14	14	13	17	12	16	16	18
Gears																				
Comp. Rotor	45	45	39	39	45	51	51	91	59	36	45	47	51	47	52	88	39	58	72	72
Comp. Stator	34	34	29	29	34	39	39	68	44	27	34	35	39	35	39	66	29	44	54	54
Combustor	30	30	27	27	30	33	33	50	36	26	30	31	60	42	22	88	18	50	58	58
HPT Rotor	69	69	60	60	69	77	77	158	93	52	68	70	102	82	59	164	42	105	129	129
HPT Stator	34	34	30	30	34	38	38	79	46	26	34	35	51	41	29	82	21	53	64	64
LPT Rotor	67	68	61	61	67	68	70	155	63	73	74	51	83	73	51	68	59	48	59	59
LPT Stator	54	56	49	49	54	55	56	125	51	59	60	41	67	59	41	55	47	39	48	48
Shaft	17	17	17	15	14	15	26	20	17	16	17	16	17	16	17	18	16	18	18	16
Main Frame	140	138	145	141	138	142	139	191	155	127	139	141	141	139	144	178	127	177	176	173
Turbine Frame	28	28	25	25	28	30	30	45	34	24	29	35	41	33	25	58	21	36	45	45
Nozzle	12	12	11	11	12	13	13	18	14	11	12	11	16	13	11	20	10	14	17	17
Outer Duct	55	50	70	65	60	56	56	64	57	52	54	54	61	60	54	68	48	74	70	67
Bearings	25	25	25	25	25	25	25	25	25	25	25	25	25	25	25	25	25	25	25	25
C & A	62	62	62	62	62	62	62	62	62	62	62	62	62	62	62	62	62	62	62	62
Trunnions	13	13	13	13	13	13	13	13	13	13	13	13	13	13	13	13	13	13	13	13
Basic Engine Wt.	751	747	740	745	774	785	817	1222	833	696	763	731	893	806	710	1111	644	912	980	988
Suppression	25	22	32	28	24	25	21	31	26	23	25	25	29	28	24	33	21	34	33	30
Splitters	62	51	74	54	53	67	56	95	71	53	60	60	82	75	54	114	42	61	90	74
TOTAL WEIGHT	838	820	846	827	851	877	894	1348	930	772	848	816	1004	909	788	1258	707	1007	1103	1092

Table VI. Geared Reversed Flow Combustor.

Case No.	1	2	3	4	5	6	7	8	9	10	11	12	13	14	15	16	17	18	19	20
Fan Blade & Disk	60	71	53	81	71	64	53	45	62	59	68	72	52	58	63	58	59	60	63	51
Fan Hub	19	22	19	26	20	20	19	18	18	19	20	24	24	19	20	20	20	19	20	21
Gears	127	139	125	132	122	122	134	130	138	125	133	146	121	124	129	128	126	127	129	122
Comp. Rotor	36	29	43	29	36	43	36	43	36	37	32	23	72	47	29	41	37	42	31	39
Comp. Stator	27	22	32	22	27	32	27	32	27	28	24	17	54	35	21	30	28	31	23	52
Combustor	26	22	29	22	26	29	26	29	26	26	43	19	42	31	22	51	36	19	16	74
HPT Rotor	57	48	65	48	57	65	57	65	56	58	68	37	123	74	44	83	67	50	37	131
HPT Stator	29	24	32	24	28	32	29	32	28	29	34	19	61	37	22	41	33	25	18	65
LPT Rotor	95	84	106	84	95	106	95	106	99	92	115	82	138	106	88	103	111	91	86	181
LPT Stator	46	41	51	41	46	51	46	51	47	44	56	40	66	51	43	50	53	44	41	87
Shaft	10	11	10	12	10	10	10	10	11	10	10	12	12	10	10	10	10	10	10	13
Front Frame (Trans.)	15	19	14	21	14	14	16	15	13	15	18	20	19	16	14	17	15	15	15	20
Main Frame	90	130	73	136	87	71	93	75	87	88	121	140	82	86	94	88	89	90	95	81
Turbine Frame	24	21	27	21	24	27	24	27	25	24	30	18	40	29	21	21	29	22	18	51
Outer Duct	57	75	52	83	56	53	59	52	51	55	67	84	59	55	57	55	56	56	60	61
Inner Duct & Nozzle	42	53	41	59	40	39	45	43	38	42	52	59	50	43	42	43	44	41	42	57
Bearings	25	25	25	25	25	25	25	25	25	25	25	25	25	25	25	25	25	25	25	25
C & A	75	75	75	75	75	75	75	75	75	75	75	75	75	75	75	75	75	75	75	75
Trunnions	13	13	13	13	13	13	13	13	13	13	13	13	13	13	13	13	13	13	13	13
Basic Engine Wt.	873	924	885	954	872	891	882	886	875	864	1004	925	1128	934	832	952	926	855	817	1249
Suppression	26	36	24	39	25	23	28	25	24	26	32	40	28	26	27	25	26	26	28	29
Splitters	41	41	48	52	35	44	46	52	30	40	38	50	66	44	40	36	43	37	39	79
TOTAL WEIGHT	940	1001	957	1045	932	958	956	963	929	930	1074	1015	1222	1004	899	1013	995	918	884	1357

Table VII. Integral Lift Engine.

Component	Material	Form	Remarks
Fan Section			
Blade	Graphite/Epoxy	Composite Layup	
Disk	Ti77XD	Forging	Development Ti Alloy
Supercharger	17-4PH	Casting	
Nose Spinner	Glass/Epoxy	Molding	Urethane Coating
Splitter Nose	Glass/Epoxy	Molding	Urethane Coating
Tip Shroud	Graphite/Epoxy	Composite Layup	
Compressor			
IGV, Stg. 1 Vane	Graphite/Epoxy with 321 SS Tube	Chopped Fiber Molding	Central Tube Section oval
Stg. 2 Vane	224-T62	Casting	
Stg. 3 & 4 Vanes	IN718	Punched & Brazed	
OGV	IN718	Casting	
Stg. 1 Blade	Graphite/Epoxy	Composite Layup	LE FOD Protection
Stg. 2-5 Blades	Ti 6Al-4V	Forging	
Spool	Ti77XD	Forging	
Fwd. Case	224-T62	Casting	
Rear Case	17-4PH	Casting	
Fwd. Rotating Seals	321SS	F.W. Ring	
Vane Tip Seals			
Stgs. 1 & 2	Polyimide	Molded in PI/Glass	
Stgs. 3 - 5	Nickel/Graphite	Honeycomb	
Combustor			
Liner	Hastelloy X	Sheet	
Middle Liner	IN625	Sheet	
Outer Liner	IN718	Sheet & Casting	
Nozzle	Hastelloy X	Sheet & Casting	
Manifold	Inco 600	Turbine	
Turbine			
Stg. 1 Vanes	MM509	Casting	Codep Coated
Stgs. 2 - 4 Vanes	Rene 120	Casting	Codep Coated
Stgs. 1 - 2 Bucket	Ni76XB	Casting	Codep Coated
Stg. 3 Bucket	Rene 120	Casting	Codep Coated
Stg. 4 Bucket	Rene 77	Casting	
Stg. 1 Disk	Ni75XD	PM Forging	
LP Spool	Ni75XD	PM Compact	
HP Conical Shafts	IN718	PM Compact	
LP Conical Shafts	IN718	PM Compact	
HP Turbine Tip Seals	MM509	Casting with Brazed Ring	
HP Turbine Tip Seals	Hastelloy X	Honeycomb Brazed to Forged Rings.	
Vane Seals	Hastelloy X	Honeycomb Brazed to Forged Rings.	
LP Shaft Seals	Hastelloy & 17-4PH	Honeycomb Brazed to Casting	
Main Shaft	4340	Forging	
Static Structures			
Fwd. Frame Struts	6061 T6		
Aft Struts	IN718	Casting & Sheet Metal	
Fwd. Outer Bearing Support & Rotating Seals	4340	Forging	
Static Seals	224-T62 & G1/Gr/P1 Seal	Casting with Composite Seal	
Fwd Cowling, Fwd Outer Fan Duct, Rear Outer Fan Duct	Glass/Epoxy	Composite Lay-up	Sound Suppression Panels
(2) Fwd Inner Fan Ducts, (3) Splitter Rings	6061-T6 & 5052H32	Forging with Monocoque Bonded Structure	
Aft Inner Fan Duct	Inco 625	Brazed Monocoque Structure	
Aft Frame	Inco 625	Brazed with Monocoque Splitter & OD Shroud	
Inner and Outer Frame Support	6061-T6 Aluminum		Bonded to Struts

Table VIII. Fan Design Parameter Summary.

Design Parameter	ILF1A1	ILF2A1	ILF2A2	TF39 Comp. (Stage 1)
Flow Rate; lb/sec	588.3	653.2	653.2	396.3
Specific Flow; lb/sec-ft^2	42.5	42.5	42.5	40.0
Pressure Ratio	1.25	1.20	1.20	1.25
Efficiency, $\eta_{ad}(\eta_p)$, %	87.0(87.3)	87.6(87.8)	88.2(88.4)	88.2(88.5)
Tip Speed, ft/sec	1180	1060	855	1100
Stall Margin, %	18.5	18.0	18.0	20.0
Bypass Ratio	12.6	11.5	11.5	---
Inlet Radius Ratio	0.471	0.468	0.468	0.361
Inlet Mach Number	0.624	0.624	0.624	0.565
Exit Mach Number	0.465	0.50	0.55	0.581
Rotor Tip Solidity	1.0	1.0	1.0	1.0
Rotor Aspect Ratio	3.25	3.9	2.9	3.25
OGV Aspect Ratio	5.6	5.6	4.2	3.5
Number of Blades	40	48	36	25
Number of OGV's	80	80	70	36

Table IX. ILF1A1 Fan and Supercharger Vector Diagrams and Blading Summary.

Stage	R_1/R_{T_1}	M_{1R}	C_{Z1} fps	U_1 fps	β_{1R} Deg.	i Deg.	R_2/R_{T_1}	β_{2R} Deg.	D_f	$\bar{\sigma}$	$\bar{\omega}$	X_f Deg.	δ Deg.
Fan Aerodynamics													
Rotor	1.000	1.296	713.9	1180.0	58.83	2.00	0.985	52.03	0.2233	1.000	0.0803	0.00	1.84
	0.790	1.091	701.2	932.0	53.07	1.00	0.794	47.38	0.2731	1.253	0.0366	1.50	5.07
	0.471	0.869	720.7	555.0	37.62	3.00	0.502	17.02	0.3720	2.041	0.0457	4.00	9.85
Stator	1.026	0.544	569.2	1211.0	21.07	-2.00	1.038	0.00	0.2741	1.103	0.0350	2.00	8.78
	0.824	0.564	586.5	972.0	21.77	-0.50	0.830	0.00	0.2529	1.377	0.0200	0.50	5.90
	0.533	0.636	600.9	629.0	31.81	2.00	0.533	0.00	0.3276	2.134	0.0490	2.00	7.90
Supercharger Aerodynamics													
Rotor	1.000	0.617	547.5	387.7	35.30	1.00	1.000	24.32	0.1605	1.505	0.0378	0.00	2.62
	0.825	0.584	549.0	319.8	30.22	1.00	0.830	17.28	0.1653	1.818	0.0270	1.00	3.97
	0.604	0.561	562.3	234.3	22.62	3.00	0.608	1.73	0.2249	2.484	0.0378	2.00	5.39
Stator	1.000	0.522	555.0	387.7	13.86	-2.00	1.000	10.00	0.0680	1.128	0.0218	2.00	9.24
	0.830	0.519	546.5	321.9	15.53	-1.00	0.846	10.00	0.0913	1.346	0.0122	0.00	6.38
	0.608	0.513	516.5	235.6	23.07	0.00	0.638	10.00	0.2274	1.810	0.0218	2.00	8.81

Table IX. ILF1A1 Fan and Supercharger Vector Diagrams and Blading Summary. (Concluded)

Stage	$\bar{R}/R_{T_1}$	σ	c In.	ϕ Deg.	β_m Deg.	t_m/c	t_e/c
Fan Blade Geometry							
Rotor	0.993	1.000	4.450	6.49	53.54	0.0300	0.0100
	0.792	1.253	4.450	10.01	47.13	0.0458	0.0100
	0.487	2.041	4.450	39.38	18.44	0.0800	0.0100
No. Blades: 40		Aspect Ratio: 3.248		Meanline: Special		t/c: Special	
Stator	1.032	1.103	2.553	31.82	7.29	0.0700	0.0100
	0.827	1.377	2.553	28.04	8.17	0.0618	0.0100
	0.533	2.134	2.553	37.71	10.95	0.0500	0.0100
No. Blades: 80		Aspect Ratio: 5.578		Meanline: Circular Arc		t/c: 65 Series	
Supercharger Blade Geometry							
Rotor	1.000	1.505	3.766	12.53	27.94	0.0800	0.0100
	0.828	1.818	3.766	16.36	21.16	0.0800	0.0100
	0.606	2.484	3.766	23.91	7.85	0.0800	0.0100
No. Blades: 24		Aspect Ratio: 1.000		Meanline: Circular Arc		t/c: 65 Series	
Stator	1.000	1.128	1.613	35.28	-1.78	0.0700	0.0100
	0.838	1.346	1.613	32.87	0.01	0.0604	0.0100
	0.623	1.810	1.613	41.33	1.62	0.0506	0.0100
No. Blades: 42		Aspect Ratio: 2.327		Meanline: Circular Arc		t/c: 65 Series	

Table X. ILF2A1 Fan and Supercharger Vector Diagrams and Blading Summary.

Stage	R_1/R_{T_1}	M_{1R}	C_{Z1} fps	U_1 fps	β_{1R} Deg.	i Deg.	R_2/R_{T_1}	β_{2R} Deg.	D_f	$\bar{\sigma}$	$\bar{\omega}$	X_f Deg.	δ Deg.
Fan Aerodynamics													
Rotor	1.000	1.181	690.0	1060.0	56.94	2.00	0.988	48.12	0.1927	1.008	0.0803	0.00	1.80
	0.786	1.019	702.9	833.2	49.85	1.00	0.793	43.11	0.2521	1.269	0.0366	1.50	5.00
	0.468	0.885	771.5	496.5	32.76	3.00	0.501	13.77	0.3659	2.068	0.0457	4.00	9.24
Stator	1.028	0.578	607.8	1090.0	18.42	-2.00	1.039	0.0	0.2296	1.081	0.0350	2.00	8.10
	0.826	0.591	617.5	875.3	19.14	-0.50	0.833	0.0	0.2188	1.347	0.0200	0.50	5.31
	0.544	0.664	647.7	576.5	27.75	2.00	0.544	0.0	0.2930	2.054	0.0490	2.00	7.21
Supercharger Aerodynamics													
Rotor	1.000	0.630	567.3	382.0	33.9	1.00	1.000	22.5	0.1403	1.514	0.0357	0.00	2.59
	0.832	0.614	584.8	318.0	28.5	1.00	0.837	16.2	0.1657	1.813	0.0248	1.00	2.86
	0.626	0.602	605.3	239.0	21.5	3.00	0.626	2.2	0.2506	2.418	0.0345	2.00	5.14
Stator	1.000	0.55	585.9	382.0	13.4	-2.00	1.000	10.0	0.0908	1.111	0.0180	2.00	9.28
	0.837	0.545	574.1	320.0	15.0	-1.00	0.849	10.0	0.0813	1.317	0.0108	0.00	6.29
	0.626	0.526	532.1	239.0	22.3	0.00	0.652	10.0	0.1875	1.739	0.0244	2.00	8.89

Table X. ILF2A1 Fan and Supercharger Vector Diagrams and Blading Summary. (Concluded)

Stage	$\bar{R}/R_{T_1}$	σ	c In.	ϕ Deg.	β_m Deg.	t_m/c	t_e/c
Fan Blade Geometry							
Rotor	0.994	1.008	4.204	9.52	51.01	0.0300	0.01
	0.790	1.269	4.204	11.14	43.40	0.0461	0.01
	0.485	2.068	4.204	37.44	15.31	0.0800	0.01
No. Blades: 48		Aspect Ratio: 3.917		Meanline: Special		t/c: Special	
Stator	1.034	1.081	2.635	28.48	6.28	0.0700	0.01
	0.834	1.347	2.635	24.74	7.14	0.0617	0.01
	0.544	2.054	2.635	32.96	9.27	0.0500	0.01
No. Blades: 80		Aspect Ratio: 5.58		Meanline: Circular Arc		t/c: 65 Series	
Supercharger Blade Geometry							
Rotor	1.000	1.514	3.577	13.01	26.35	0.0800	0.01
	0.835	1.813	3.577	15.67	19.86	0.0800	0.01
	0.626	2.418	3.577	21.80	7.72	0.0800	0.01
No. Blades: 28		Aspect Ratio: 1.101		Meanline: Circular Arc		t/c: 65 Series	
Stator	1.000	1.111	1.531	34.67	-1.94	0.0700	0.01
	0.843	1.317	1.531	34.22	-0.20	0.0603	0.01
	0.639	1.739	1.531	40.77	1.24	0.0506	0.01
No. Blades: 48		Aspect Ratio: 2.483		Meanline: Circular Arc		t/c: 65 Series	

Table XI. ILF2A2 Fan and Supercharger Vector Diagrams and Blading Summary.

Stage	R_1/R_{T_1}	M_{1R}	C_{Z1} fps	U_1 fps	β_{1R} Deg.	i Deg.	R_2/R_{T_1}	β_{2R} Deg.	D_f	$\bar{\sigma}$	$\bar{\omega}$	X_f Deg.	δ Deg.
Fan Aerodynamics													
Rotor	1.000	1.101	790.3	855.0	47.25	2.00	1.000	41.05	0.3121	1.002	0.0743	0.00	3.27
	0.787	0.911	703.4	672.5	43.72	1.00	0.800	31.50	0.3026	1.263	0.0376	0.00	4.40
	0.468	0.720	622.7	399.9	32.71	4.00	0.523	1.12	0.1856	2.022	0.0500	4.00	11.64
Stator	1.030	0.563	578.4	880.3	22.59	-2.00	1.033	0.00	0.2029	1.264	0.0296	2.00	8.73
	0.822	0.626	638.7	702.9	22.52	-0.45	0.826	0.00	0.2379	1.548	0.0206	0.45	5.64
	0.551	0.725	676.9	470.9	31.28	2.00	0.551	0.00	0.3260	2.316	0.0419	2.00	7.53
Supercharger Aerodynamics													
Rotor	1.000	0.597	574.3	299.8	27.57	1.00	1.000	18.12	0.0994	1.514	0.0245	0.00	2.02
	0.832	0.854	581.4	249.4	23.22	1.00	0.837	12.79	0.1072	1.814	0.0165	1.00	3.26
	0.626	0.856	605.5	187.7	17.22	3.00	0.626	2.09	0.1931	2.419	0.0214	2.00	4.39
Stator	1.000	0.549	587.2	299.1	10.39	-2.00	1.000	10.00	0.0804	1.111	0.0115	2.00	8.32
	0.837	0.546	581.9	250.7	11.52	-1.00	0.849	10.00	0.0548	1.317	0.0065	0.00	5.34
	0.626	0.523	544.7	187.7	17.12	0.00	0.652	10.00	0.1023	1.731	0.0131	1.86	7.27

Table XI. ILF2A2 Fan and Supercharger Vector Diagrams and Blading Summary. (Concluded)

Stage	$\bar{R}/R_{T_1}$	σ	c In.	ϕ Deg.	β_m Deg.	t_m/c	t_e/c
Fan Blade Geometry							
Rotor	1.000	1.002	5.25	7.47	41.52	0.0300	0.0100
	0.794	1.263	5.25	16.62	34.68	0.0464	0.0100
	0.497	2.022	5.25	51.11	5.55	0.0800	0.0100
No. Blades: 36		Aspect Ratio: 2.886		Meanline: Special		t/c: Special	
Stator	1.032	1.264	3.439	33.13	8.04	0.0700	0.0100
	0.824	1.548	3.439	28.48	8.64	0.0614	0.0100
	0.551	2.316	3.439	36.81	10.88	0.0500	0.0100
No. Blades: 70		Aspect Ratio: 4.197		Meanline: Circular Arc		t/c: 65 Series	
Supercharger Blade Geometry							
Rotor	1.000	1.514	3.577	10.47	21.33	0.0800	0.0100
	0.835	1.814	3.577	13.00	15.85	0.0800	0.0100
	0.626	2.419	3.577	16.75	5.84	0.0800	0.0100
No. Blades: 28		Aspect Ratio: 1.101		Meanline: Circular Arc		t/c: 65 Series	
Stator	1.000	1.111	1.531	30.41	-3.11	0.0700	0.0100
	0.843	1.317	1.531	27.61	-1.57	0.0602	0.0100
	0.639	1.731	1.531	34.55	-0.67	0.0505	0.0100
No. Blades: 48		Aspect Ratio: 2.465		Meanline: Circular Arc		t/c: 65 Series	

Table XII. ILF1A1 Compressor Vector Diagrams and Blading Summary.

Rotor Aerodynamics													
Stage	R_1/R_{T_1}	M_{1R}	C_{Z1} fps	U_1 fps	β_{1R} Deg.	i Deg.	R_2/R_{T_1}	β_{2R} Deg.	D_f	$\bar{\sigma}$	$\bar{\omega}$	X_f Deg.	δ Deg.
Rotor 1	1.000	1.336	659.2	1401.0	62.91	0.00	0.991	54.42	0.4404	1.294	0.1460	0.00	5.74
	0.851	1.172	653.9	1192.0	58.92	-1.00	0.871	45.83	0.4470	1.439	0.0824	2.00	8.09
	0.655	0.905	511.1	917.0	58.44	-1.00	0.732	31.87	0.4555	1.629	0.0832	4.00	10.34
Rotor 2	0.989	1.211	711.7	1385.0	60.54	0.00	0.989	48.66	0.5206	1.222	0.1122	0.00	6.89
	0.894	1.127	699.7	1252.0	58.20	-1.00	0.912	42.79	0.4989	1.338	0.0627	1.80	8.97
	0.784	1.023	653.8	1099.0	56.39	-1.00	0.813	32.08	0.5225	1.496	0.0817	3.50	11.18
Rotor 3	0.987	1.079	657.3	1383.0	62.59	0.00	0.981	52.03	0.5252	1.183	0.1157	0.00	7.07
	0.922	1.043	680.0	1292.0	59.88	-1.00	0.923	47.05	0.4964	1.262	0.0639	1.50	9.01
	0.855	0.991	704.0	1197.0	56.74	-1.00	0.865	38.29	0.5281	1.355	0.0777	3.00	11.36
Rotor 4	0.969	0.998	607.7	1358.0	64.85	0.00	0.954	53.56	0.5240	1.186	0.1108	0.00	7.27
	0.917	0.977	624.1	1286.0	62.91	-1.00	0.908	50.22	0.4886	1.250	0.0630	1.30	8.92
	0.865	0.933	647.7	1212.0	60.49	-1.00	0.862	43.37	0.5251	1.321	0.0804	2.50	11.05
Rotor 5	0.918	0.931	599.8	1311.0	65.06	0.00	0.893	55.82	0.5183	1.197	0.1116	0.00	7.14
	0.877	0.919	600.4	1252.0	64.00	0.00	0.854	53.35	0.5757	1.253	0.0624	1.00	7.91
	0.837	0.884	625.4	1192.0	60.49	0.00	0.814	47.86	0.5183	1.315	0.0806	2.00	10.00

Table XII. ILF1A1 Compressor Vector Diagrams and Blading Summary. (Continued)

Stator Aerodynamics														
Stage	R_1/R_{T_1}	M_{1R}	C_{Z1} fps	U_1 fps	β_{1R} Deg.	i Deg.	R_2/R_{T_1}	β_{2R} Deg.	D_f	$\bar{\sigma}$	$\bar{\omega}$	X_f Deg.	δ Deg.
Stator 1	0.991	0.725	607.1	1389.0	44.64	-3.00	0.989	10.00	0.3872	1.189	0.0715	2.00	13.21
	0.871	0.739	607.6	1224.0	44.58	-3.00	0.894	10.00	0.3689	1.331	0.0422	0.00	10.00
	0.732	0.801	578.0	1025.0	49.02	-2.00	0.784	10.00	0.4156	1.552	0.0784	2.00	12.44
Stator 2	0.989	0.713	610.9	1385.0	48.52	-3.00	0.987	10.00	0.5211	1.271	0.0654	2.00	14.27
	0.912	0.742	644.7	1278.0	46.57	-3.00	0 922	10.00	0.4823	1.370	0.0429	0.00	10.73
	0.831	0.804	665.8	1164.0	48.27	-2.00	0.855	10.00	0.4901	1.491	0.0832	2.00	12.75
Stator 3	0.981	0.614	556.8	1374.0	49.89	-3.00	0.969	6.00	0.5590	1.266	0.0632	2.00	15.63
	0.923	0.641	606.0	1293.0	46.66	-3.00	0.917	6.00	0.5303	1.342	0.0441	0.00	11.84
	0.865	0.694	646.3	1212.0	47.34	-2.00	0.865	6.00	0.5498	1.427	0.0759	2.00	13.73
Stator 4	0.954	0.541	536.4	1337.0	48.71	-3.00	0.936	2.00	0.5316	1.301	0.0688	2.00	15.87
	0.908	0.557	576.8	1272.0	45.13	-3.00	0.894	2.00	0.5073	1.365	0.0432	0.00	12.05
	0.862	0.594	608.0	1208.0	46.17	-2.00	0.851	2.00	0.5234	1.436	0.0750	2.00	14.08
Stator 5	0.918	0.468	502.7	1286.0	47.38	-3.00	0.893	0.00	0.4965	1.466	0.0722	2.00	14.93
	0.877	0.479	538.6	1229.0	43.18	-2.00	0.854	0.00	0.4756	1.534	0.0448	0.00	10.79
	0.837	0.507	558.8	1173.0	44.80	-2.00	0.814	0.00	0.4976	1.608	0.0742	2.00	13.28

Table XII. ILF1A1 Compressor Vector Diagrams and Blading Summary. (Continued)

Rotor Blade Geometry							
Stage	R/R_{T_1}	σ	c In.	ϕ Deg.	β_m Deg.	t_m/c	t_e/c
Rotor 1	0.996	1.294	2.276	15.63	54.95	0.0300	0.0100
	0.861	1.439	2.193	24.16	48.03	0.0500	0.0100
	0.694	1.629	1.995	48.48	34.88	0.0700	0.0100
No. Blades: 34		Aspect Ratio: 1.32		Meanline: Special		t/c: Special	
Rotor 2	0.989	1.222	1.451	18.77	51.15	0.0300	0.0100
	0.903	1.338	1.451	27.39	45.69	0.0500	0.0100
	0.808	1.496	1.451	43.63	36.17	0.0700	0.0100
No. Blades: 50		Aspect Ratio: 1.17		Meanline: Special		t/c: Special	
Rotor 3	0.984	1.183	0.999	16.96	53.94	0.0300	0.0100
	0.923	1.262	0.999	22.85	49.50	0.0500	0.0100
	0.860	1.355	0.999	32.81	41.78	0.0700	0.0100
No. Blades: 70		Aspect Ratio: 1.17		Meanline: Special		t/c: Special	
Rotor 4	0.962	1.186	0.926	17.59	55.71	0.0300	0.0100
	0.913	1.250	0.926	21.40	53.04	0.0500	0.0100
	0.864	1.321	0.926	28.29	47.24	0.0700	0.0100
No. Blades: 74		Aspect Ratio: 1.00		Meanline: Special		t/c: Special	
Rotor 5	0.927	1.197	0.926	16.00	56.96	0.0300	0.0100
	0.886	1.253	0.926	16.83	55.14	0.0500	0.0100
	0.844	1.315	0.926	20.98	50.80	0.0700	0.0100
No. Blades: 72		Aspect Ratio: 0.86		Meanline: Circular Arc		t/c: DCA	

Table XII. ILF1A1 Compressor Vector Diagrams and Blading Summary. (Concluded)

Stator Blade Geometry							
Stage	$\bar{R}/R_{T_1}$	σ	c In.	ϕ Deg.	β_m Deg.	t_m/c	t_e/c
Stator 1	0.990	1.189	1.009	50.92	22.20	0.0700	0.0100
	0.883	1.331	1.009	47.20	23.71	0.0600	0.0100
	0.758	1.552	1.009	52.03	23.51	0.0500	0.0100
No. Blades: 70		Aspect Ratio: 2.144		Meanline: Circular Arc		t/c: 65 Series	
Stator 2	0.988	1.271	1.019	55.87	23.55	0.0700	0.0100
	0.917	1.370	1.019	50.24	24.44	0.0600	0.0100
	0.843	1.491	1.019	52.73	23.28	0.0500	0.0100
No. Blades: 74		Aspect Ratio: 1.338		Meanline: Circular Arc		t/c: 65 Series	
Stator 3	0.975	1.266	0.883	62.58	21.00	0.0700	0.0100
	0.920	1.342	0.883	55.60	21.80	0.0600	0.0100
	0.865	1.427	0.883	56.99	20.78	0.0500	0.0100
No. Blades: 84		Aspect Ratio: 1.183		Meanline: Circular Arc		t/c: 65 Series	
Stator 4	0.945	1.301	0.820	65.10	17.76	0.0700	0.0100
	0.901	1.365	0.820	58.73	18.64	0.0600	0.0100
	0.857	1.436	0.820	60.18	18.47	0.0500	0.0100
No. Blades: 90		Aspect Ratio: 0.021		Meanline: Circular Arc		t/c: 65 Series	
Stator 5	0.906	1.466	0.831	63.87	15.35	0.0700	0.0100
	0.866	1.534	0.831	58.30	16.74	0.0600	0.0100
	0.826	1.608	0.831	59.95	17.74	0.0500	0.0100
No. Blades: 96		Aspect Ratio: 0.921		Meanline: Circular Arc		t/c: 65 Series	

Table XIII. ILF2A1 Compressor Vector Diagrams and Blading Summary.

Rotor Aerodynamics													
Stage	R_1/R_{T_1}	M_{1R}	C_{Z1} fps	U_1 fps	β_{1R} Deg.	i Deg.	R_2/R_{T_1}	β_{2R} Deg.	D_f	$\bar{\sigma}$	$\bar{\omega}$	X_f Deg.	δ Deg.
Rotor 1	1.000	1.358	672.6	1421.0	62.76	0.00	0.992	54.71	0.4916	1.300	0.1460	0.00	6.22
	0.853	1.194	669.4	1213.0	58.71	-1.00	0.873	45.21	0.4967	1.462	0.0824	2.00	8.74
	0.663	0.933	548.0	942.0	57.14	-1.00	0.730	29.76	0.5465	1.751	0.0832	4.00	11.37
Rotor 2	0.984	1.185	636.0	1398.0	63.69	0.00	0.972	51.18	0.5105	1.221	0.1122	0.00	7.04
	0.887	1.106	664.0	1261.0	59.87	-1.00	0.894	44.40	0.4969	1.341	0.0627	1.80	9.26
	0.781	1.029	679.6	1110.0	55.55	-1.00	0.812	32.02	0.5352	1.499	0.0817	3.50	11.61
Rotor 3	0.959	1.081	648.0	1363.0	63.17	0.00	0.945	53.18	0.5067	1.181	0.1157	0.00	7.01
	0.892	1.039	664.8	1268.0	60.69	-1.00	0.884	48.57	0.4826	1.265	0.0639	1.50	9.05
	0.823	0.982	694.9	1170.0	57.29	-1.00	0.823	39.88	0.5230	1.366	0.0777	3.00	11.51
Rotor 4	0.928	0.993	584.0	1319.0	65.78	0.00	0.909	57.82	0.5063	1.194	0.1108	0.00	6.83
	0.871	0.963	588.8	1238.0	64.19	-1.00	0.854	54.31	0.4821	1.272	0.0630	1.30	8.78
	0.812	0.875	609.9	1154.0	61.70	-1.00	0.798	47.35	0.5345	1.363	0.0804	2.50	11.20

Table XIII. ILF2A1 Compressor Vector Diagrams and Blading Summary. (Continued)

Stator Aerodynamics														
Stage	R_1/R_{T_1}	M_{1R}	C_{Z1} fps	U_1 fps	β_{1R} Deg.	i Deg.	R_2/R_{T_1}	β_{2R} Deg.	D_f	$\bar{\sigma}$	$\bar{\omega}$	X_f Deg.	δ Deg.
Stator 1	0.992	0.707	546.0	1410.0	49.48	-3.00	0.984	10.00	0.4881	1.206	0.0715	2.00	14.78
	0.873	0.750	589.2	1240.0	47.67	-3.00	0.887	10.00	0.4509	1.354	0.0422	0.00	10.96
	0.753	0.812	538.4	1037.0	53.57	-2.00	0.781	10.00	0.4248	1.577	0.0784	2.00	13.35
Stator 2	0.972	0.676	579.0	1381.0	48.83	-3.00	0.959	7.20	0.5177	1.250	0.654	2.00	15.08
	0.894	0.710	622.2	1270.0	46.73	-3.00	0.892	7.20	0.4967	1.351	0.0429	0.00	11.49
	0.812	0.785	662.0	1154.0	48.18	-2.00	0.823	7.20	0.5182	1.476	0.0832	2.00	13.41
Stator 3	0.945	0.582	553.5	1343.0	47.48	-3.00	0.928	2.00	0.5614	1.270	0.0632	2.00	15.71
	0.884	0.604	593.6	1257.0	44.55	-3.00	0.871	2.00	0.5378	1.355	0.0441	0.00	11.95
	0.823	0.652	626.9	1169.0	45.84	-2.00	0.812	2.00	0.5580	1.455	0.0759	2.00	13.92
Stator 4	0.909	0.603	483.0	1293.0	47.38	-3.00	0.883	0.00	0.5320	1.424	0.0722	2.00	15.16
	0.854	0.601	514.1	1214.0	44.10	-3.00	0.829	0.00	0.5088	1.516	0.0448	0.00	11.40
	0.798	0.535	533.7	1134.0	46.09	-2.00	0.773	0.00	0.5354	1.625	0.0742	2.00	13.55

Table XIII. ILF2A1 Compressor Vector Diagrams and Blading Summary. (Continued)

Rotor Blade Geometry							
Stage	$\bar{R}/R_{T_1}$	σ	c In.	ϕ Deg.	β_m Deg.	t_m/c	t_e/c
Rotor 1	0.961	1.300	2.379	13.44	55.91	0.030	0.01
	0.863	1.462	2.319	25.17	47.29	0.050	0.01
	0.697	1.751	2.241	51.87	32.57	0.070	0.01
No. Blades: 36		Aspect Ratio: 1.361		Meanline: Special		t/c: Special	
Rotor 2	0.978	1.221	1.580	18.44	54.13	0.030	0.01
	0.891	1.341	1.580	26.52	47.81	0.050	0.01
	0.797	1.499	1.580	42.13	36.70	0.070	0.01
No. Blades: 50		Aspect Ratio: 1.180		Meanline: Special		t/c: Special	
Rotor 3	0.952	1.181	1.328	15.76	54.95	0.030	0.01
	0.888	1.265	1.328	21.19	50.96	0.050	0.01
	0.823	1.366	1.328	29.60	43.55	0.070	0.01
No. Blades: 56		Aspect Ratio: 1.010		Meanline: Special		t/c: Special	
Rotor 4	0.919	1.194	1.396	13.87	58.56	0.030	0.01
	0.863	1.272	1.396	17.90	55.97	0.050	0.01
	0.805	1.363	1.396	23.98	50.31	0.070	0.01
No. Blades: 52		Aspect Ratio: 0.850		Meanline: Special		t/c: Special	

Table XIII. ILF2A1 Compressor Vector Diagrams and Blading Summary. (Concluded)

Stator Blade Geometry							
Stage	$\bar{R}/R_{T_1}$	σ	c In.	ϕ Deg.	β_m Deg.	t_m/c	t_e/c
Stator 1	0.988	1.206	1.095	57.54	23.59	0.070	0.01
	0.880	1.354	1.095	51.38	24.86	0.060	0.01
	0.756	1.577	1.095	57.00	24.89	0.050	0.01
No. Blades: 72		Aspect Ratio: 2.18		Meanline: Circular Arc		t/c: 65 Series	
Stator 2	0.966	1.250	1.247	59.99	21.52	0.070	0.01
	0.893	1.351	1.247	54 06	22.68	0.060	0.01
	0.818	1.476	1.247	56.24	21.72	0.050	0.01
No. Blades: 64		Aspect Ratio: 1.23		Meanline: Circular Arc		t/c: 65 Series	
Stator 3	0.937	1.270	1.192	64.12	17.65	0.070	0.01
	0.878	1.355	1.192	57.86	18.58	0.060	0.01
	0.818	1.455	1.192	59.78	18.27	0.050	0.01
No. Blades: 66		Aspect Ratio: 1.05		Meanline: Circular Arc		t/c: 65 Series	
Stator 4	0.896	1.424	1.279	65.09	16.33	0.070	0.01
	0.842	1.516	1.279	59.70	17.36	0.060	0.01
	0.786	1.625	1.279	62.11	18.21	0.060	0.01
No. Blades: 66		Aspect Ratio: 0.89		Meanline: Circular Arc		t/c: 65 Series	

Table XIV. ILF1A1 Compressor and Supercharger Design Parameter Summary.

Design Parameter	Supercharger	Compressor	Overall
Design Flow; lb/sec	46.6	44.9	46.6
Specific Flow; lb/sec-ft^2	36.8	39.4	---
Pressure Ratio	1.048	9.54	10.0
Efficiency, η_{ad} (η_p); %	83.6(83.6)	83.8(88.0)	83.6(87.9)
Tip Speed; ft/sec	395	1390	---
Inlet Radius Ratio	0.604	0.655	---
Last Rotor Exist Radius Ratio	---	0.912	---
Exit Mach Number	---	0.35	---
Number of Variable Stators	1	1	2
Stall Margin; %	>18.0	18.0(1)	18.0(1)

(1) With 5% for Casing Treatment

Table XV. ILF2A1 Compressor and Supercharger Design Parameter Summary.

Design Parameter	Fan	Compressor	Overall
Design Flow; lb/sec	56.6	55.1	56.6
Specific Flow; $lb/sec\text{-}ft^2$	38.5	40.1	---
Pressure Ratio	1.048	5.68	7.0
Efficiency, η_{ad} (η_p); %	83.6(83.6)	84.6(88.1)	84.4(88.0)
Tip Speed; ft/sec	372	1410	---
Inlet Radius Ratio	0.626	0.663	---
Last Rotor Radius Ratio	---	0.879	---
Exit Mach Number	---	0.35	---
Number of Variable Stators	1	1	2
Stall Margin, %	>18.0	18.0(1)	18.0(1)

(1) With 5% for Casing Treatment

Table XVI. ILF2A1 Compressor and ILF2A2 Supercharger Design Parameter Summary.

Design Parameter	Supercharger	Compressor[1]	Overall
Design Flow; lb/sec	56.6	55.1	56.6
Specific Flow; lb/sec-ft^2	38.5	40.6	---
Pressure Ratio	1.029	6.80	7.0
Efficiency, η_{ad} (η_p); %	83.6(83.6)	84.0(87.6)	83.9(87.5)
Tip Speed; ft/sec	300	1437	---
Inlet Radius Ratio	0.626	0.663	---
Last Rotor Radius Ratio	---	0.879	---
Exit Mach Number	---	0.35	---
Number of Variable Stators	1	1	2
Stall Margin; %	>18.0	18.0[2]	18.0[2]

(1) Rematched to yield overall p/p = 7.0 at 56.6 lb/sec flow into the supercharger. Resultant compressor speed is 101.9%.

(2) With 5% for Casing Treatment.

Table XVII. Effect of Casing Treatment on Stall Margin.

Stage	$N/\sqrt{\theta}$	$SM^{(1)}$ for solid casing	$SM^{(1)}$ with casing treatment(2)	ΔSM
	%	%	%	%
Task I	100	21.3	27.8	6.5
	90	20.8	23.8	3.0
	70	29.3	32.6	3.3
Task II	100	17.8	26.0	8.2
	90	16.2	30.5	14.3
	70	26.9	38.4	11.5

(1) Constant Speed Stall Margin.

(2) Circumferential Deep Groove Configuration.

Table XVIII. Core Turbines Vector Diagram Details.

Engine	ILF1A1	ILF2A1 and ILF2A2
$\alpha_{IH}^{(o)}$	71.5	70.7
$\alpha_{IT}^{(o)}$	69.1	67.1
$\beta_{IH}^{(o)}$	50.6	40.6
$\beta_{2H}^{(o)}$	51.1	53.3
RX_H	0.24	0.35
$\Gamma_H^{(o)}$	0.9	0.9
$\Gamma_P^{(o)}$	0.9	0.9
M_{1H}	1.16	1.01
M_{0T}	0.20	0.21
M_{1T}	1.01	0.84
M_{R1H}	0.58	0.44
M_{R2H}	0.88	0.88
M_{R1T}	0.42	0.33
M_{R2T}	0.95	0.99
$AA_{W/T})_B$	1.75	1.23
$A_{W/T})_V$	1.02	0.95

Table XIX. Fan Drive Turbine Blading Summary.

ILF1A1

Stage	1	2	3
No. Nozzles	122	112	122
No. Blades	118	120	124
Rotor Pitch Axial Width (in).	1.0	1.0	0.9

ILF2A1

Stage	1	2	3
GJ $h/2U_P^2$	2.14	2.13	1.86
No. Nozzles	146	134	140
No. Blades	142	136	142
Rotor Pitch Axial Width (in.)	0.85	0.90	0.85

ILF2A2

Stage	1	2	3	4
No. Nozzles	148	142	140	158
No. Blades	144	150	148	156
Rotor Pitch Axial Width (in.)	0.90	0.91	0.93	0.79

Table XX. ILF1A1 Fan Drive Turbine Vector Diagram Details.

Stage No.	1	2	3
$\alpha_{1H}(o)$	56.8	62.6	60.6
$\alpha_{1T}(o)$	52.1	56.1	50.6
$\beta_{1H}(o)$	54.8	58.4	55.6
$\beta_{2H}(o)$	58.4	59.1	55.6
BX_H	0.10	0.10	0.10
$\Gamma_H(o)$	53.1	53.8	45.9
$\Gamma_P(o)$	49.8	48.9	38.8
M_{1H}	1.07	1.08	0.87
M_{0T}	0.56	0.66	0.63
M_{1T}	0.93	0.87	0.66
M_{R1H}	0.83	0.90	0.71
M_{R2H}	0.95	0.96	0.75
M_{R1T}	0.67	0.64	0.46
M_{R2T}	0.89	0.87	0.70
$A_W/t)_B$	1.64	1.64	1.58
$A_W/t)_V$	1.49	1.75	2.12

Table XXI. ILF2A1 Fan Drive Turbine Vector Diagram Details.

Stage No.	1	2	3
$\alpha_{IH}(o)$	54.0	59.7	59.8
$\alpha_{IT}(o)$	47.5	51.3	48.2
$\beta_{IH}(o)$	48.1	53.6	54.0
$\beta_{2H}(o)$	53.9	55.7	54.3
RX_H	0.10	0.10	0.10
$\Gamma_H(o)$	44.8	47.2	44.4
$\Gamma_P(o)$	40.4	41.3	36.7
M_{1H}	0.85	0.88	0.83
M_{OT}	0.53	0.52	0.51
M_{1T}	0.73	0.69	0.62
M_{R1H}	0.67	0.71	0.68
M_{R2H}	0.74	0.76	0.71
M_{R1T}	0.53	0.50	0.43
M_{R2T}	0.71	0.71	0.67
$A_W(t)_B$	1.57	1.58	1.58
$A_W(t)_V$	1.45	1.81	2.00

Table XXII. ILF2A2 Fan Drive Turbine Vector Diagram Details.

Stage No.	1	2	3	4
α_{1H}(o)	52.4	57.4	57.9	54.2
α_{1T}(o)	46.2	49.8	48.8	41.9
β_{1H}(o)	48.5	51.9	53.2	48.4
β_{2H}(o)	53.7	53.5	53.2	49.2
RX_H	0.10	0.10	0.10	0.10
Γ_H(o)	47.2	45.8	47.3	40.1
Γ_P(o)	43.2	41.1	41.2	32.7
M_{1H}	0.82	0.82	0.86	0.72
M_{0T}	0.52	0.54	0.53	0.54
M_{1T}	0.72	0.67	0.68	0.56
M_{R1H}	0.67	0.68	0.74	0.61
M_{R2H}	0.75	0.73	0.77	0.64
M_{R1T}	0.54	0.52	0.53	0.43
M_{R2T}	0.70	0.68	0.70	0.60
$A_W/t)_B$	1.67	1.74	1.77	1.66
$A_W/t)_V$	1.41	2.33	2.27	2.57

Table XXIII. HP Turbine Cooling Design Integral Lift Fan Engines.

	ILF1A1	ILF2A1 and ILF2A2
$T_{4\ cycle}/T_{4\ design}$ (including margin)	2500° F/2634° F	2000° F/2110° F
Vane:		
Design Gas Temperature	3087° F	2434° F
Bulk Metal Temperature	1850° F	1700° F
Cooling Effectiveness & Type	0.52-Convection & Film	0.40-Convection
Cooling Flow	33% Thru Flow and 4% Film	38% Thru Flow and 1% T.E.
Blade:		
Design Gas Temperature	2485° F	1977° F
Bulk Metal Temperature	1610° F	1610° F
Cooling Effectiveness & Type	0.50-Film/ Convection Holes	0.27-Convection
Cooling Flow	3.1%	1.1%

Table XXIV. LP Turbine Cooling Design Integral Lift Fan Engine.

	ILF1A1		ILF2A1 & ILF2A2
	Stage 1	Stage 2	Stage 1
Vane:			
Design Gas Temperature	2366° F	2101° F	1944° F
Bulk Metal Temperature	1900° F	1900° F	1900° F
Cooling Effectiveness & Type	0.29-Conv.	0.15 Conv.	0.04-Convection
Cooling Flow	3.95%(*)	1.0%	1.3% (Seal Blockage)
Blade:			
Design Gas Temperature	2120° F	Cooling	Cooling
Bulk Metal Temperature	1900° F	Not	Not
Cooling Effectiveness & Type	0.18-Conv.	Required	Required
Cooling Flow	1.25%		

(*) Includes LP Blade Coolant.

Table XXV. ILF1A1 Turbine Performance Integral Lift Fan Engine.

Clean Aerodynamic Efficiency: η_{HP} = 89.8% η_{LP} = 83.5%

Cooling and Leakage Flow Effects	Amount of Flow	Returned to Cycle	Net $\Delta\eta$
HP Turbine:			
Vane Coolant	4.0%	Station 4.0	-0.40 pts.
Aft Band Coolant	0.6%	Station 5.1	-0.05 pts.
Inducer Seal Leakage	1.5%	Station 5.1	-1.64 pts.
Blade & Shroud Coolant	3.6%	Station 5.1	-0.69 pts.
LP Turbine:			
Vane 1 Fwd. Leakage and T.E. Coolant	1.1%	Station 5.4	-0.22 pts.
Vane 1 Aft Leakage	0.9%	Station 5.6	+0.13 pts.
Blade Coolant	1.25%	Station 5.6	+0.40 pts.
Vane 2 Fwd. Leakage and T.E. Coolant	0.9%	Station 5.6	+0.04 pts.
Vane 2 Seal and Shroud 2 Leakage	0.4%	Station 5.6	-0.06 pts.

Net HP Efficiency: η_{HP} = 87.0%

Net LP Efficiency: η_{LP} = 83.8%

Table XXVI. ILF2A1 and ILF2A2 Turbine Performance Integral Lift Fan Engine.

Clean Aerodynamic Efficiency: η_{HP} = 90.0% η_{LP} = 86.6%

Cooling and Leakage Flow Effects	Amount of Flow	Returned to Cycle	Net $\Delta\eta$
HP Turbine:			
Vane Coolant	1.0%	Station 4.0	-0.10 pts.
Inducer Seal Leakage	1.1%	Station 5.1	-1.22 pts.
Blade & Shroud Coolant	1.3%	Station 5.1	-0.06 pts.
LP Turbine:			
Vane 1 Fwd. Leakage	0.1%	Station 5.4	-0.02 pts.
Vane 1 Aft. Leakage	0.6%	Station 5.6	+0.12 pts.
Stages 1 & 2 Shroud Leakage	0.3%	Station 5.6	-0.10 pts.

Net HP Efficiency: η_{HP} = 88.6%

Net LP Efficiency: η_{LP} = 86.6%

Table XXVII. Acoustic Splitter Design.

Cycle	ILF1A1	ILF2A1	ILF2A2
Fan P/P (Design Pt)	1.25	1.20	1.20
Fan Exhaust			
Number	3	3	3
Length	15"	15"	15"
Thickness	0.75"	0.75"	0.75"
Total Square Ft.	126.6	110.1	116.5
Design Frequency	3.2 KHz	3.2 KHz	3.2 KHz
Turbine Exhaust			
Number	2	2	2
Length	5"	6"	6.5"
Thickness	0.5"	0.5"	0.5"
Total Square Ft.	13.1	16.5	19.9
Design Frequency	4 KHz	4 KHz	4 KHz

Table XXVIII. Noise Constituents.

Noise Rating Point (10000 lb) PNdB, 500 ft. Sideline
12 Engines 90° F Day

Engine	ILF1A1	ILF2A1	ILF2A2
Fan P/P (design pt.)	1.25	1.20	1.20
Fan Unsuppressed	115.6	114.1	116.7
Fan Suppressed	93.9	93.7	91.8
Fan Jet	85	78.9	78.9
Core Jet	85.8	82.4	82.4
Total Jet	88.7	84.2	84.2
Turbine Unsuppressed	96.4	96.3	97.6
Turbine Suppressed	83.8	83.7	85.0
Total Jet plus Turbine	90.2	87.8	88.3
Total System	96.1*	95.3	94.5
Objective	98	95	95

* Could be reduced to 95 PNdb with additional treatment (Δ3" splitter length).

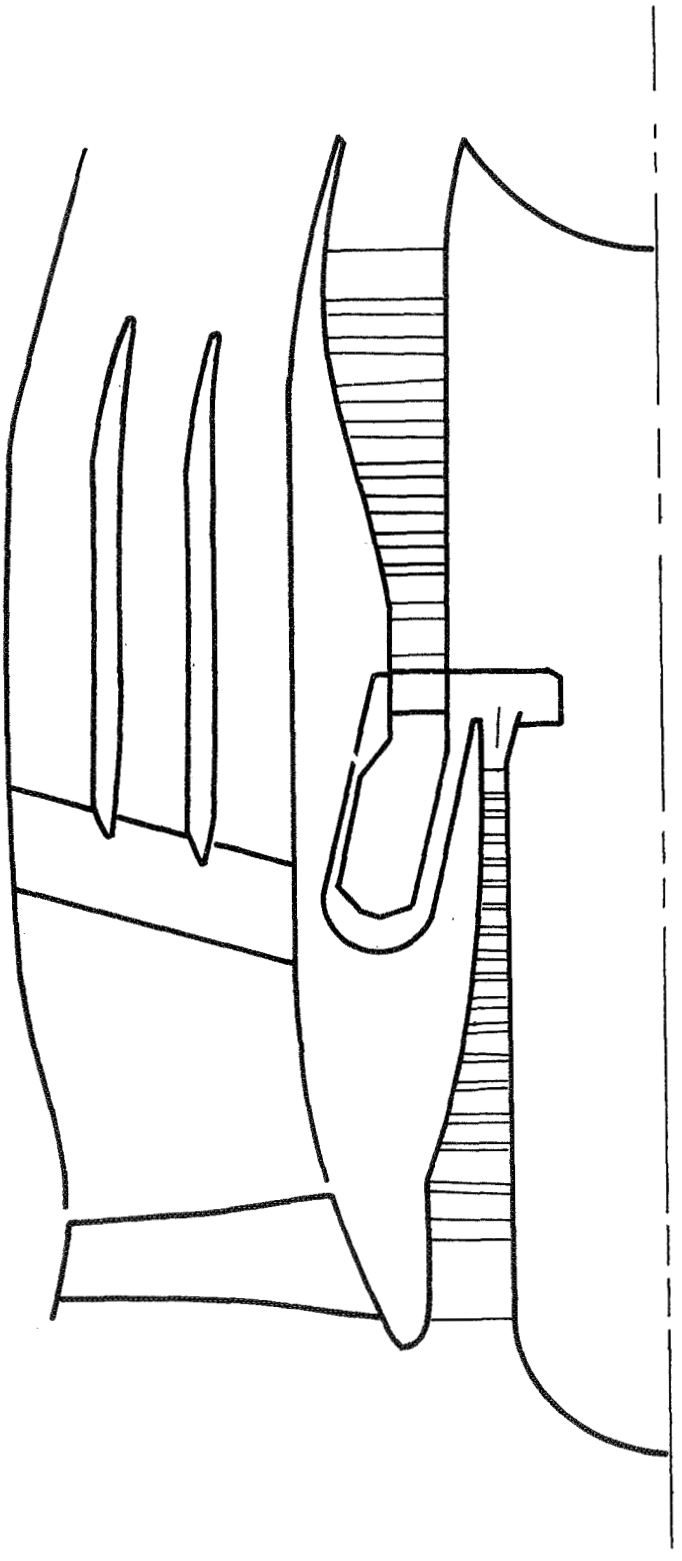

Figure 1. Non-Geared Parametric Engine.

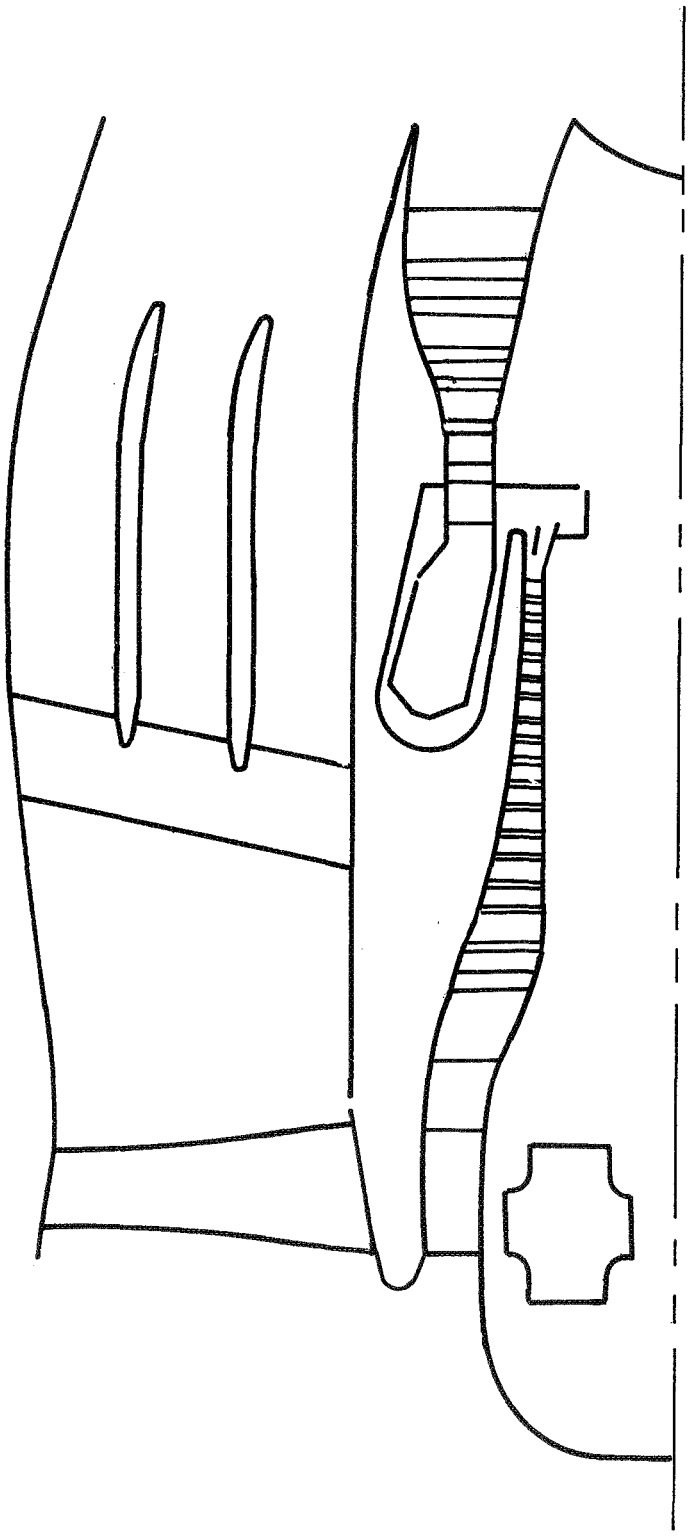

Figure 2. Geared Parametric Engine.

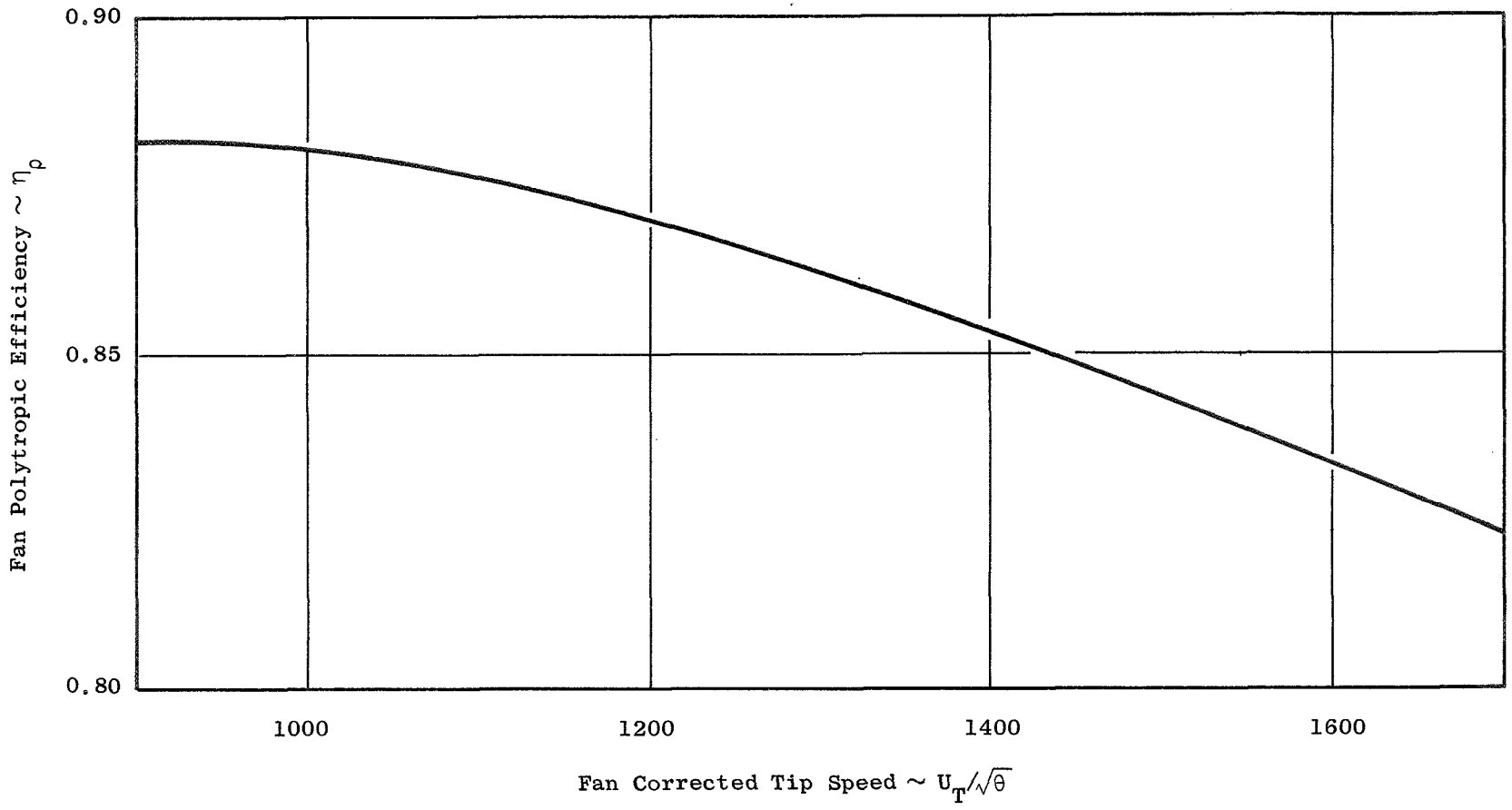

Figure 3. Relation Between Tip Speed and Polytropic Efficiency for Parametric Study.

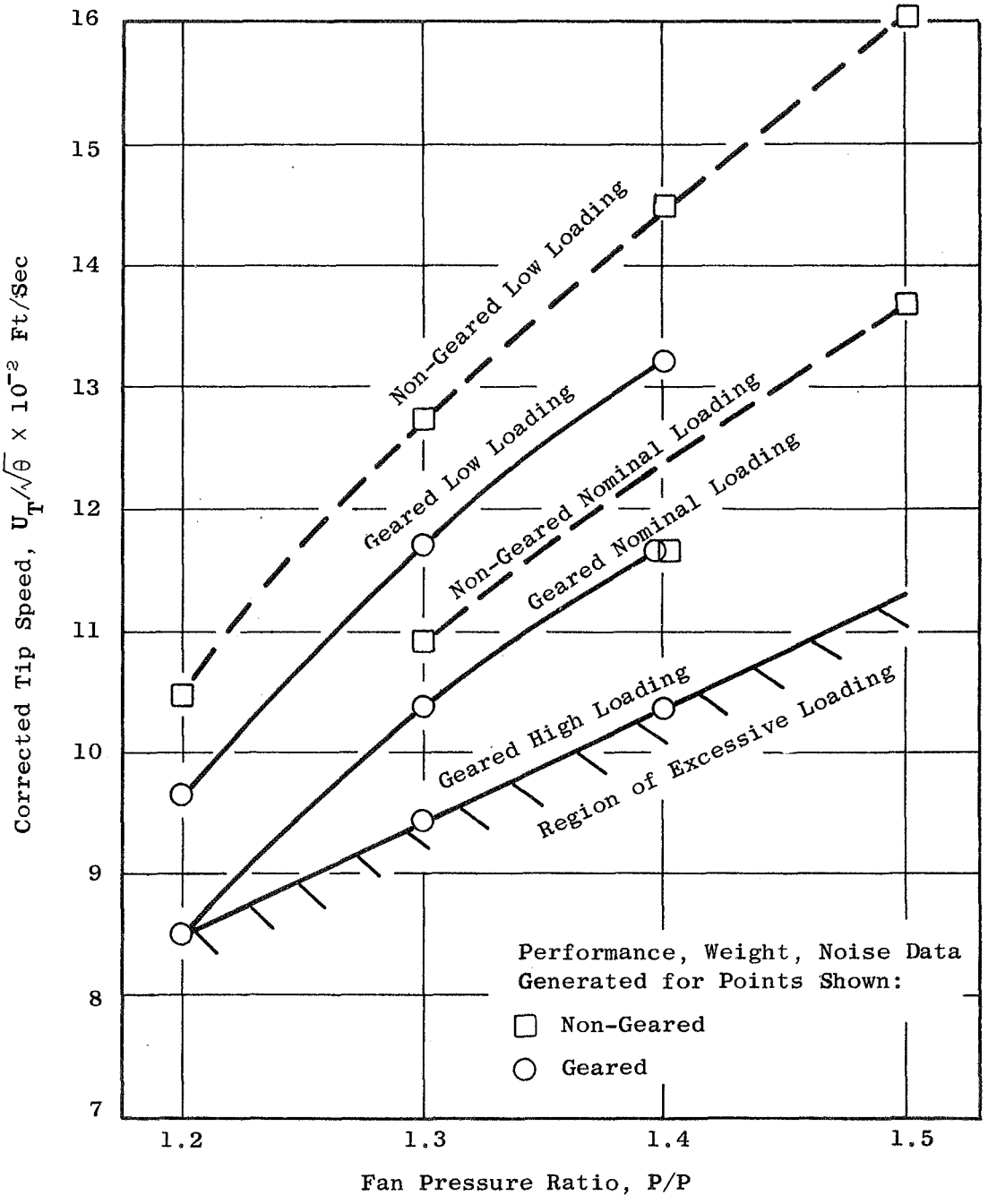

Figure 4. Integral Lift Fan Study Task I Selected Relation Between Fan P/P and Tip Speed.

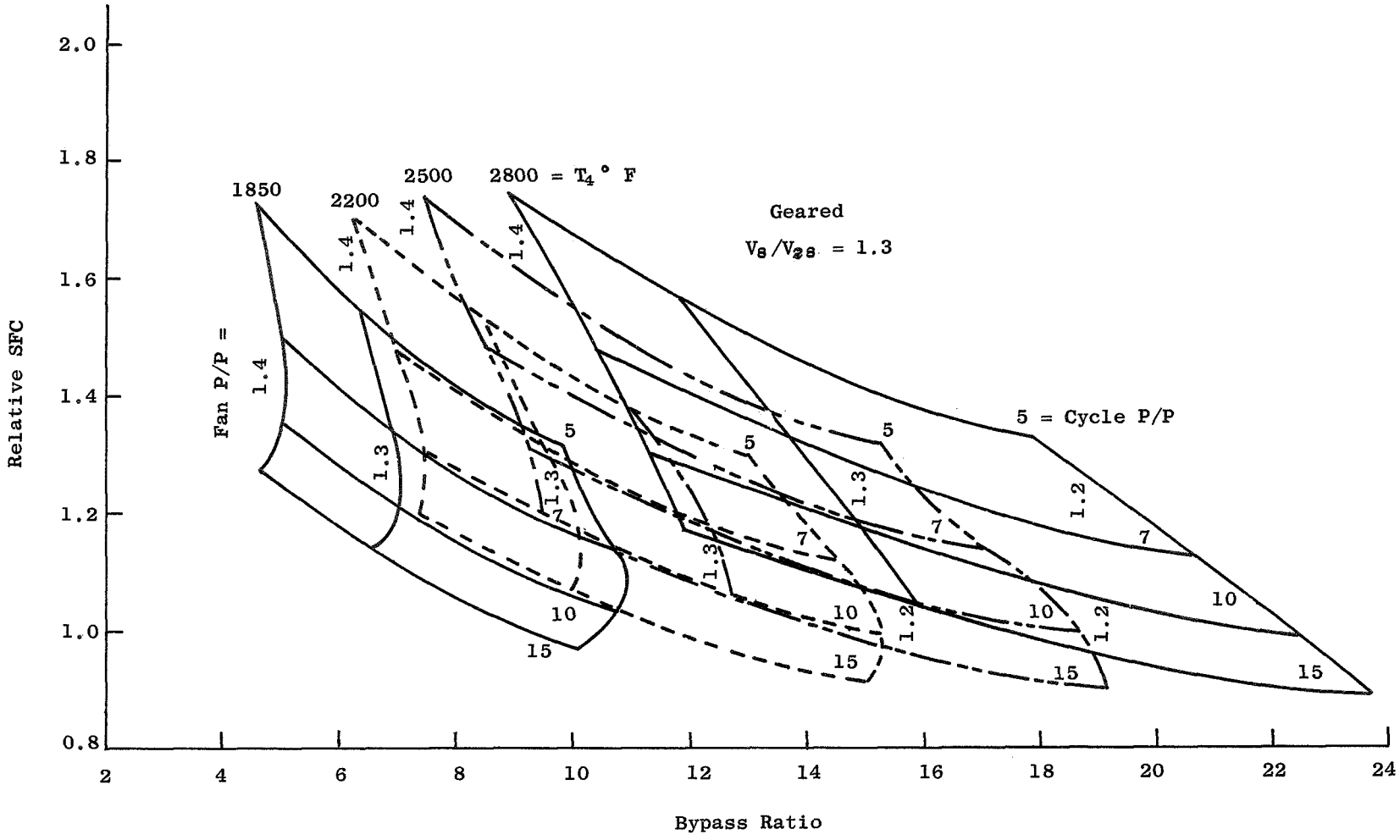

Figure 5. Integral Lift Fan Engine Study Task I Parametric Data.

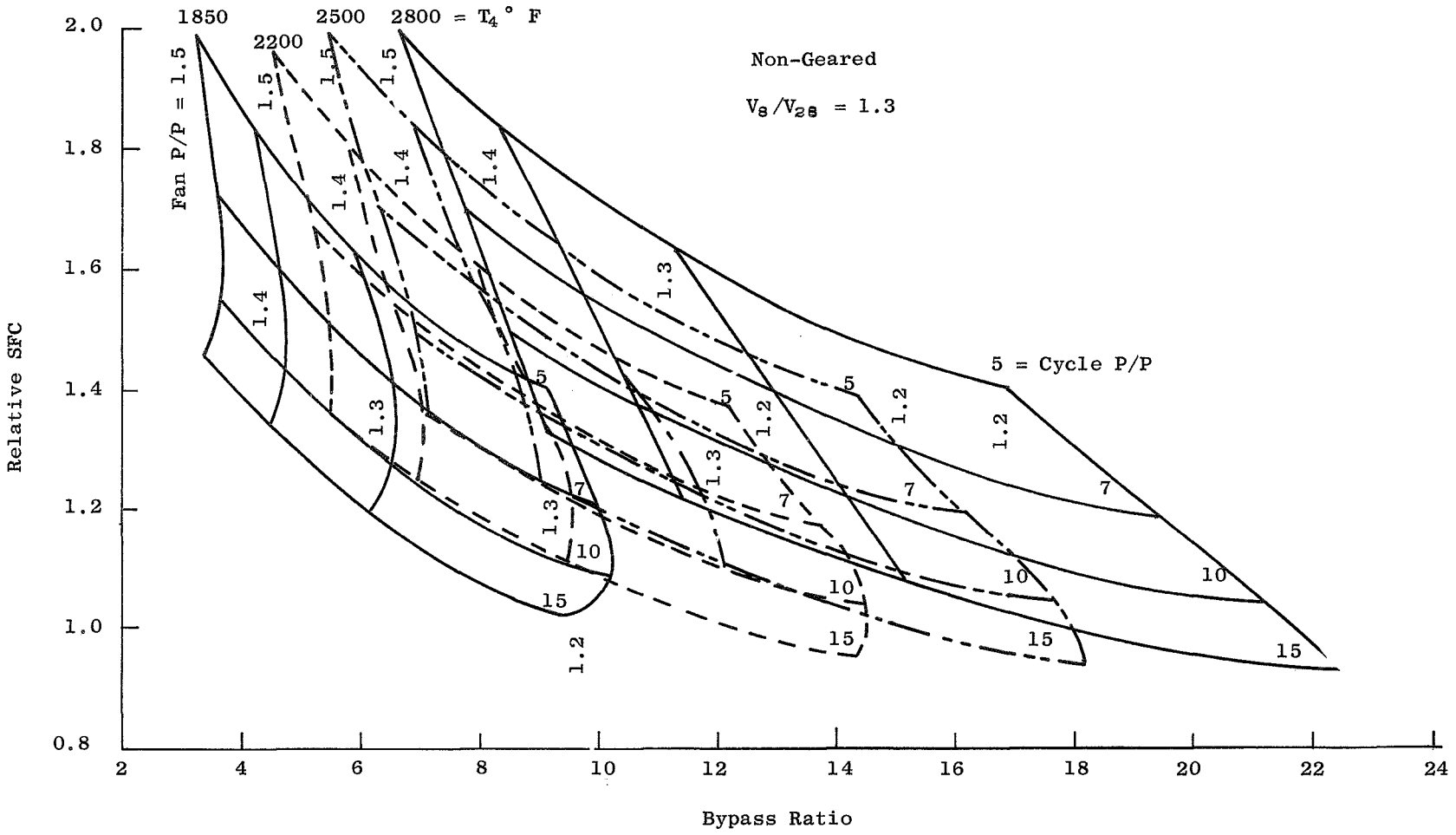

Figure 6. Integral Lift Fan Engine Study Task I Parametric Data.

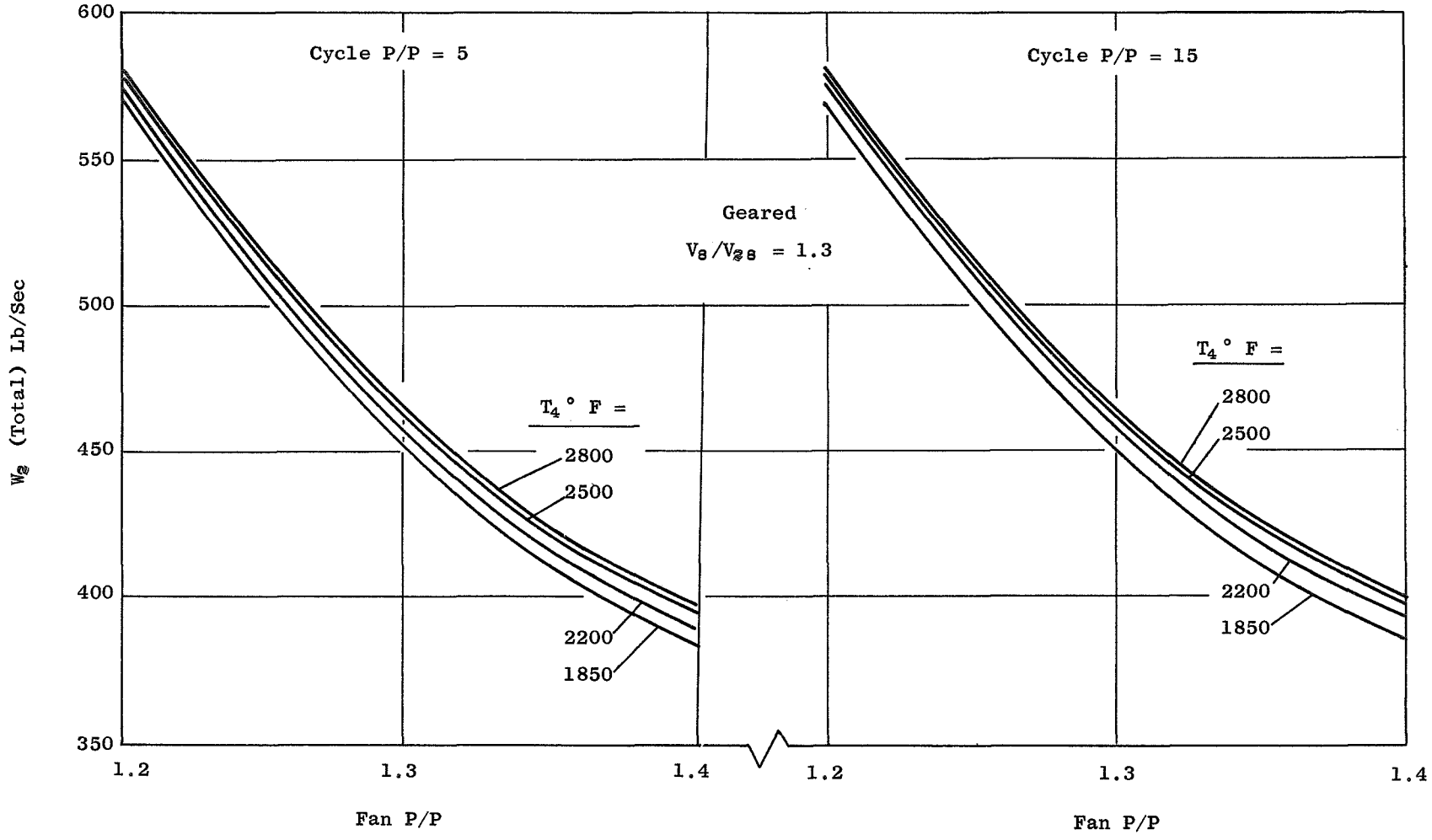

Figure 7. Integral Lift Fan Engine Study Task I Parametric Data.

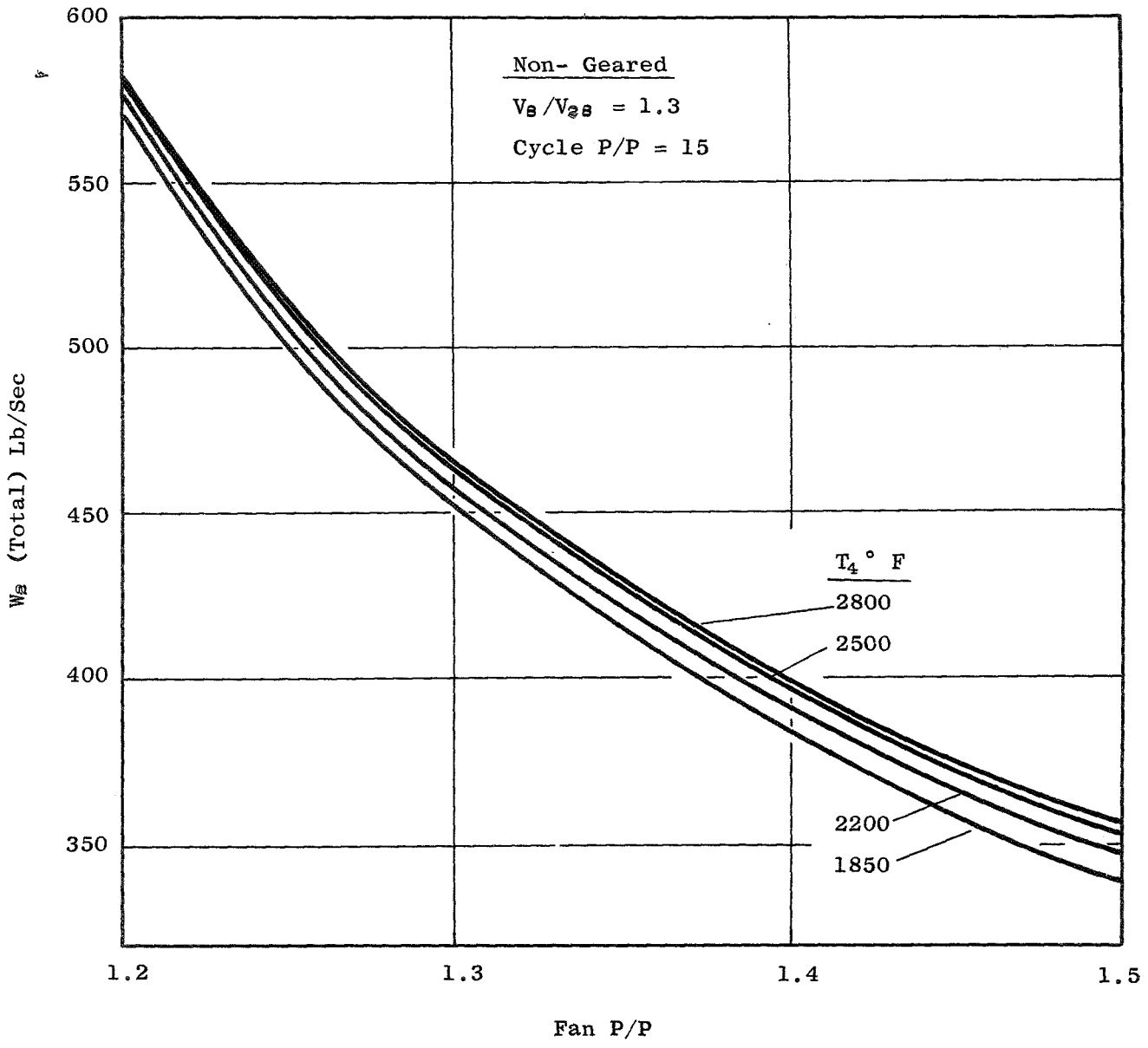

Figure 8. Integral Lift Fan Engine Study Task I Parametric Data.

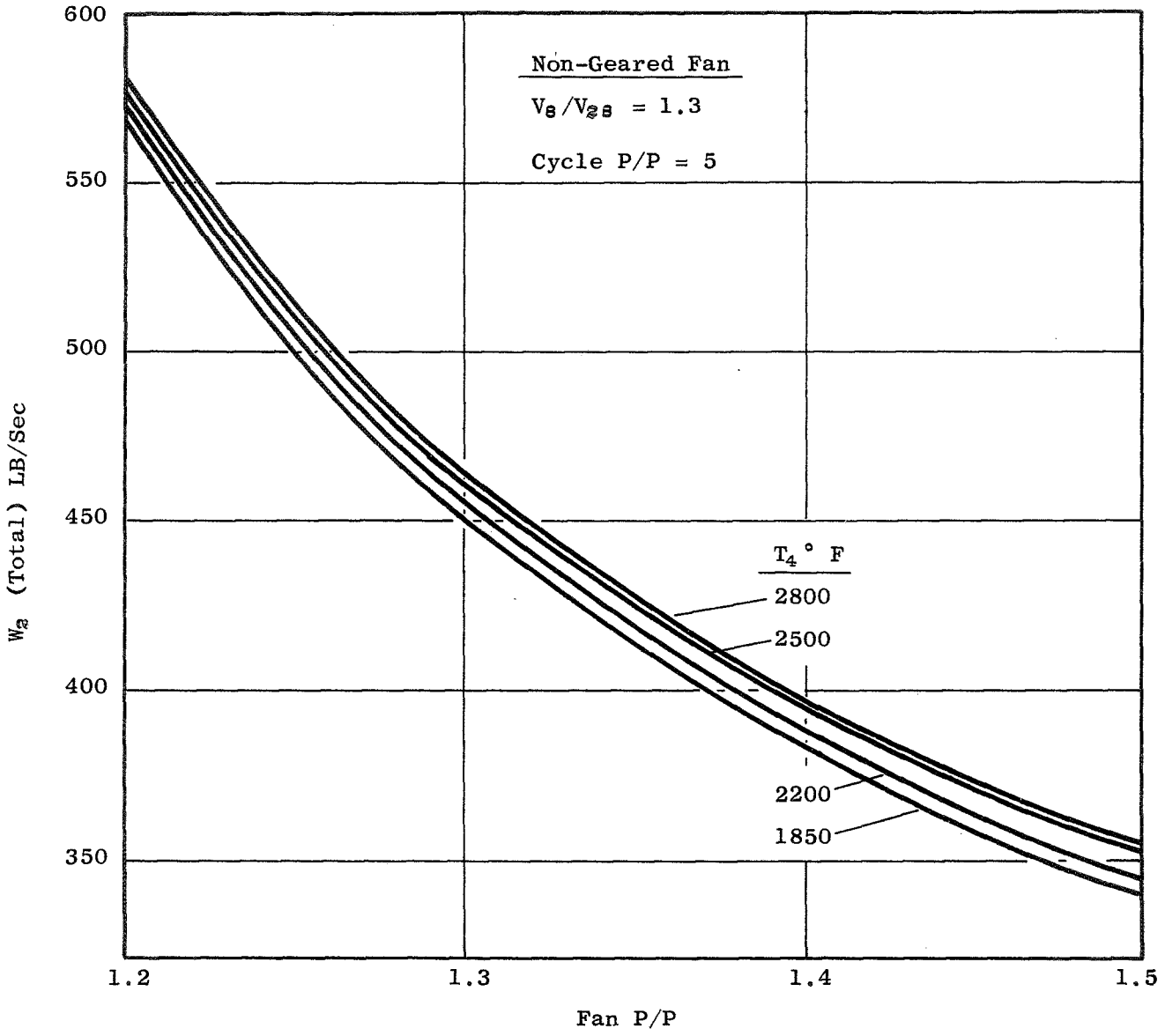

Figure 9. Integral Lift Fan Engine Study Task I Parametric Data.

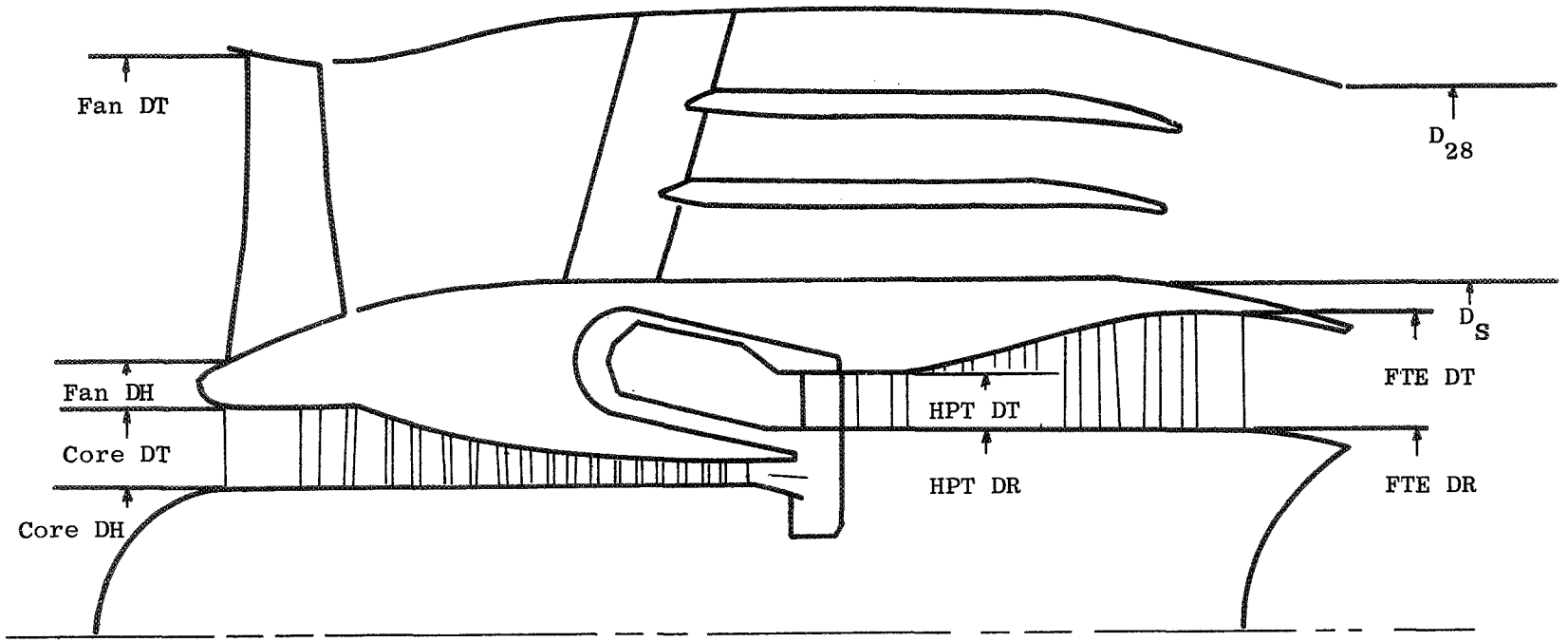

Figure 10. Sizing Procedures - Dimensions, Non-Geared Configurations.

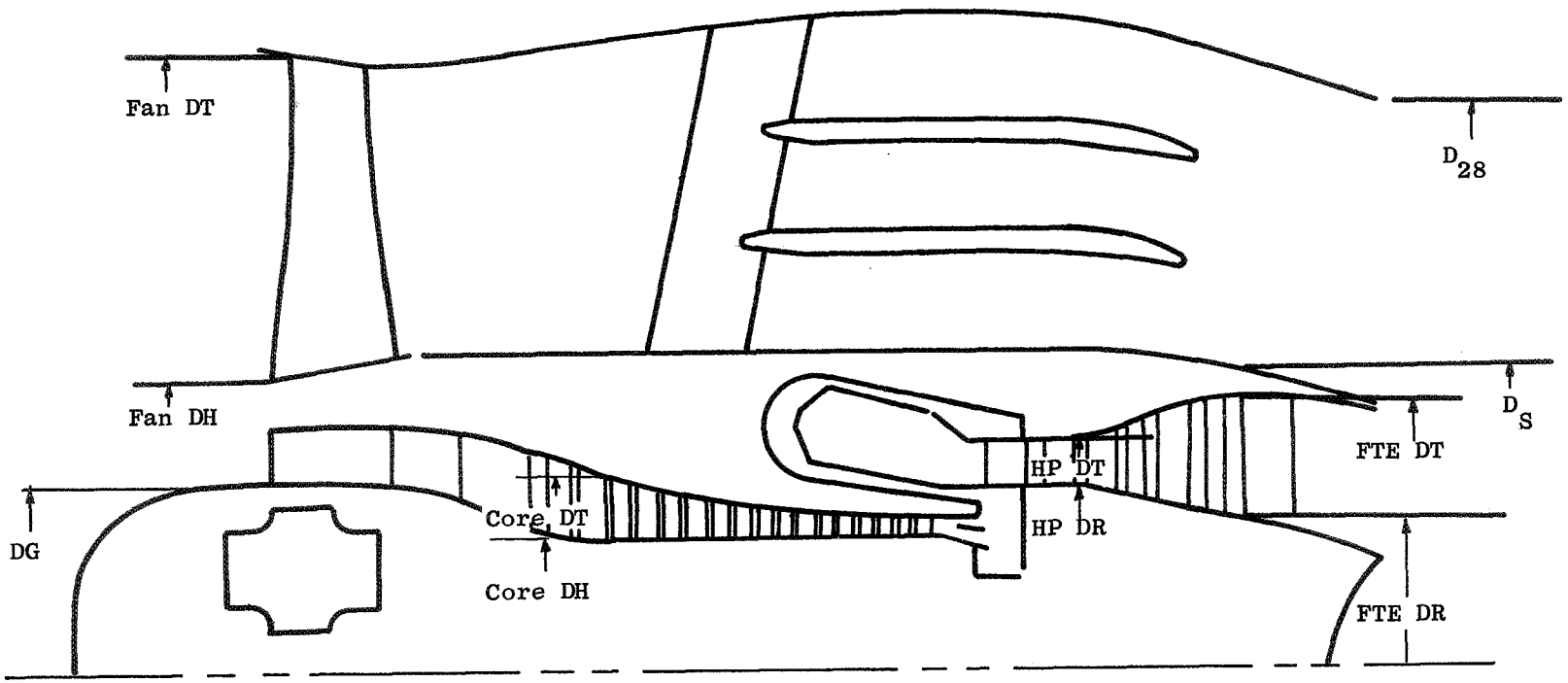

Figure 11. Sizing Procedures - Dimensions, Geared Configuration.

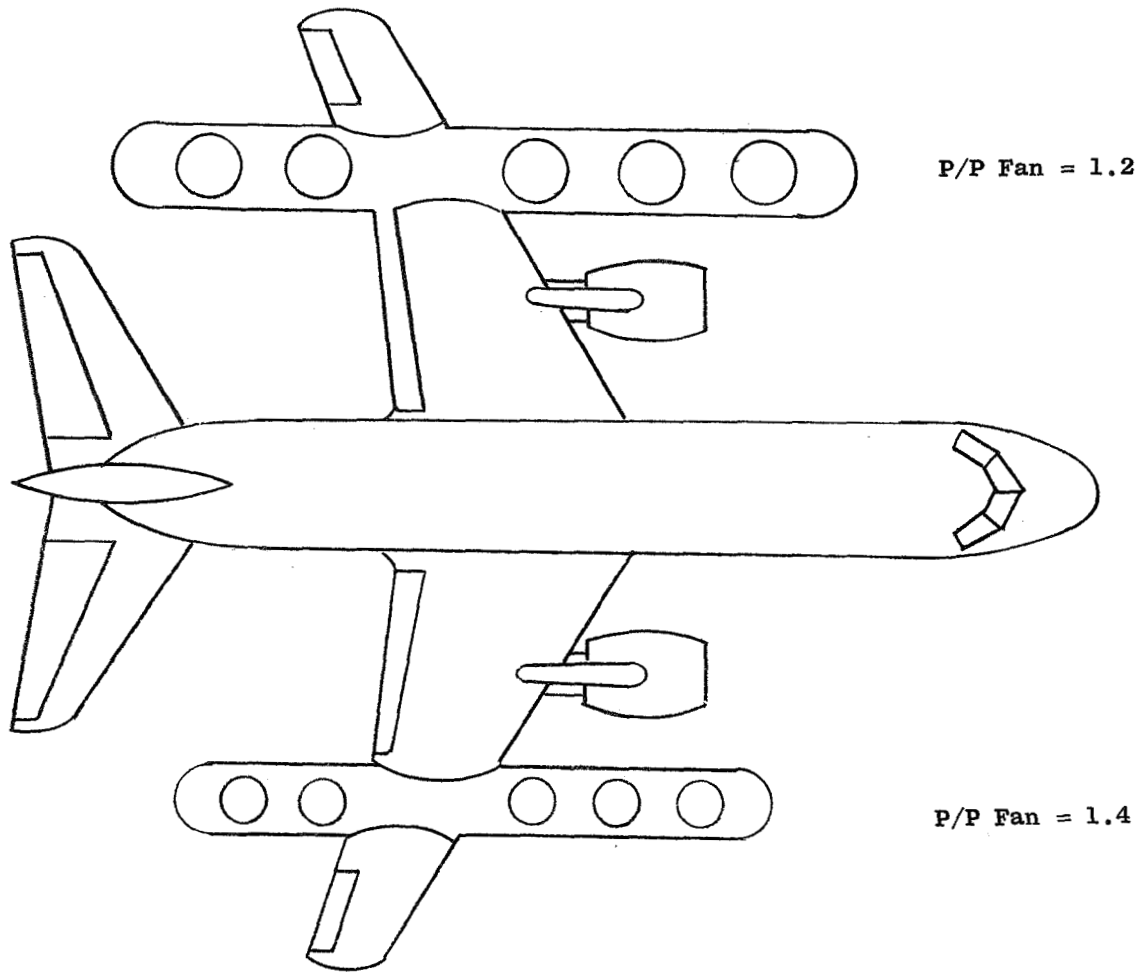

Figure 12. Effect of Fan Pressure Ratio on POD Size.

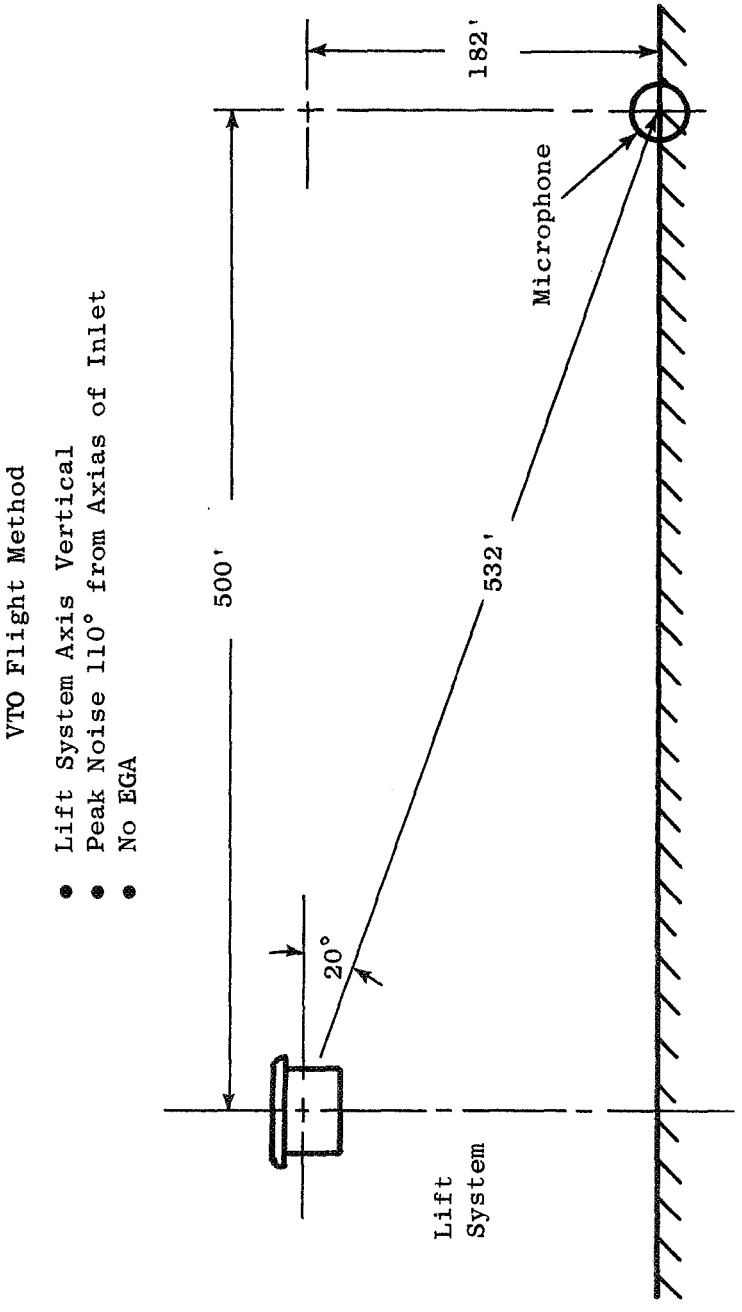

Figure 13. 500 Foot Sideline Definition.

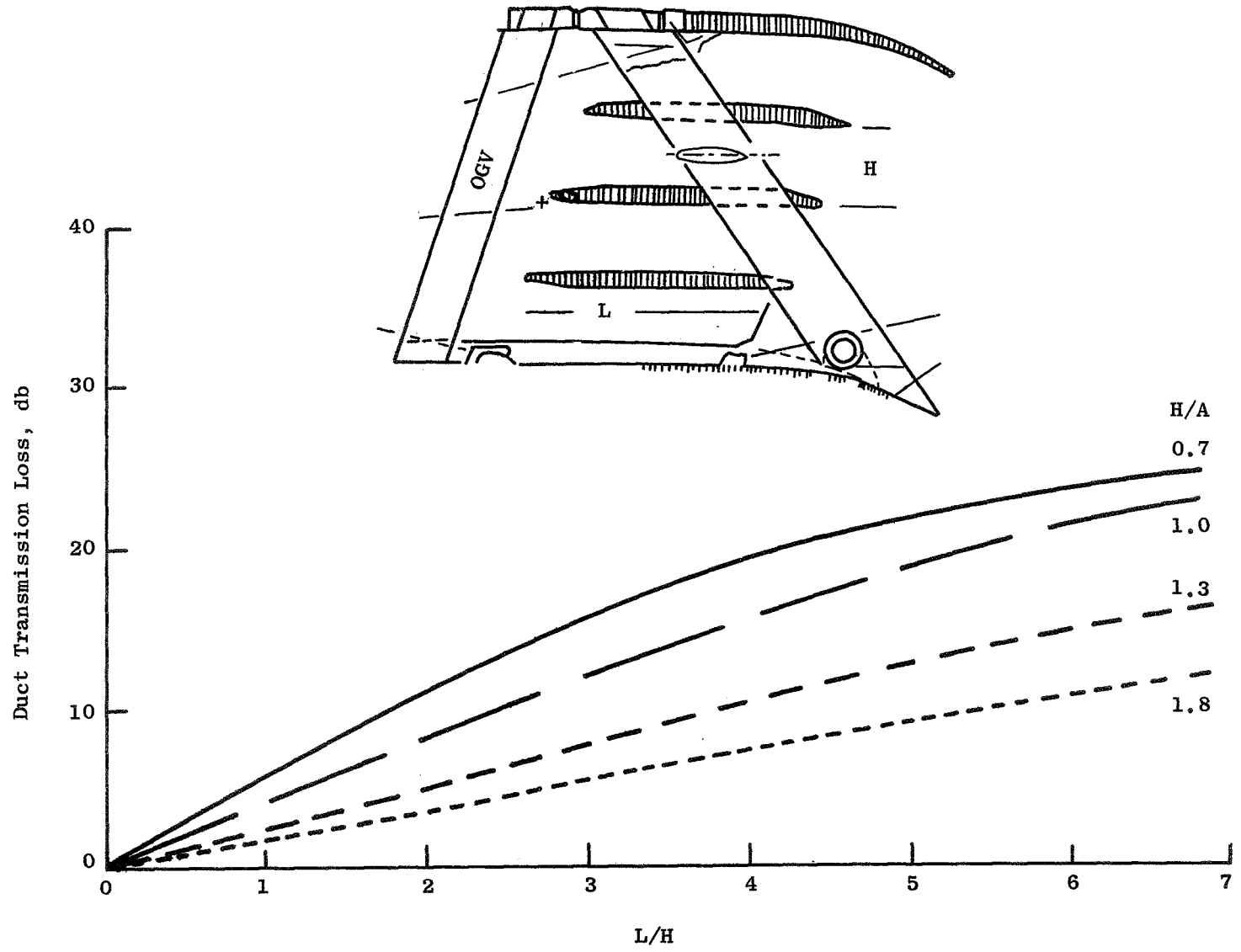

Figure 14. Acoustic Splitter Suppression Characteristics.

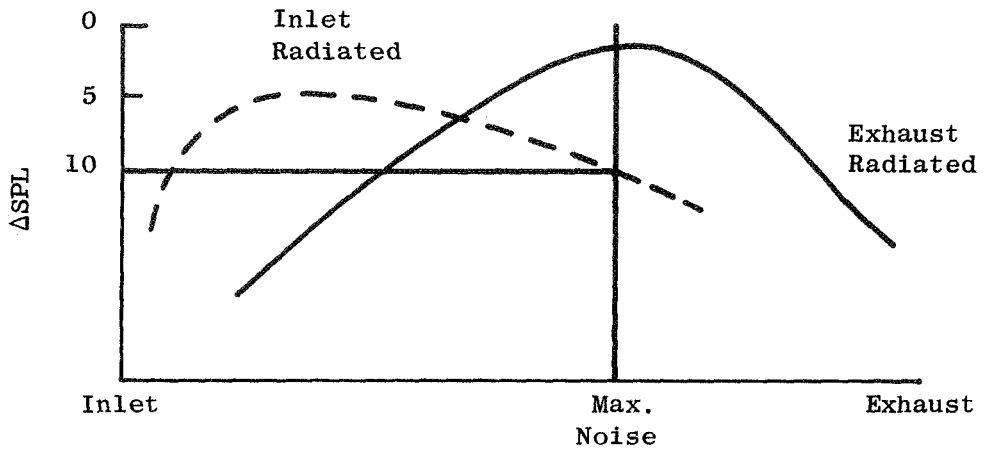

- Exhaust Noise Suppressed to Equal Inlet Noise Before Inlet Suppression Required
- Inlet Radiated Noise 10 db Below Exhaust Radiated Noise
- Inlet Suppression = Fan Suppression, 7 PNdB
- As Source Noise is Reduced, Inlet Suppression Requirements Reduced to Maintain Constant Total Noise
- ΔPNdB Inlet = ΔPNdB Exhaust - 7 PNdB - ΔPNdB Source

Figure 15. Inlet Suppression Requirements.

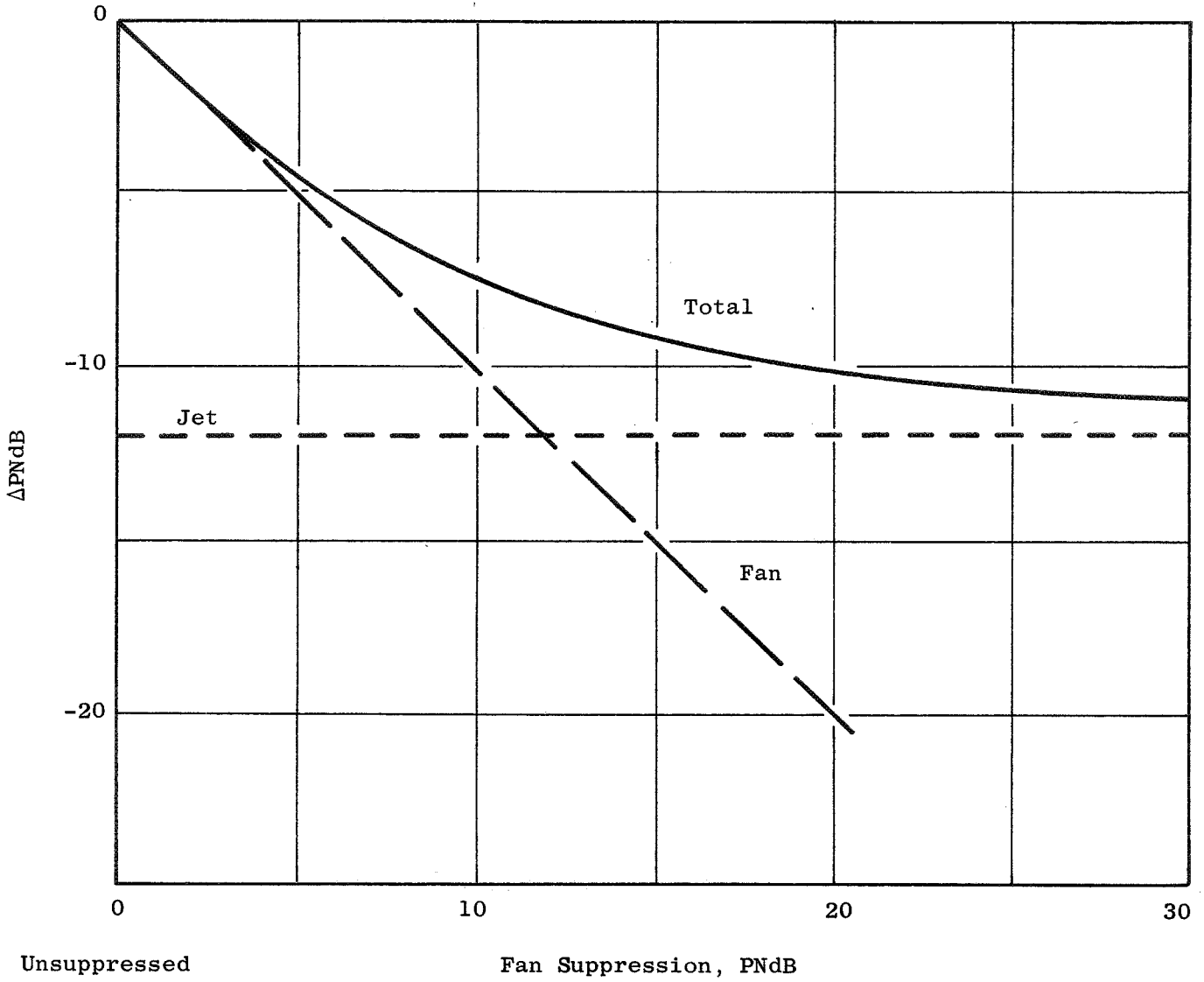

Figure 16. Effect of Fan Suppression on Total Noise.

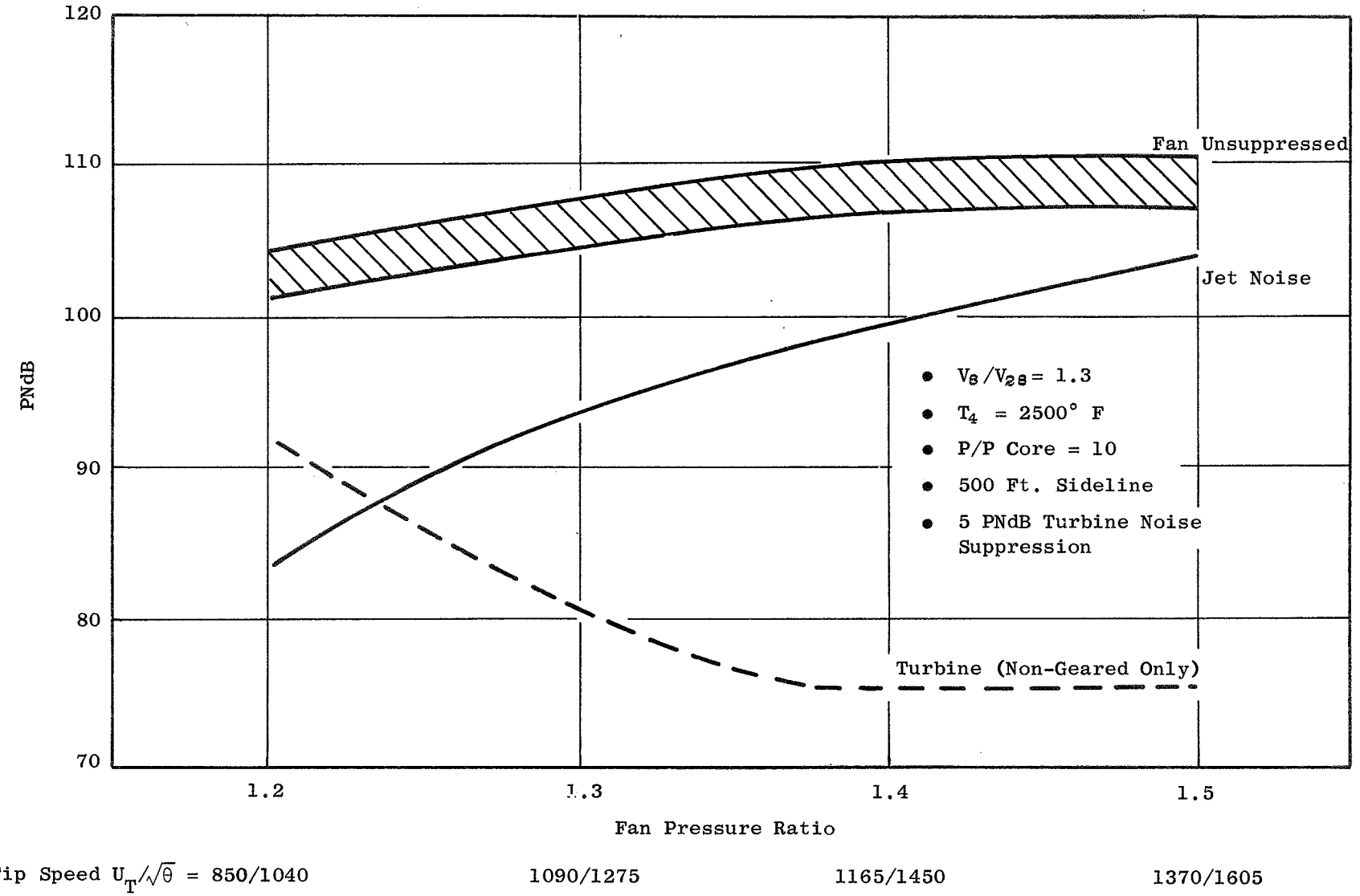

Figure 17. Noise Constituents at 100% Design Thrust.

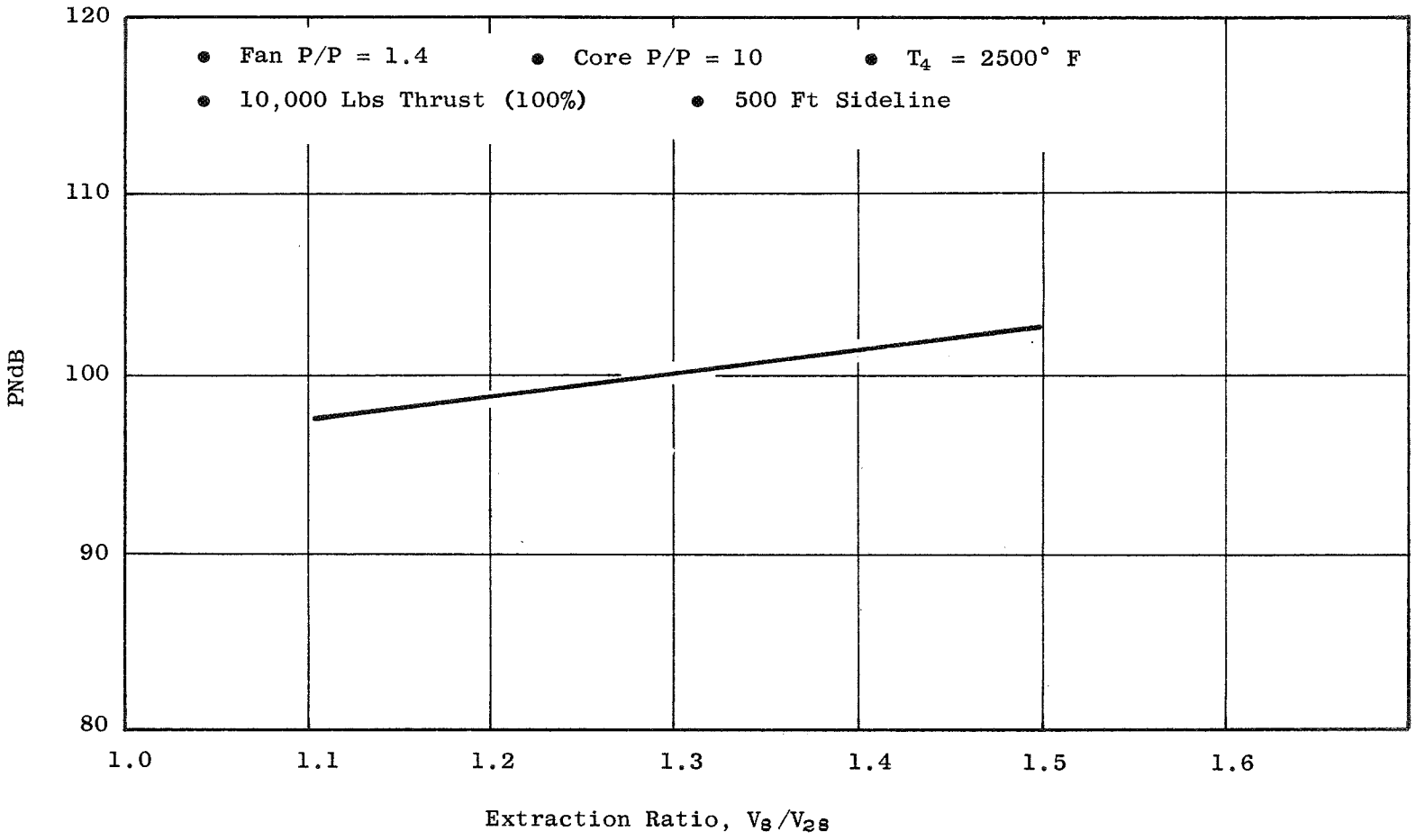

Figure 18. Effect of Cycle Extraction Ratio on Jet Noise.

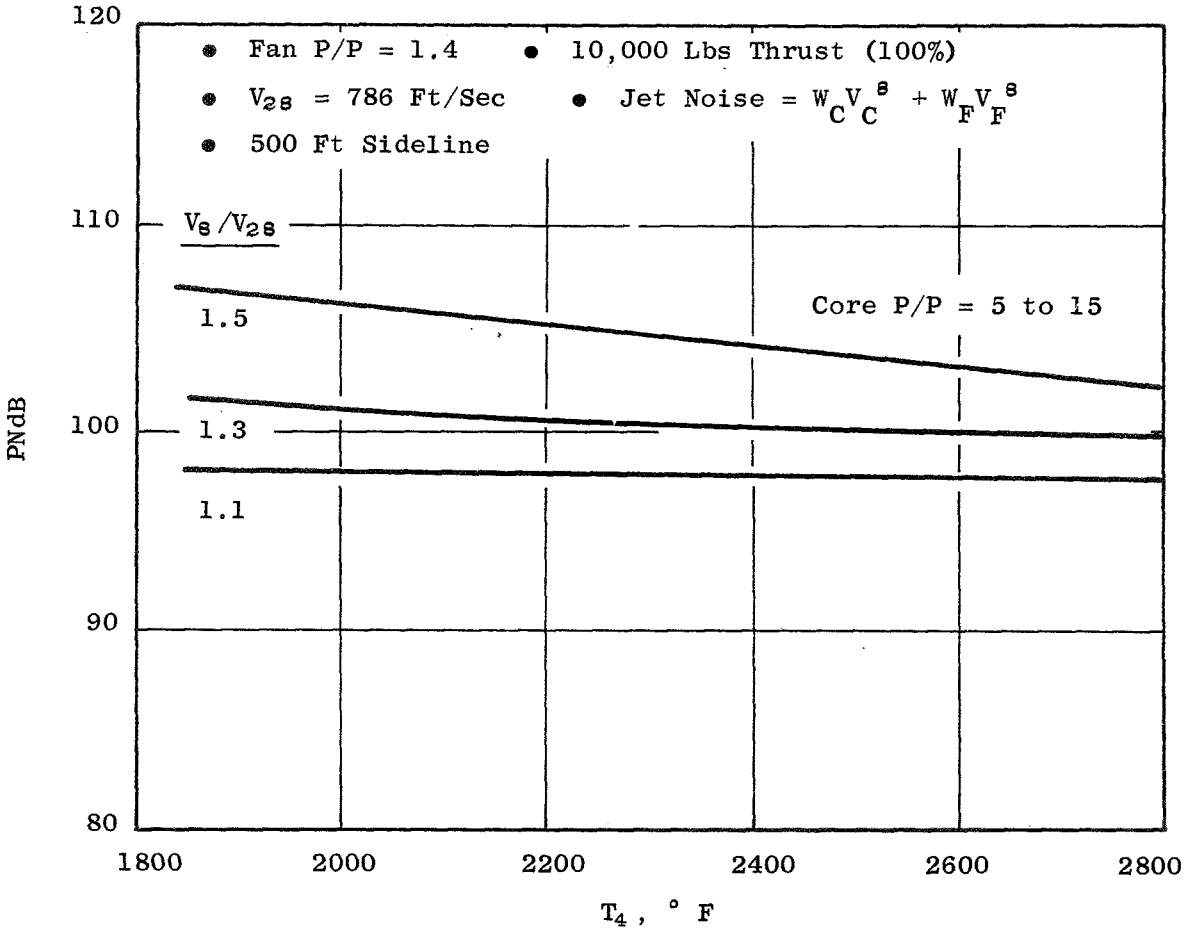

Figure 19. Effect of Cycle T_4 on Jet Noise.

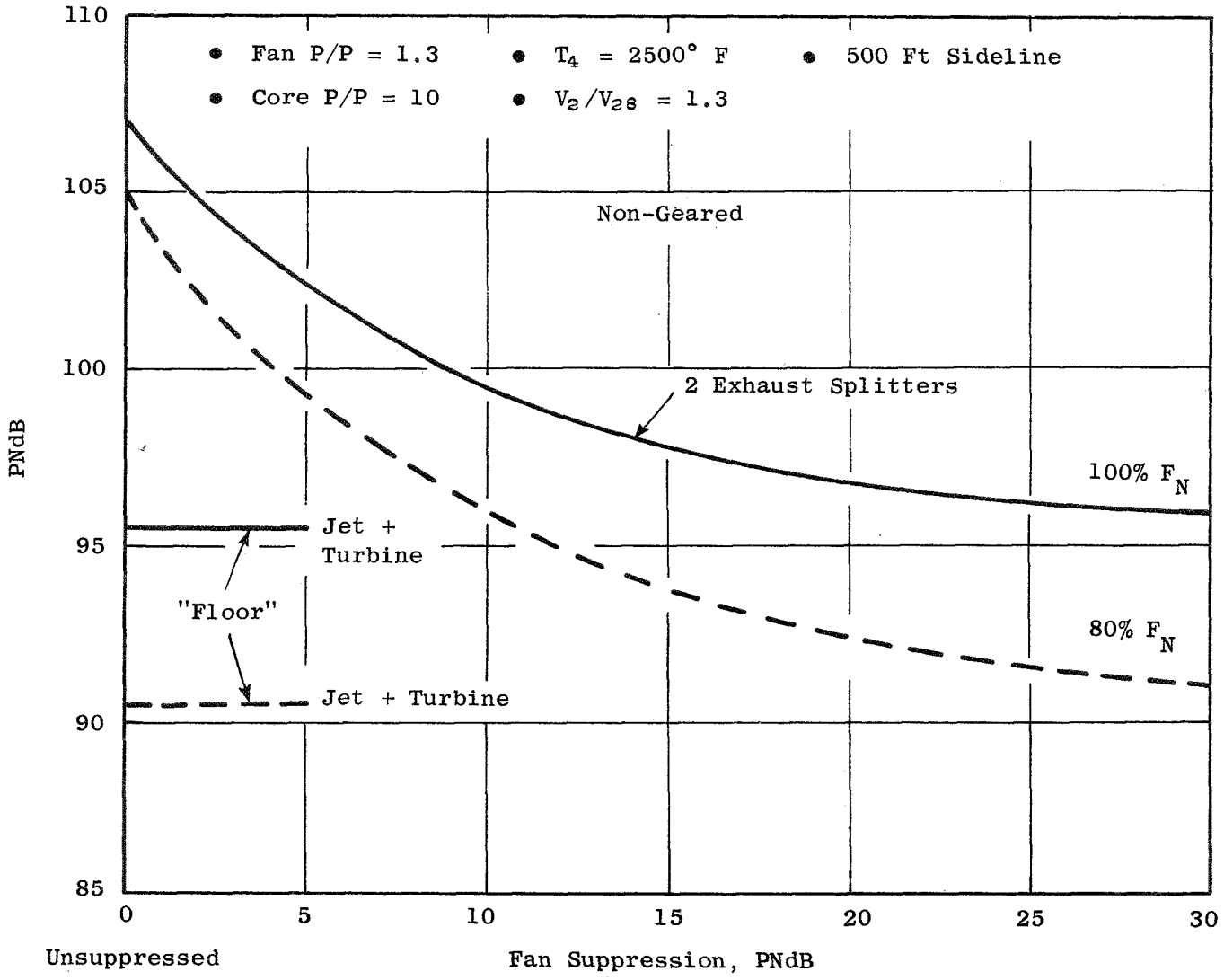

Figure 20. Effect of Thrust on Suppressed Noise.

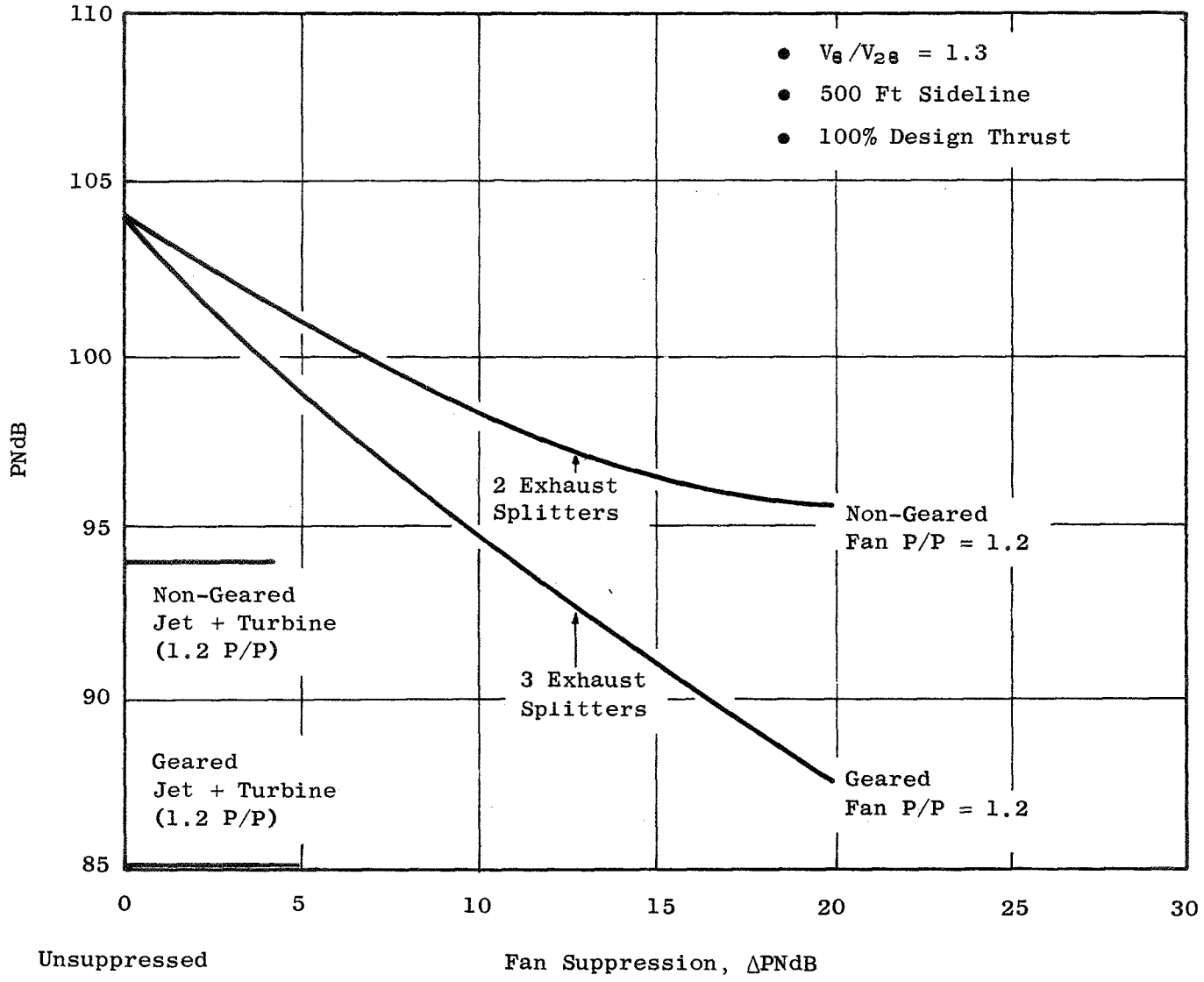

Figure 21. Effect of Pressure Ratio on Noise.

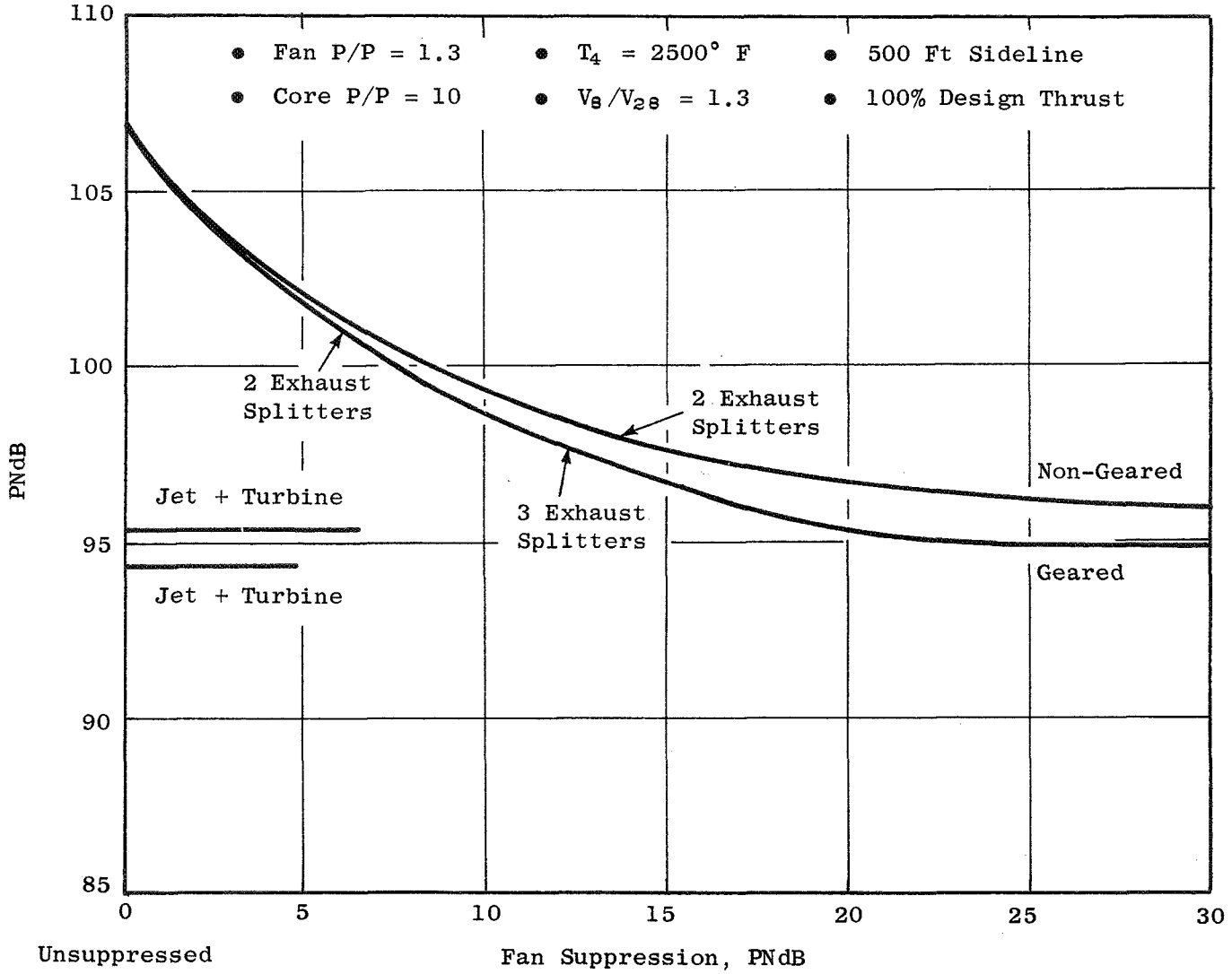

Figure 22. Comparison of Non-Geared and Geared Suppressed Noise.

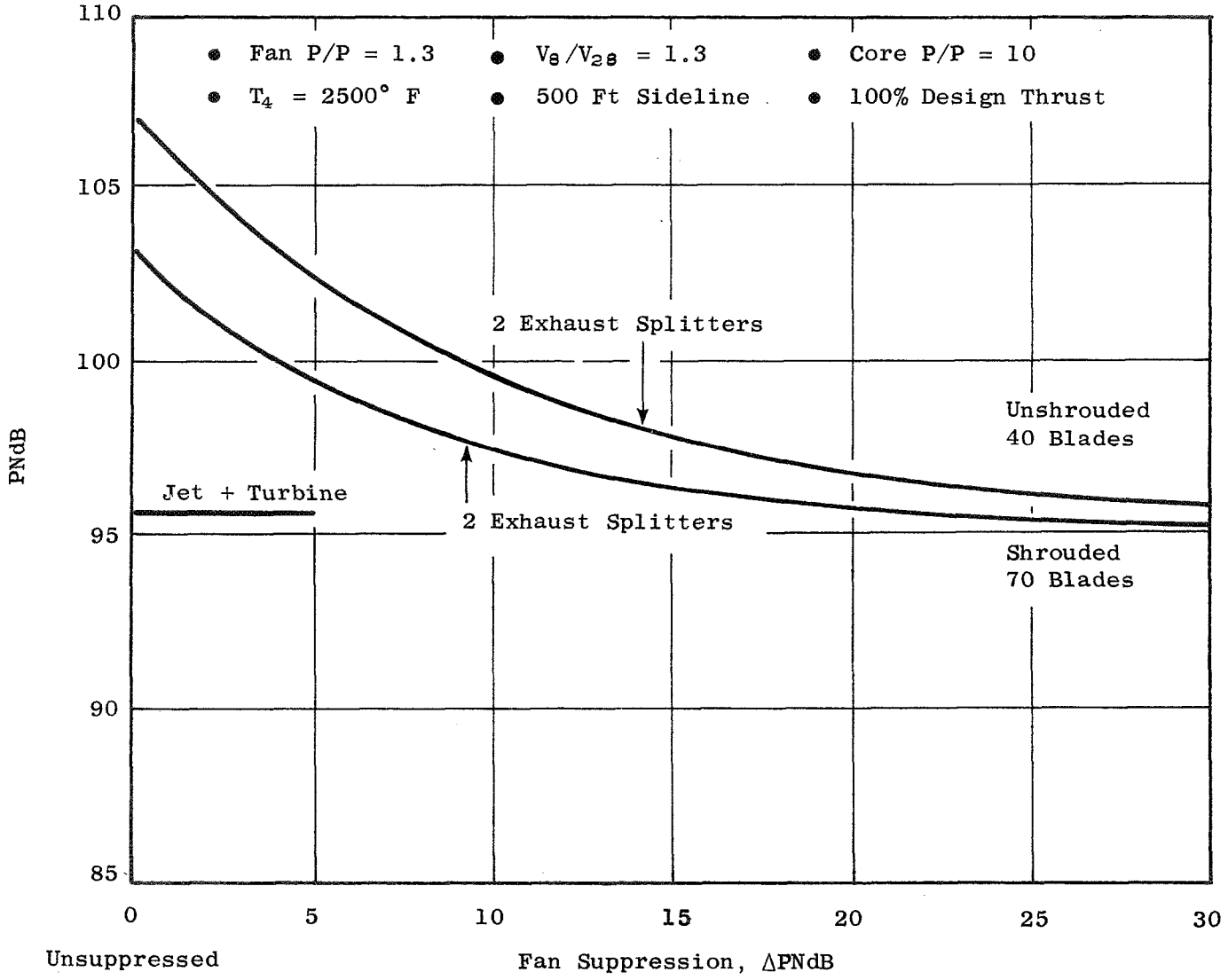

Figure 23. Effect of Blade Number on Non-Geared Noise.

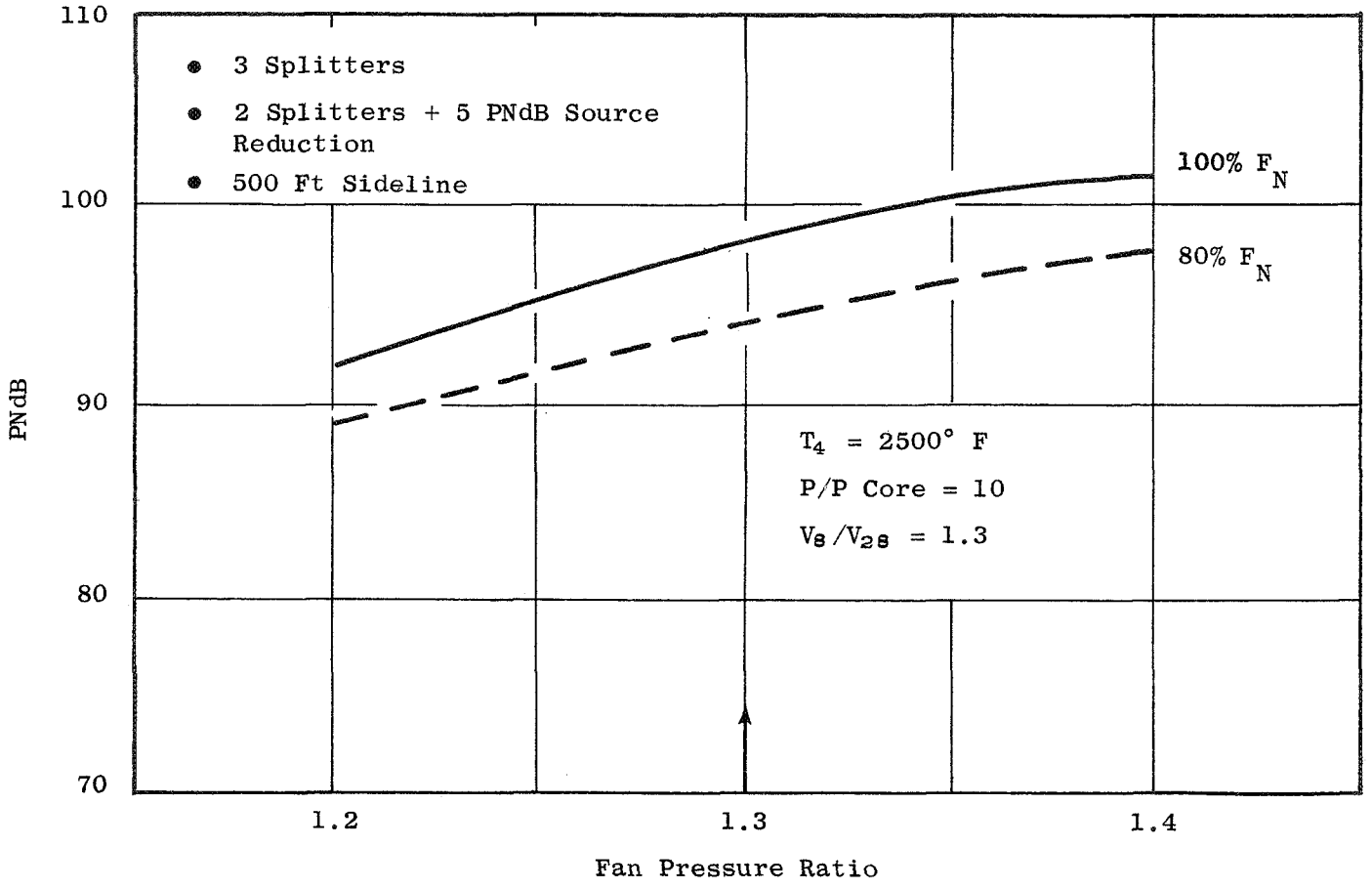

Figure 24. Geared Unshrouded Fan Suppressed Noise.

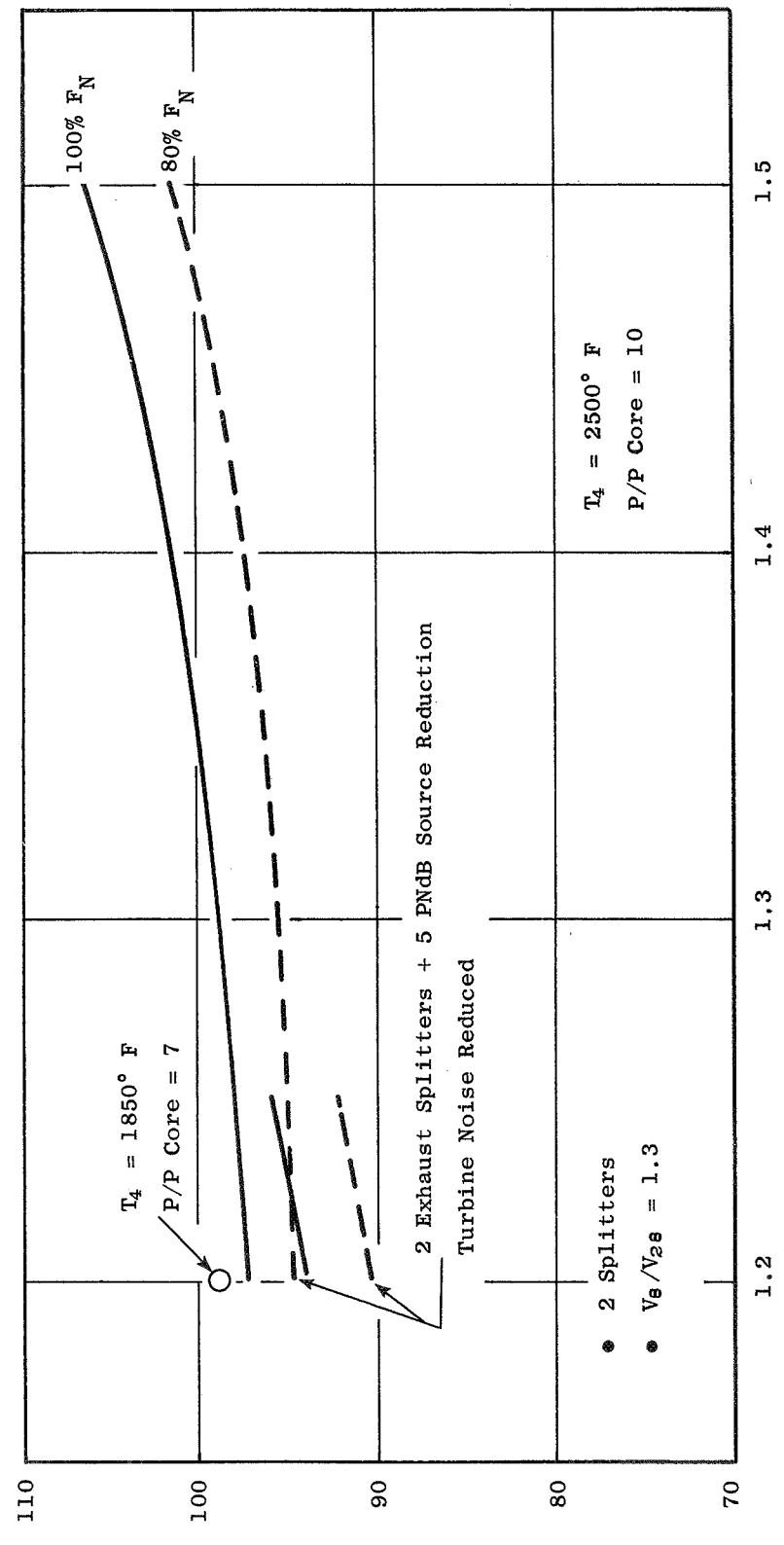

Figure 25. Non-Geared Unshrouded Fan Suppressed Noise.

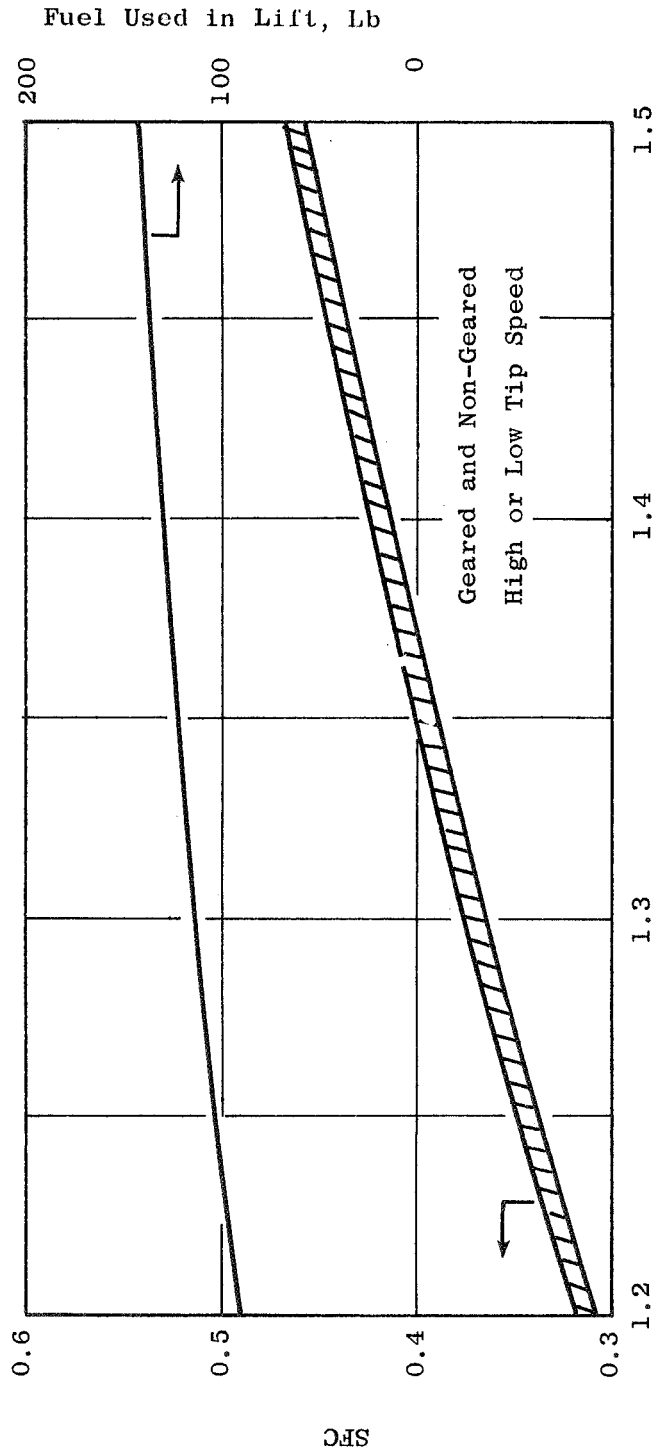

Figure 26. Effect of Fan Pressure Ratio on SFC.

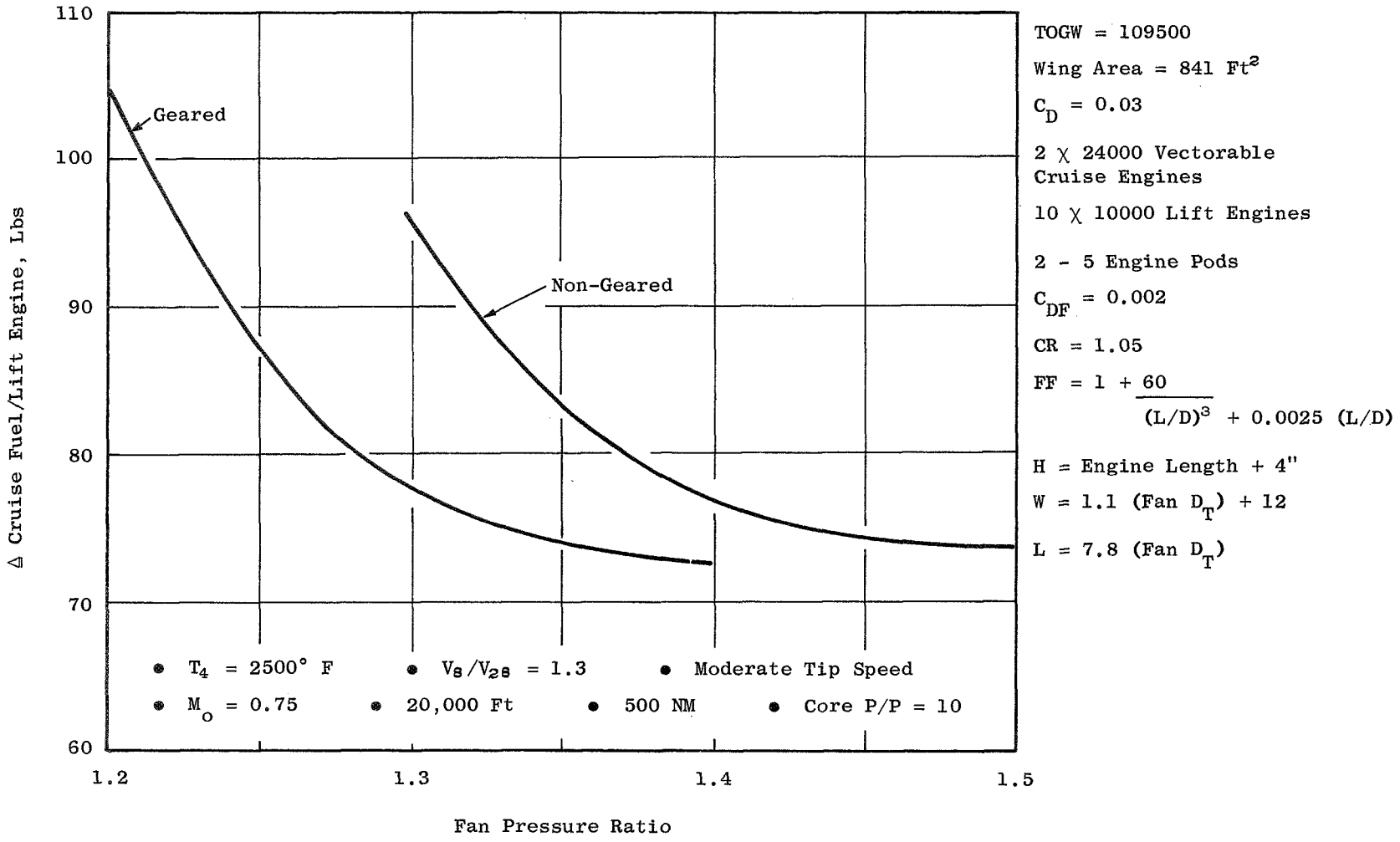

Figure 27. Effect of Fan Pressure Ratio on Δ Cruise Fuel.

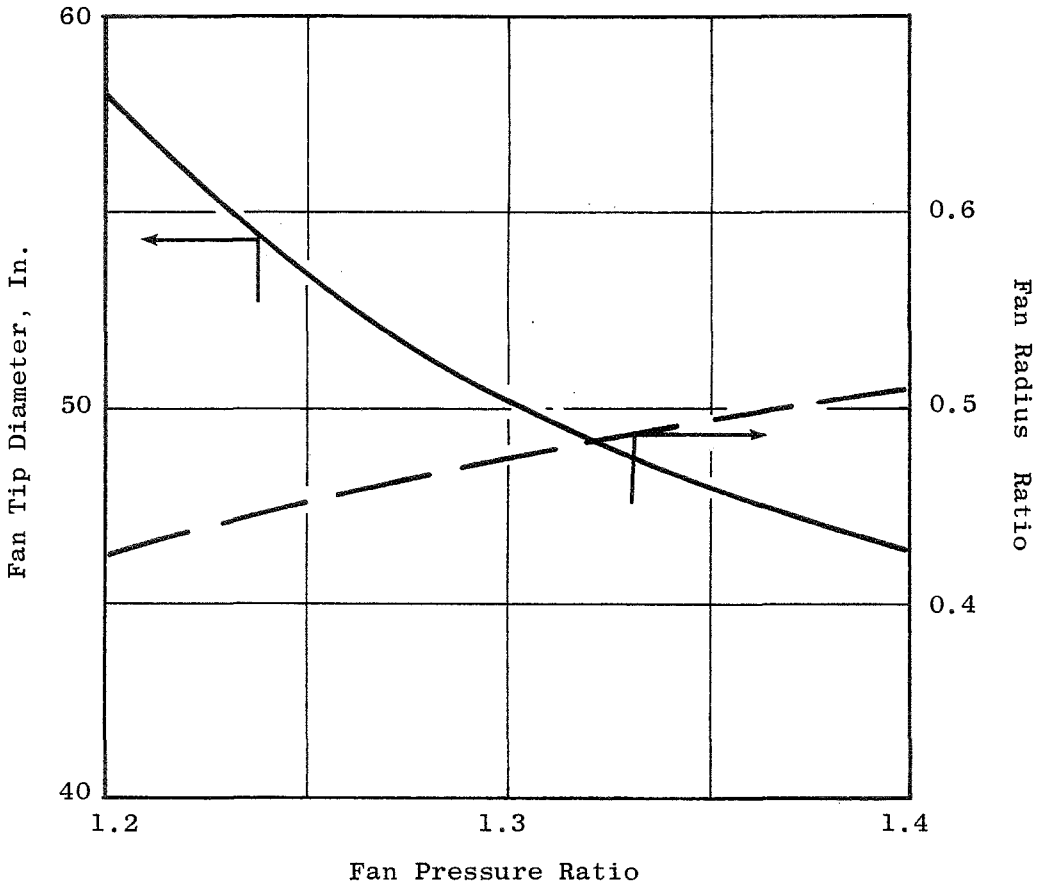

Figure 28. Effect of Fan Pressure Ratio on Fan Tip Diameter.

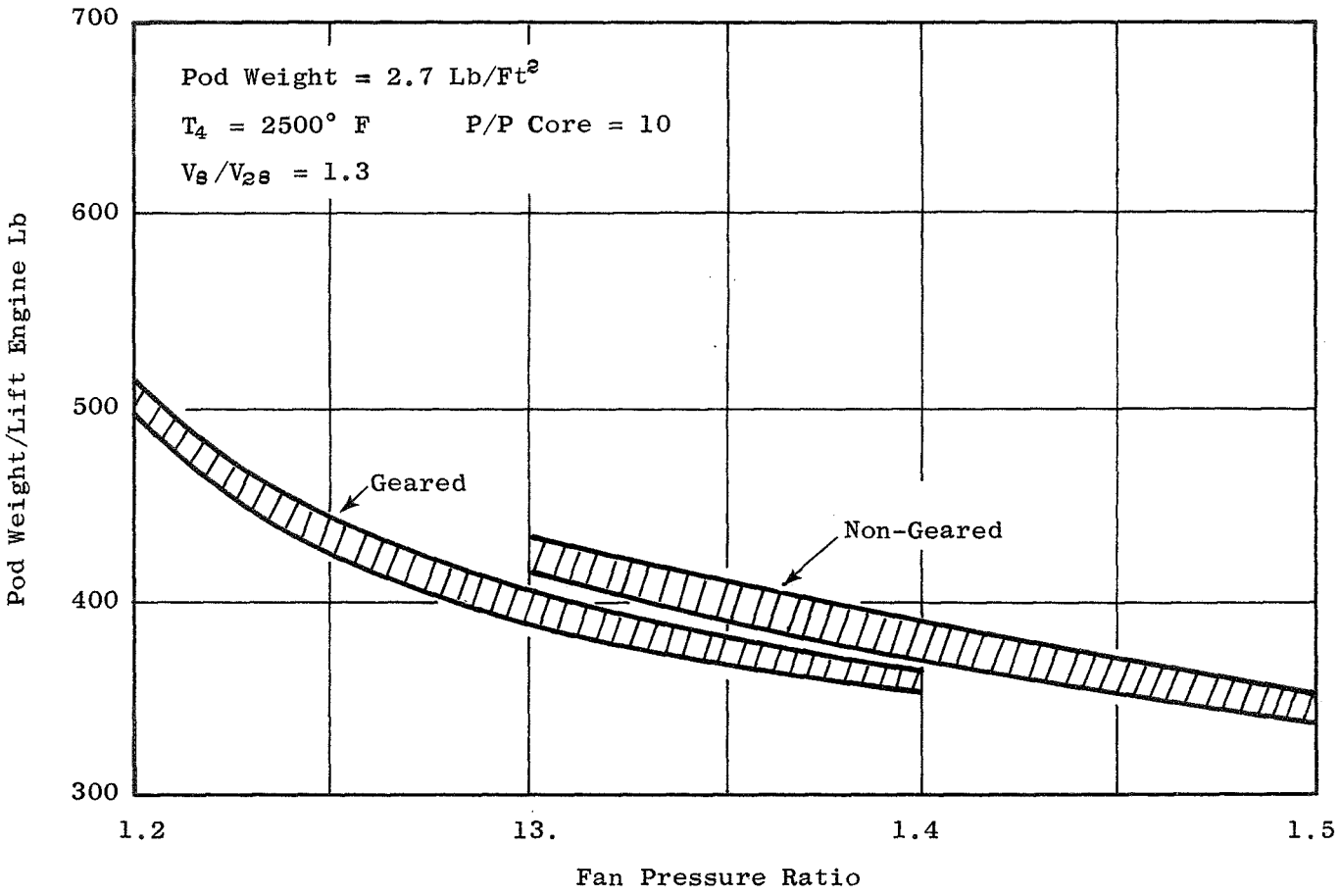

Figure 29. Effect of Fan Pressure Ratio on POD Weight.

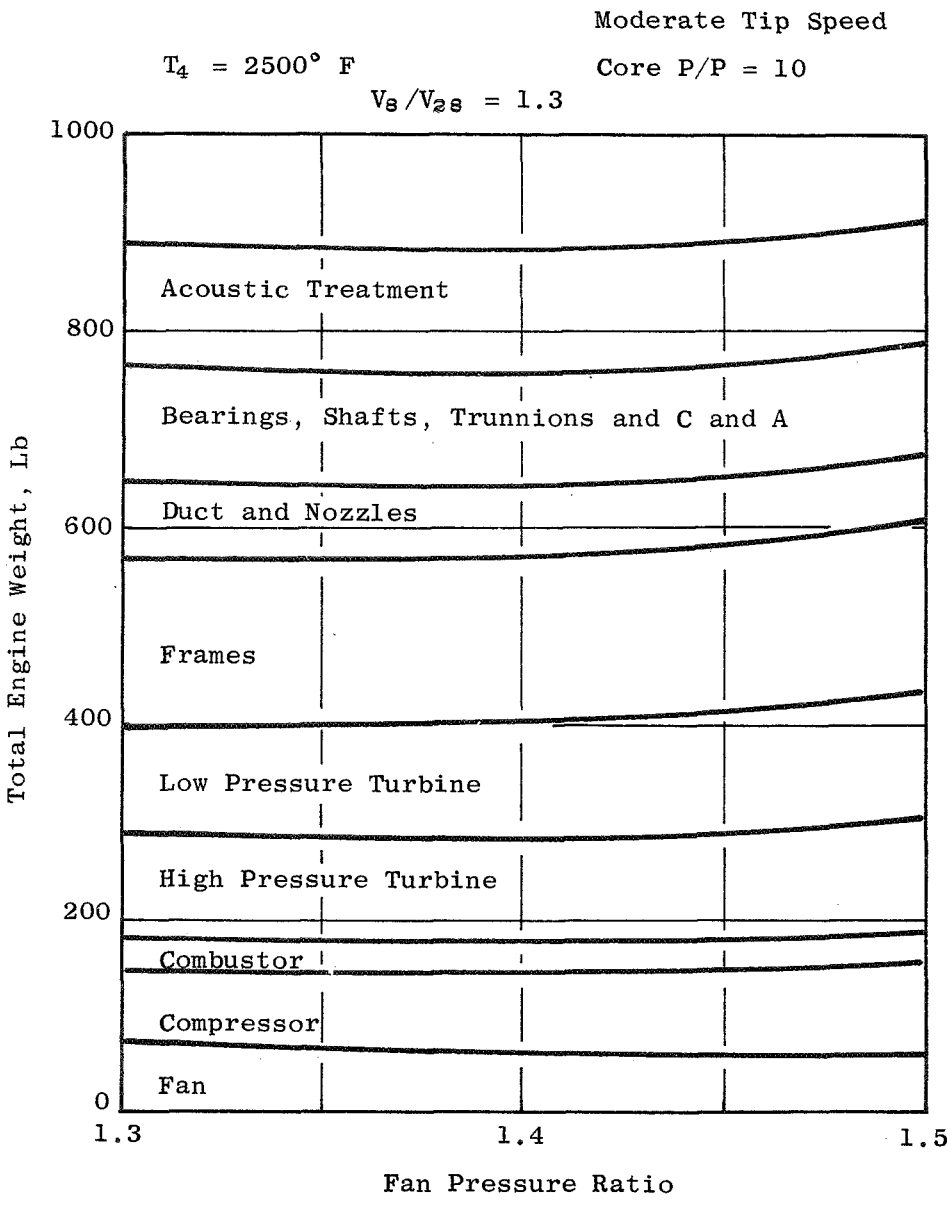

Figure 30. Non-Geared Weight Constituents.

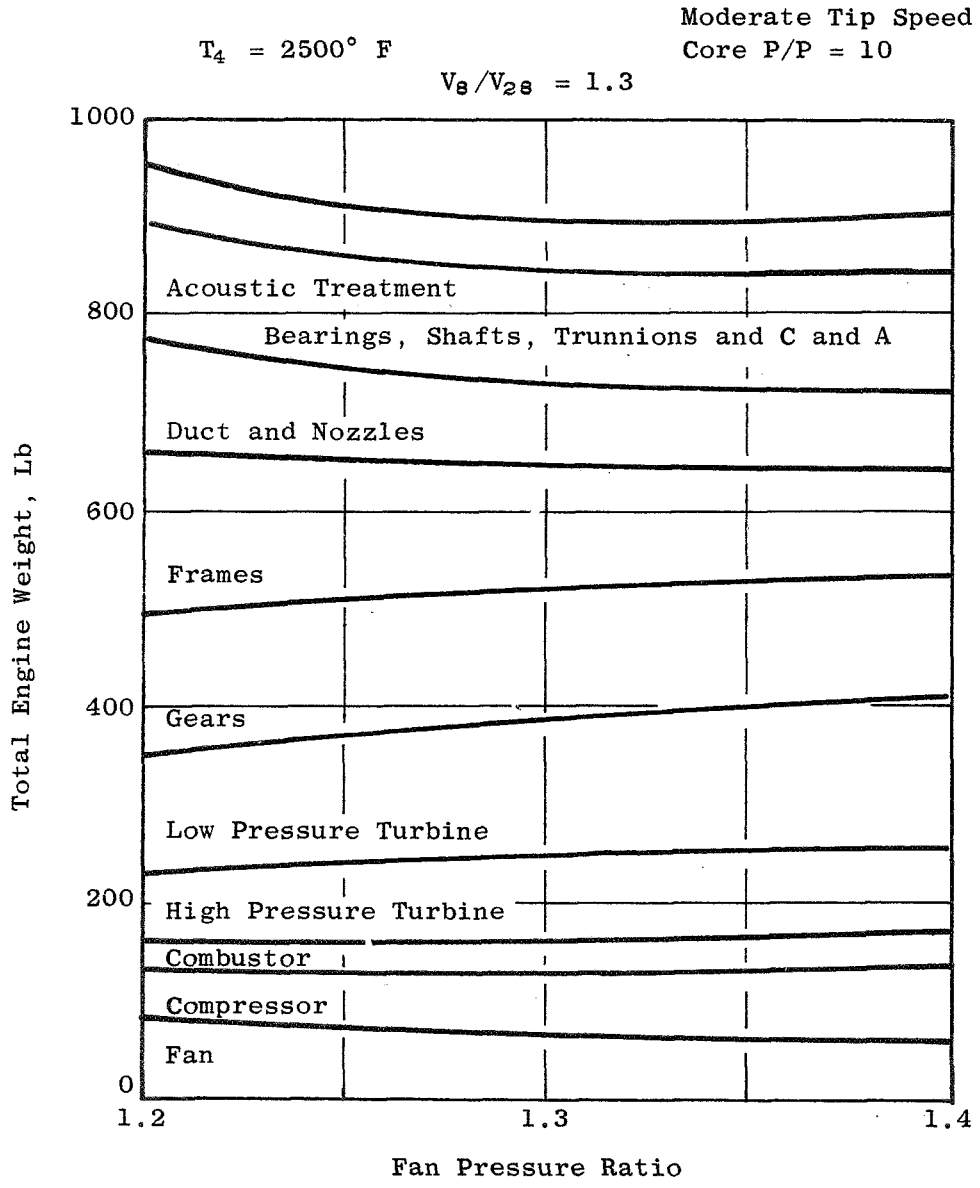

Figure 31. Geared Weight Constituents.

- T_4 = 2500° F
- V_s/V_{ss} = 1.3
- Core P/P = 10
- Moderate Tip Speed

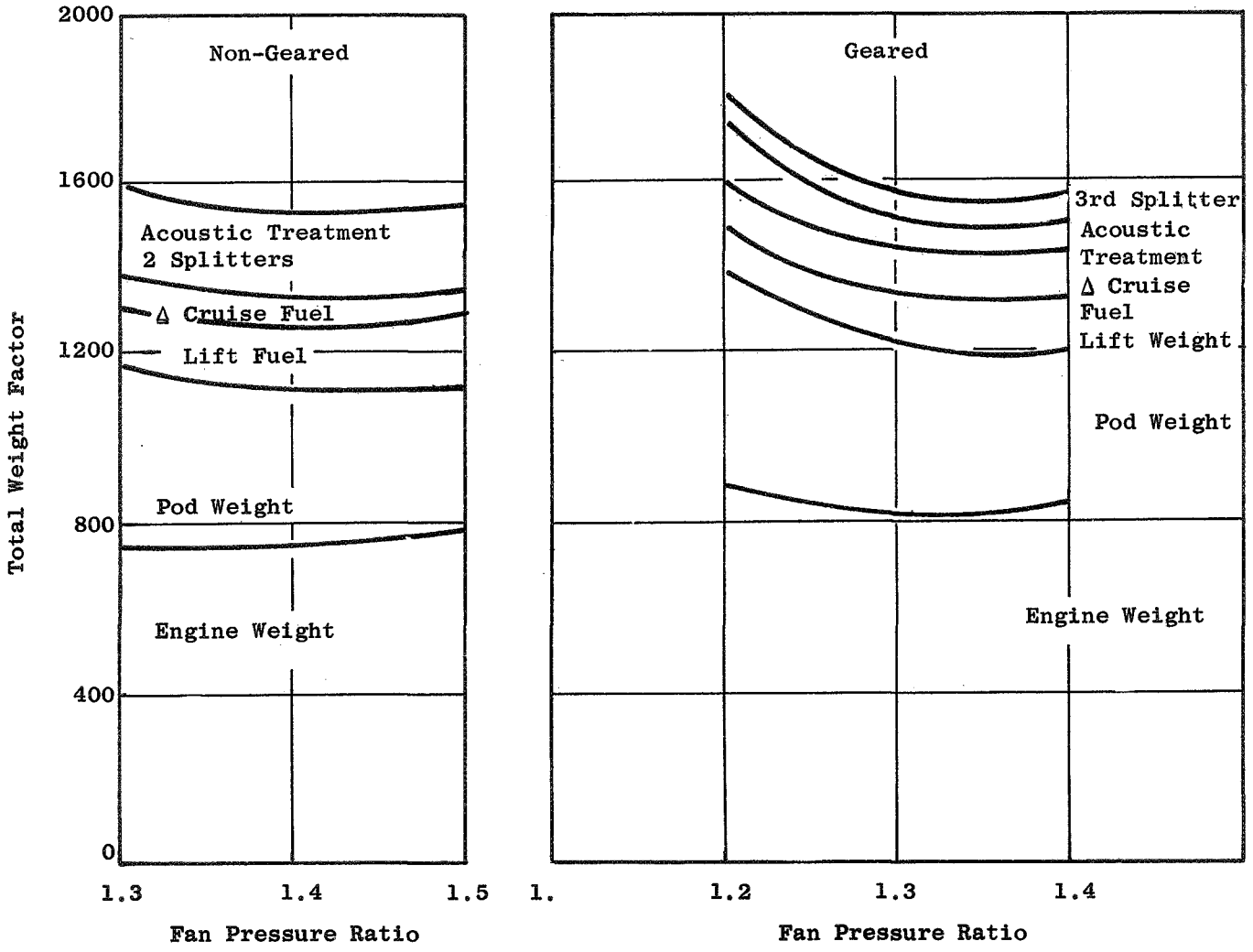

Figure 32. Merit Factor Constituents.

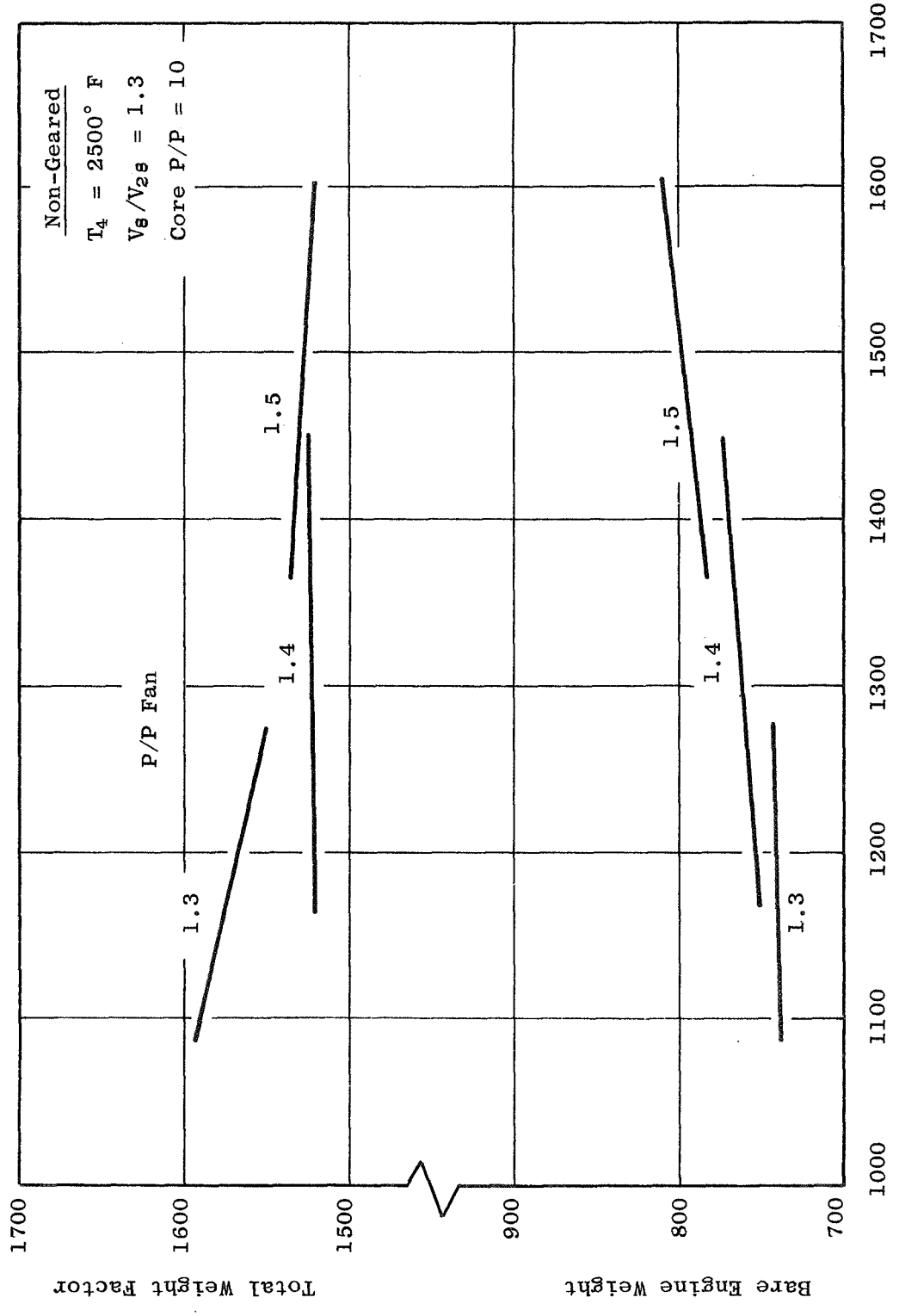

Figure 33. Effect of Fan Tip Speed.

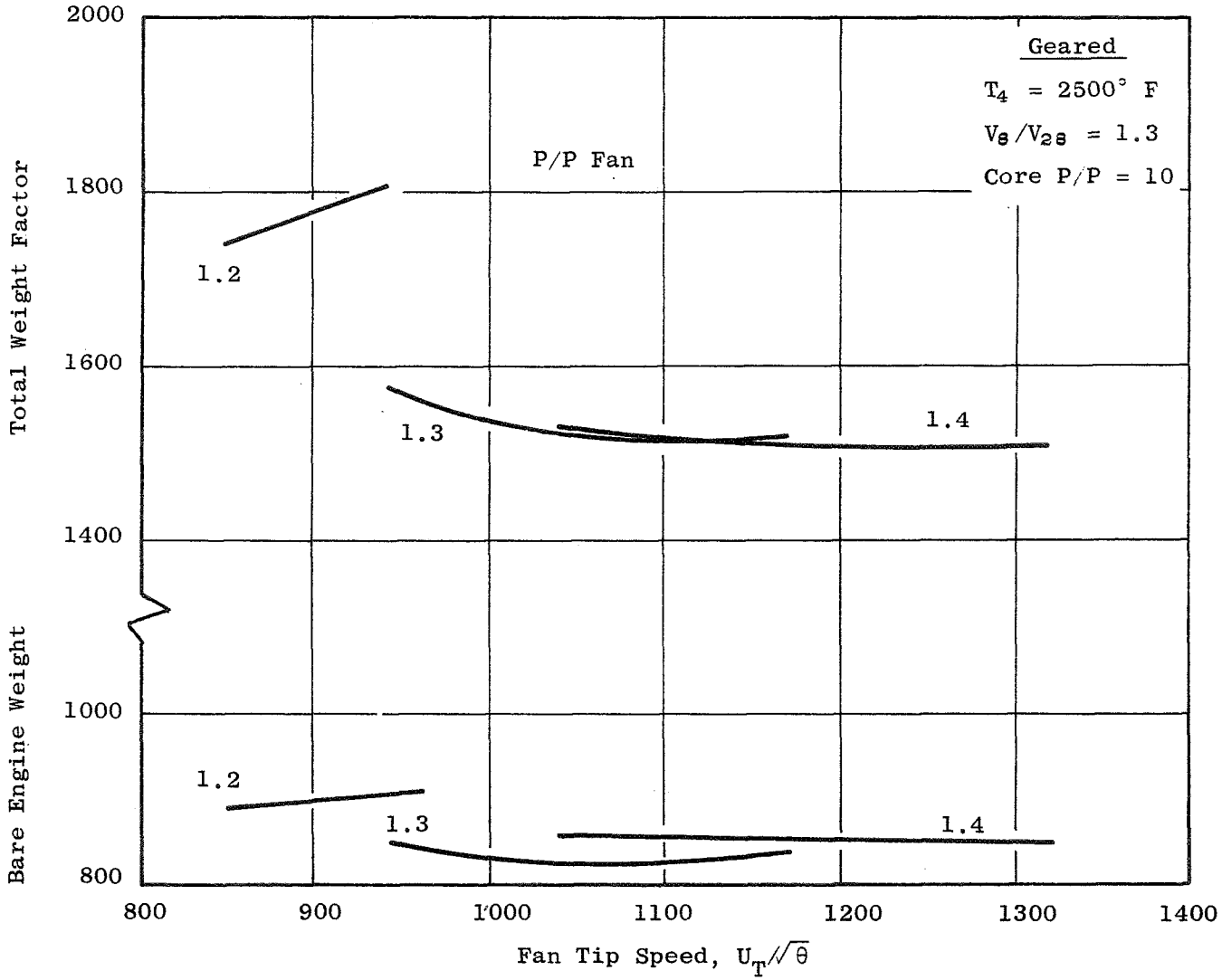

Figure 34. Effect of Fan Tip Speed.

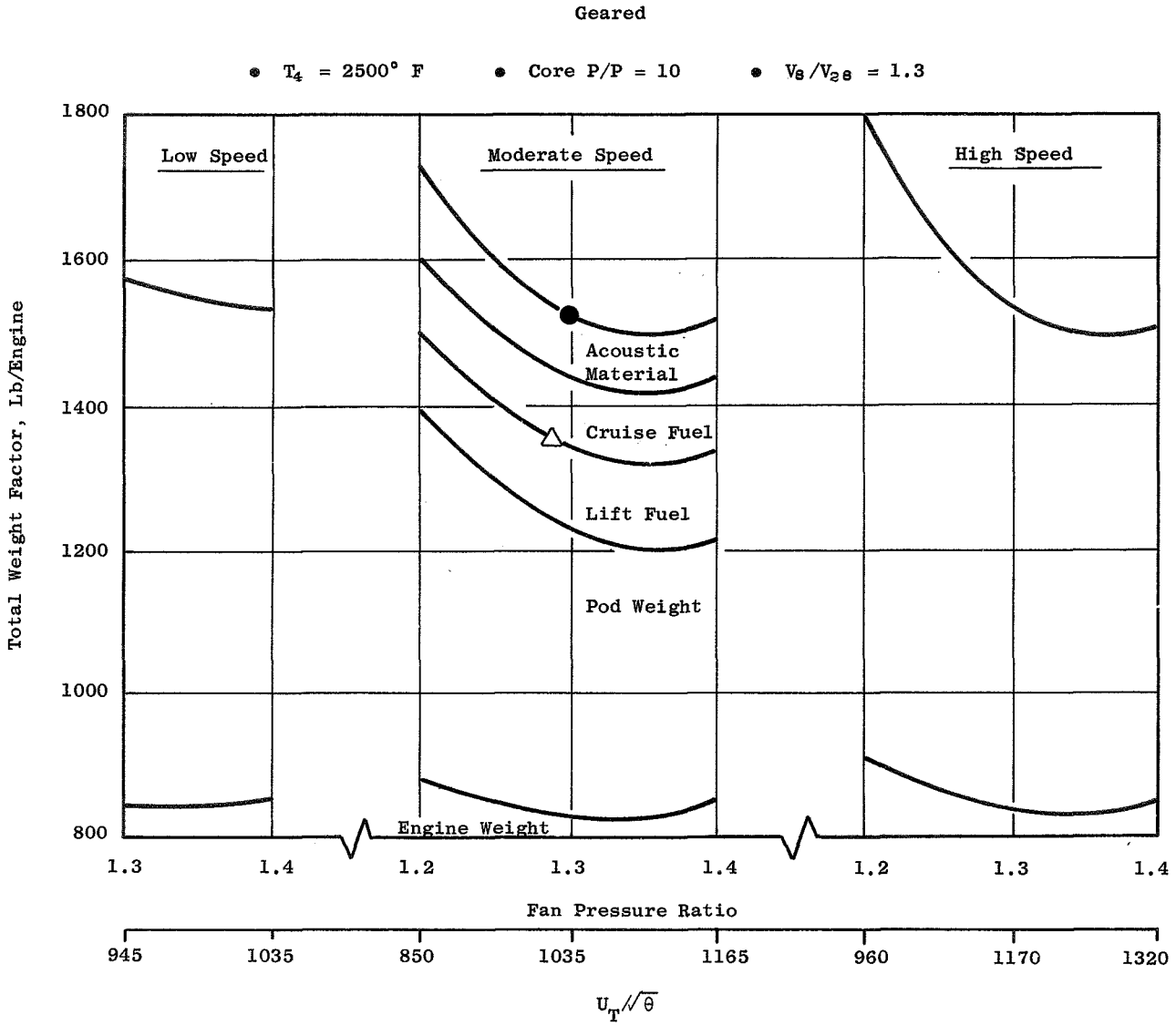

Figure 35. Effect of Fan Pressure Ratio and Tip Speed.

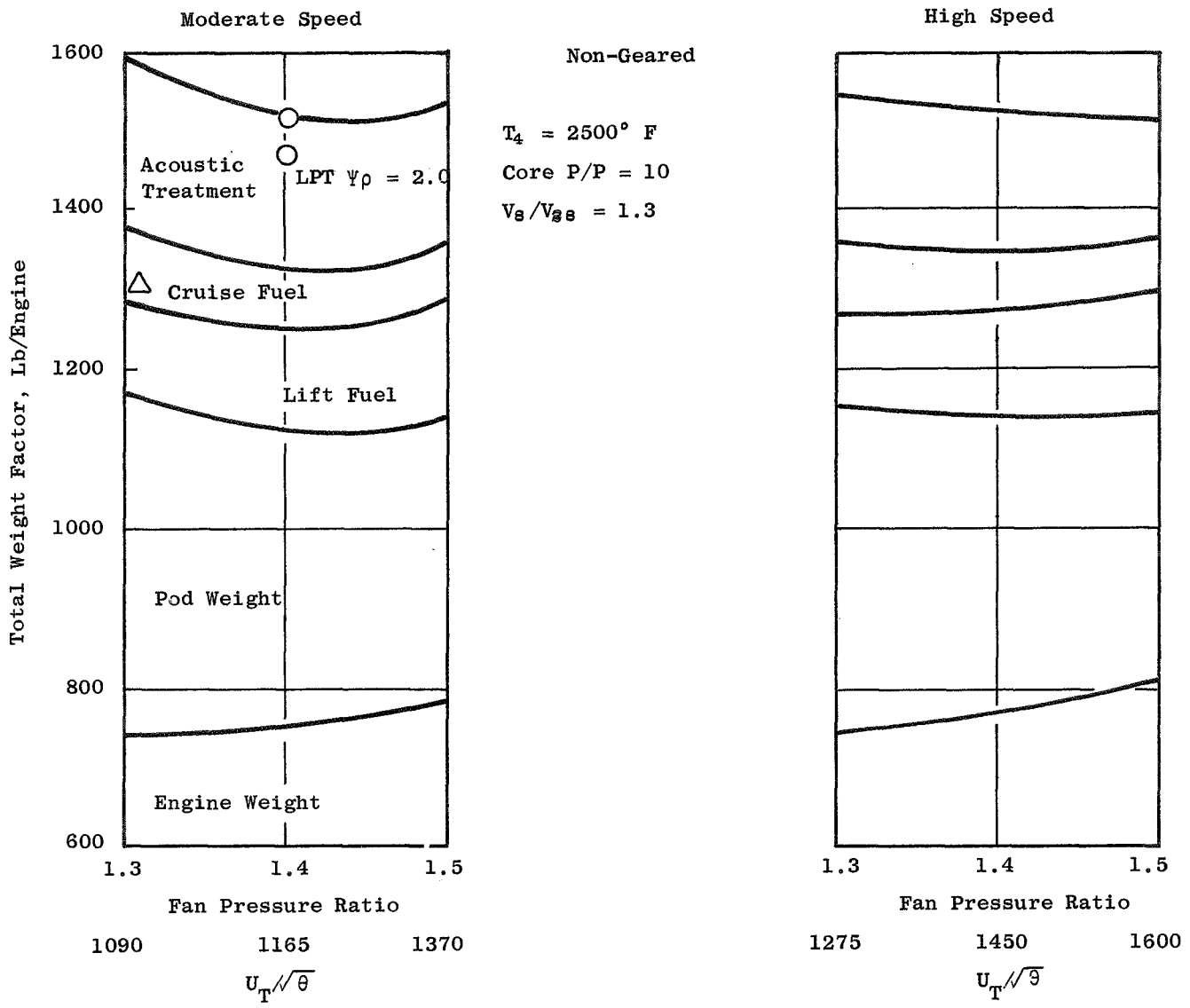

Figure 36. Effect of Fan Pressure Ratio and Tip Speed.

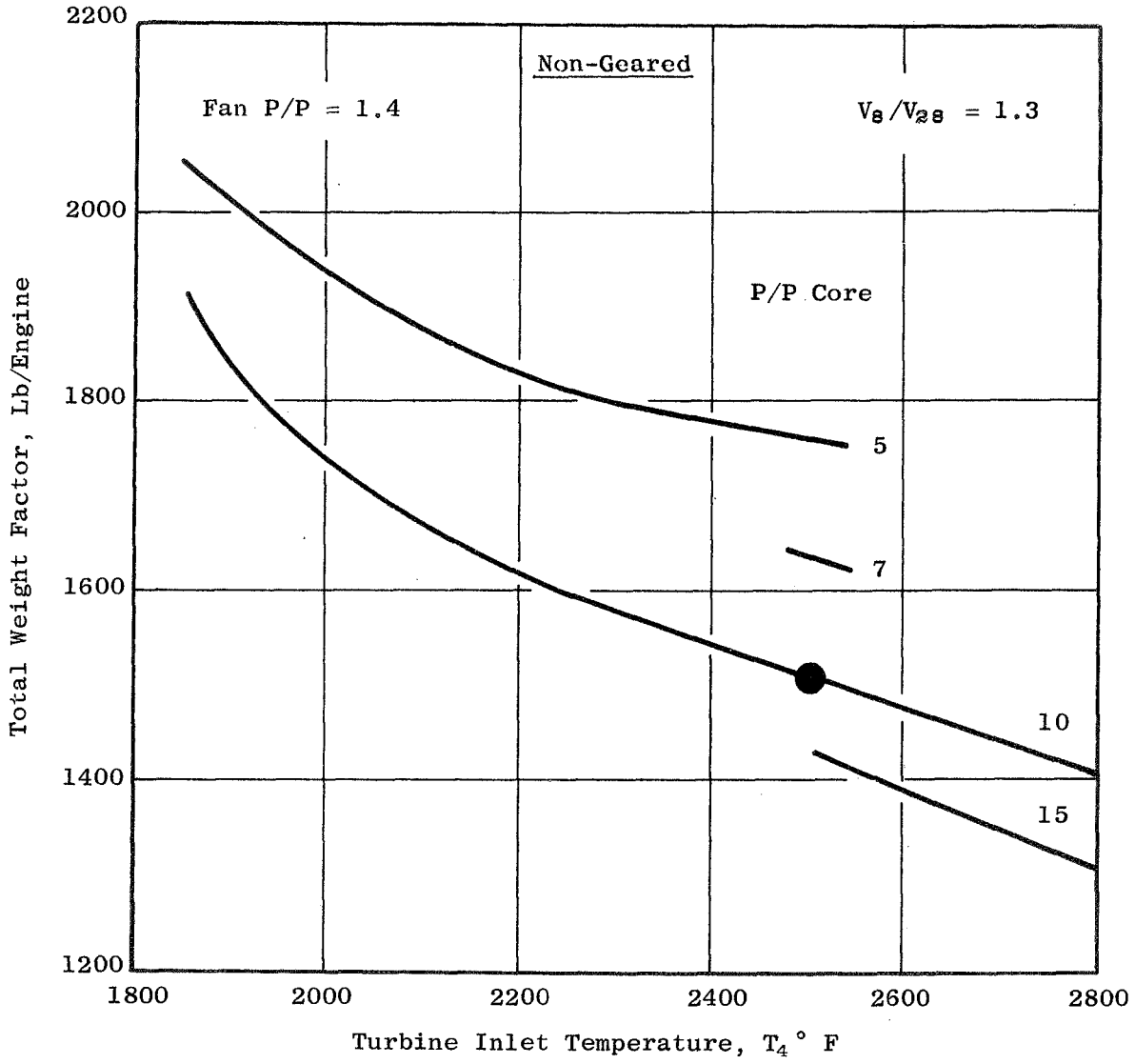

Figure 37. Effect of Cycle T_4 and Core P/P.

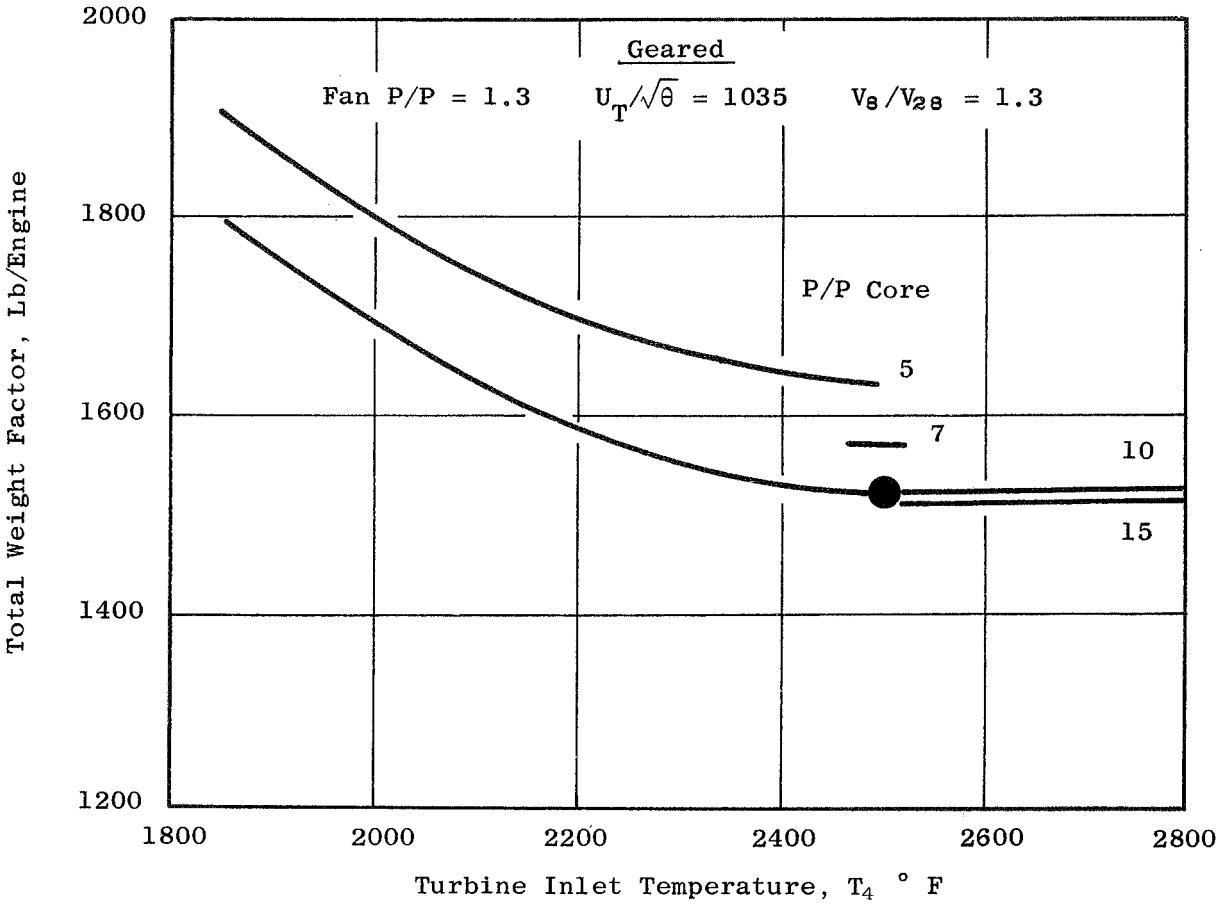

Figure 38. Effect of Cycle T_4 and Core P/P.

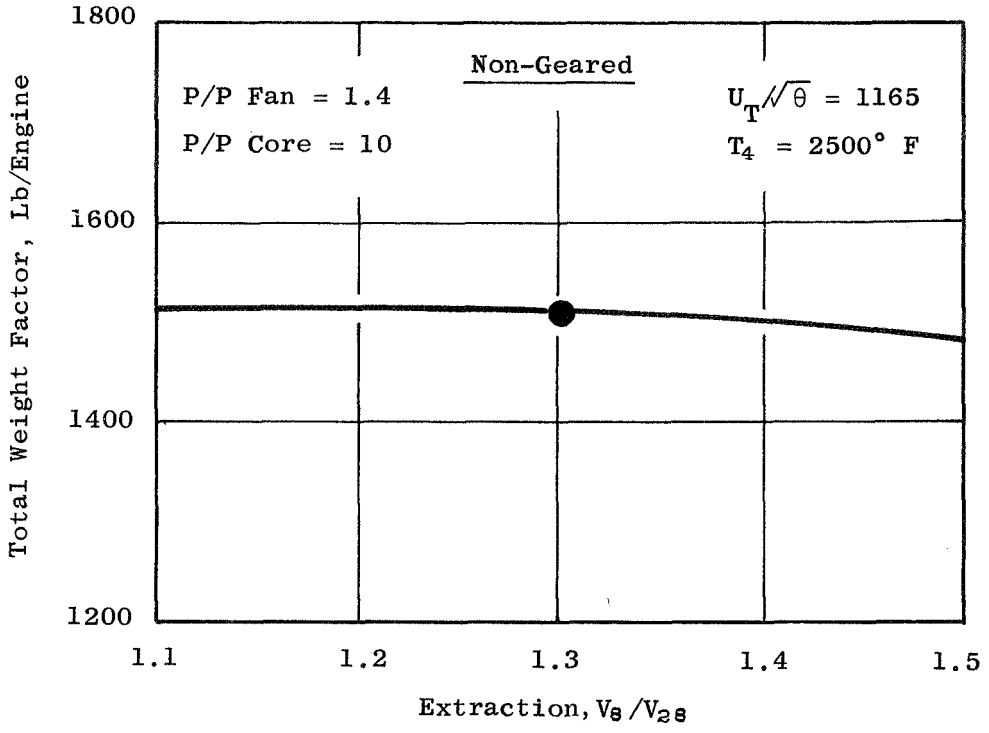

Figure 39. Effect of Extraction.

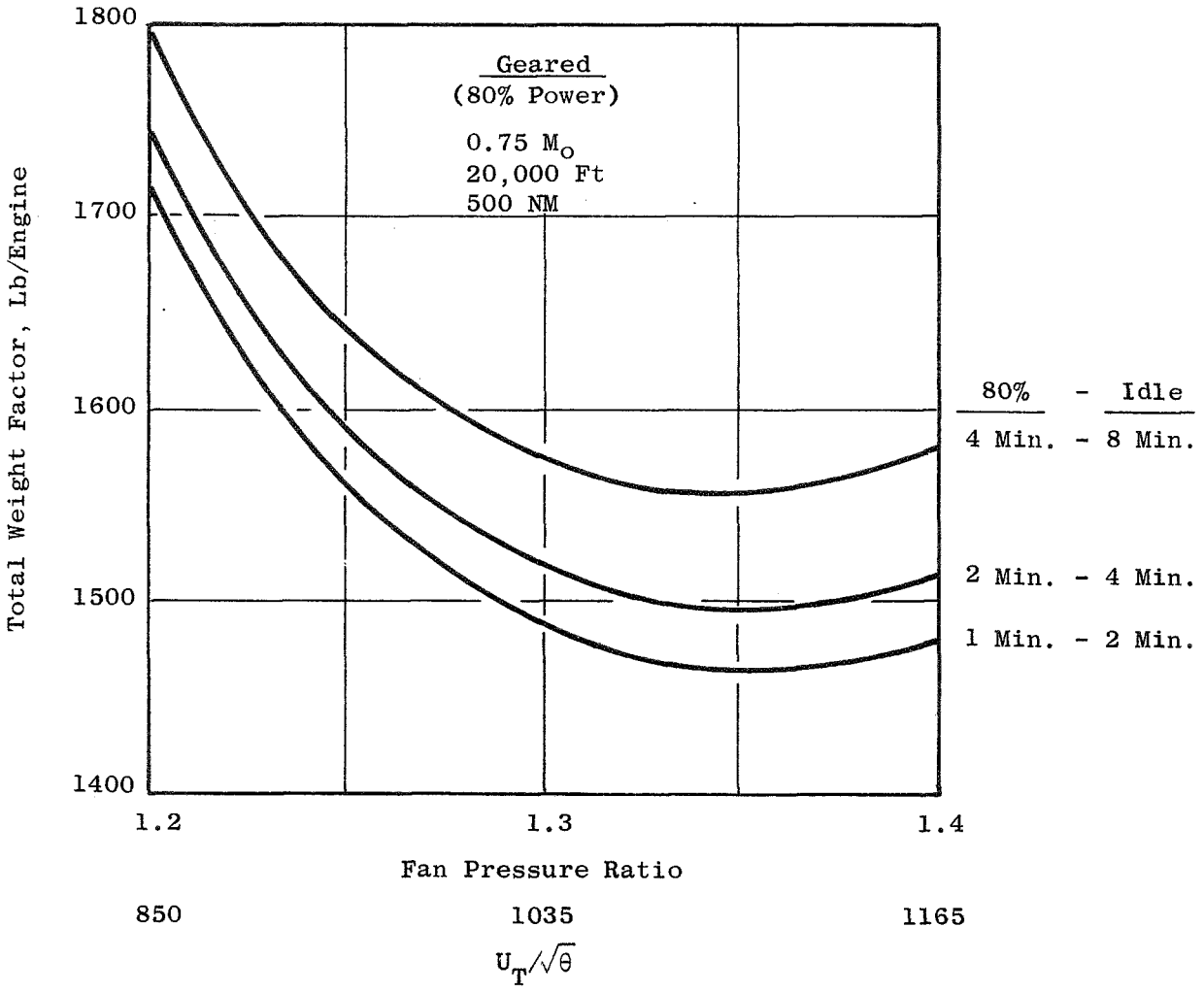

Figure 40. Effect of Time in Lift.

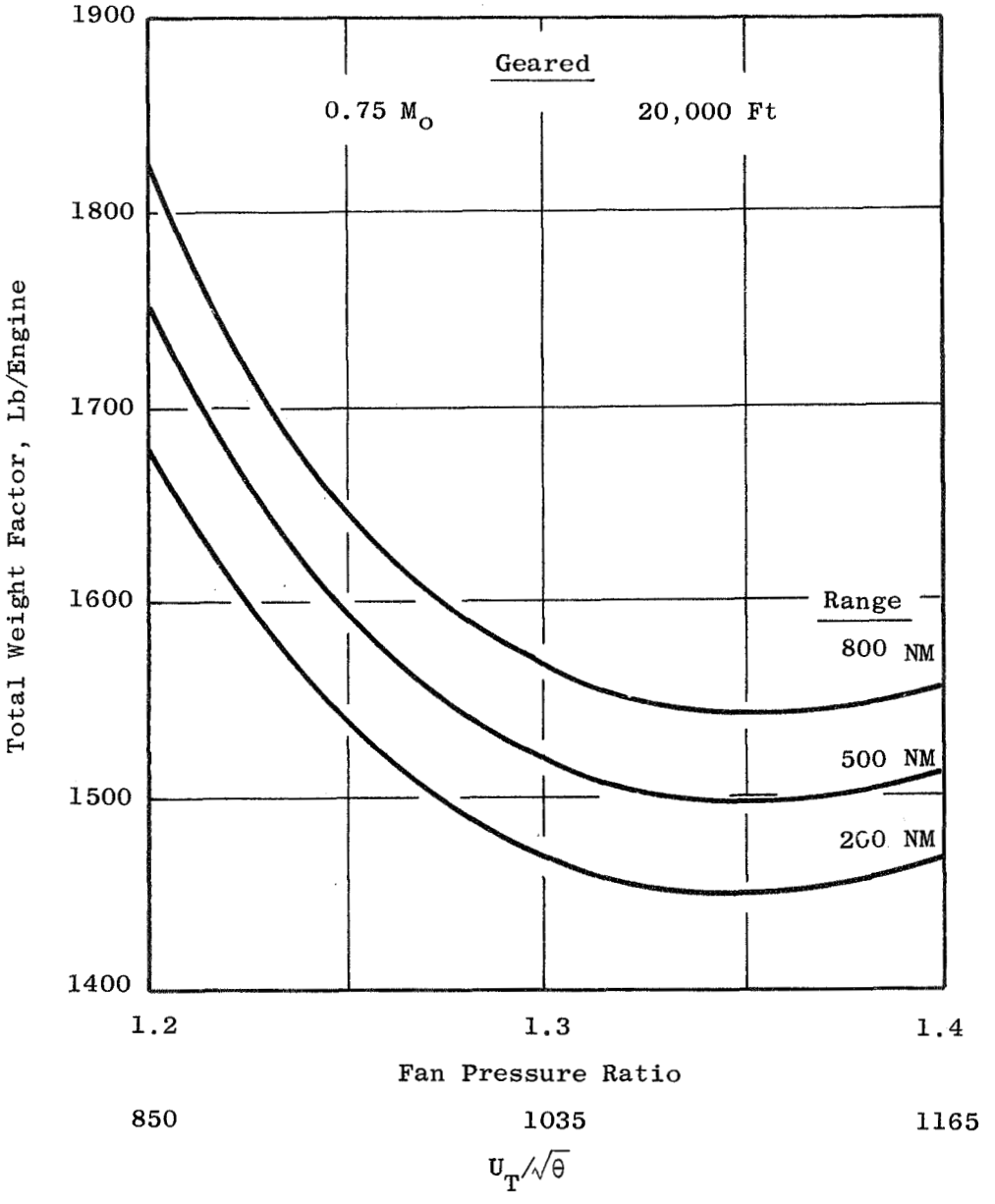

Figure 41. Effect of Range - VTOL Airplane.

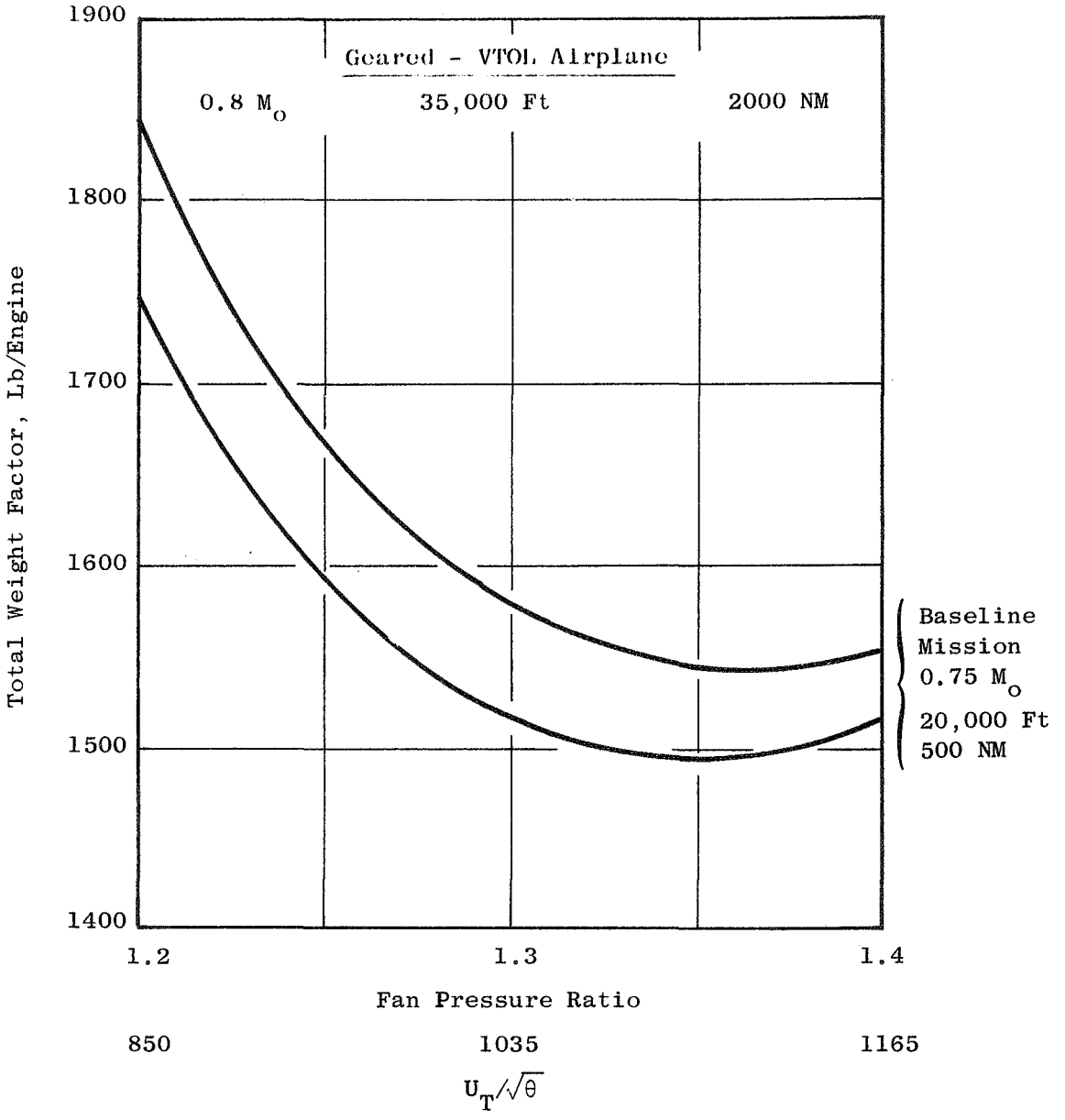

Figure 42. Effect of Alternate STOL Mission.

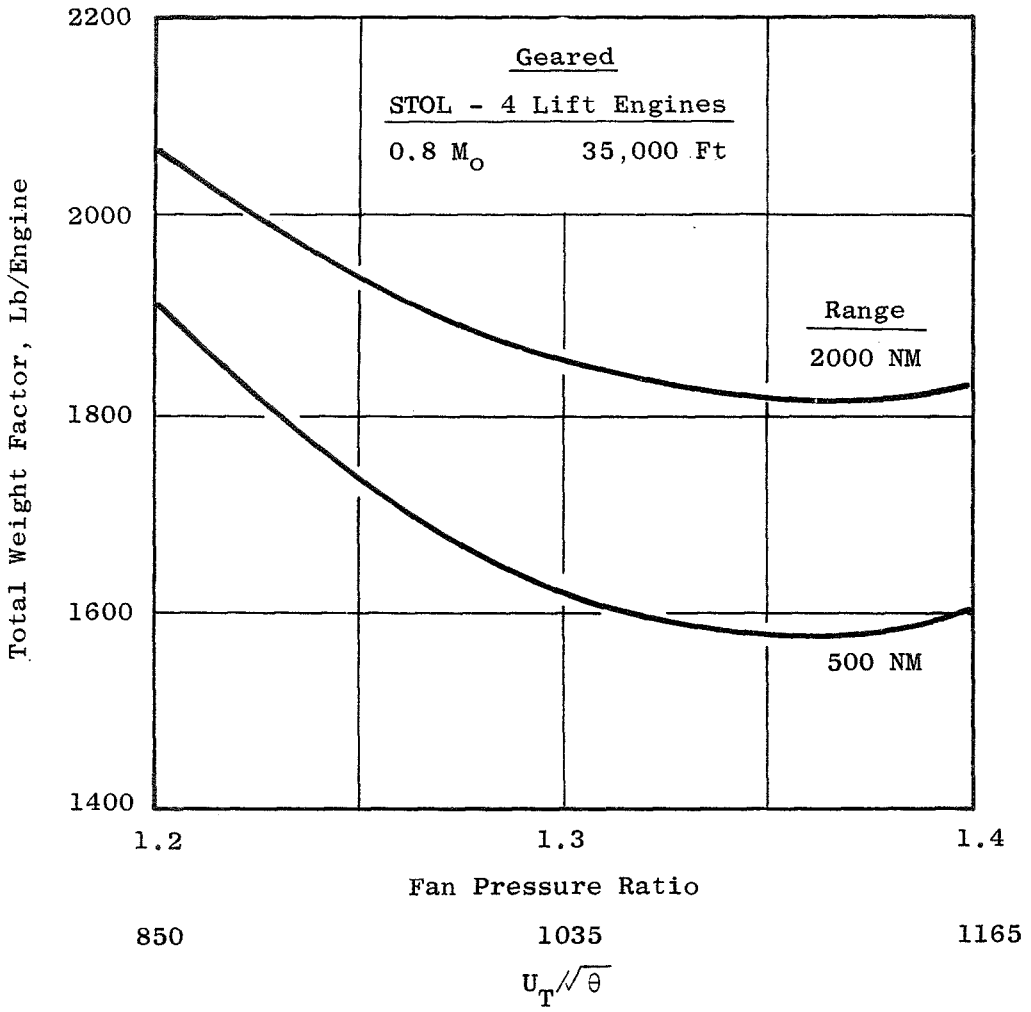

Figure 43. Effect of Alternate Airplane.

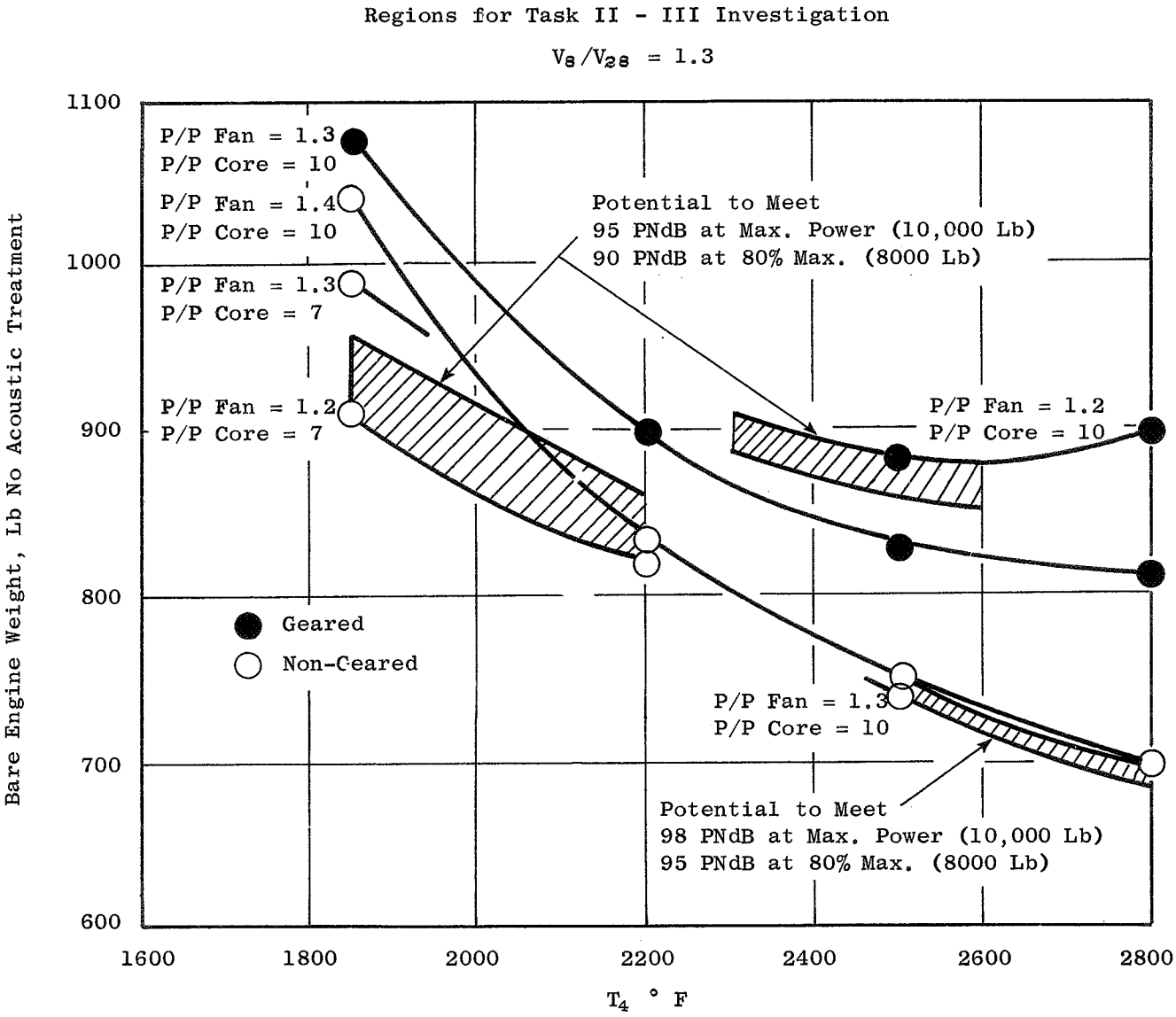

Figure 44. Engine Weight Results - Recommended.

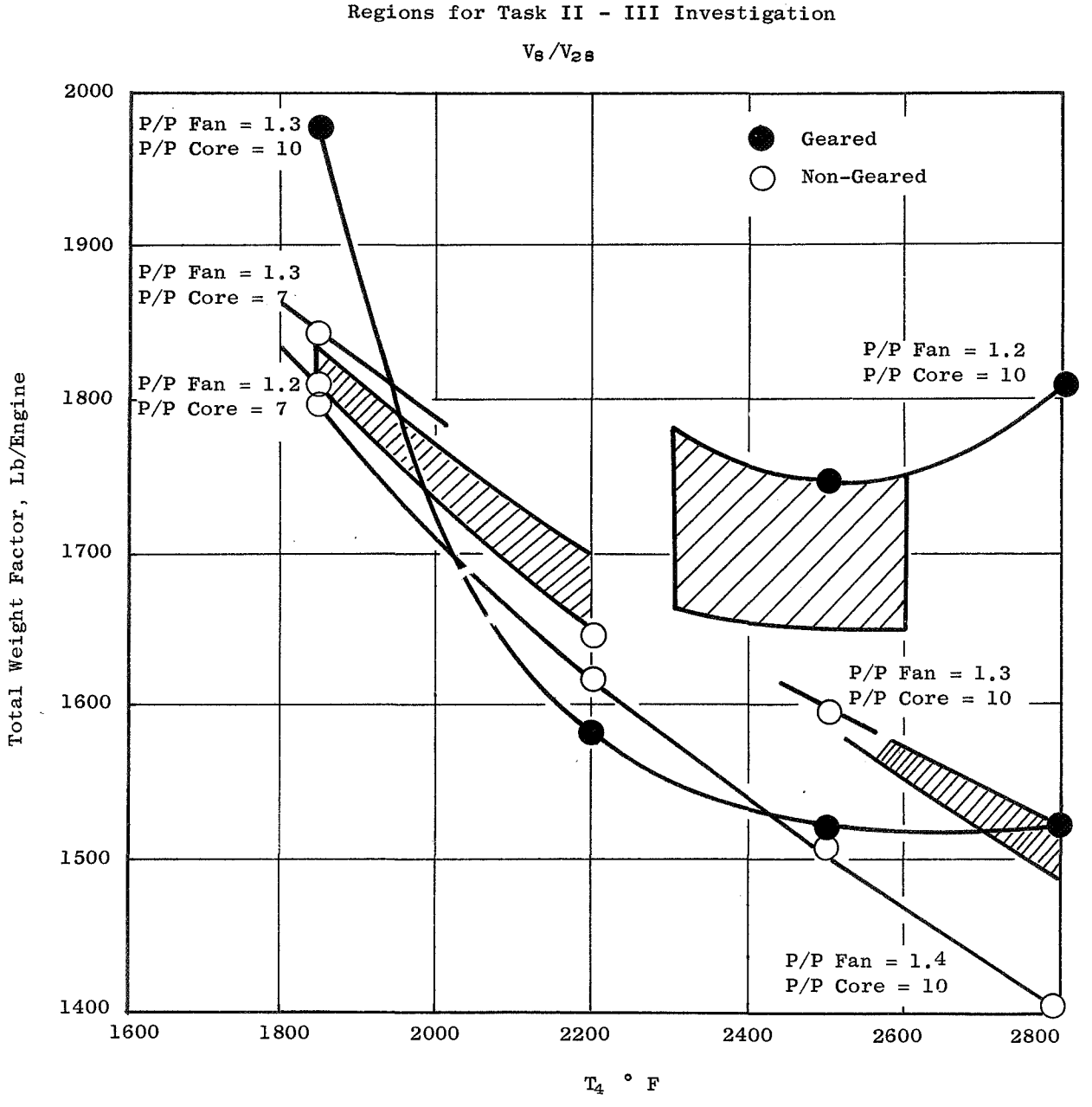

Figure 45. Weight Factor Results - Recommended.

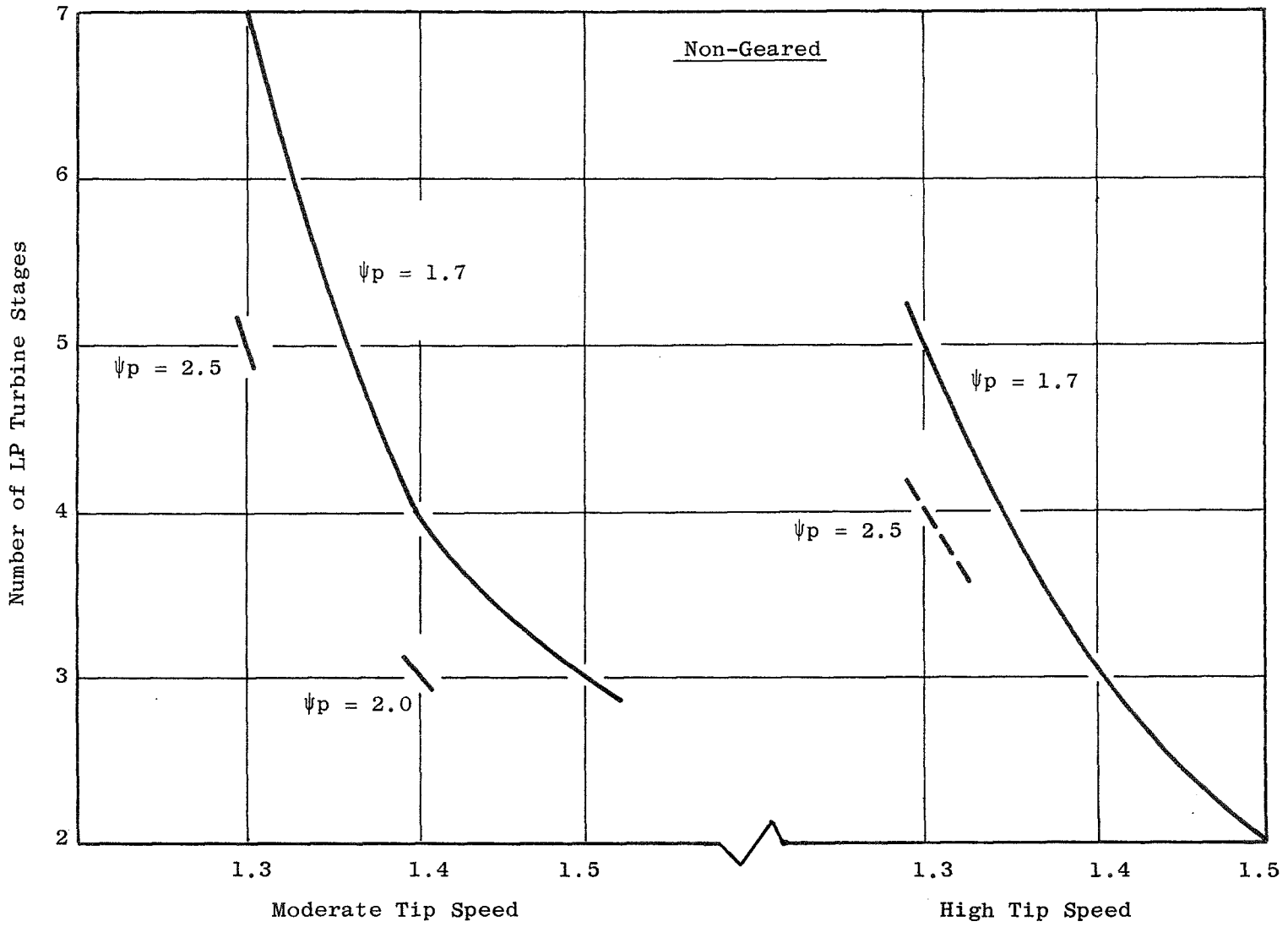

Figure 46. Effect of LPT Loading and Tip Speed on Number of LP Turbine Stages.

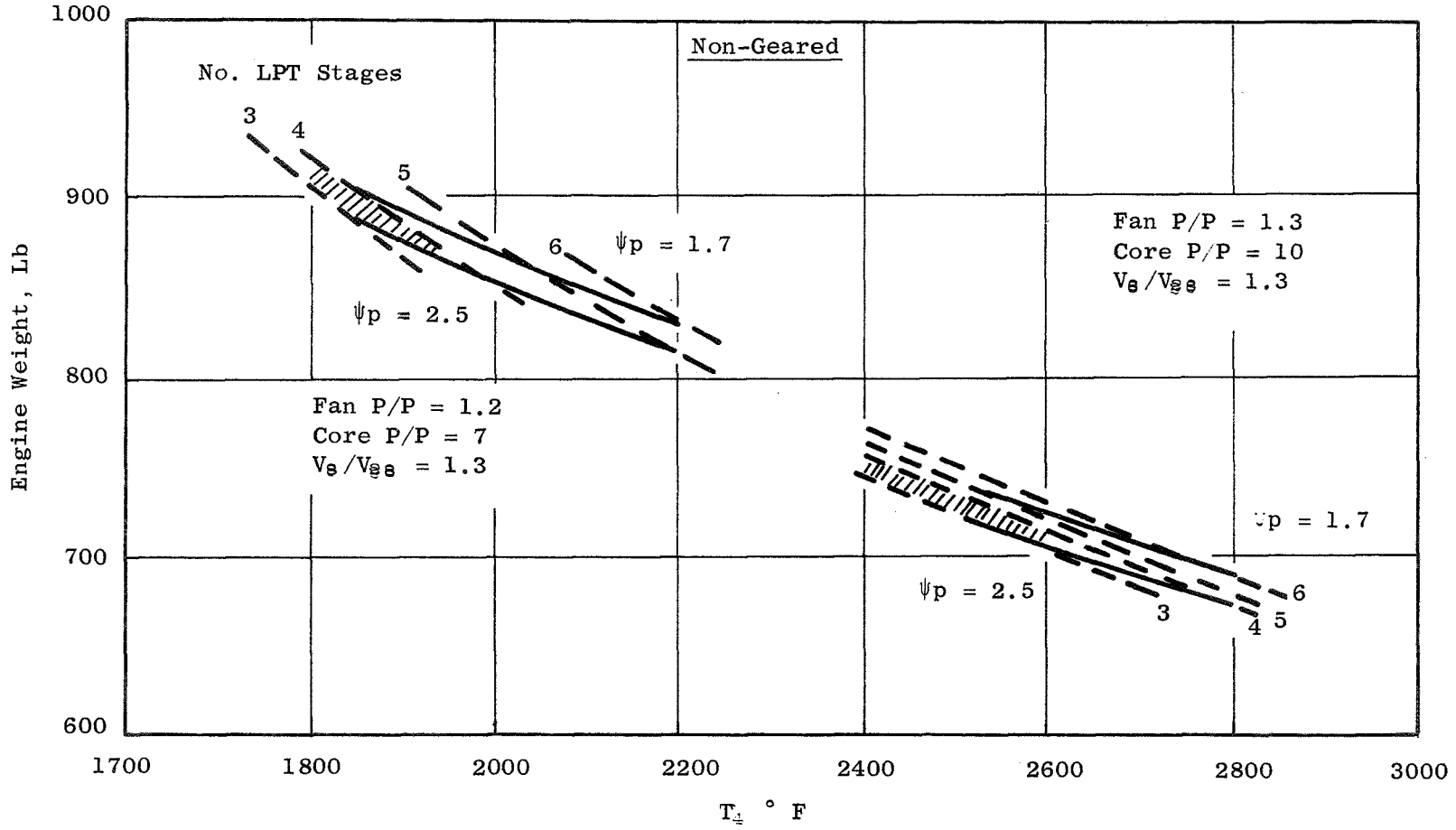

Figure 47. Effect of LPT Loading on Engine Weight.

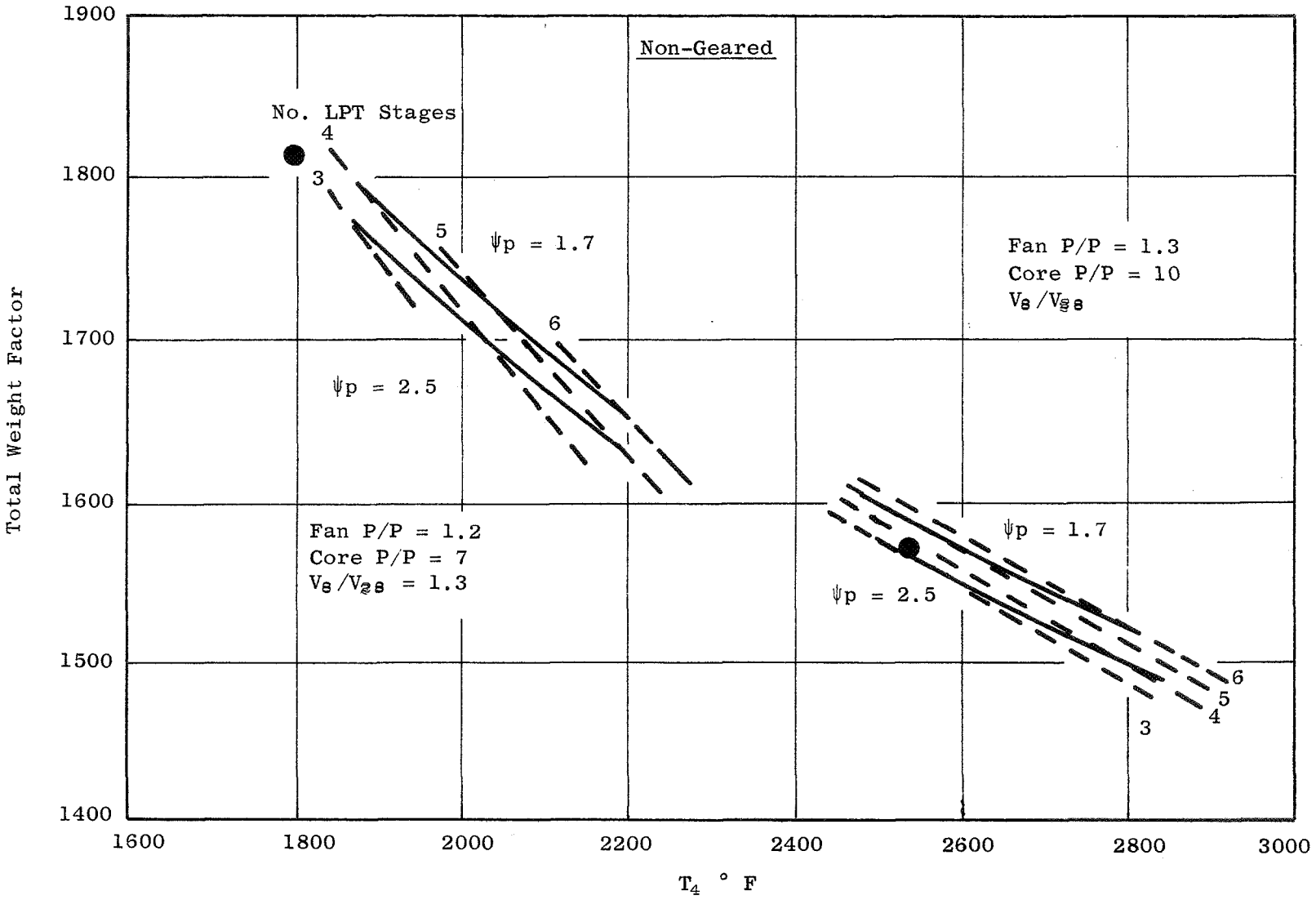

Figure 48. Effect of LPT Loading on Total Weight Factor.

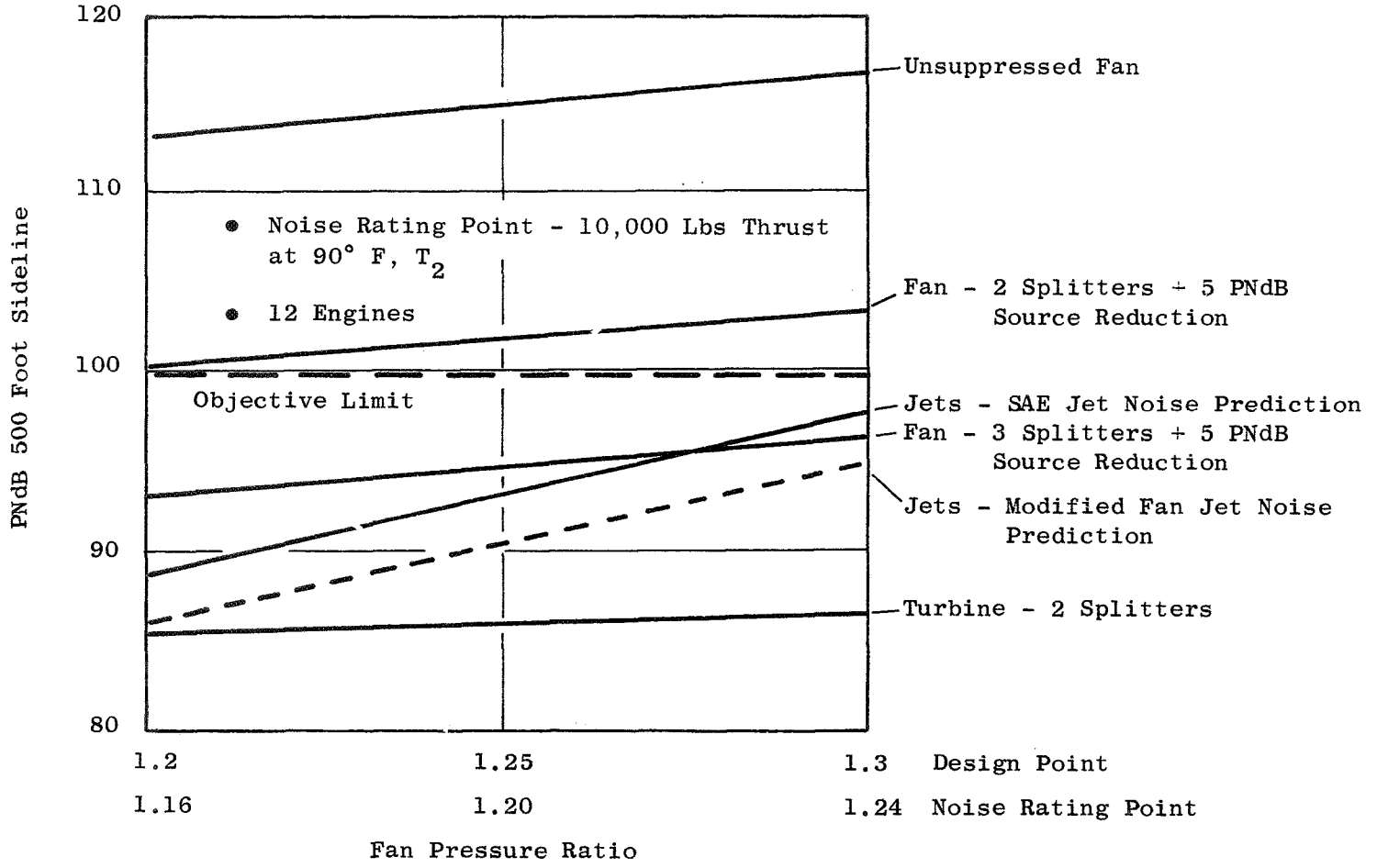

Figure 49. Noise Constituents.

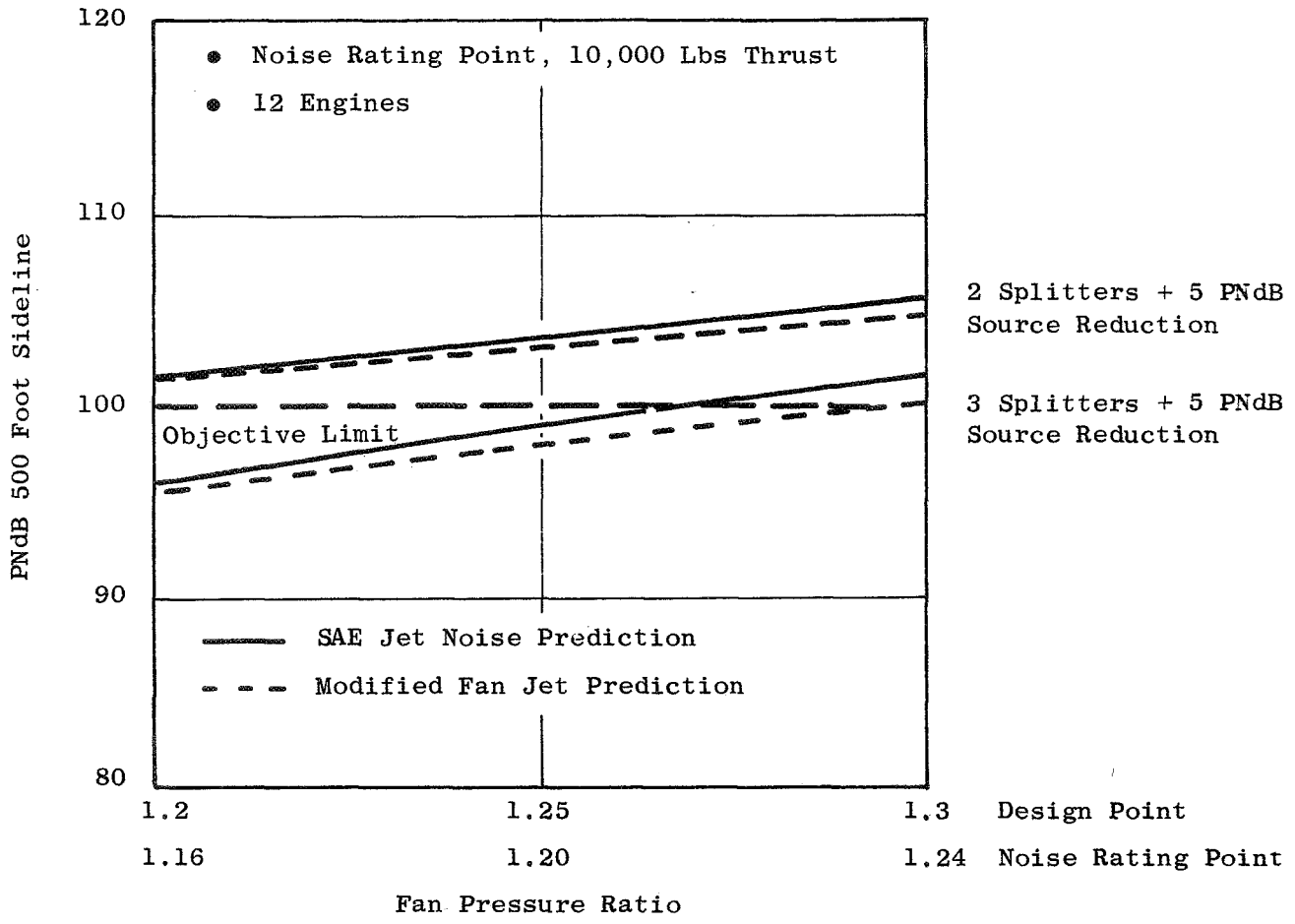

Figure 50. Total Noise Level with Turbine.

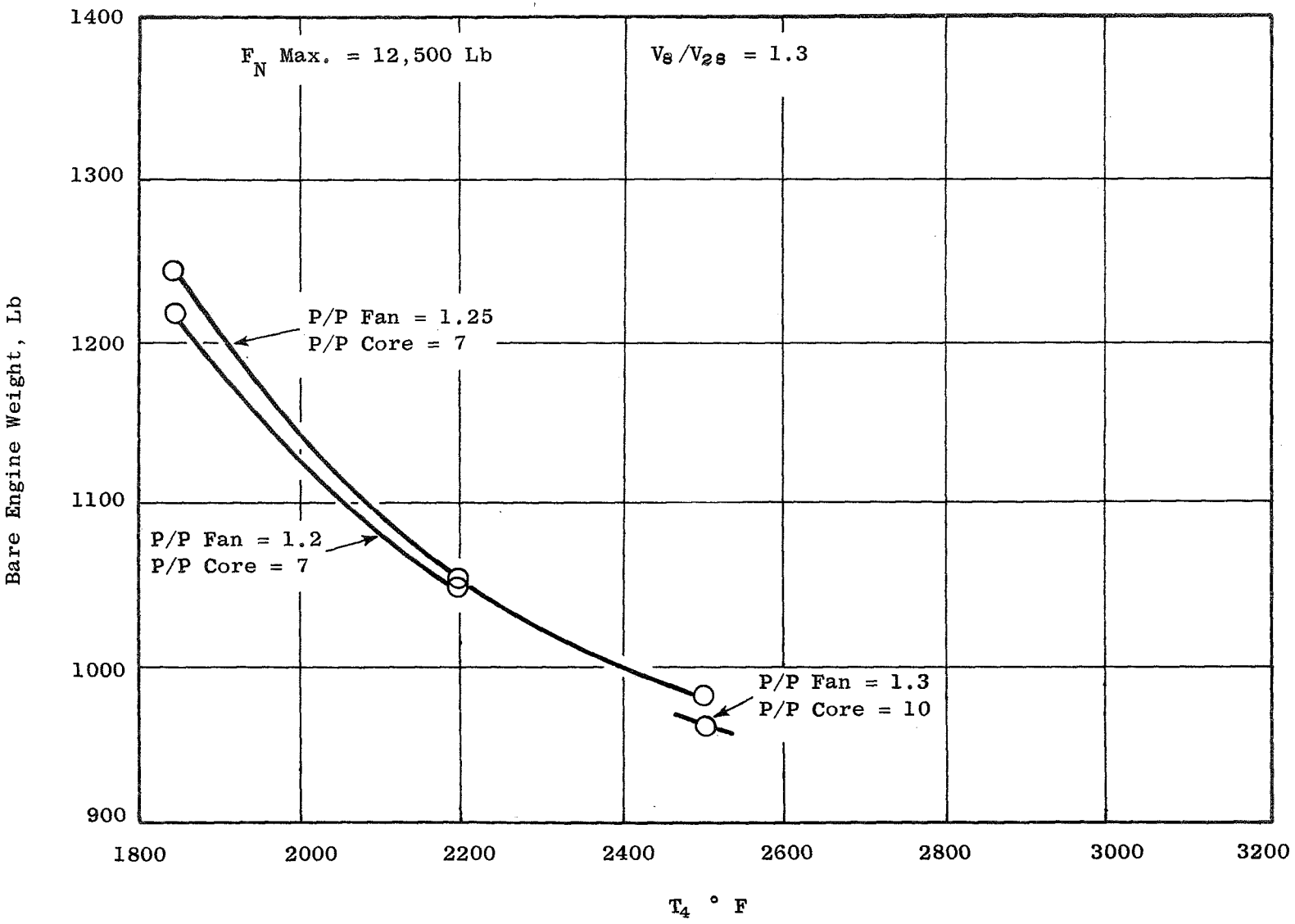

Figure 51. Results - Bare Engine Weight.

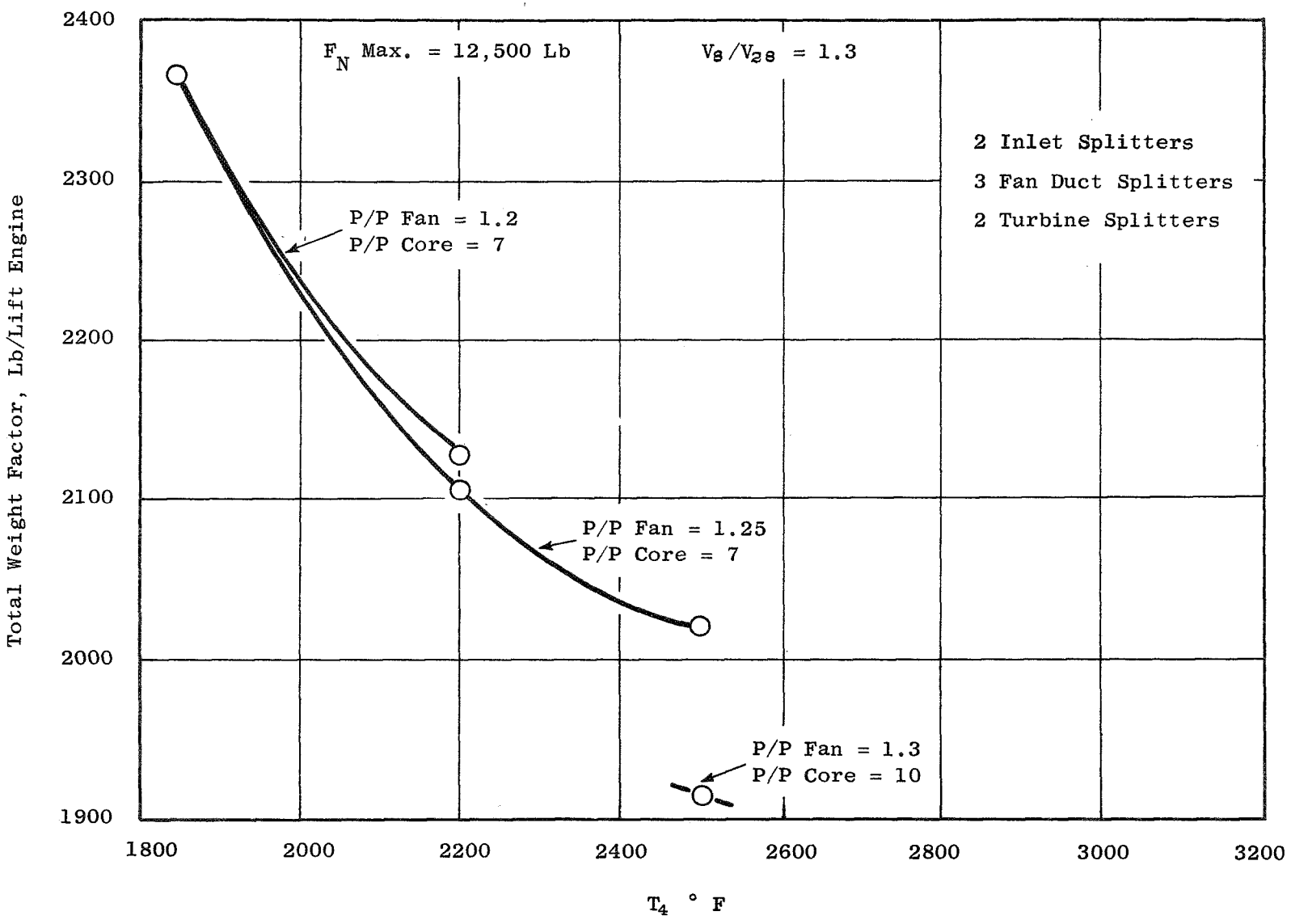

Figure 52. Results - Total Weight Factor.

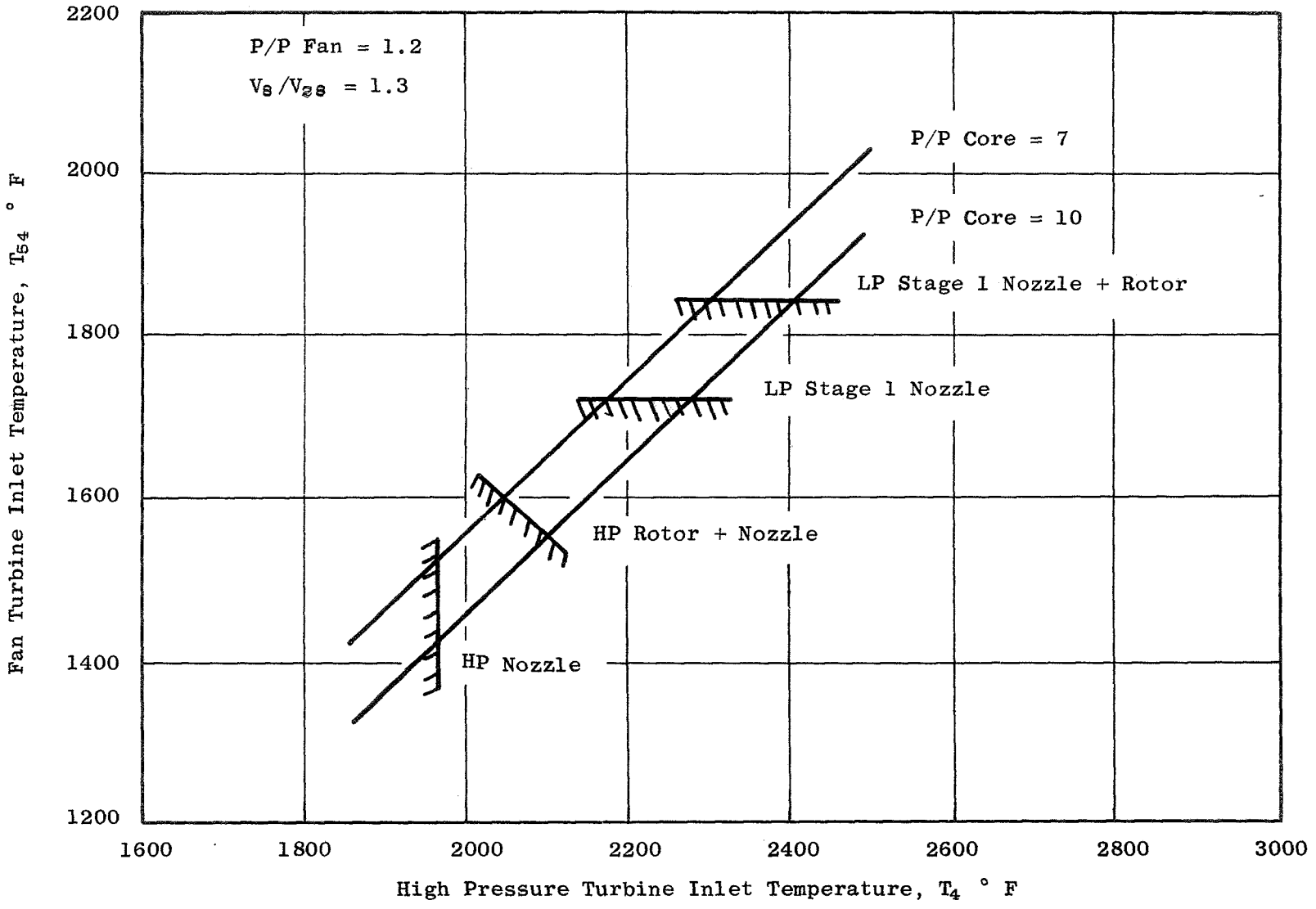

Figure 53. Effect of T_4 and P/P Core on Fan Turbine Inlet Temperature and Cooling Requirements.

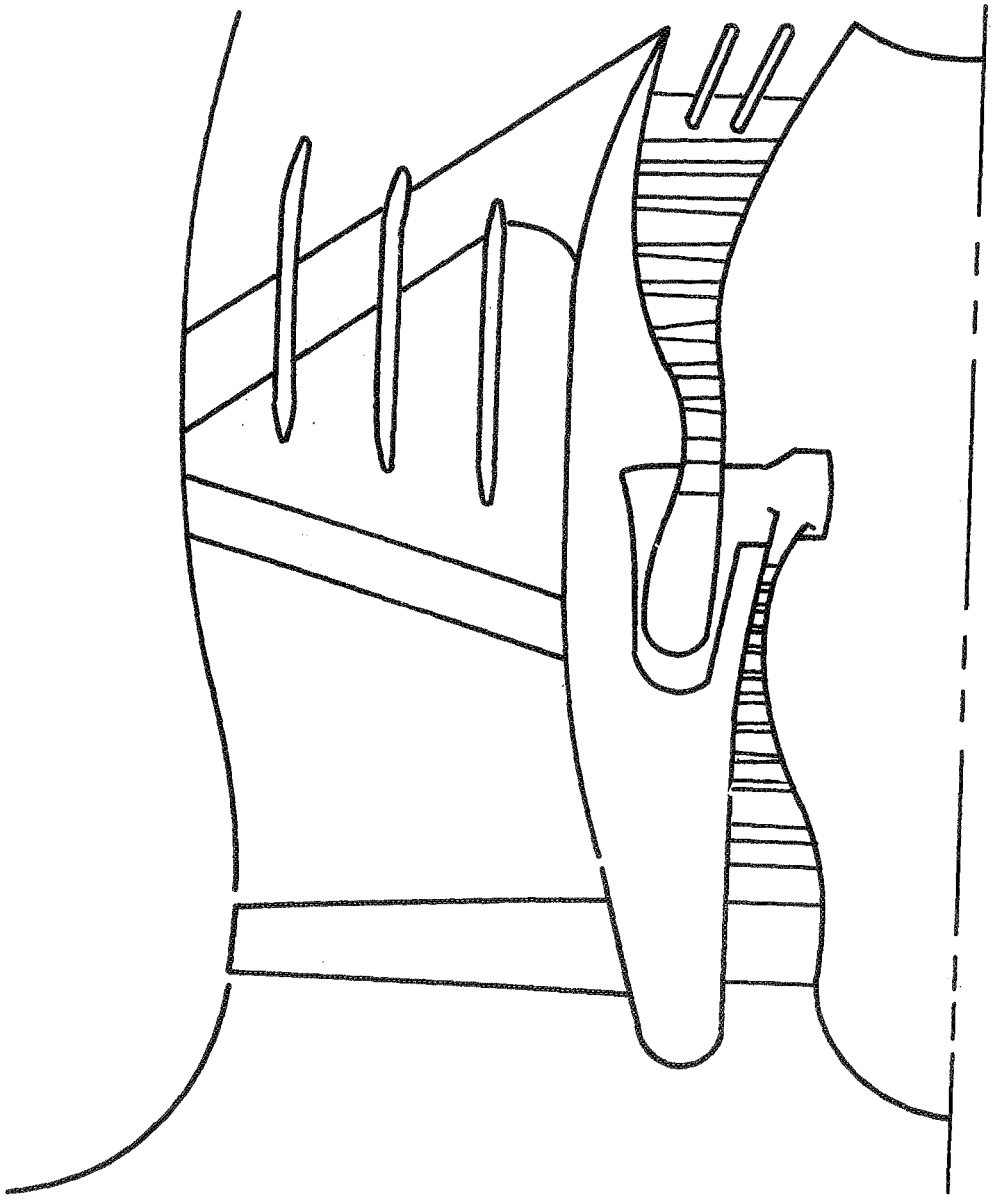

Figure 54. Task II/III Component Arrangement.

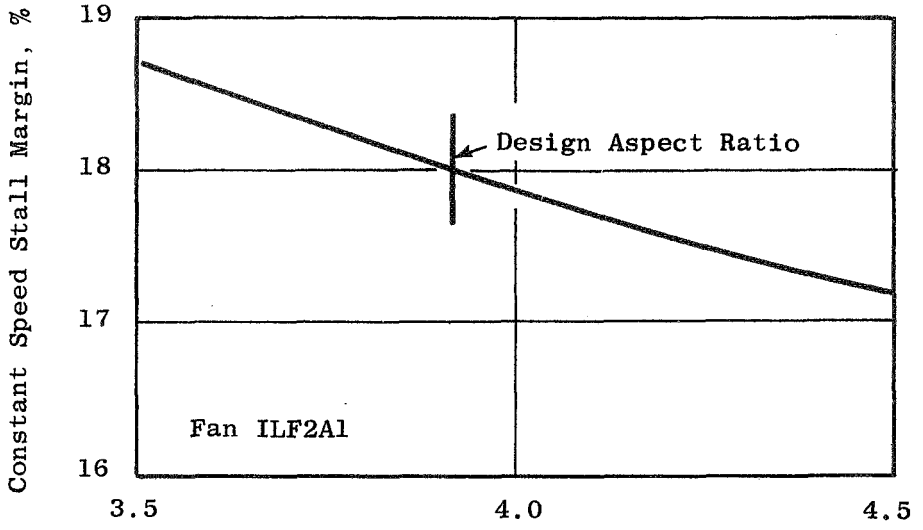

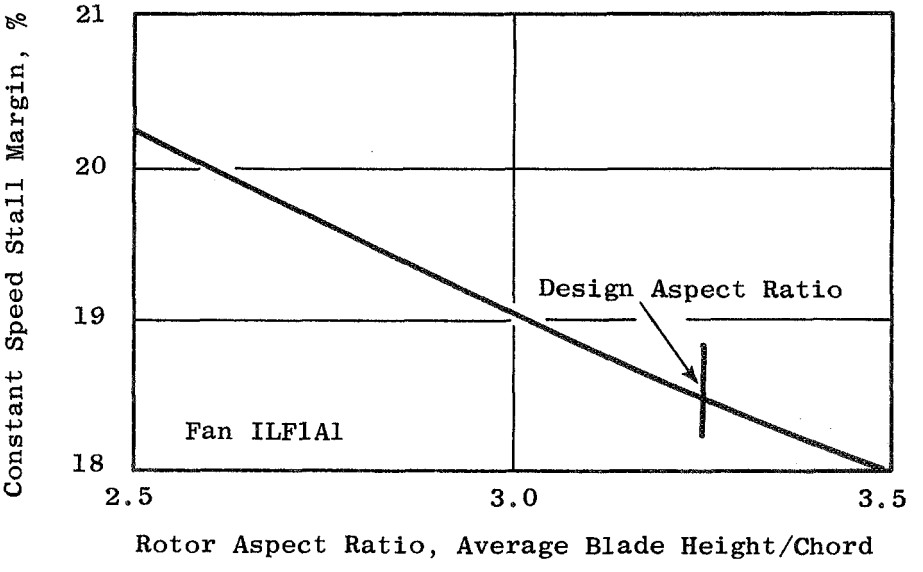

Figure 55. Fans ILF1A1 and ILF2A1 Parametric Study.

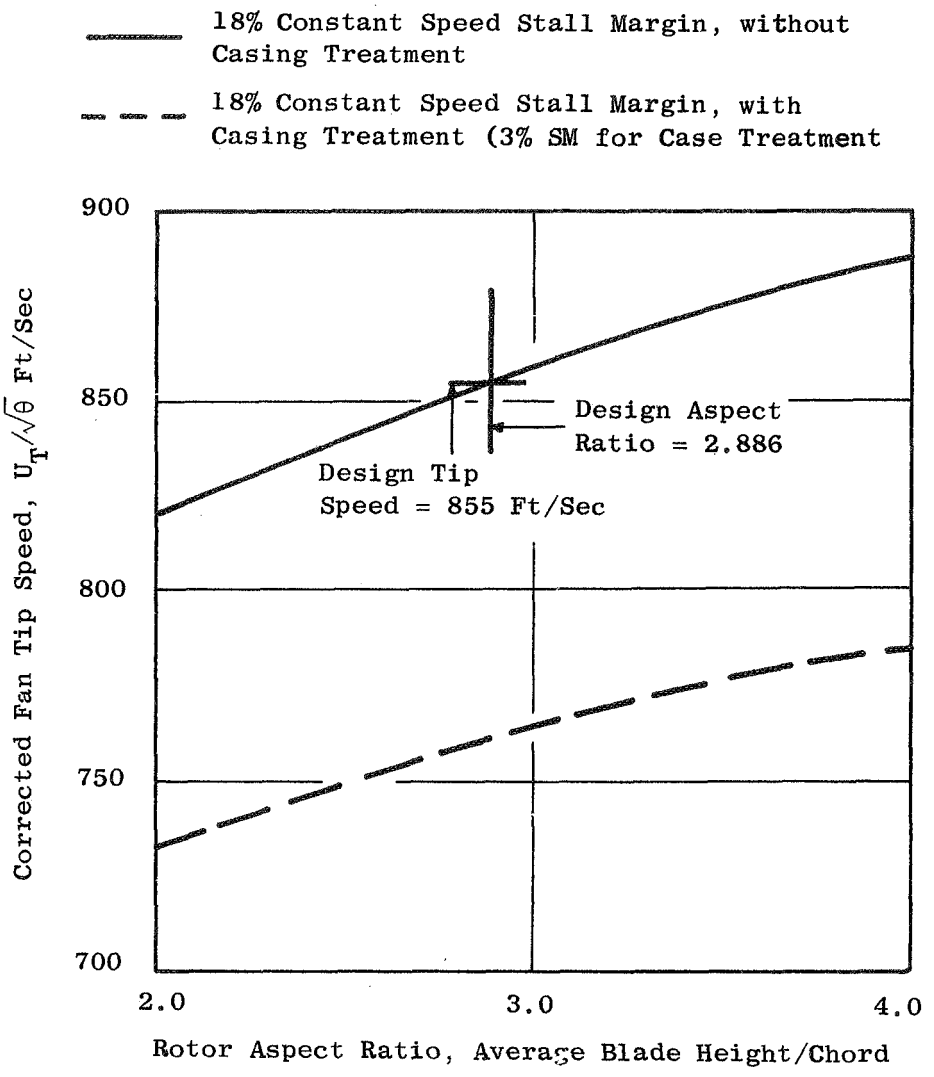

Figure 56. Fan ILF2A2 Parametric Study.

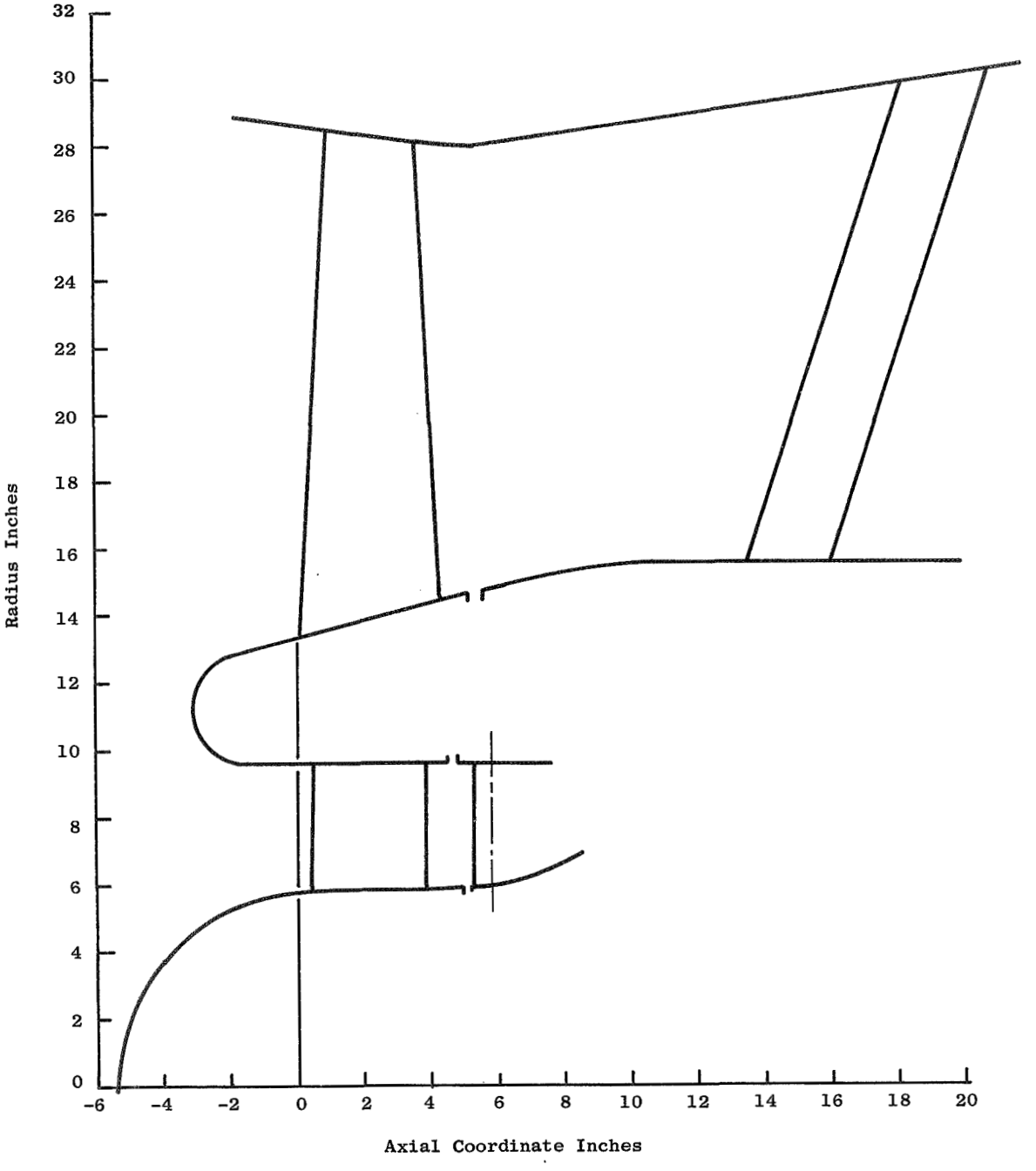

Figure 57. Fan Flow Path ILF1A1.

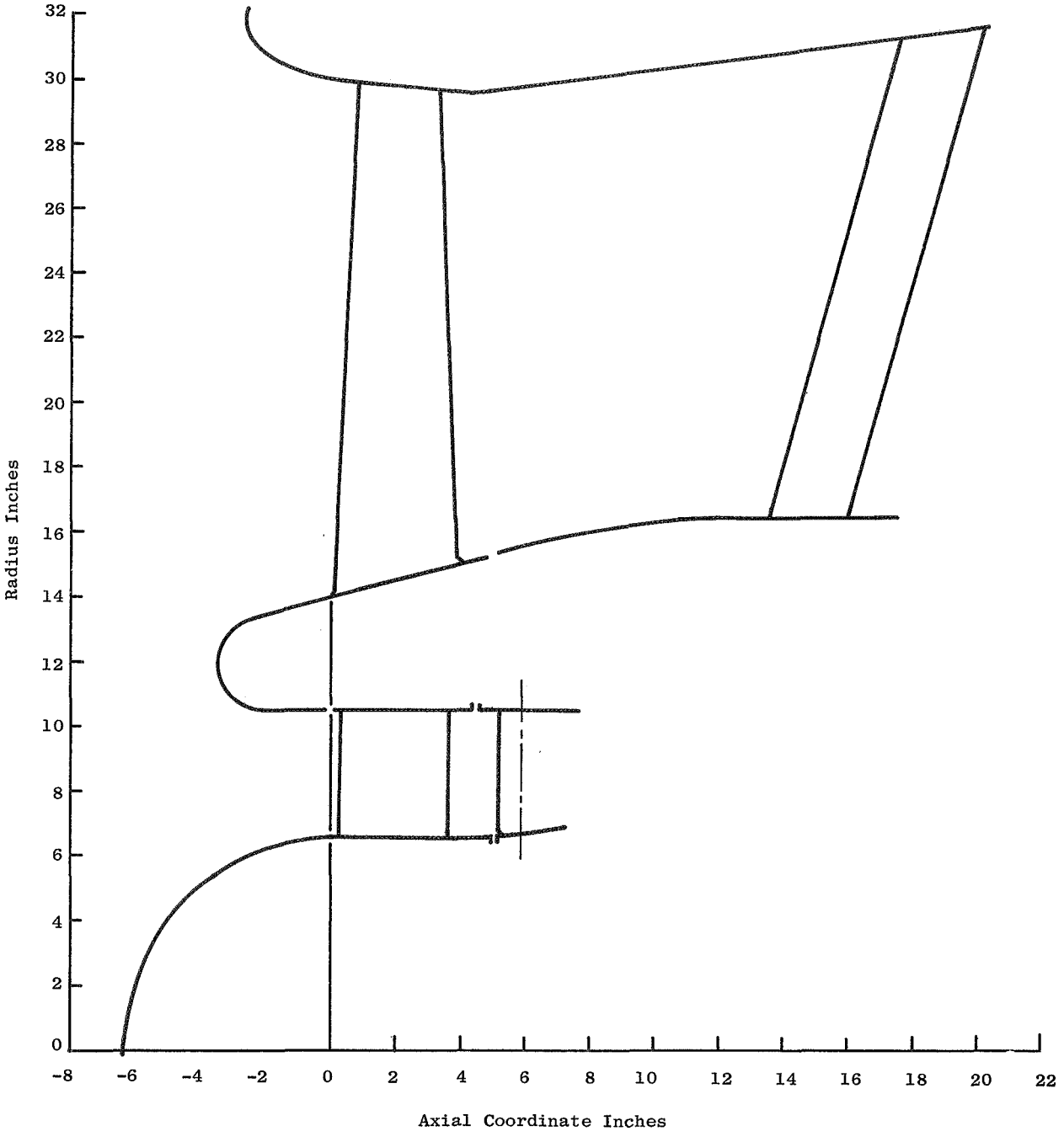

Figure 58. Fan Flow Path ILF2A1.

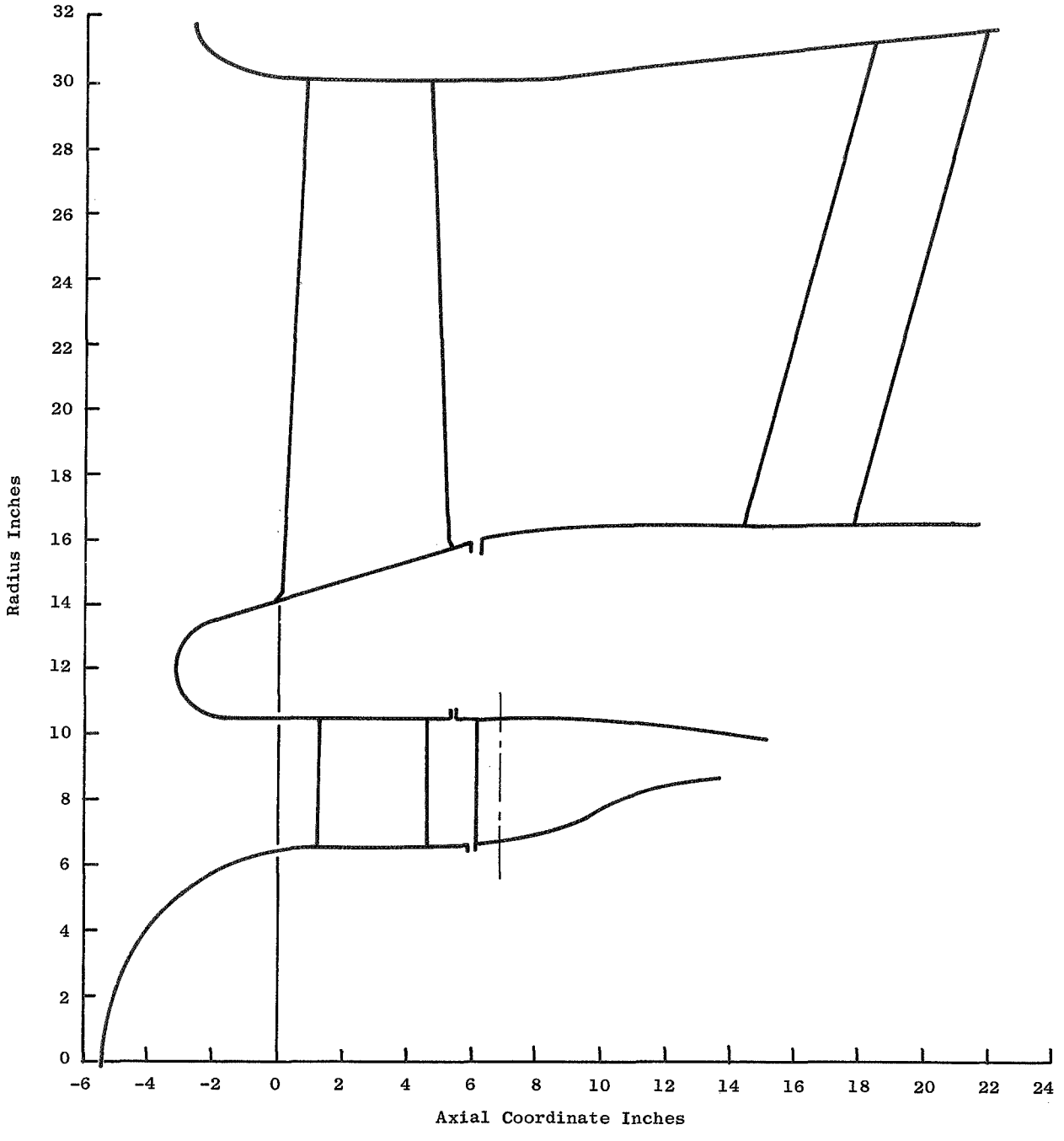

Figure 59. Fan Flow Path ILF2A2.

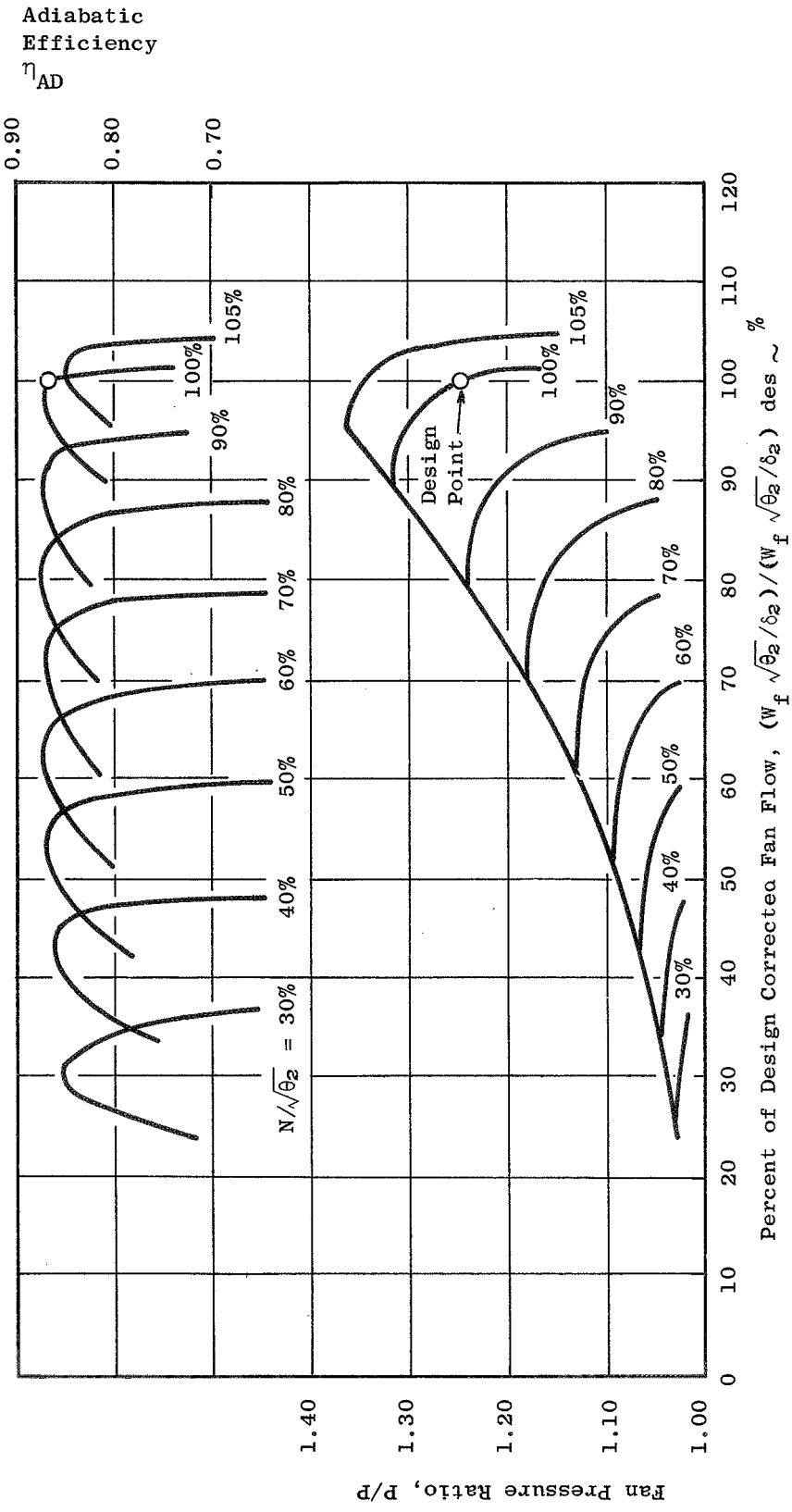

Figure 60. Fan ILF1A1 Performance Map.

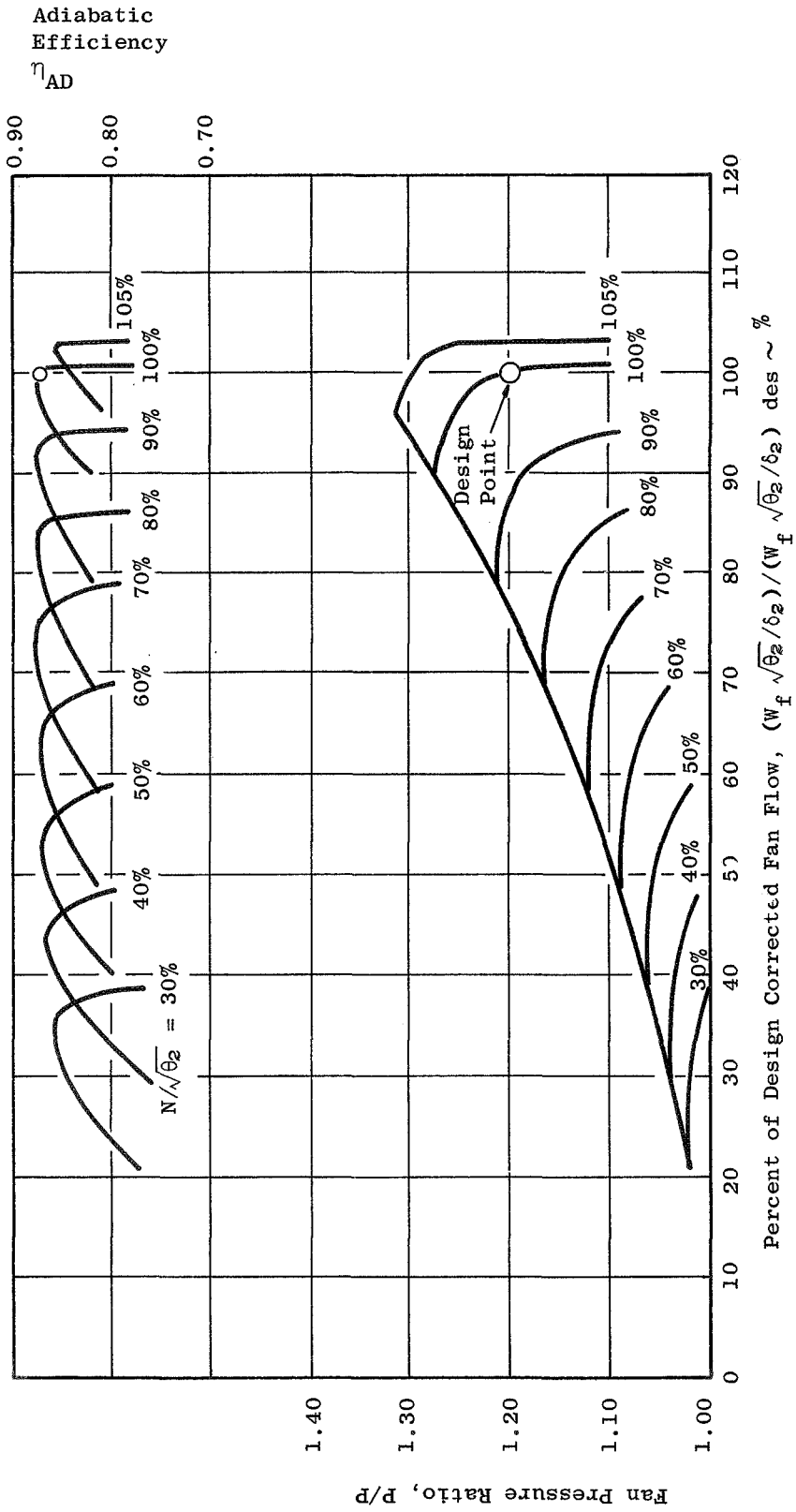

Figure 61. Fan ILF2A1 Performance Map.

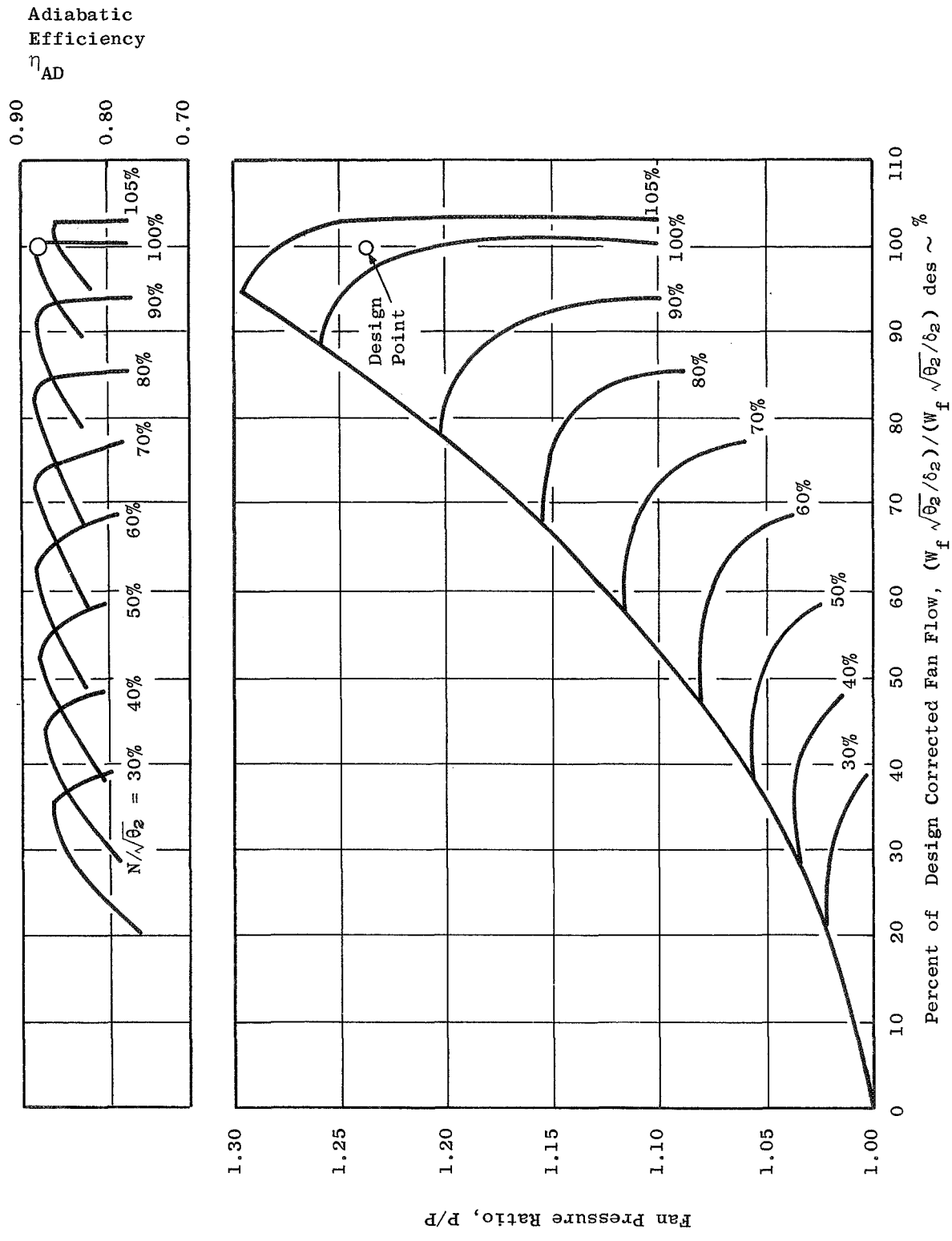

Figure 62. Fan ILF2A2 Performance Map.

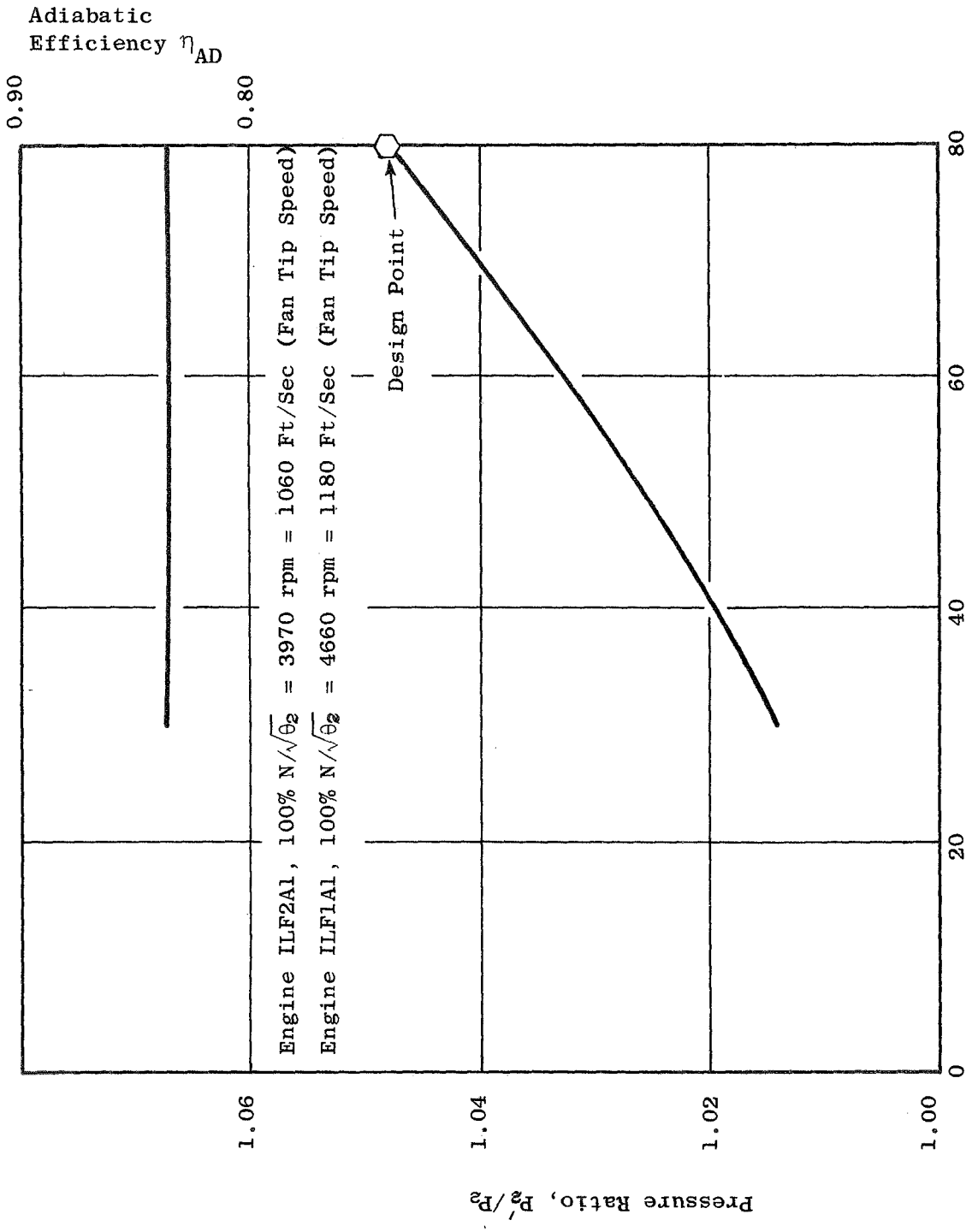

Figure 63. Supercharger ILF1A1 and ILF2A1 Operating Line Performance.

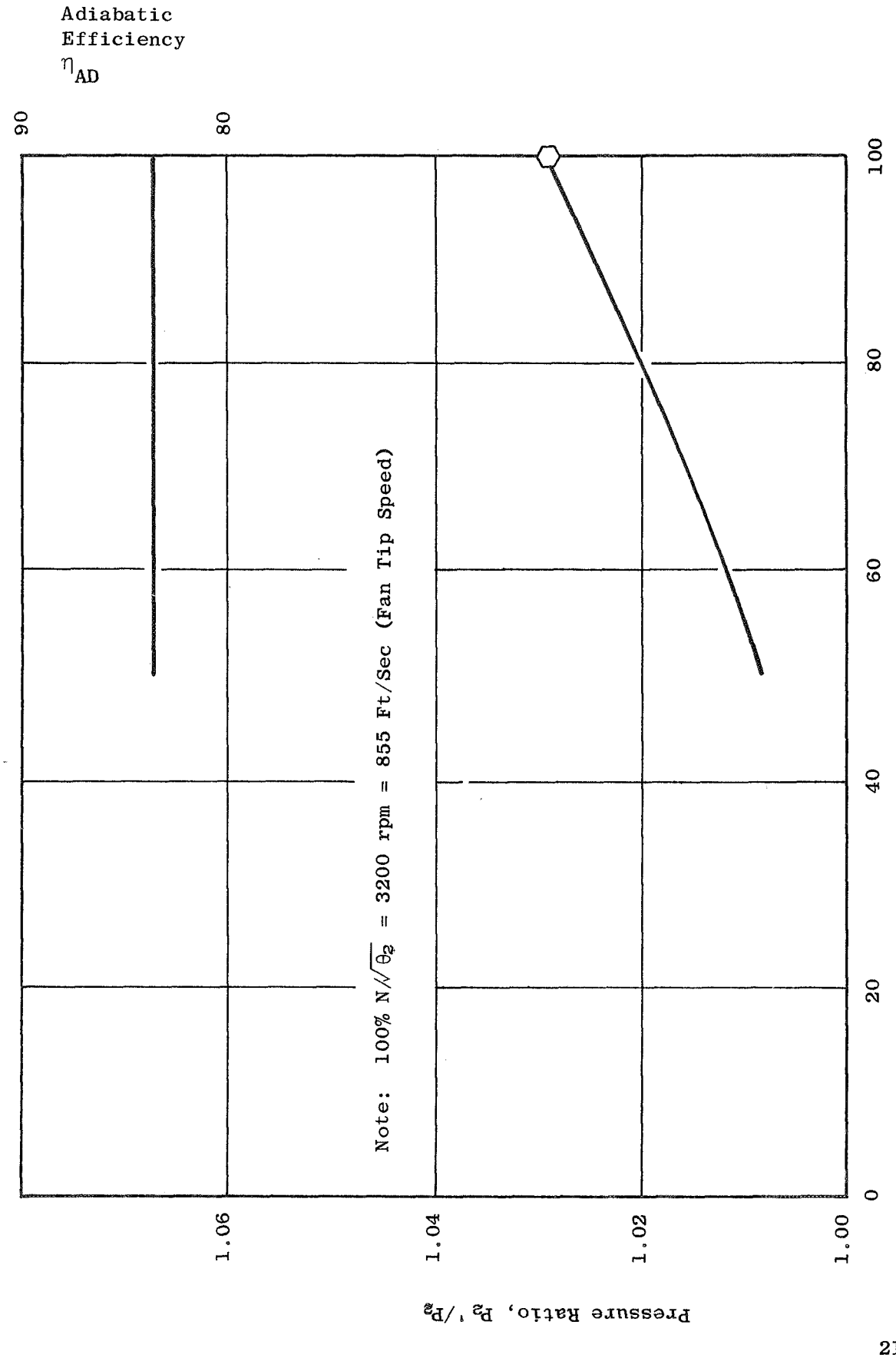

Figure 64. Supercharger ILF2A2 Operating Line Performance.

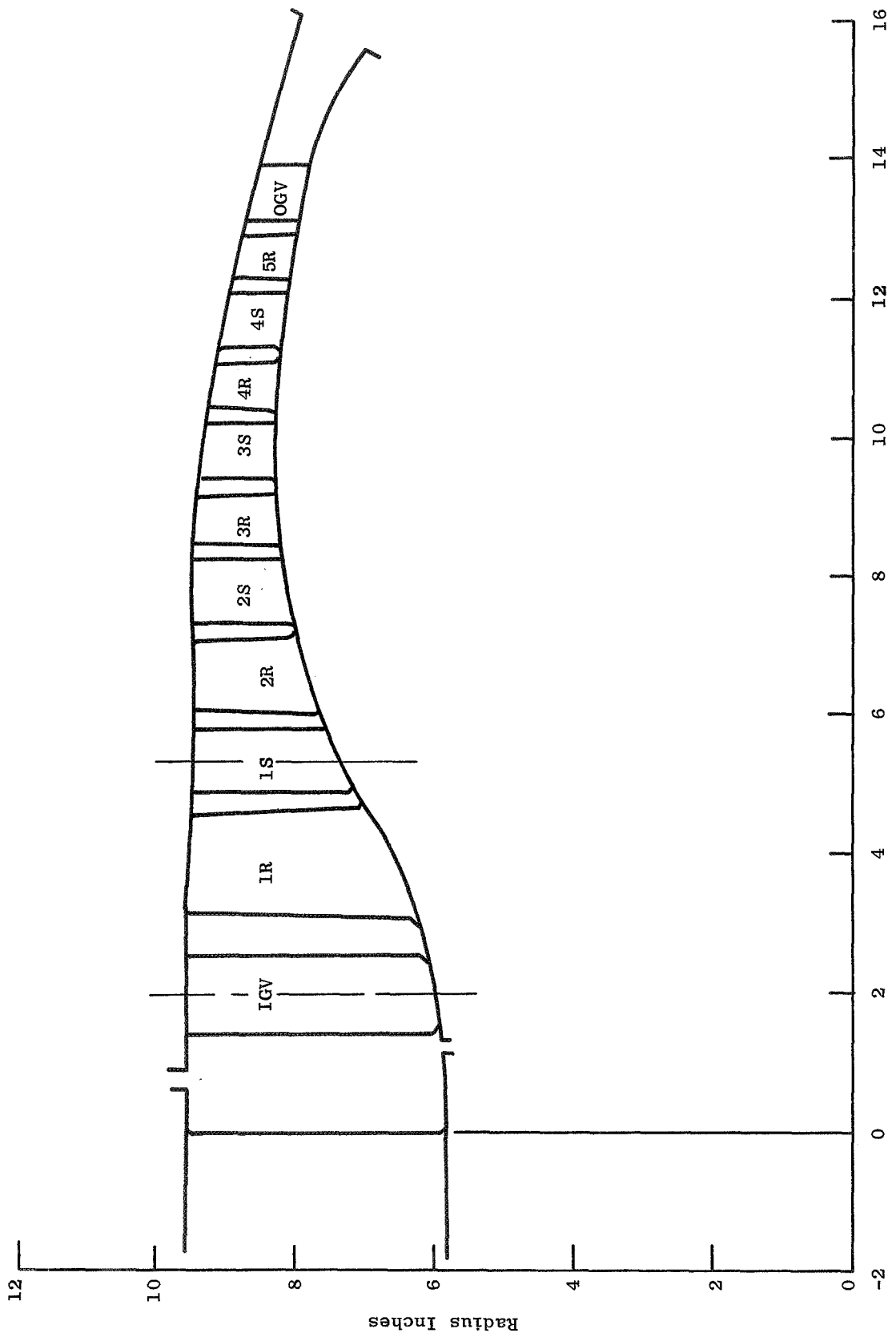

Figure 65. Compressor Flow Path ILF1A1.

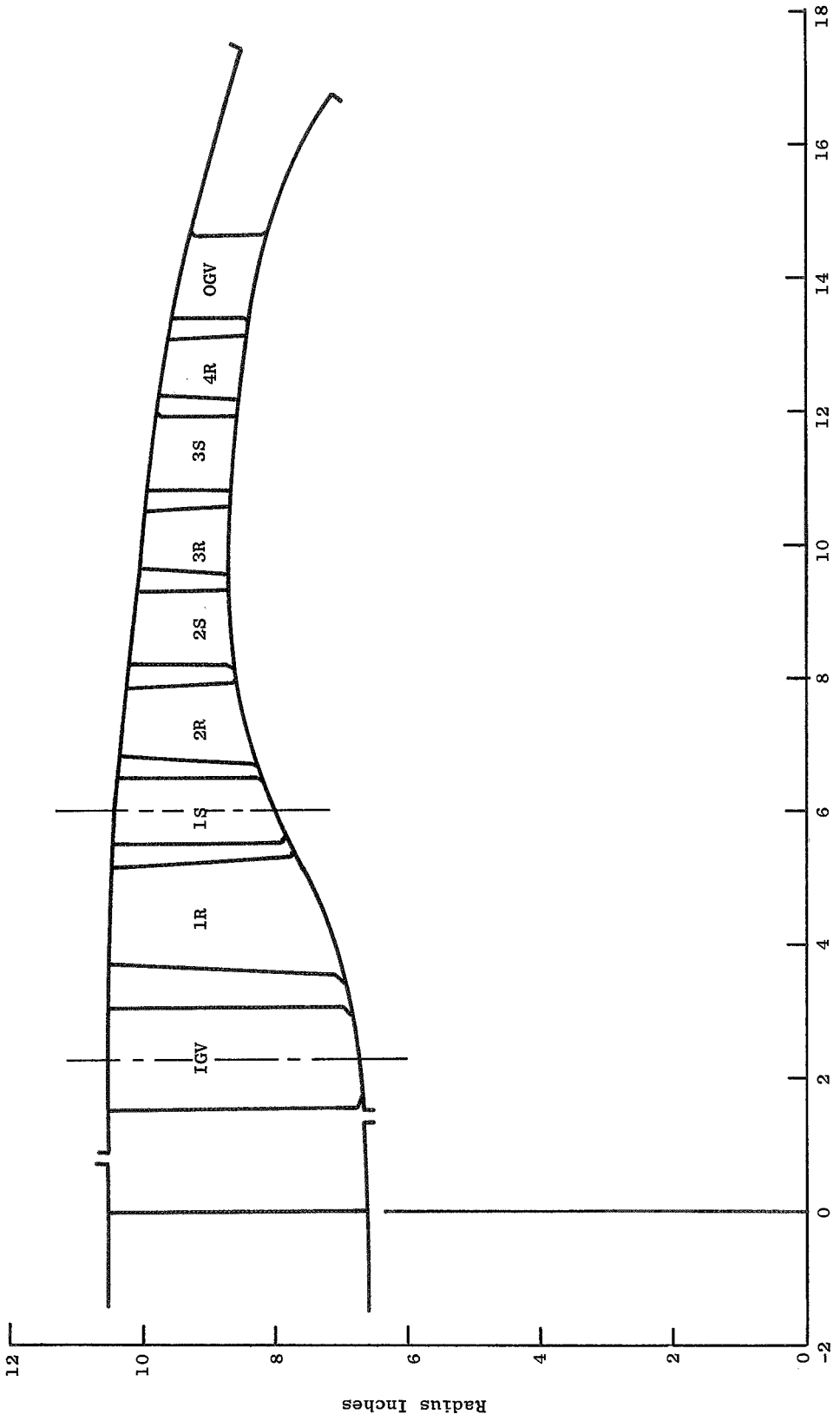

Figure 66. Compressor Flow Path ILF2A1 and ILF2A2.

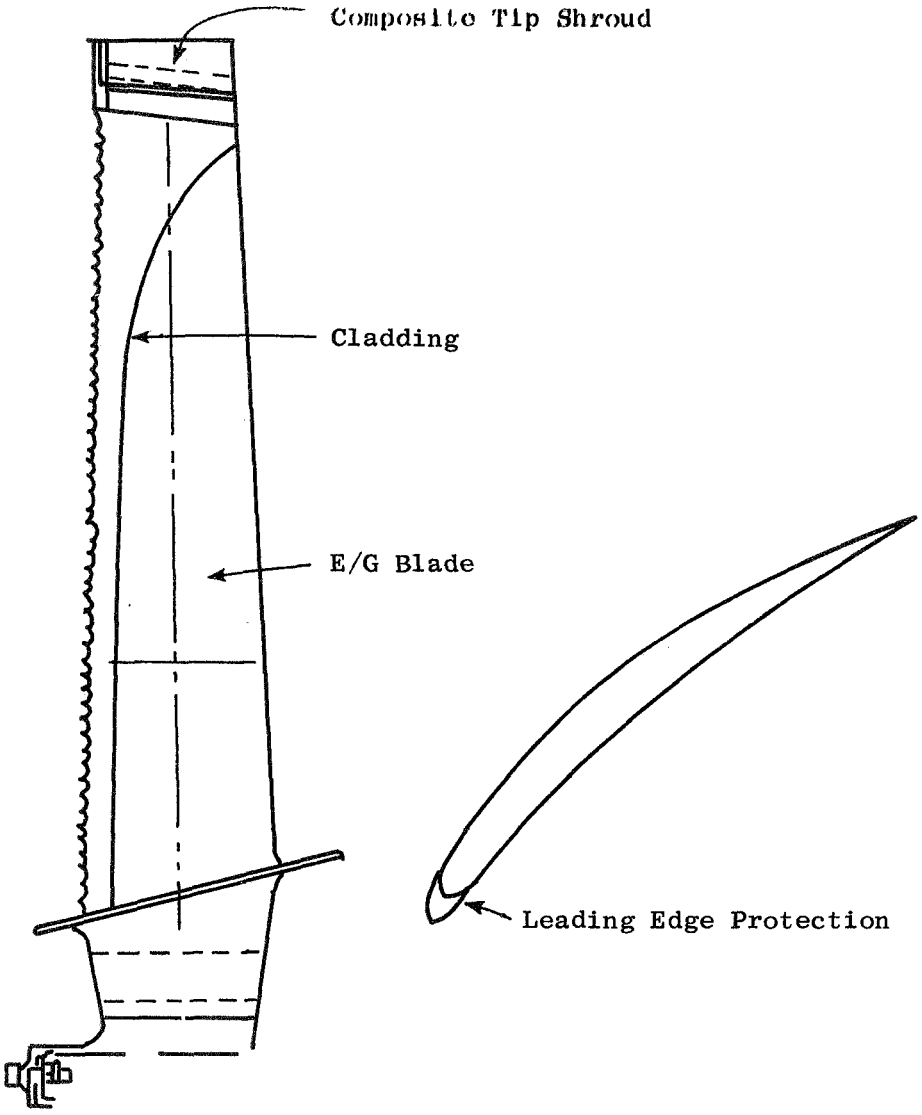

Figure 67. Epoxy/Graphite Fan.

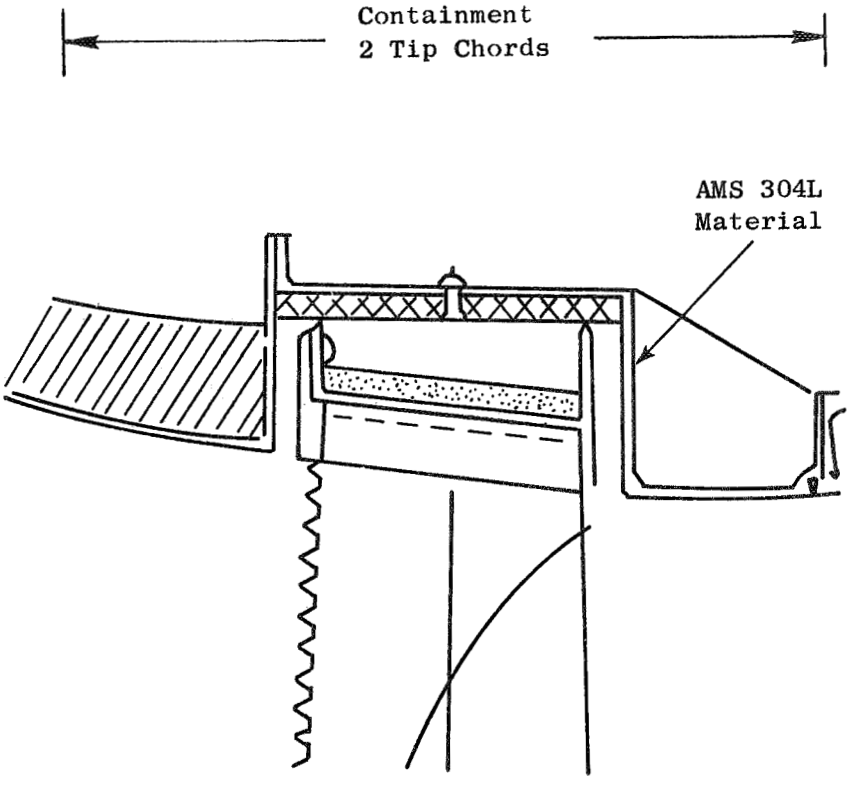

Figure 68. Fan.

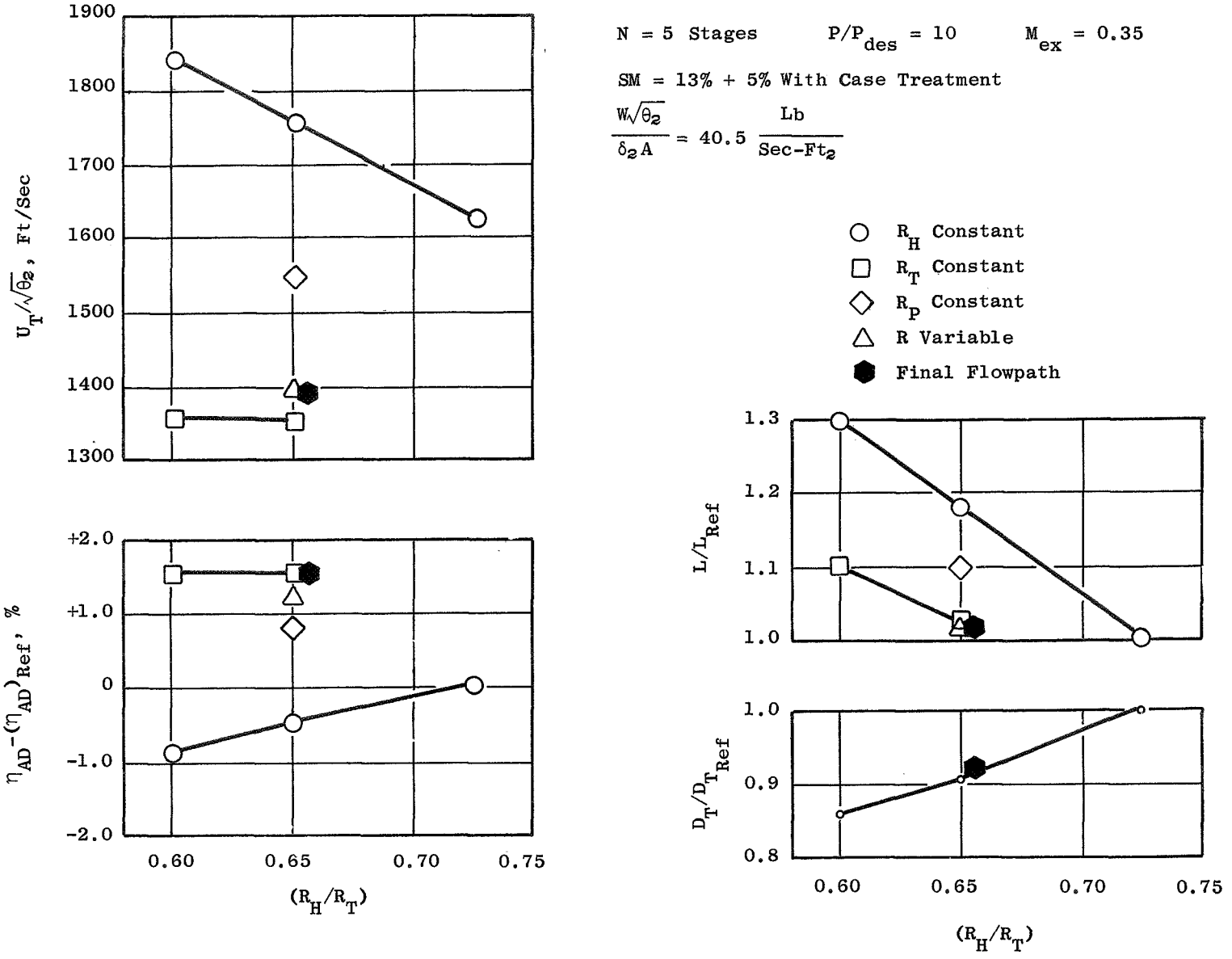

Figure 69. ILF1A1 Compressor Parametric Study.

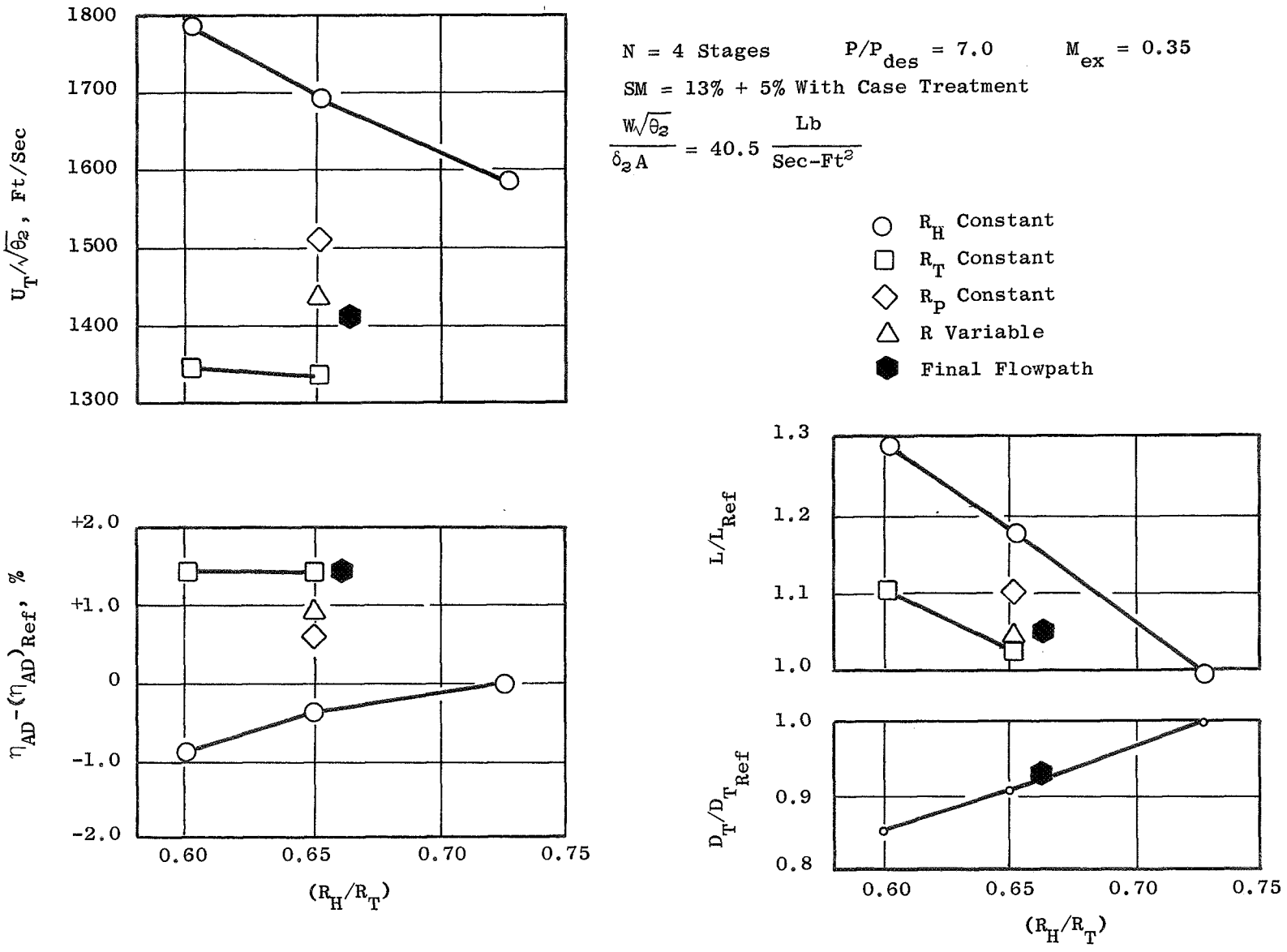

Figure 70. ILF2A1 Compressor Parametric Study.

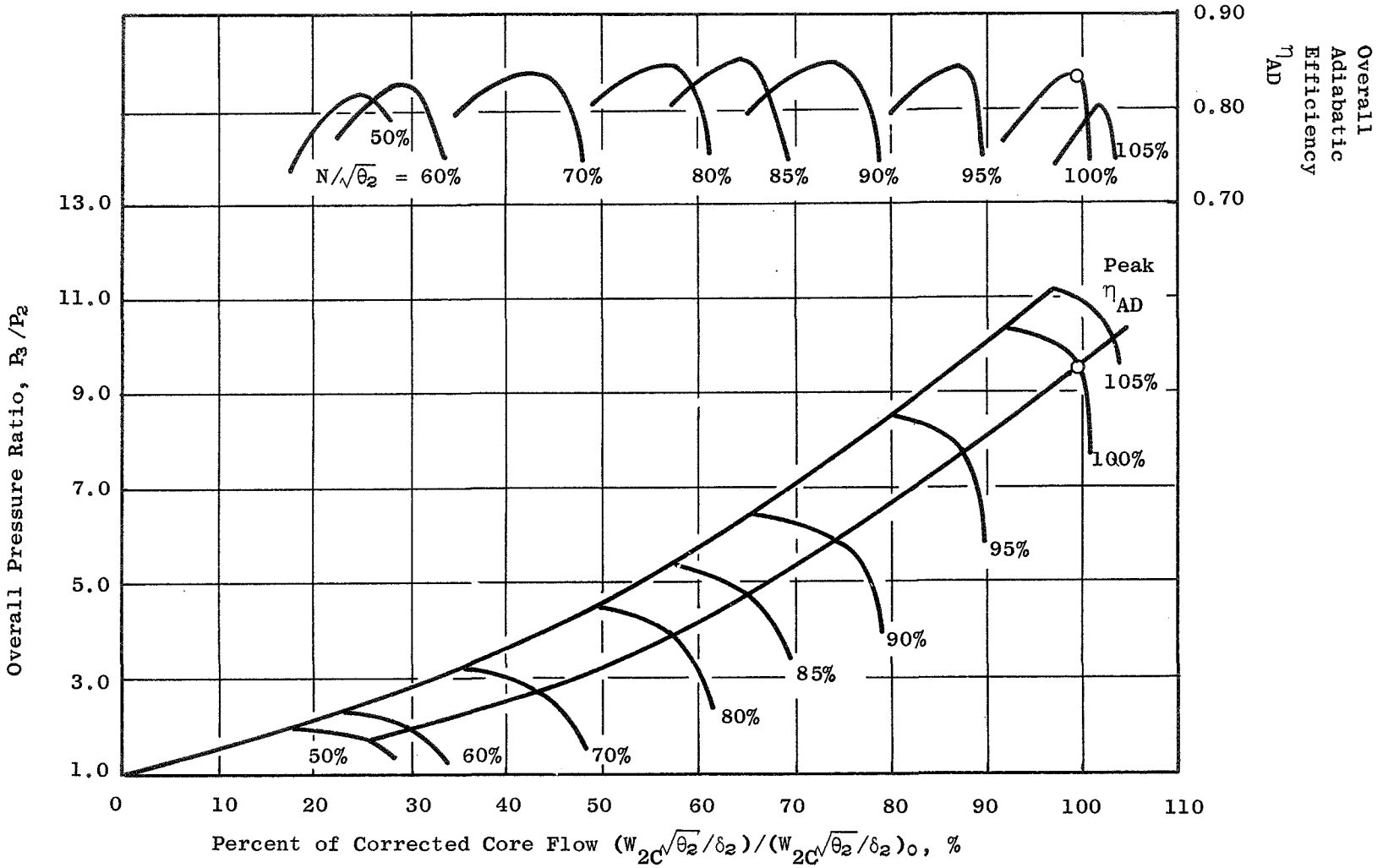

Figure 71. ILF1A1 Compressor Performance Map.

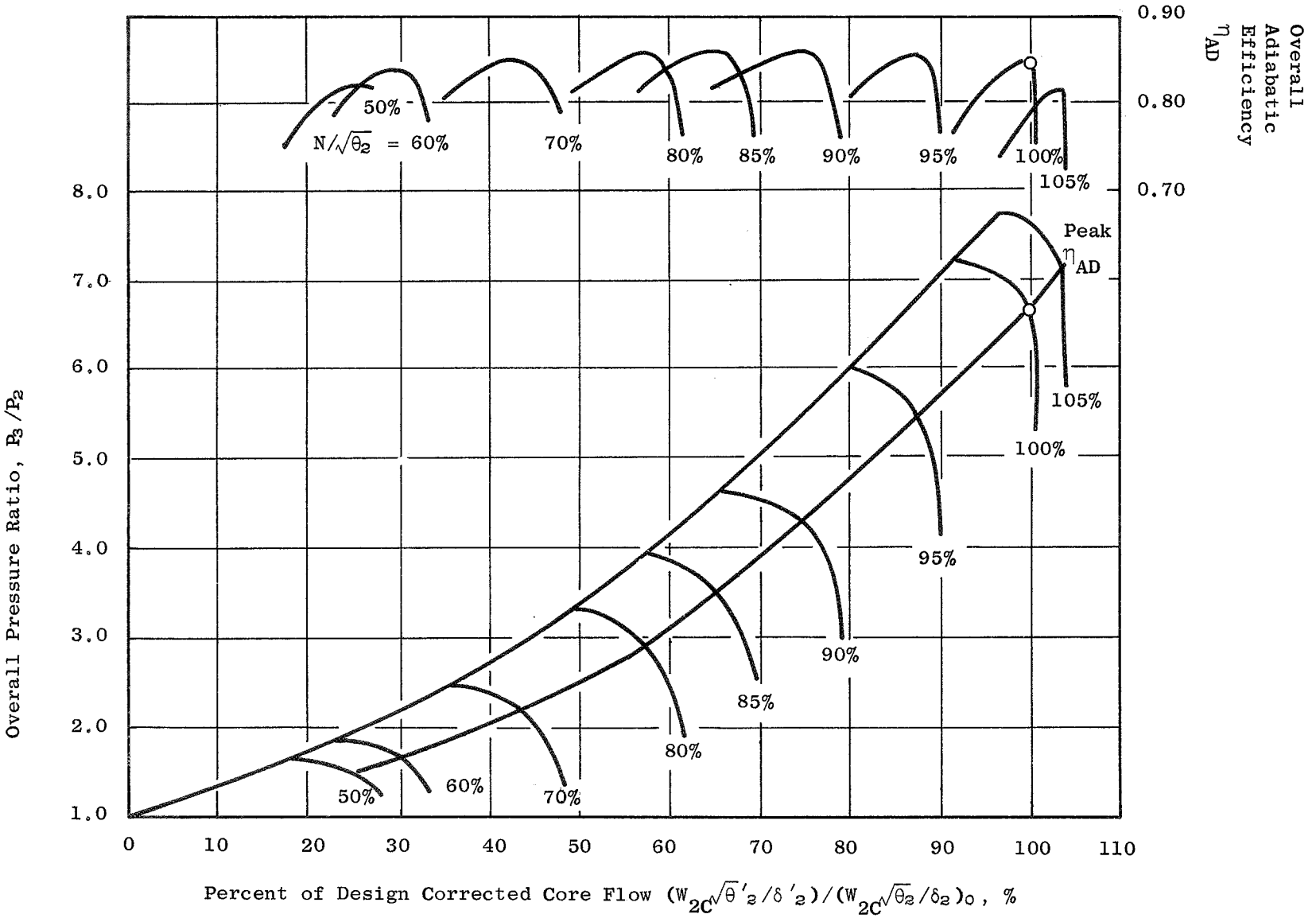

Figure 72. ILF2A1 Compressor Performance Map.

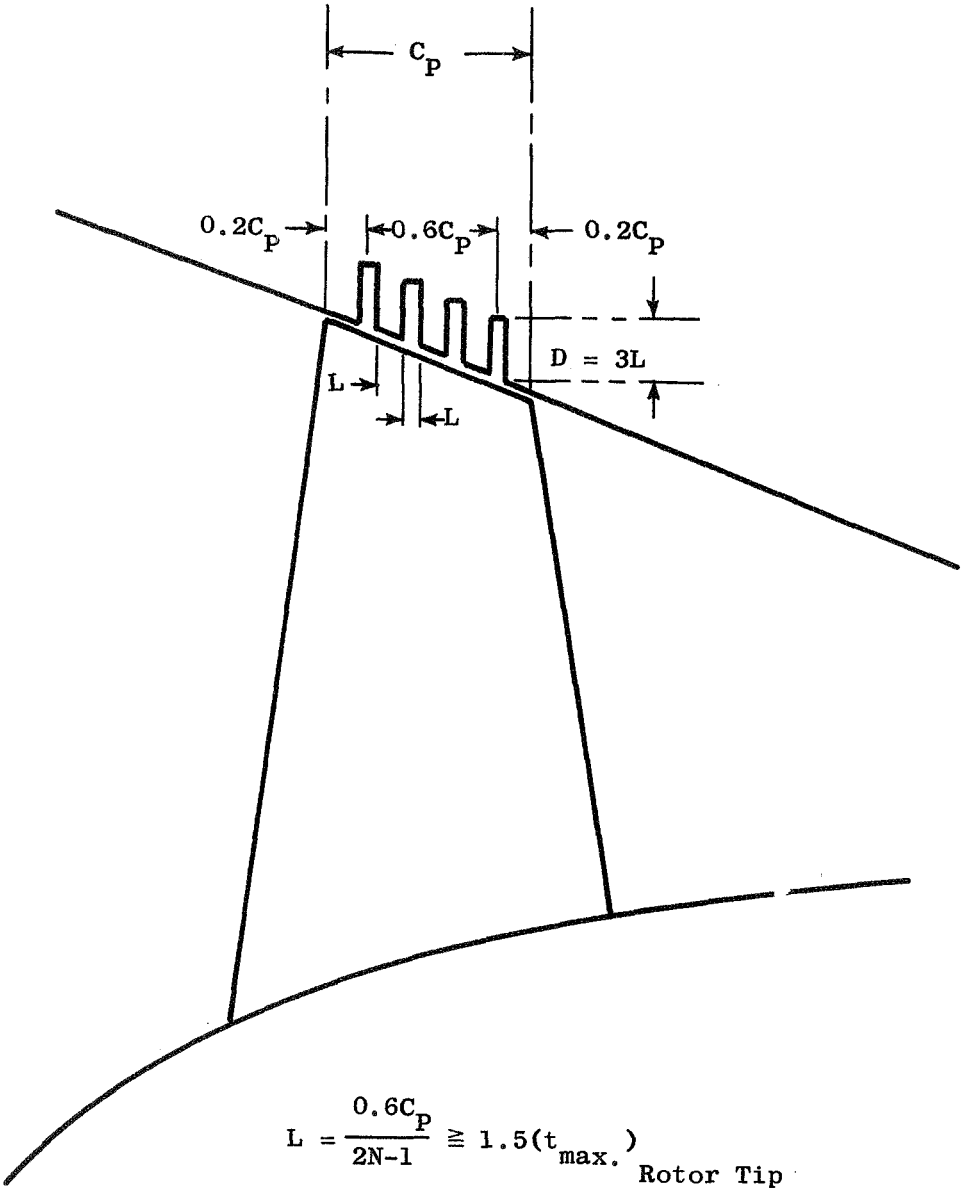

Figure 73. Circumferential Groove Casing Treatment Configuration.

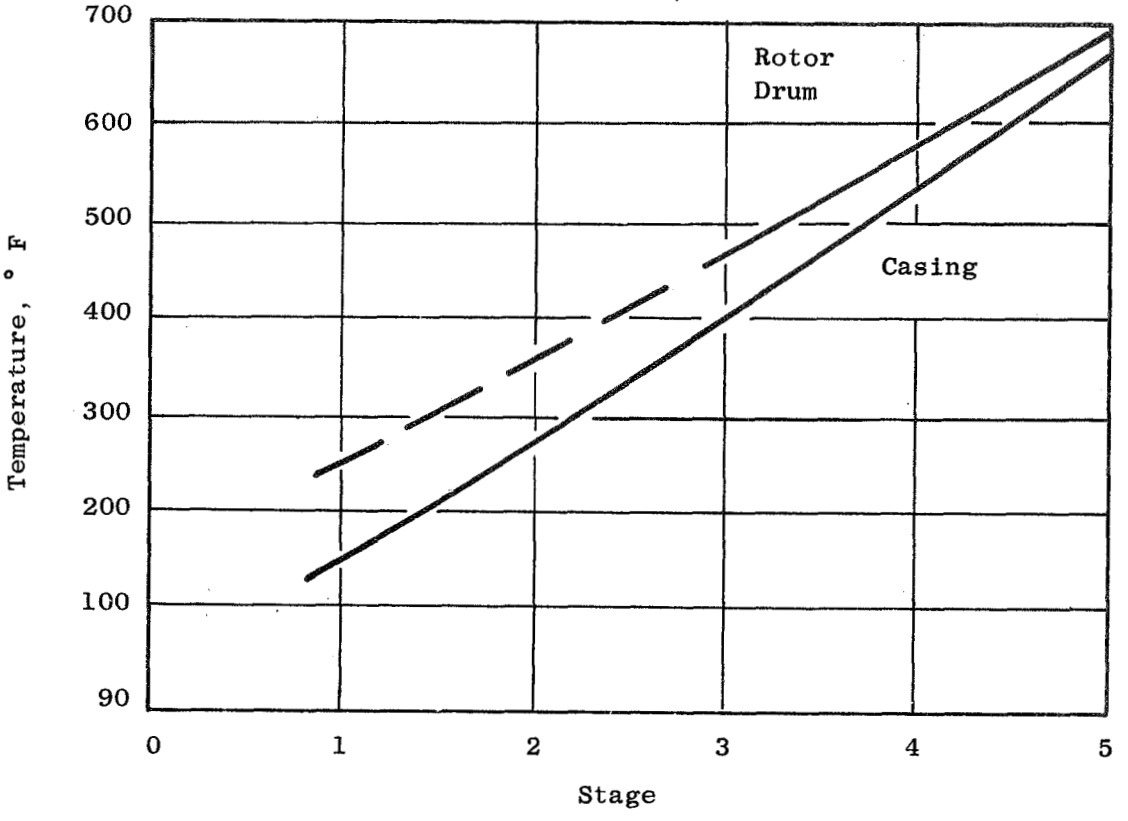

Figure 74. Compressor Average Metal Temperature.

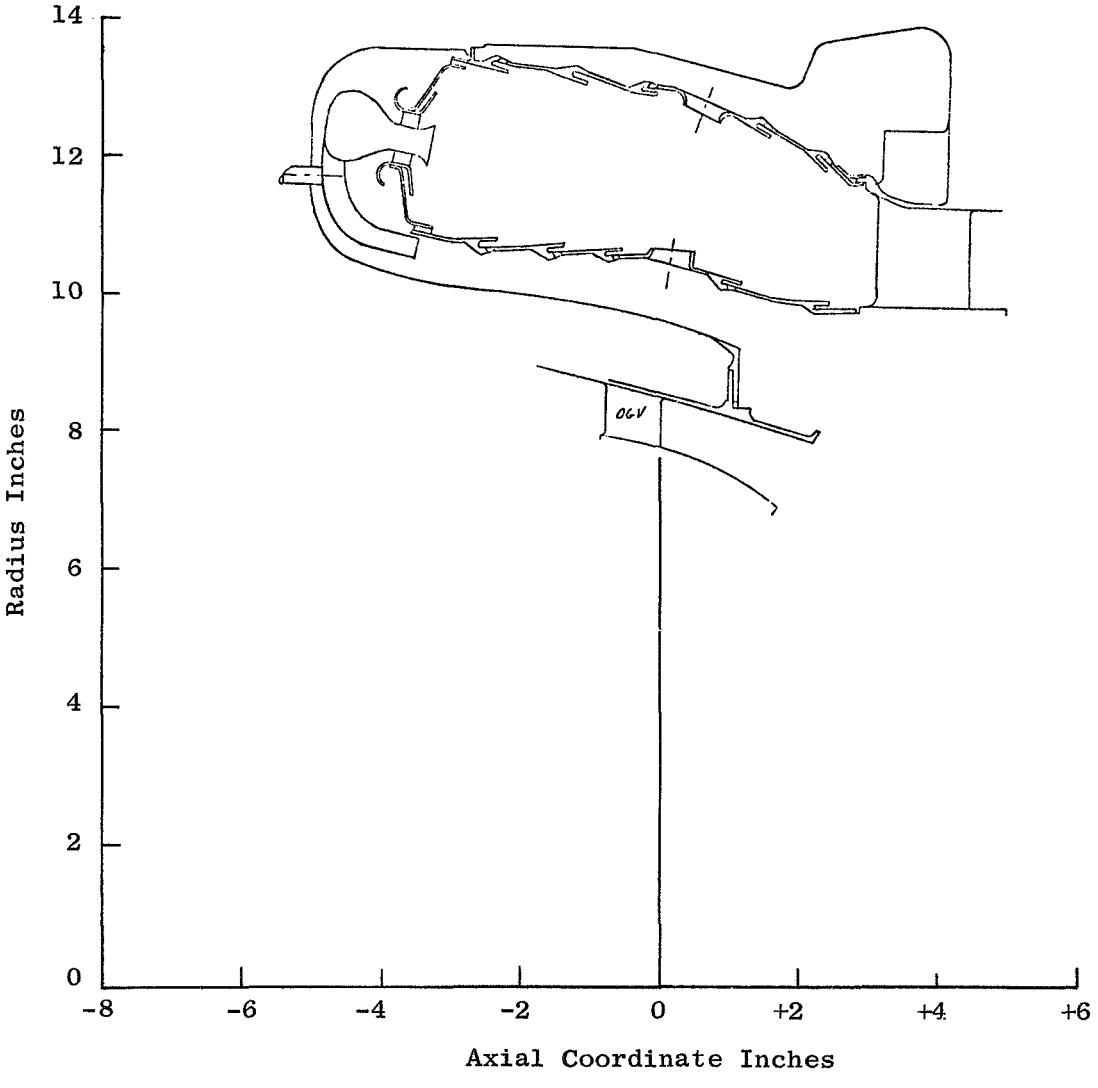

Figure 75. Combustor Flowpath ILF1A1.

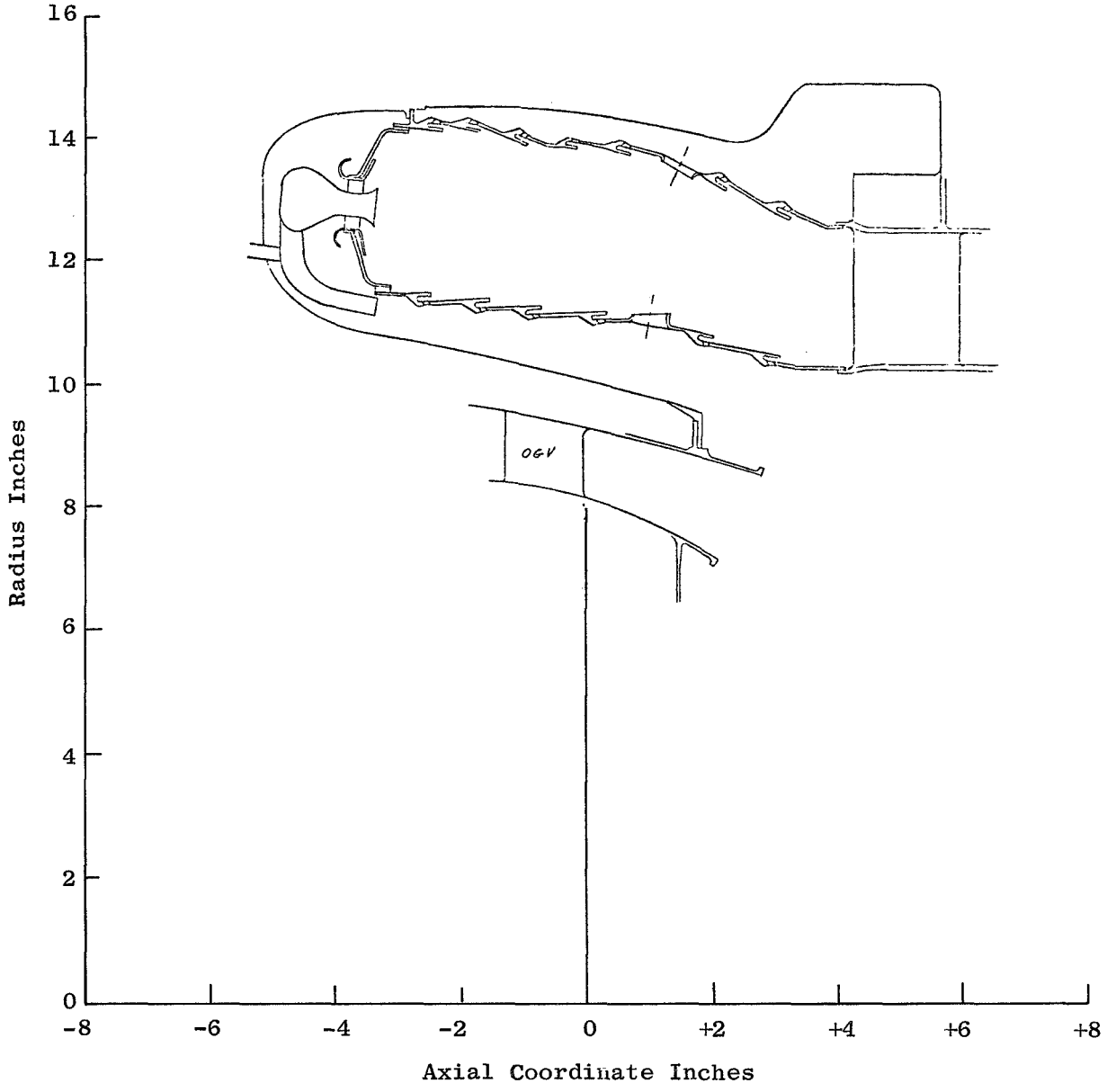

Figure 76. Combustor Flowpath ILF2A1 and ILF2A2.

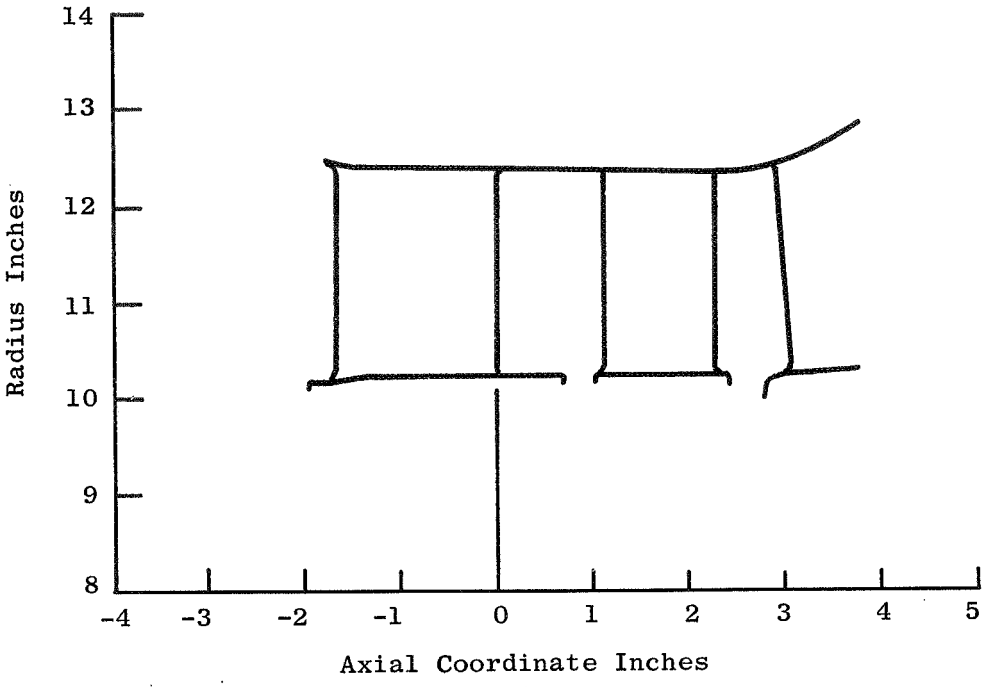

Figure 78. High Pressure Turbine Flowpath ILF2A1 and ILF2A2.

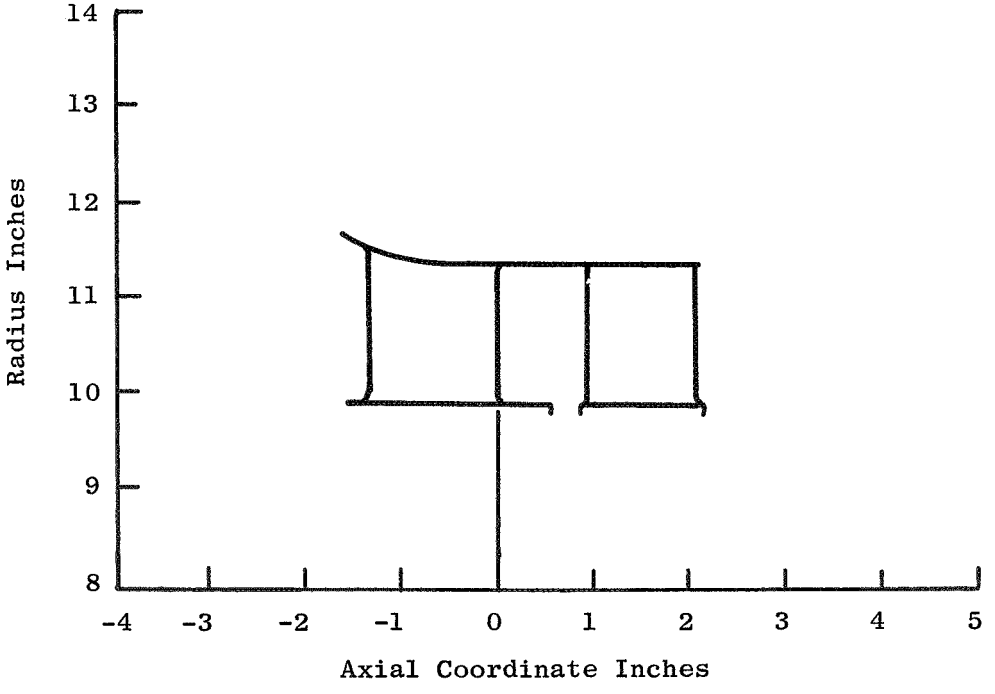

Figure 77. High Pressure Turbine Flowpath ILF1A1.

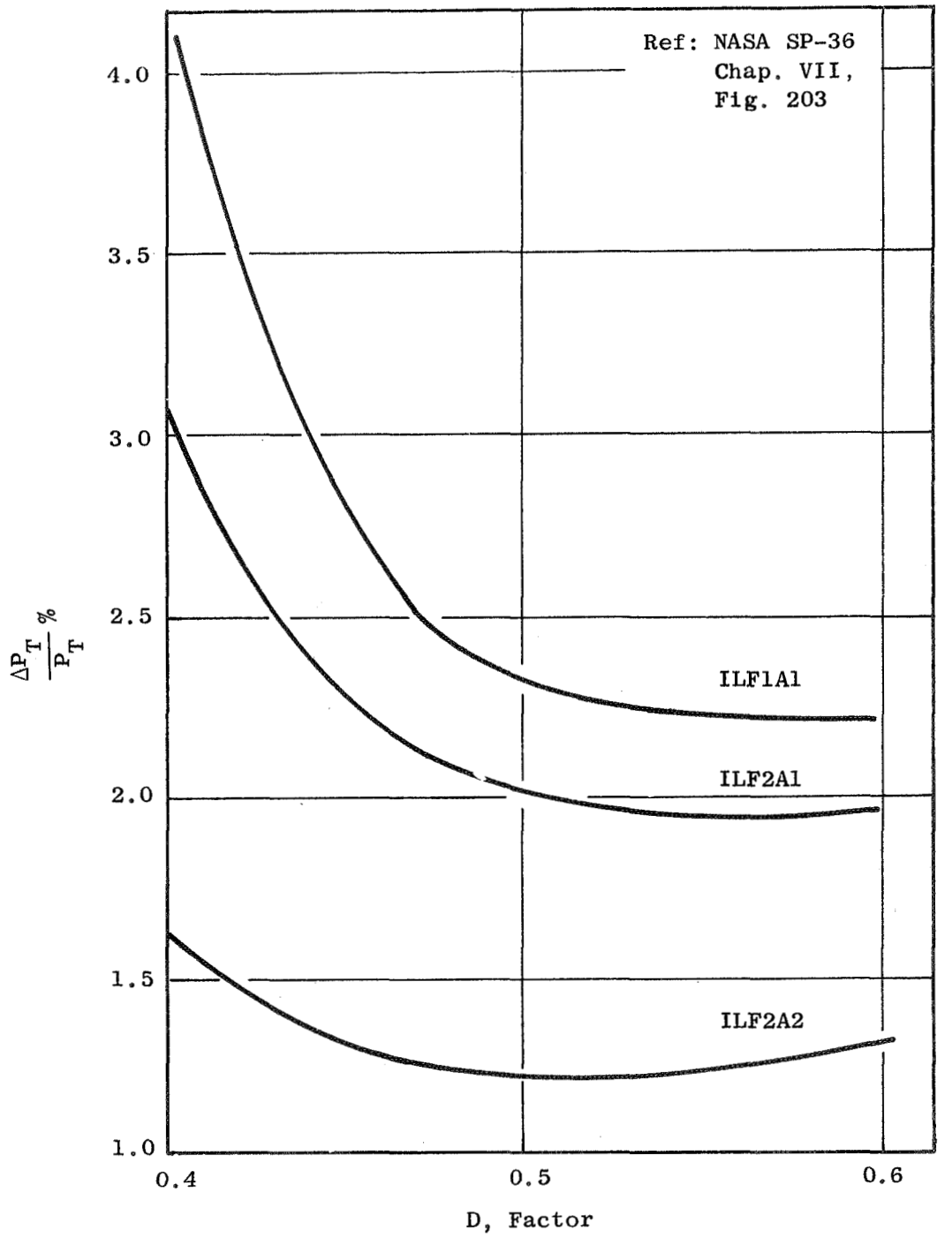

Figure 79. OGV Loss Vs. D-Factor.

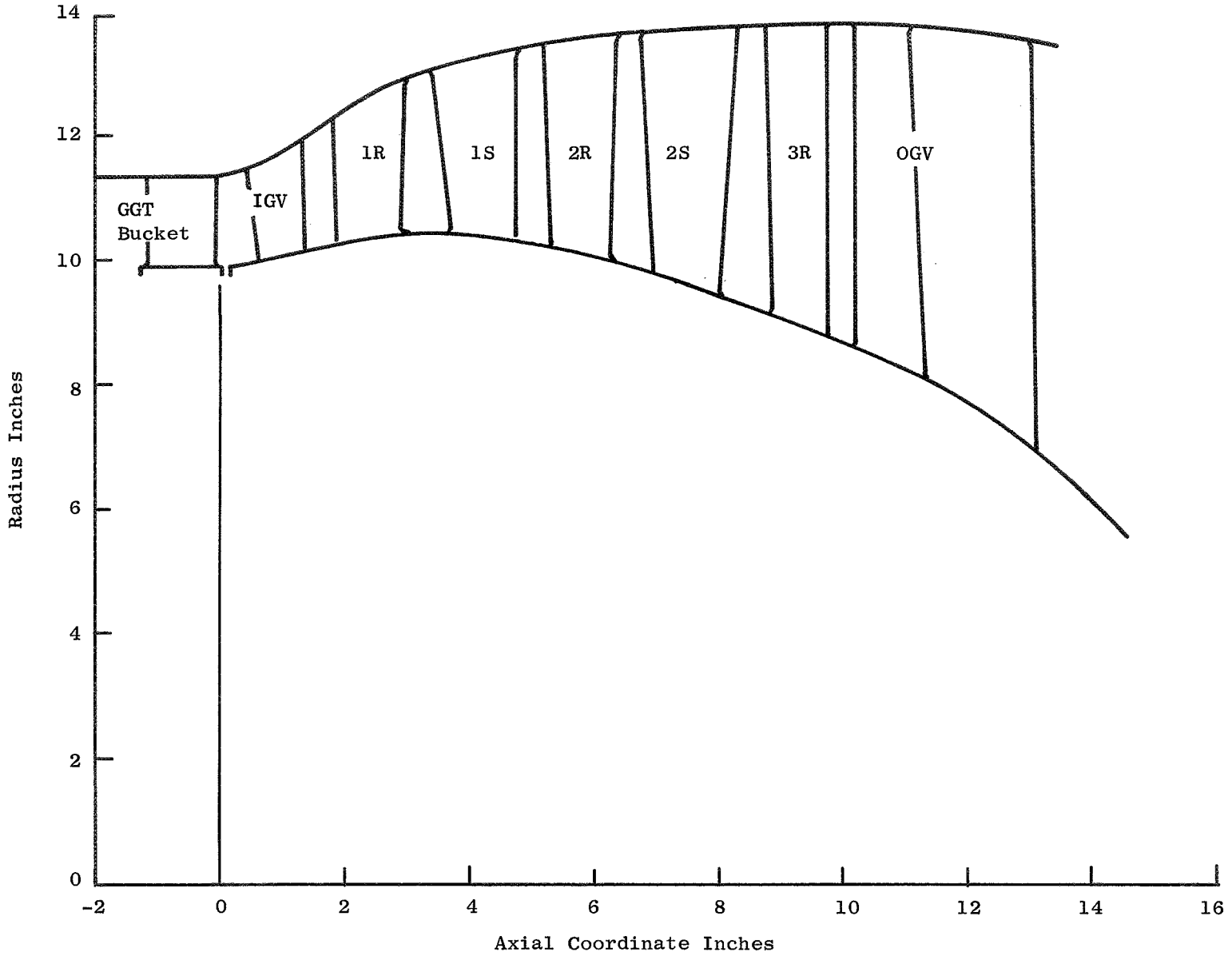

Figure 80. Low Pressure Turbine Flowpath ILF1A1.

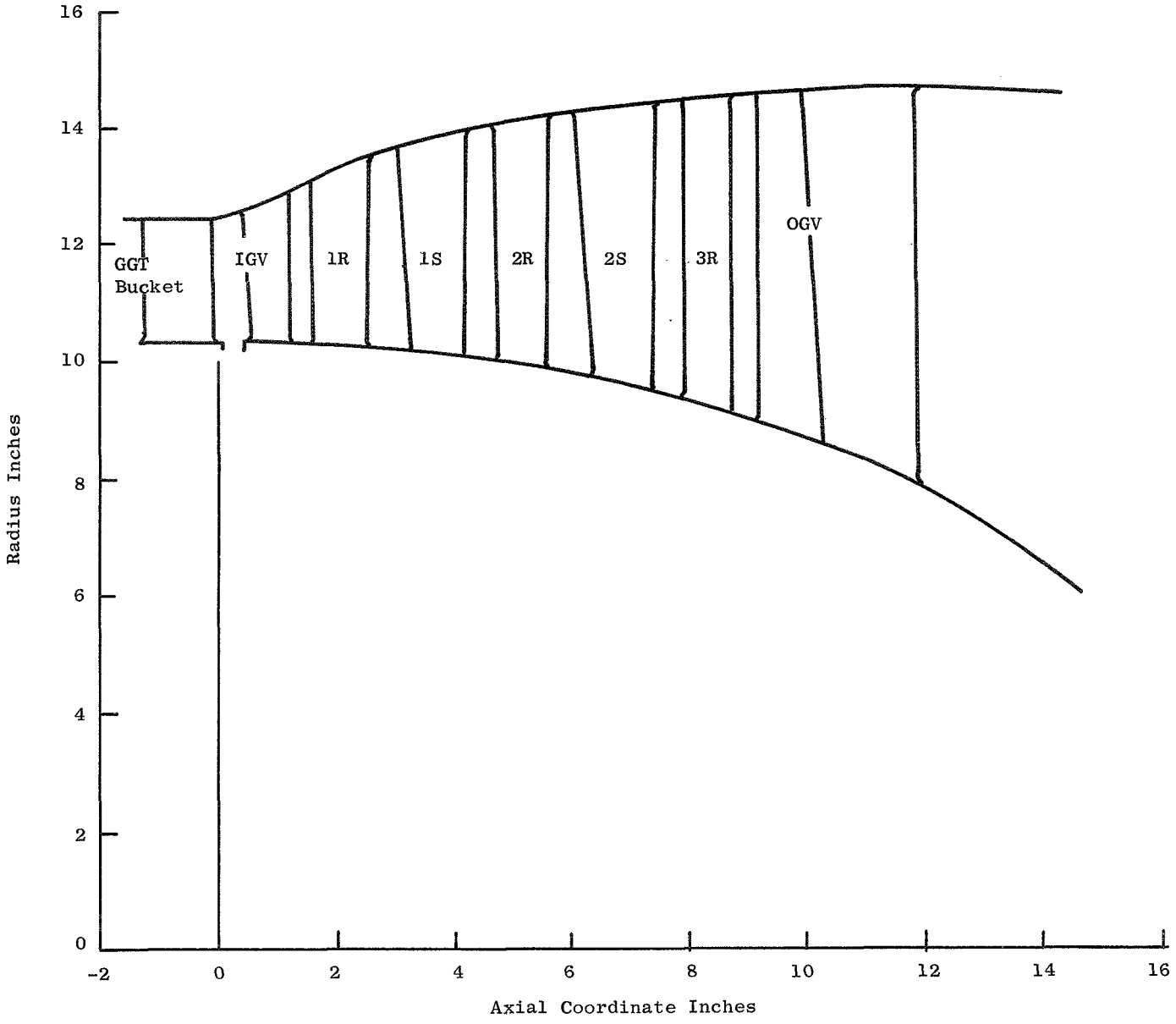

Figure 81. Low Pressure Turbine Flow Path ILF2A1.

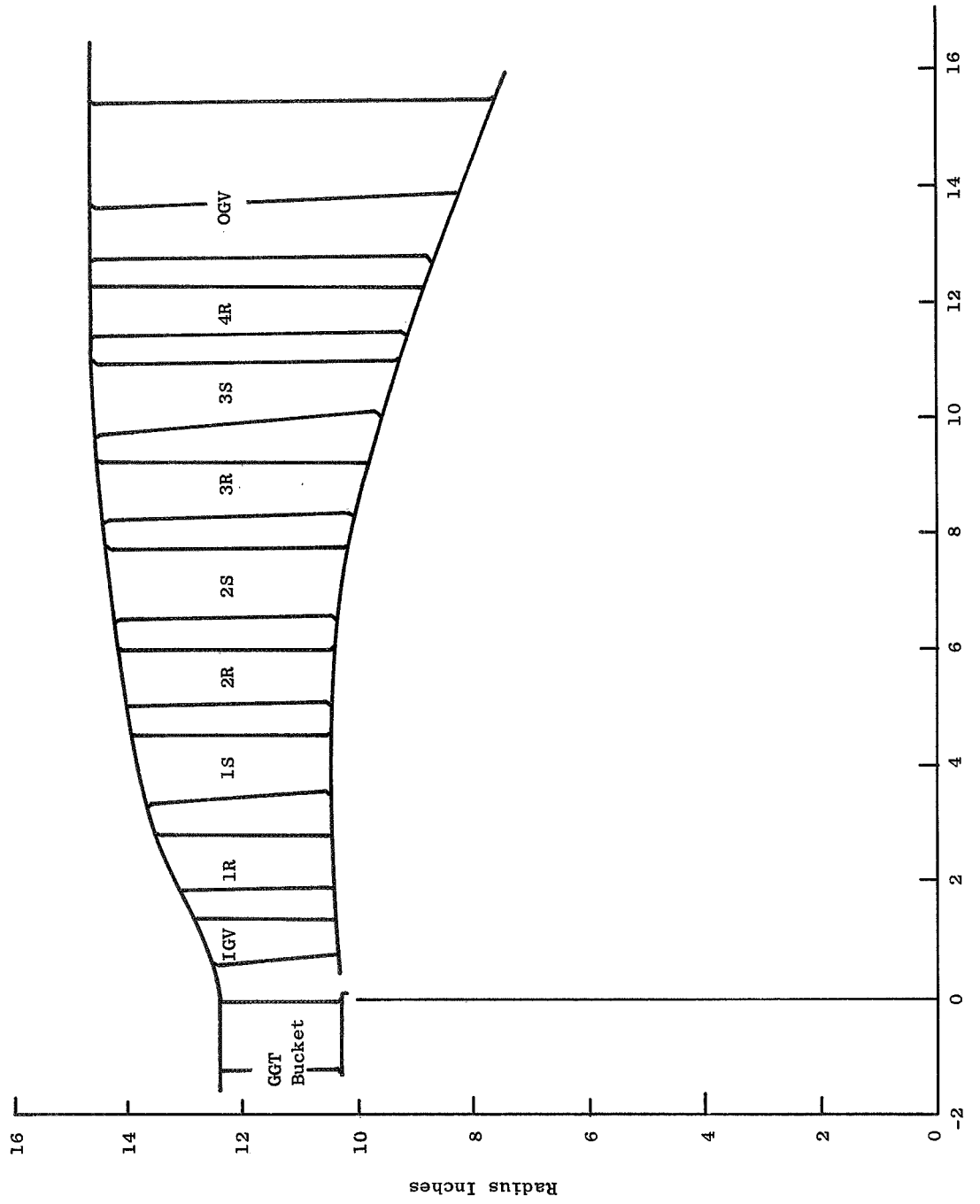

Figure 82. Low Pressure Turbine Flow Path ILF2A2.

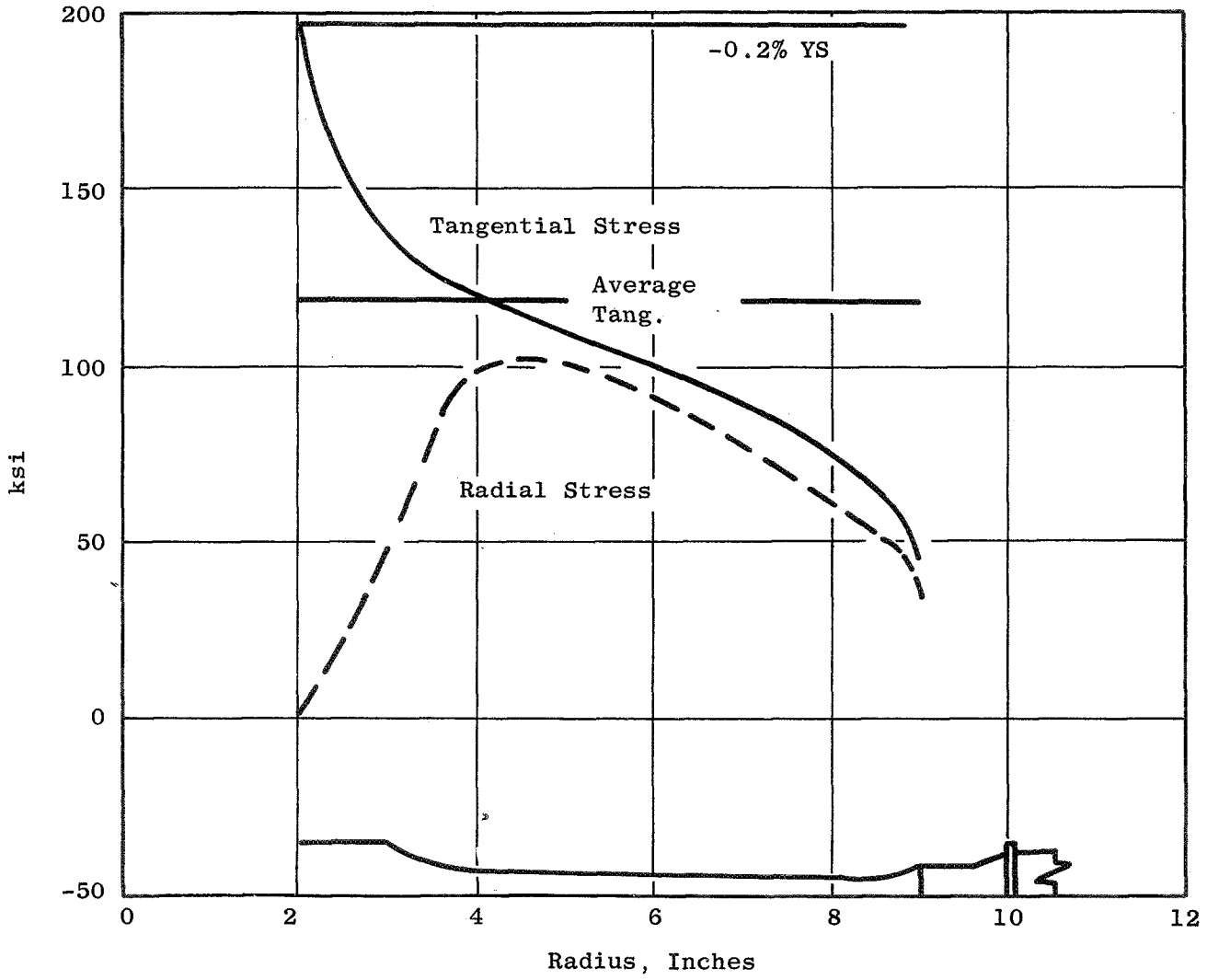

Figure 83. High Pressure Turbine Disc Stress.

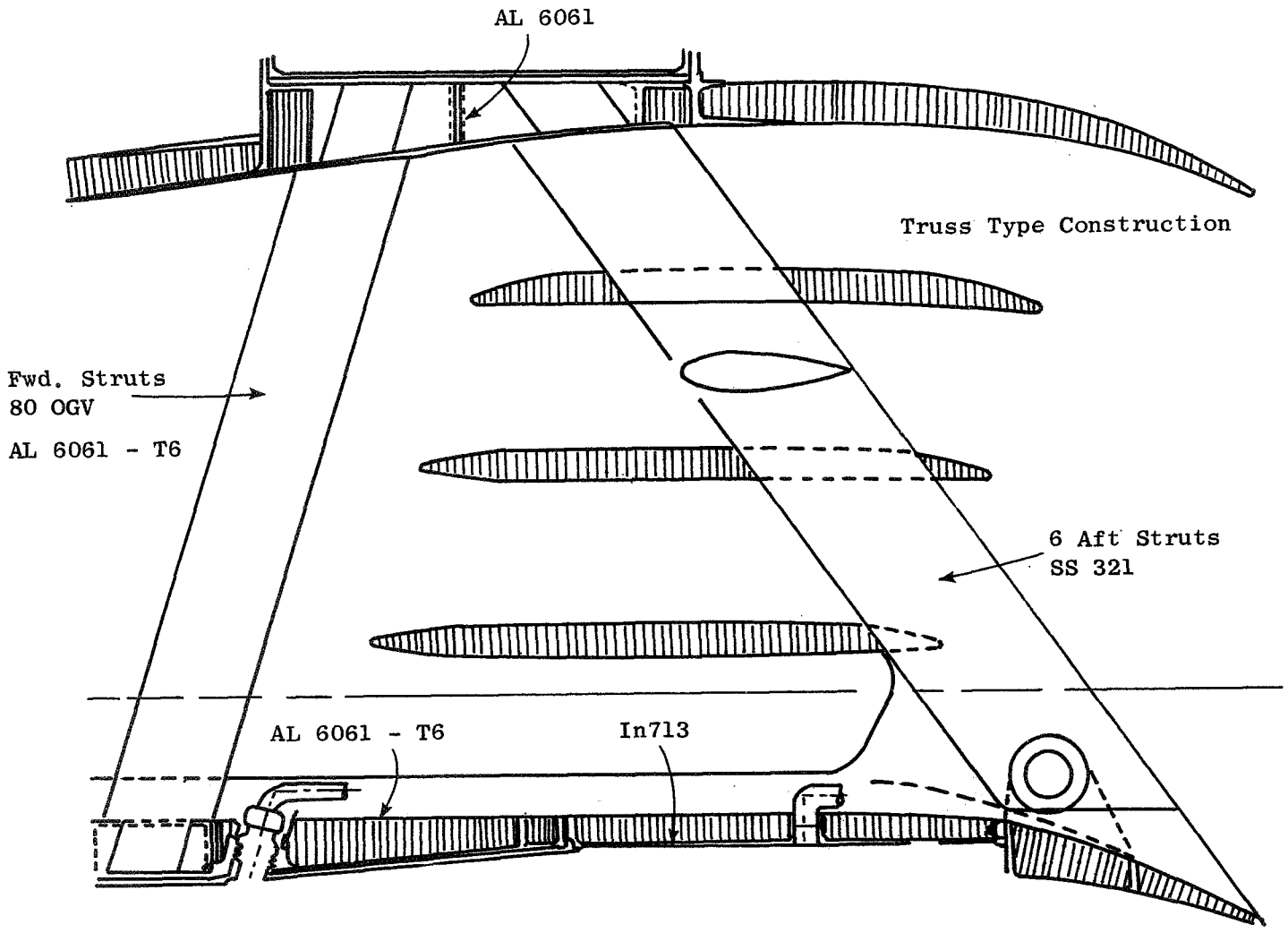

Figure 84. Frame Arrangement.

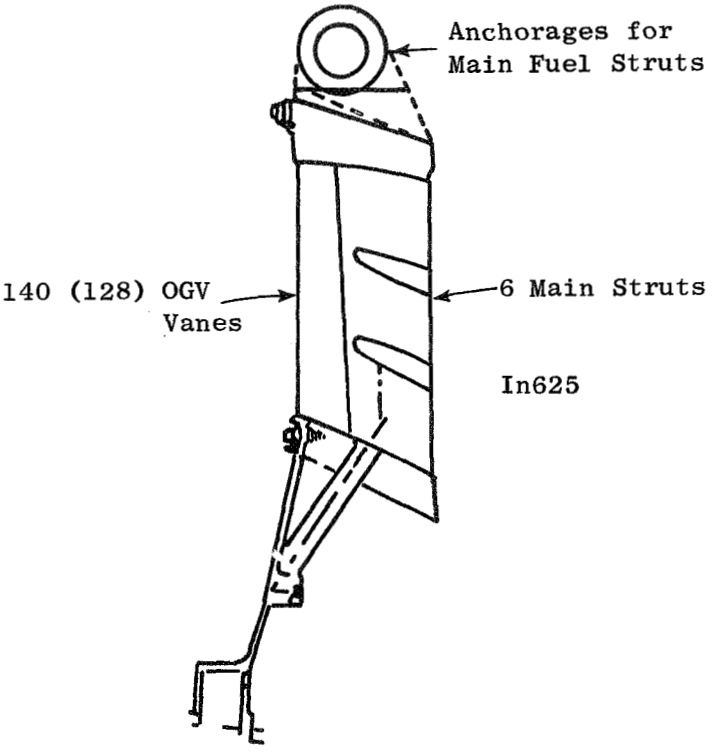

Figure 85. Turbine Rear Frame.

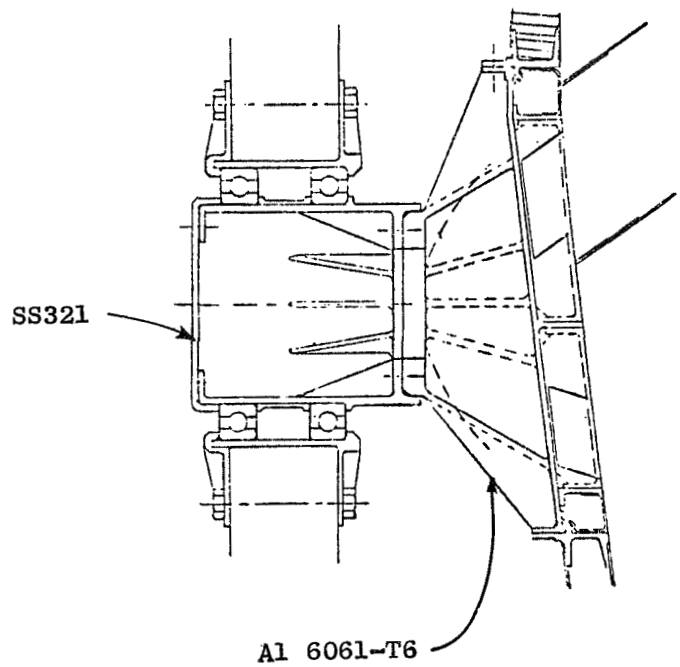

Figure 86. Trunnion Support.

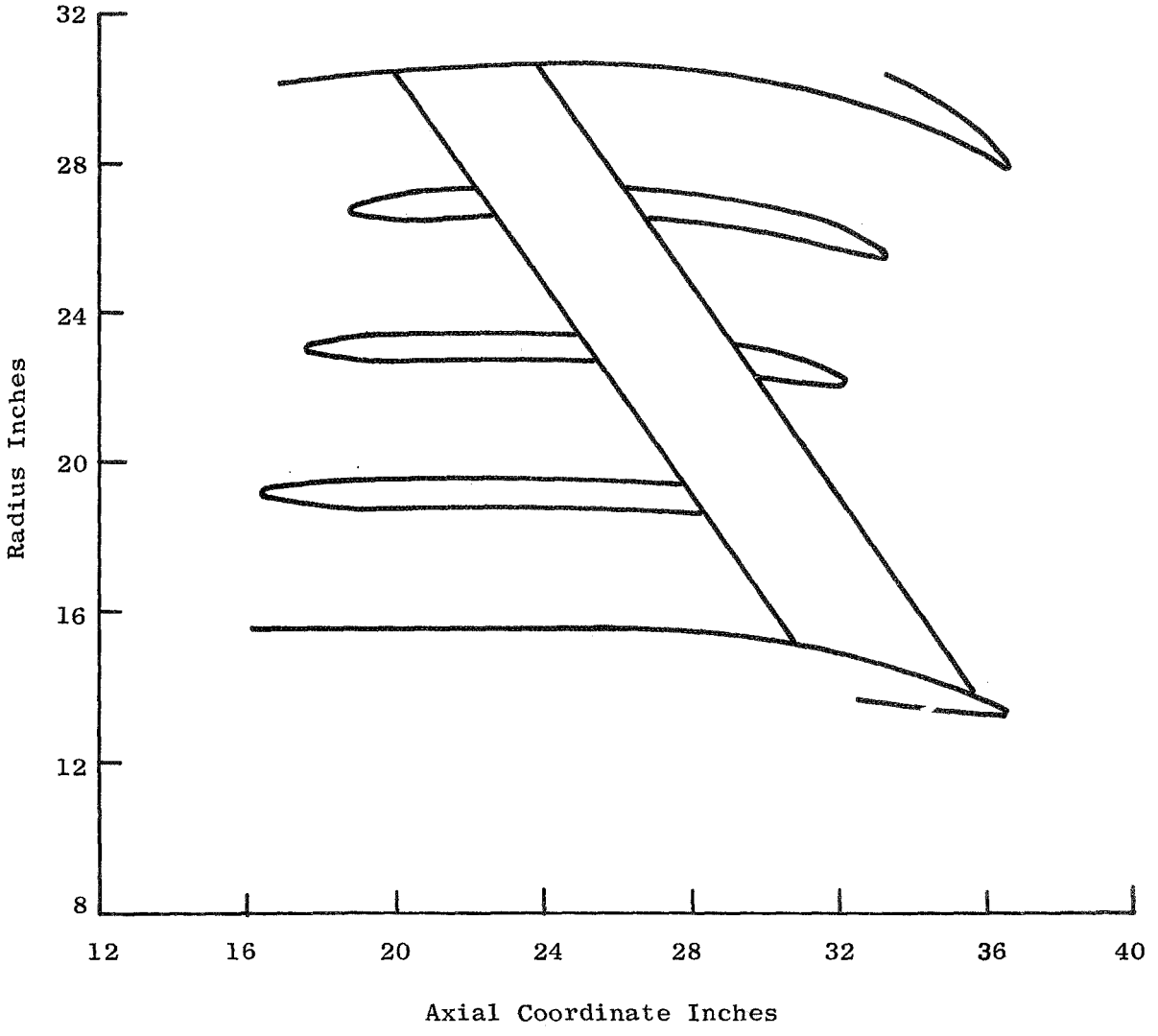

Figure 87. Fan Duct Flowpath ILF1A1.

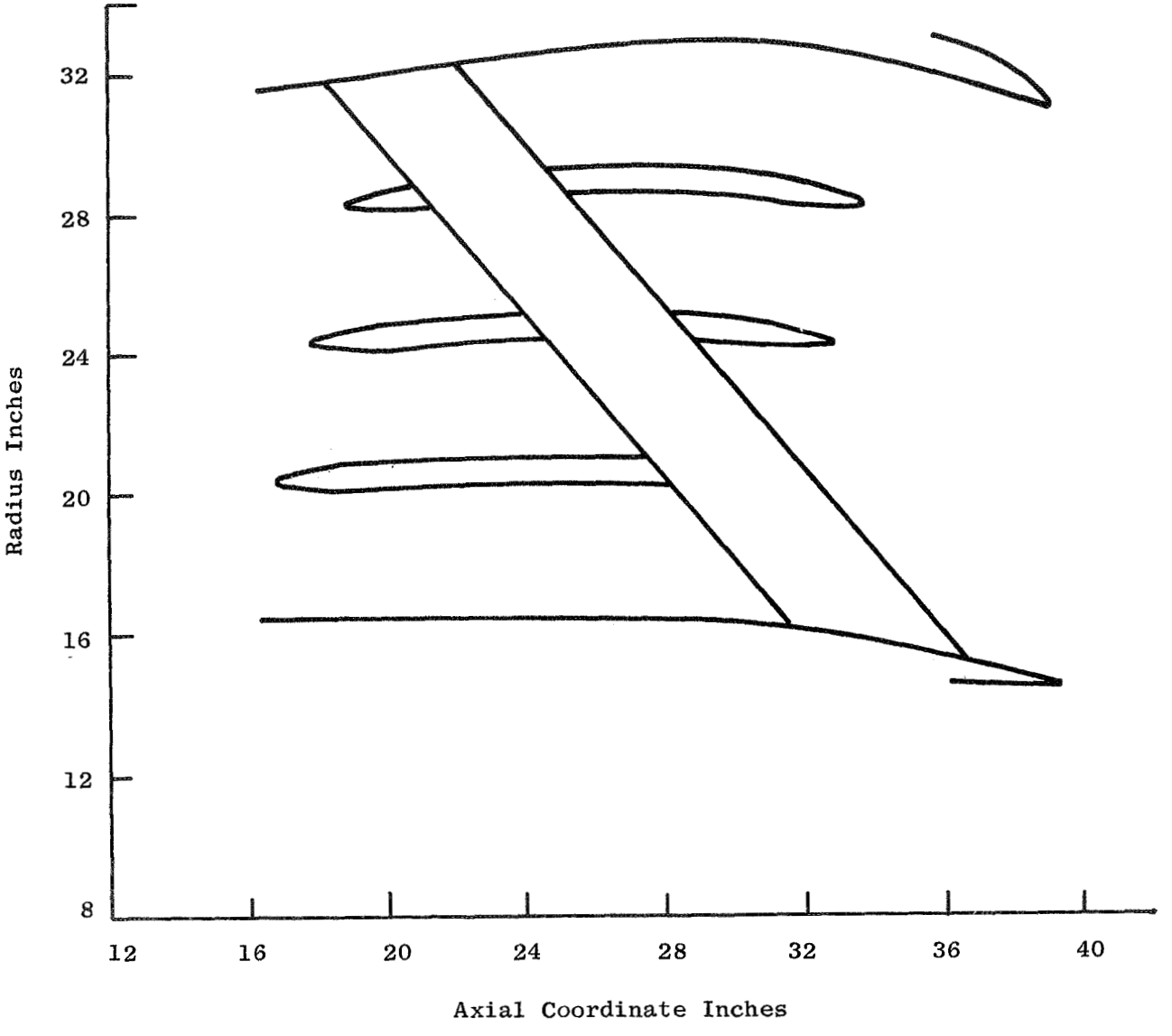

Figure 88. Fan Duct Flowpath ILF2A1.

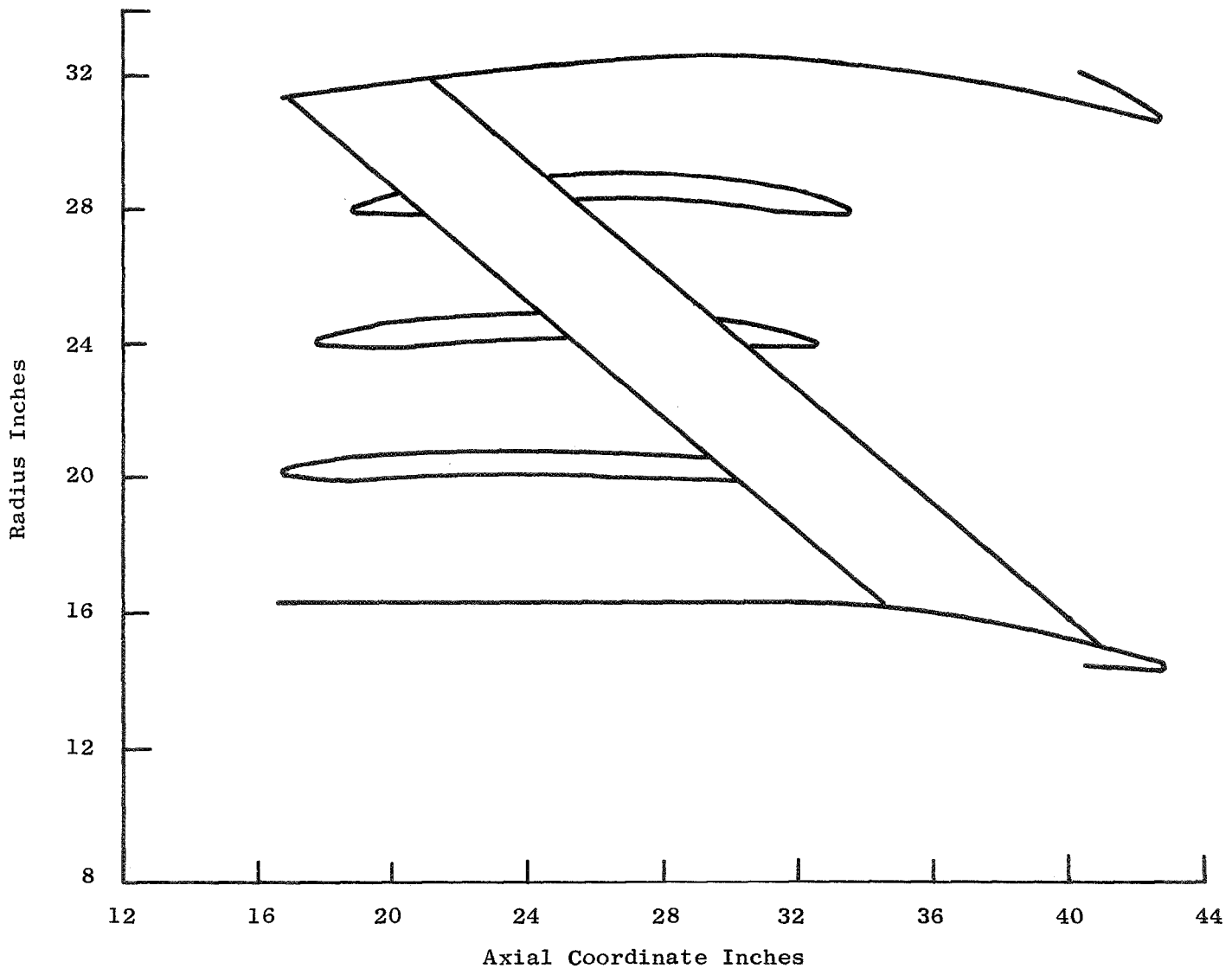

Figure 89. Fan Duct Flowpath ILF2A2.

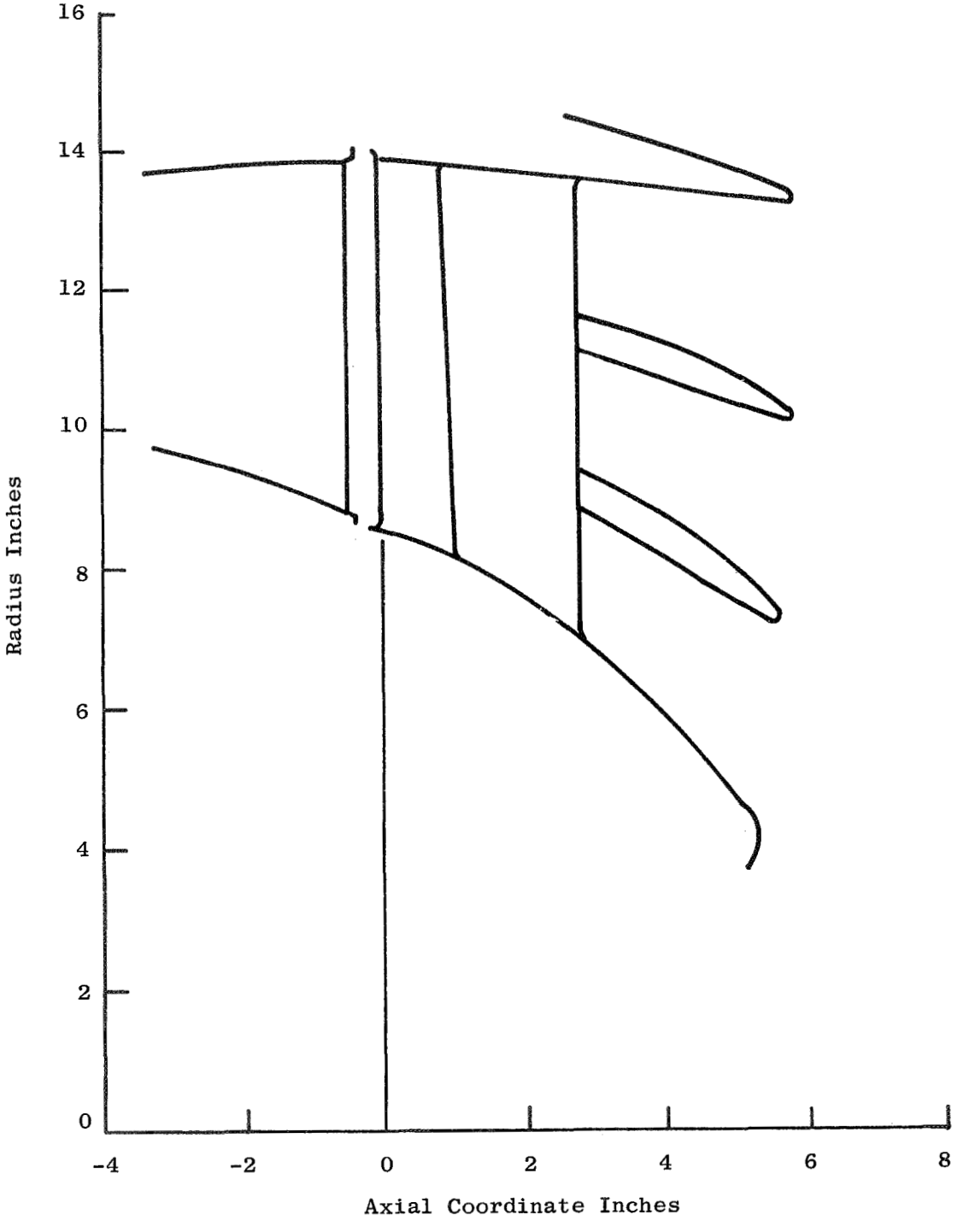

Figure 90. Core Duct Flowpath ILF1A1.

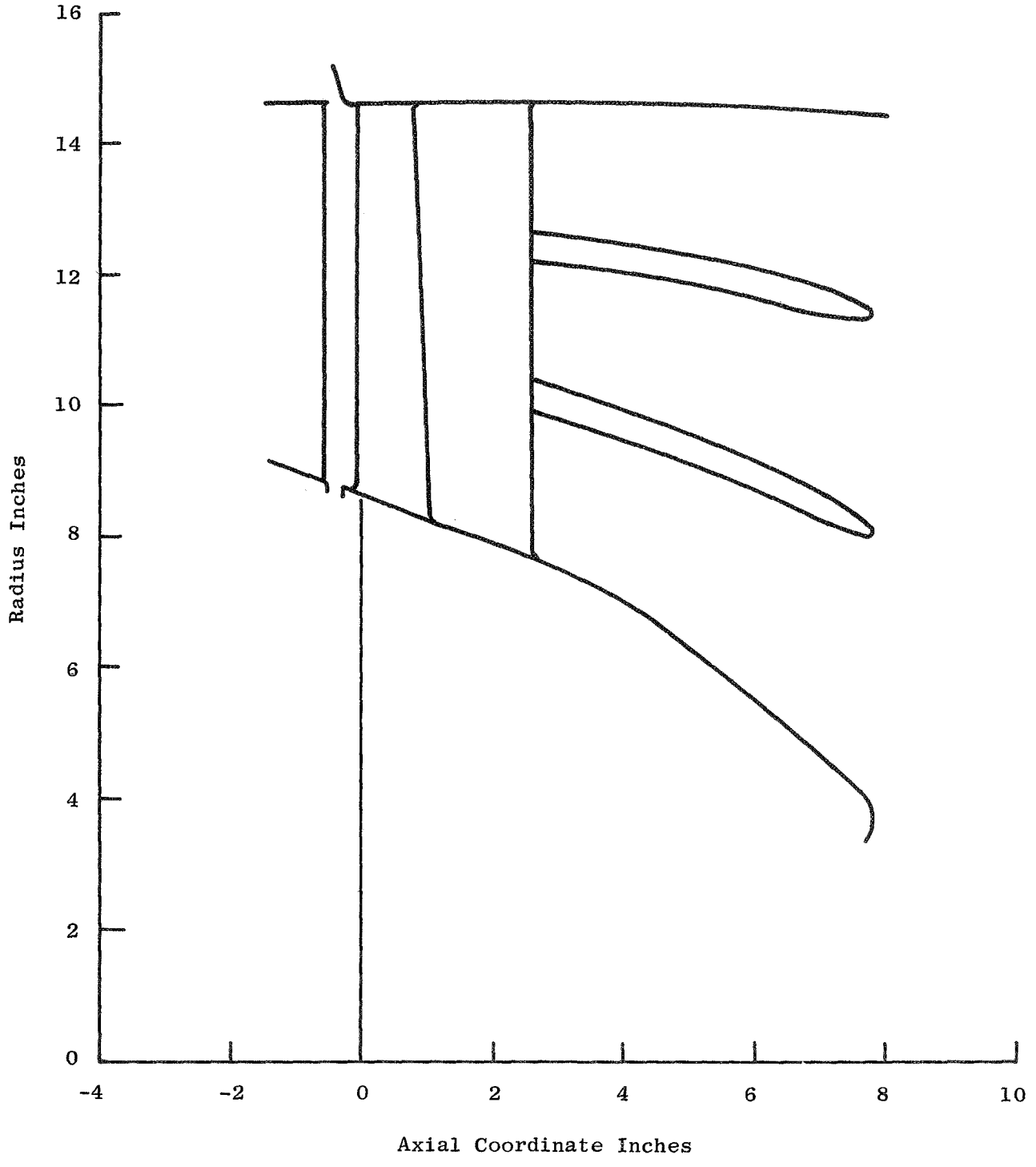

Figure 91. Core Duct Flowpath ILF2A1 and ILF2A2.

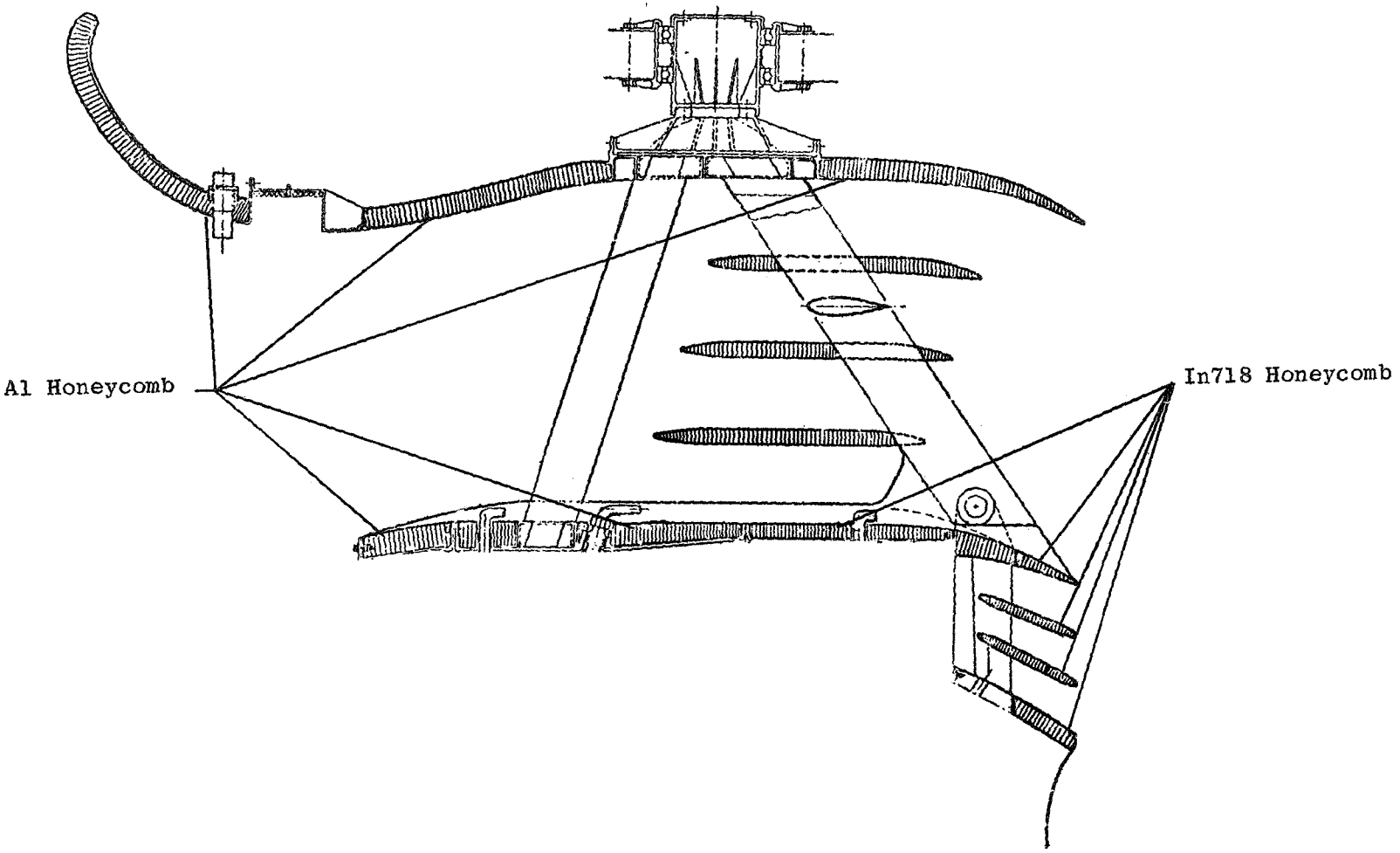

Figure 92. Fan Duct Detail.

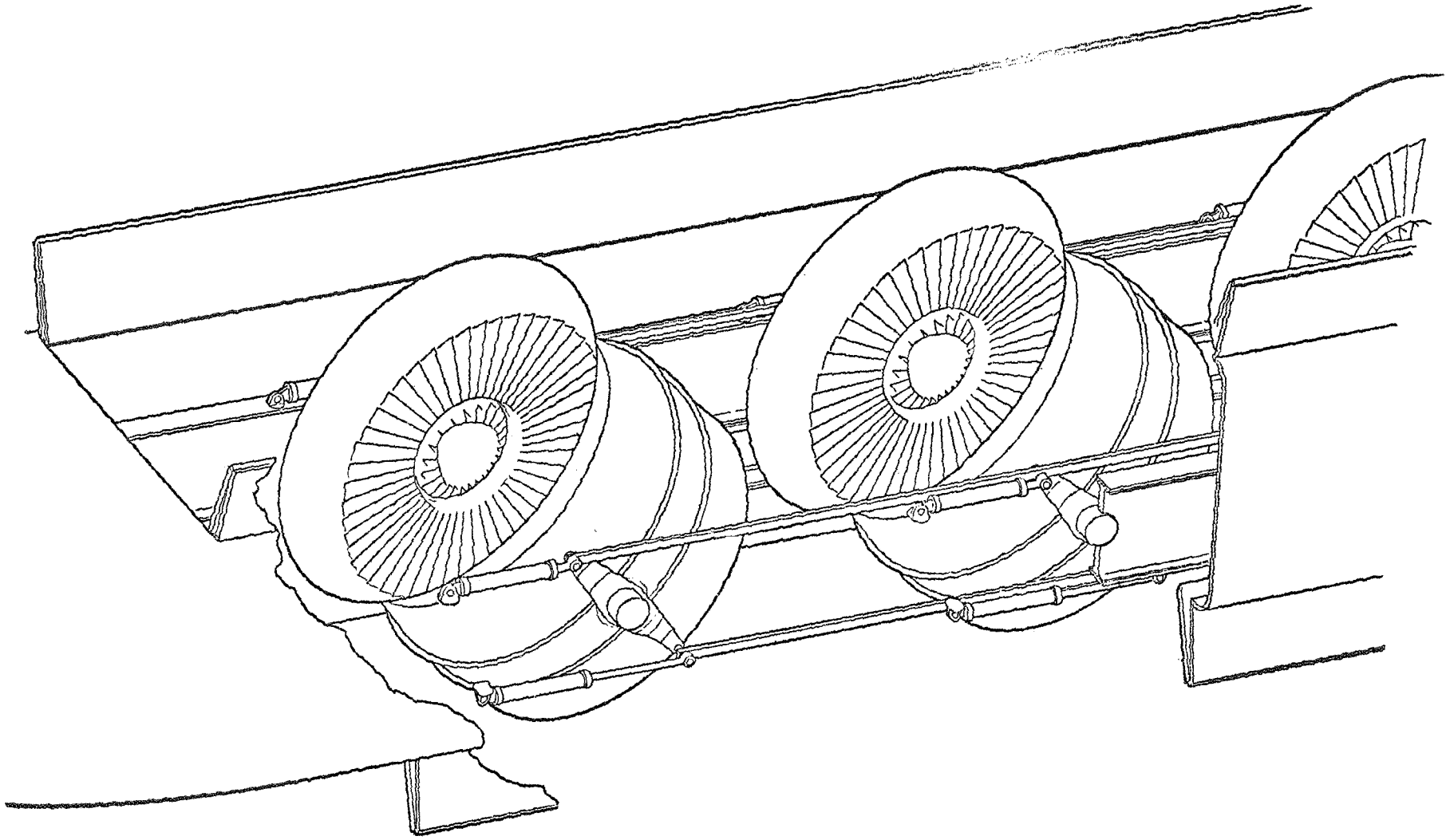

Figure 93. Pod Cutaway.

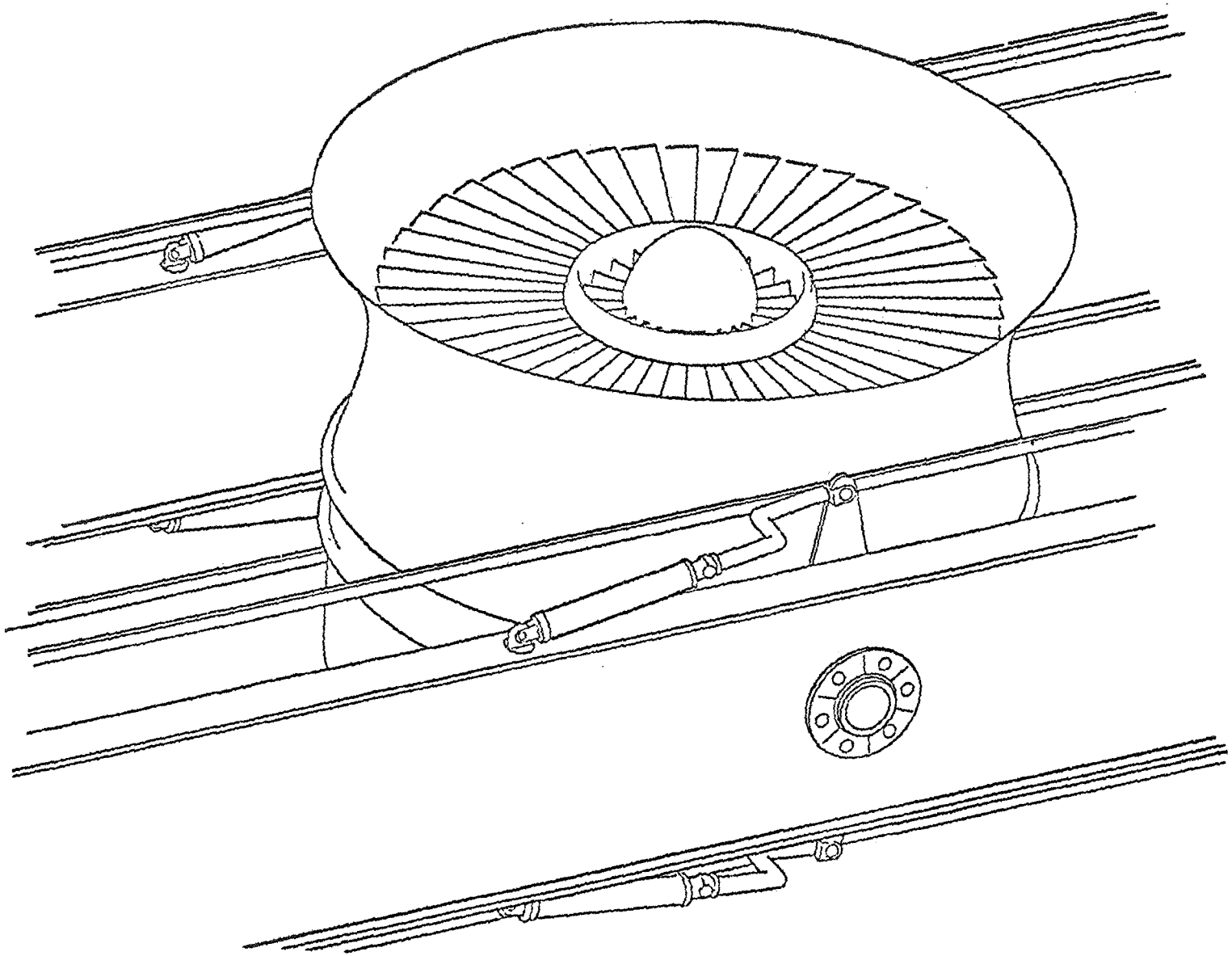

Figure 94. Engine Support Beam.

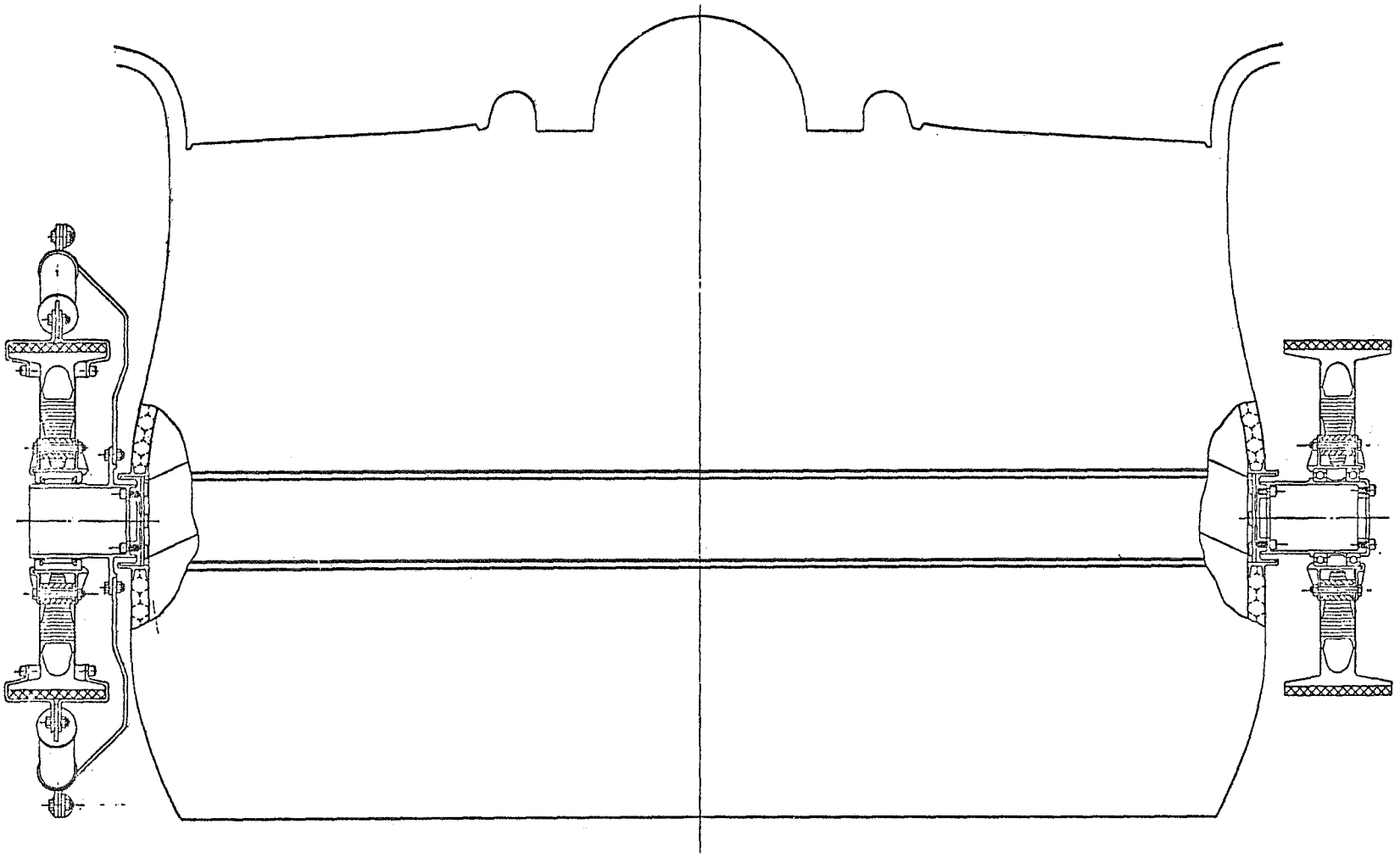

Figure 95. Vectoring and Support System Cross Section.

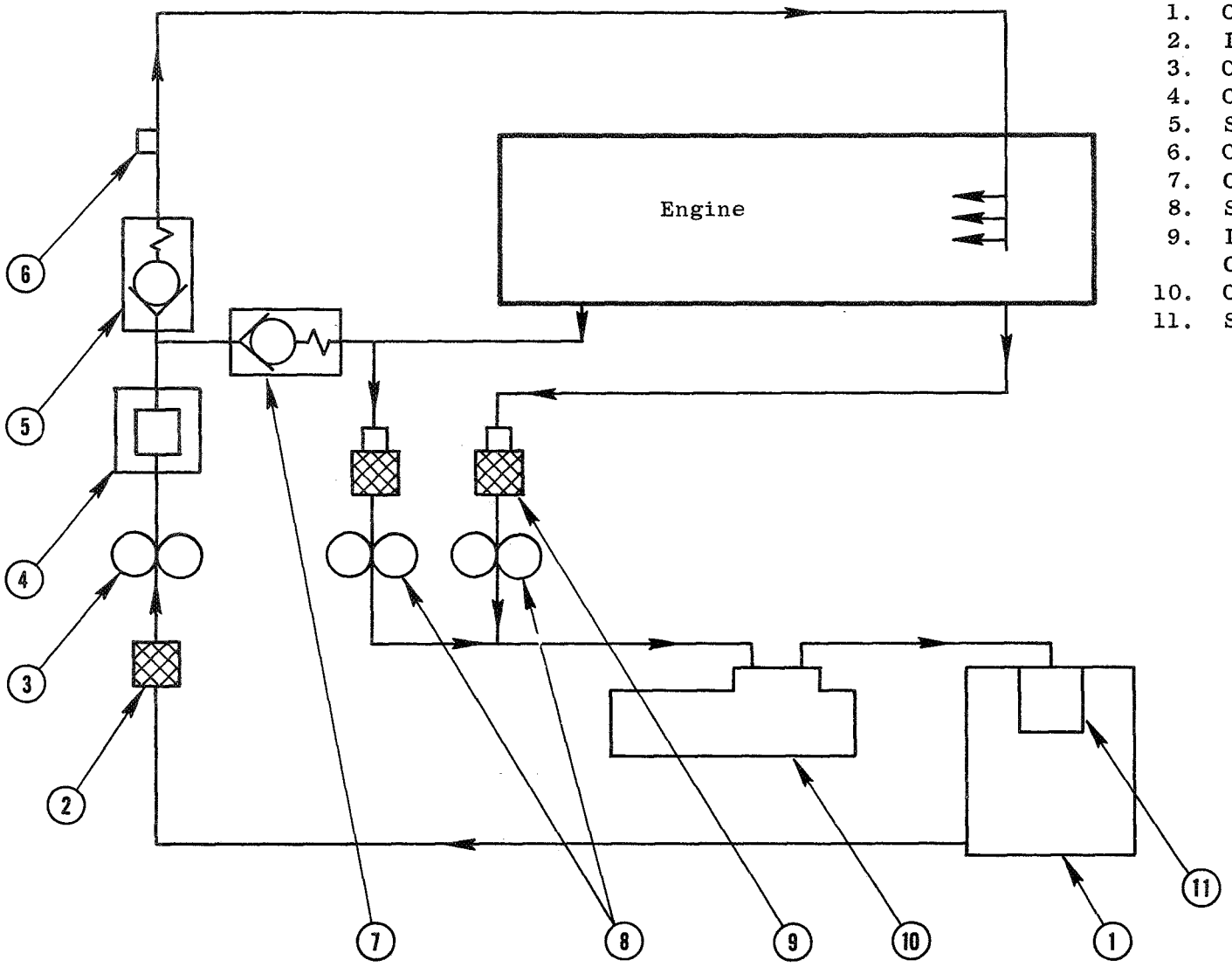

1. Oil Tank
2. Inlet Screen
3. Oil Supply Pump
4. Oil Supply Filter
5. Static Leak Check Valve
6. Oil Pressure Tap
7. Cold Start Bypass Valve
8. Scavenge Pumps
9. Inlet Screen with Magnetic Chip Collector
10. Oil Cooler
11. Scavenge Oil Deaerator

Figure 96. Integral Lift Fan Lubrication System Schematic.

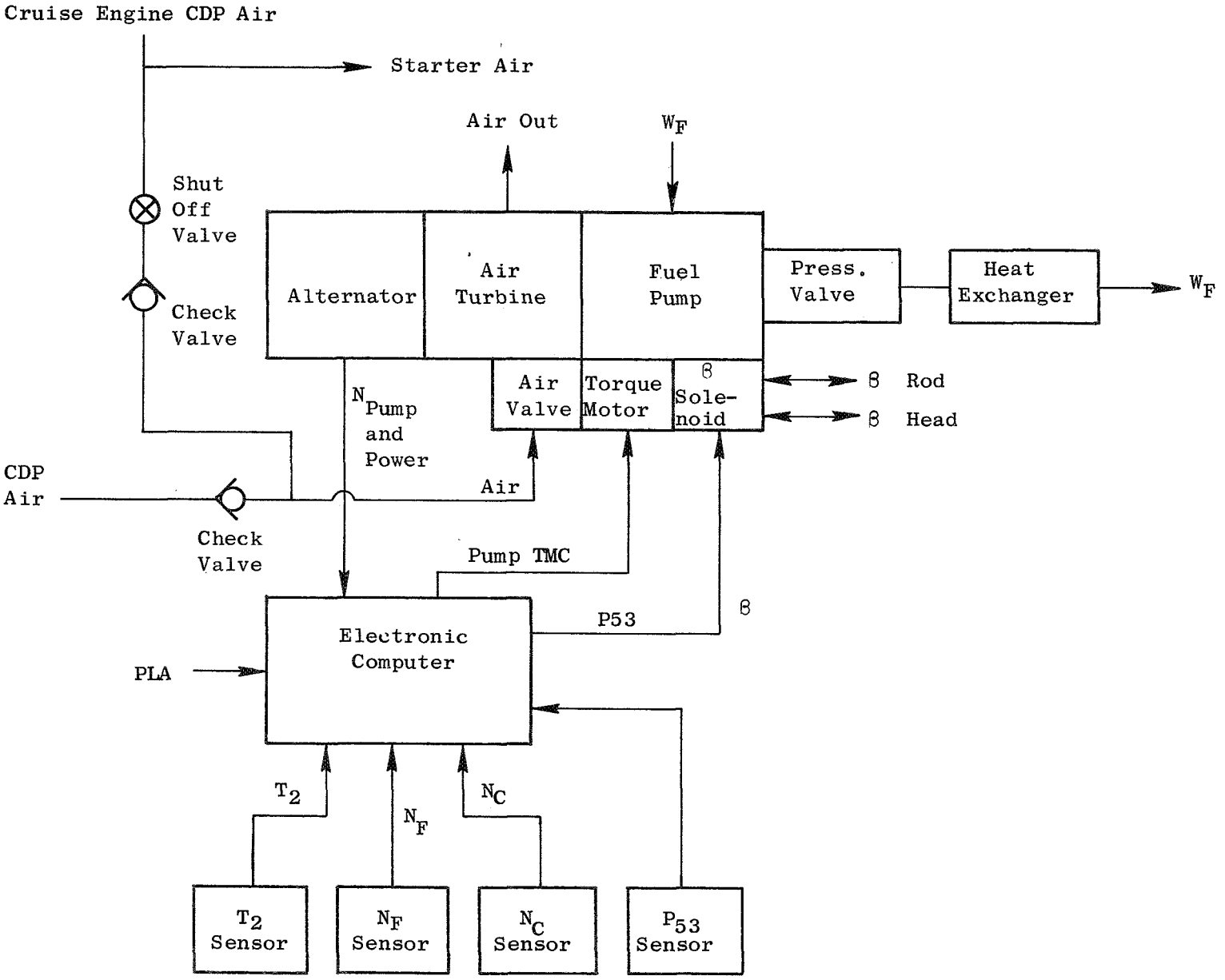

Figure 97. Controls & Accessories Schematic.

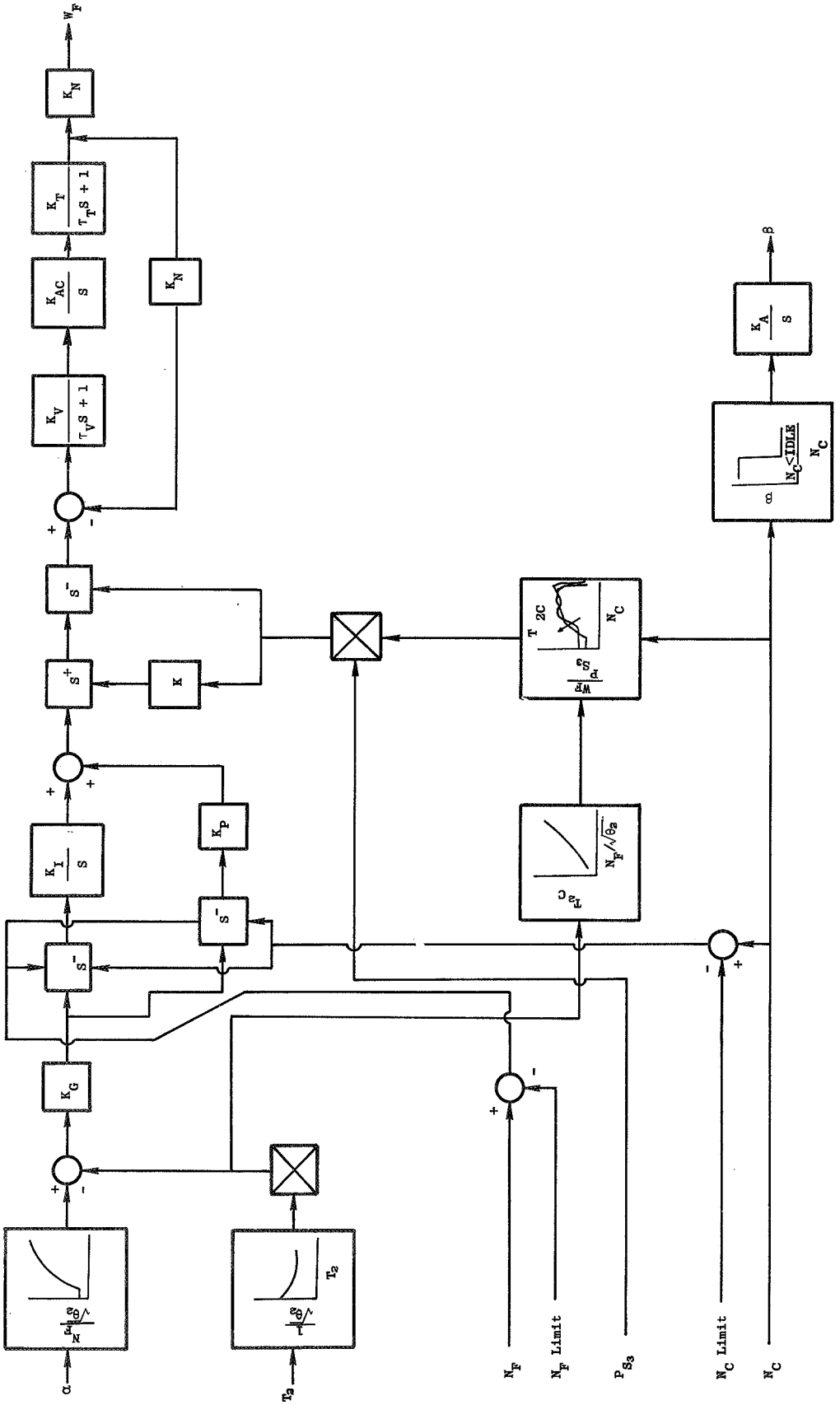

Figure 98. Control Block Diagrams.

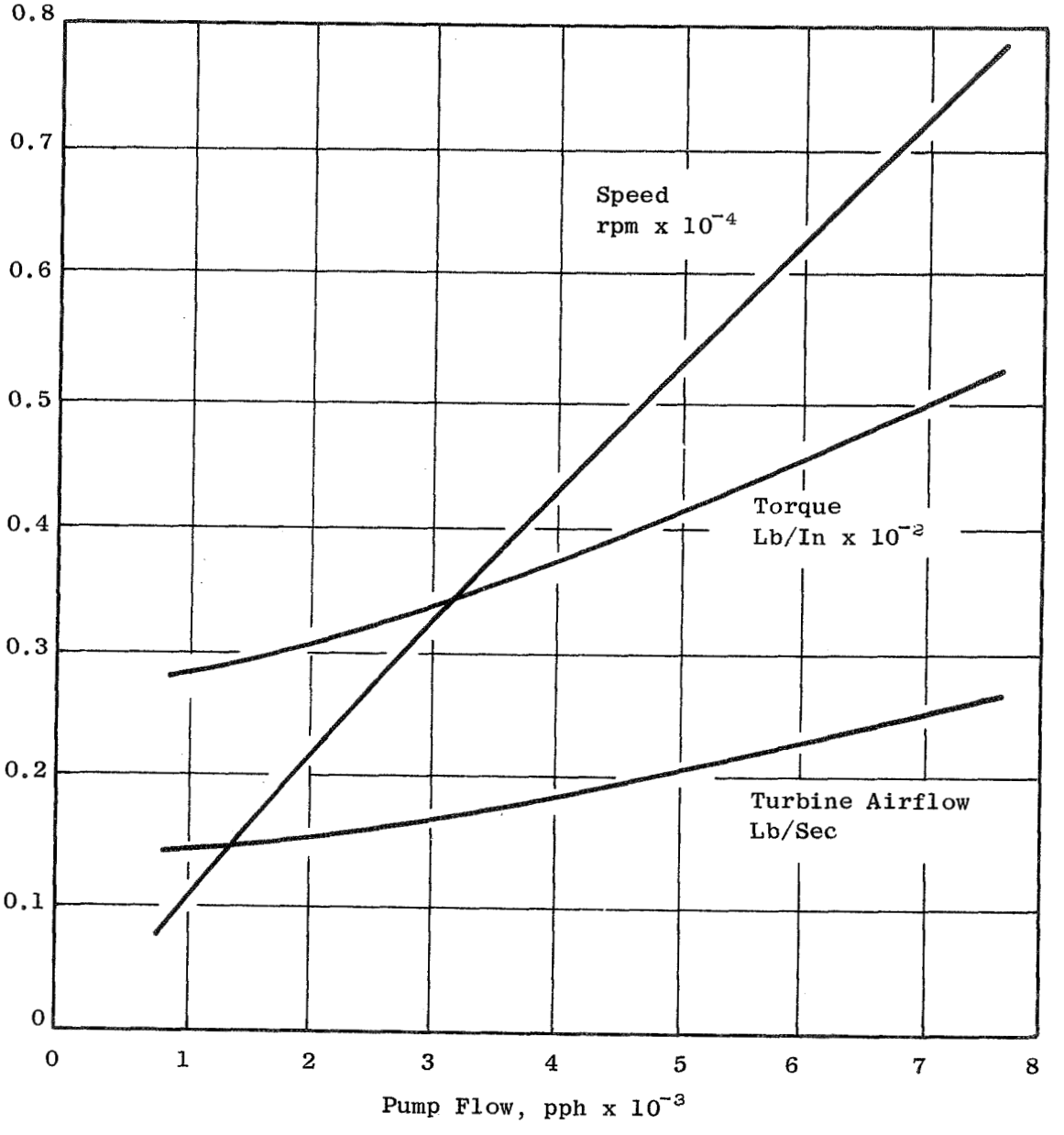

Figure 99. Pump/Turbine Characteristics.

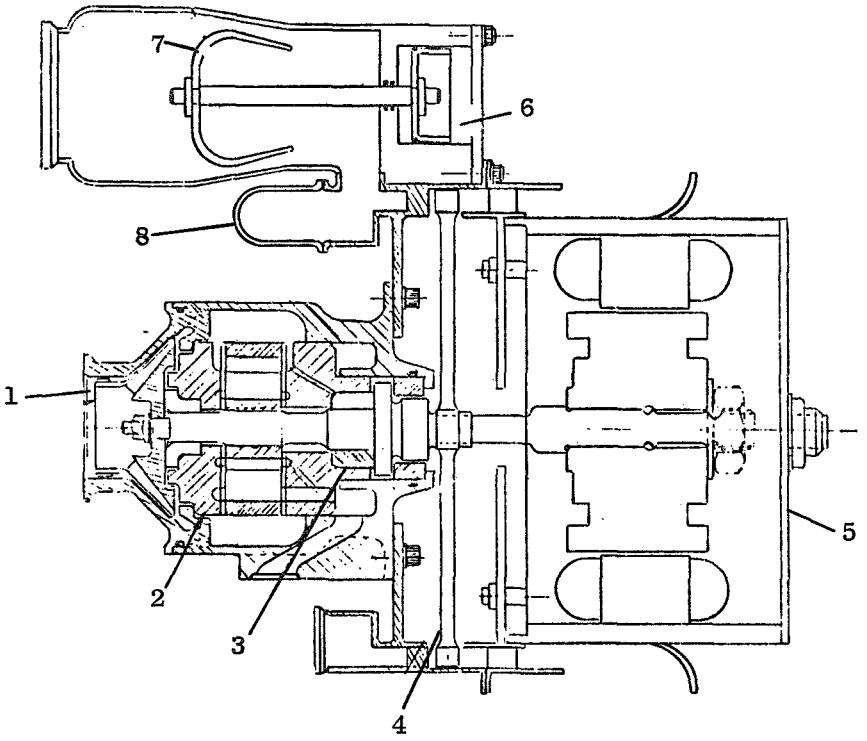

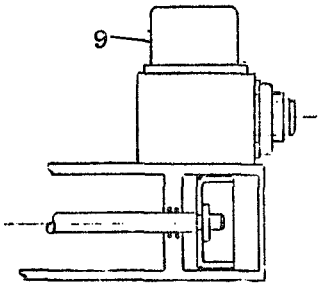

1. Boost Impeller
2. Vane Element
3. Fuel Lubricated Bearing
4. Air Turbine Rotor
5. Alternator
6. Fuel Powered Actuator
7. Air Valve
8. Air Manifold
9. Servo Valve

Figure 100. Controls & Accessories Package.

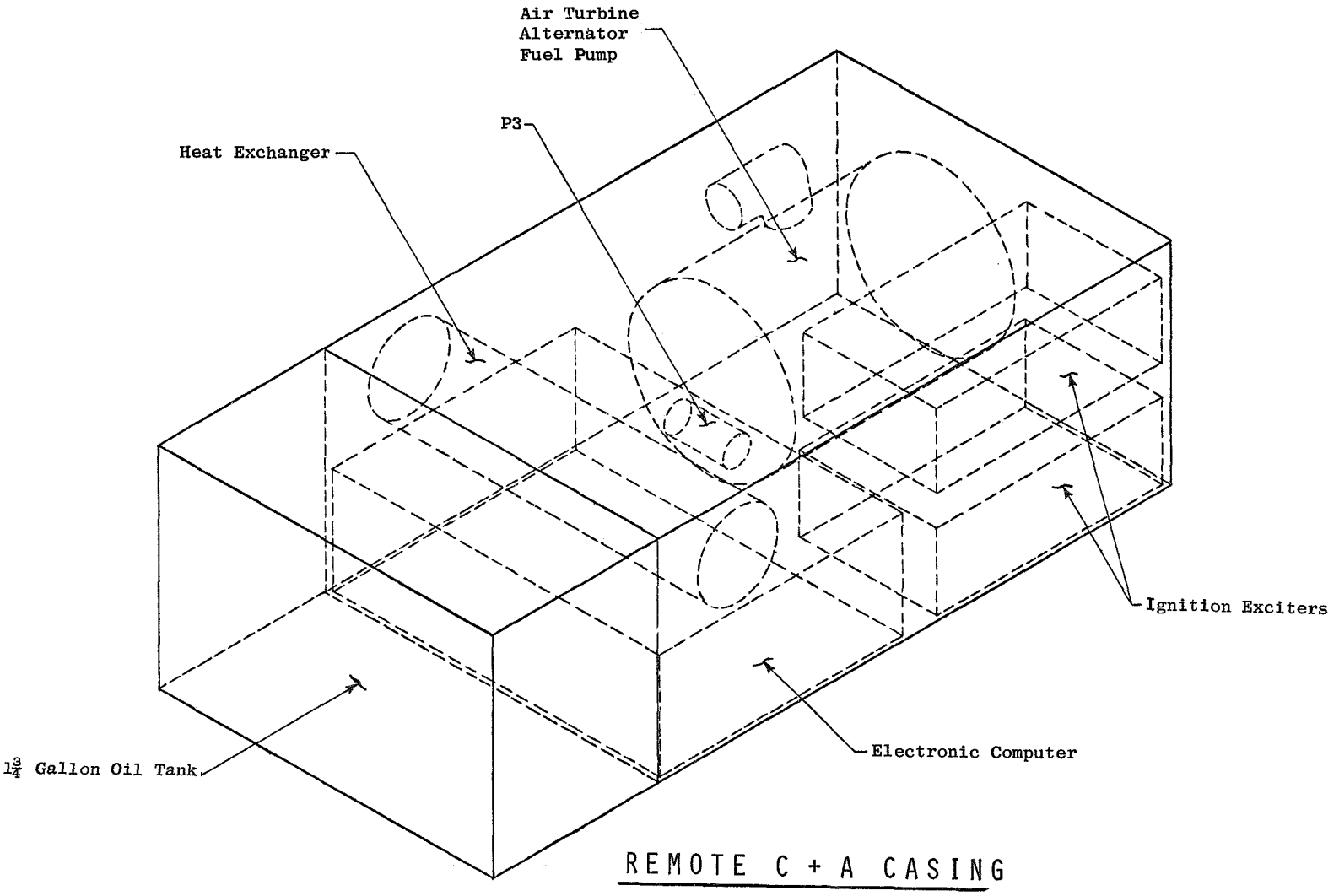

Figure 101. Controls and Accessories Packaging Schematic.

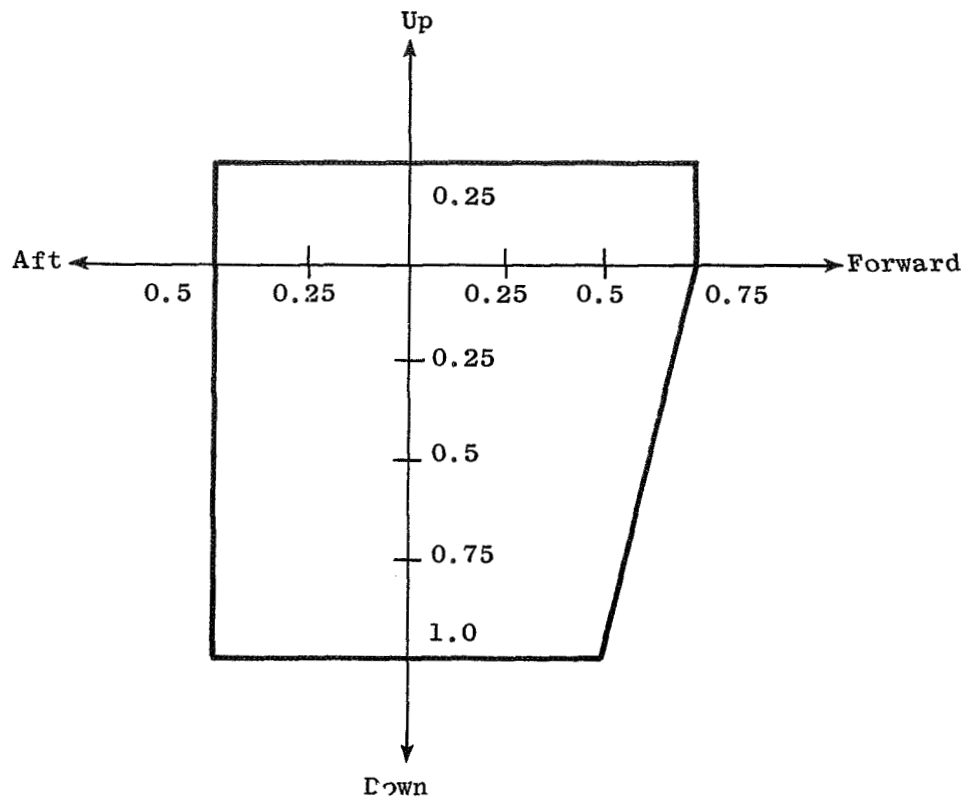

Side Load ±0.5 g
$\dot{\theta}$ Pitch Velocity = 0.1 rad/sec
$\ddot{\theta}$ Pitch Acceleration = 0.5 rad/sec^2
$\dot{\phi}$ Roll Velocity = 0.1 rad/sec
$\ddot{\phi}$ Roll Acceleration = 1.0 rad/sec^2

} can occur in any combination

NOTES:

1) Load factors, angular velocities and accelerations to be taken about the C.G. of the fan.
2) Side load factors act to either side.
3) Side loads and gyro loads do not act simultaneously.
4) Zero to maximum thrust for all conditions.

Figure 102. Engine Steady Maneuver Load Requirements.

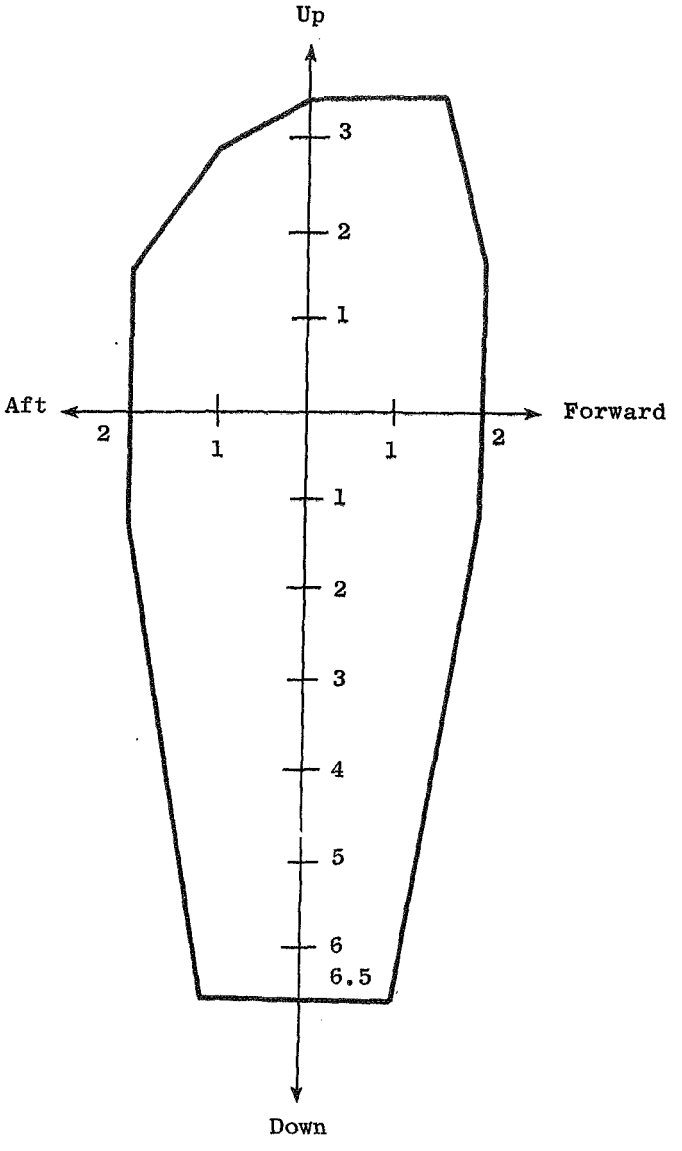

Side Load = ±2.0 g
$\dot{\theta}$ Pitch Velocity = 0
$\ddot{\theta}$ Pitch Acceleration = ±7 rad/sec^2
$\dot{\phi}$ Roll Velocity = 0
$\ddot{\phi}$ Roll Acceleration = ±12 rad/sec^2

} can occur in any combination

NOTES:

1) Load factors, angular velocities and accelerations to be taken about the C.G. of the engine.
2) Side load factors act to either side.
3) Side loads and gyro loads do not act simultaneously.
4) Zero to maximum thrust for all conditions.

Figure 103. Engine Vertical Landing Maneuver Load Requirements.

FLIGHT
(0 to Max. Thrust)

$\theta = \pm 6$ rad/sec^2

$\Psi = 0$

$\dot{\Psi} = 0$

$\dot{\theta} = \pm 2$ rad/sec

S.L. = 4.0 Applicable to complete crosshatched area

$\dot{\theta} = 0$

S.L. = 1.5 Applicable to complete rectangle from 7 Up to 10 Down

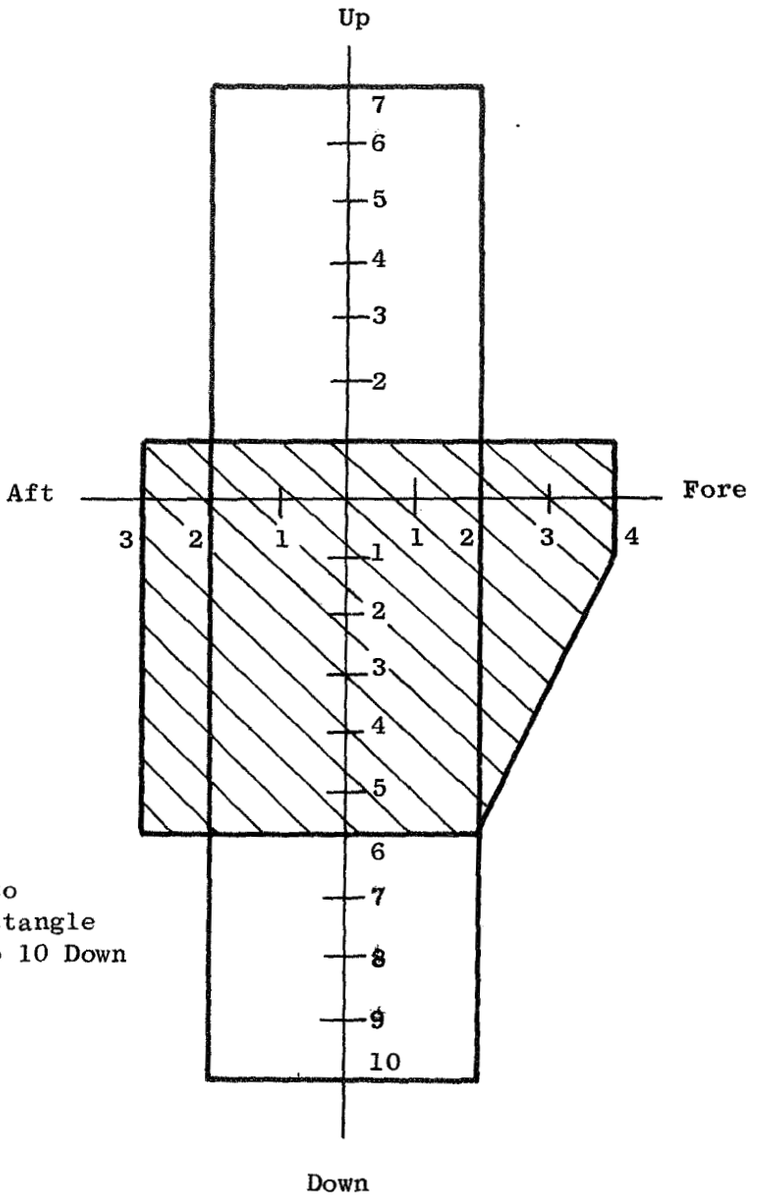

NOTES:

1) Load factors and angular velocities and accelerations should be taken at or about the C.G. of the fan.
2) Side load factors (S.L.) act to either side.
3) θ and $\dot{\theta}$ are pitching velocity and acceleration.
4) $\dot{\Psi}$ and $\ddot{\Psi}$ are yawing velocity and acceleration.
5) Down loads occur during pull out.
6) Fore loads occur during arrested landing.

Figure 104. Engine Unpowered Flight Maneuver Loads.

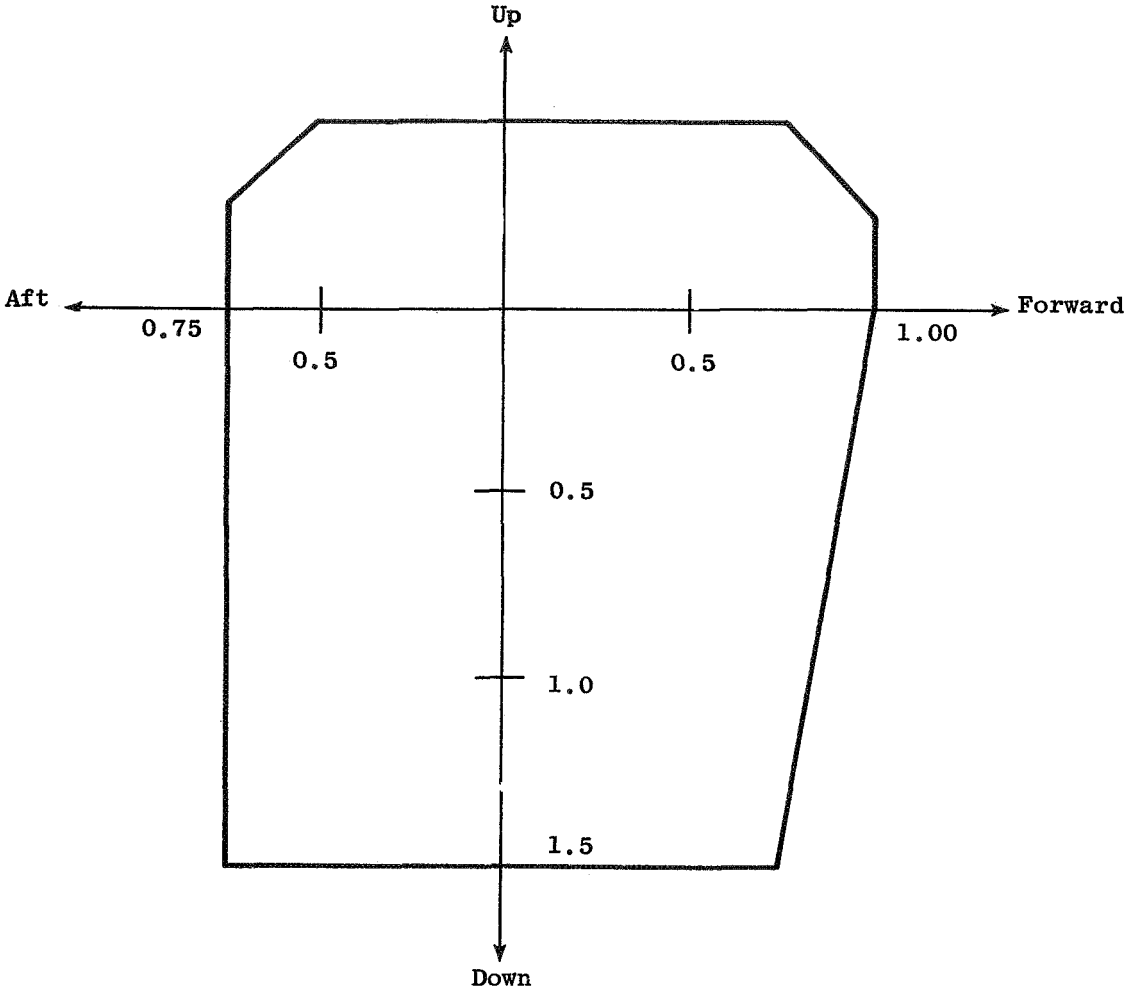

Side Load = ±1.0 g
$\dot{\theta}$ Pitch Velocity = 0.5 rad/sec
$\ddot{\theta}$ Pitch Acceleration = 1.0 rad/sec^2
$\dot{\phi}$ Roll Velocity = 0.5 rad/sec
$\ddot{\phi}$ Roll Acceleration = 2.0 rad/sec^2

} can occur in any combination

NOTES:

1) Load factors, angular velocities and accelerations to be taken about the C.G. of the engine.
2) Side load factors act to either side.
3) Side loads and gyro loads do not act simultaneously.
4) Zero to maximum thrust for all conditions.

Figure 105. Engine Frequent Maneuver Load Requirements.

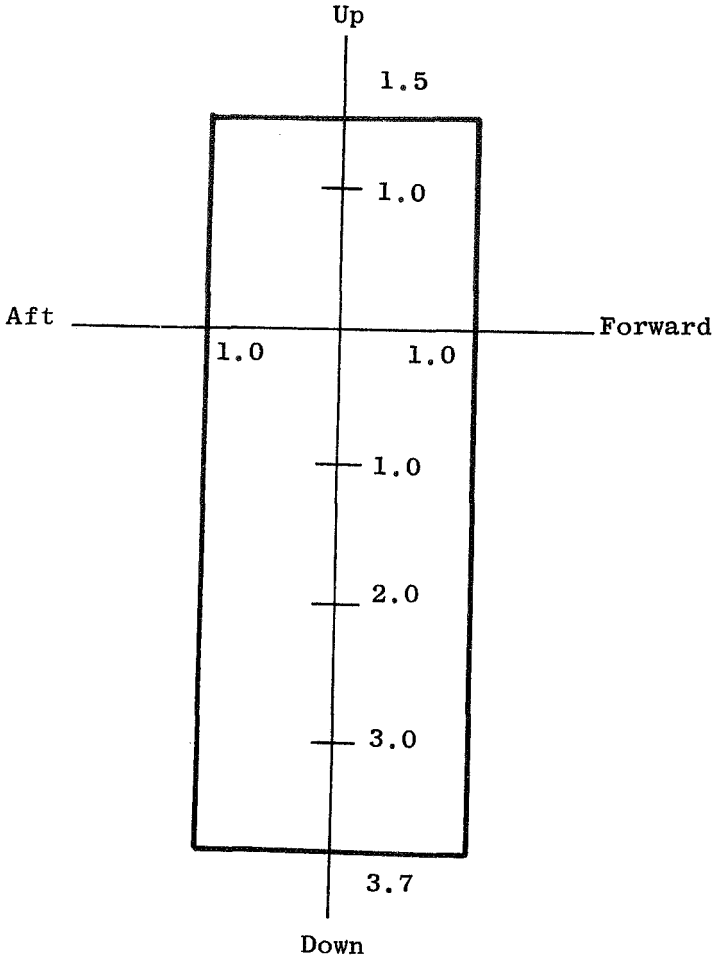

Side Load = ±1.0 g
θ Pitch Velocity = 1.0 rad/sec
θ Pitch Acceleration = 1.0 rad/sec^2
φ Roll Velocity = 1.0 rad/sec
φ Roll Acceleration = 3.0 rad/sec^2

Maximum combined velocity = 1.0 rad/sec

NOTES:

1) Load factors, angular velocities and accelerations to be taken about the C.G. of the engine.
2) Side load factors act to either side.
3) Side loads and gyro loads do not act simultaneously.
4) Zero to maximum thrust for all conditions.

Figure 106. Engine Infrequent Maneuver Load Requirements.

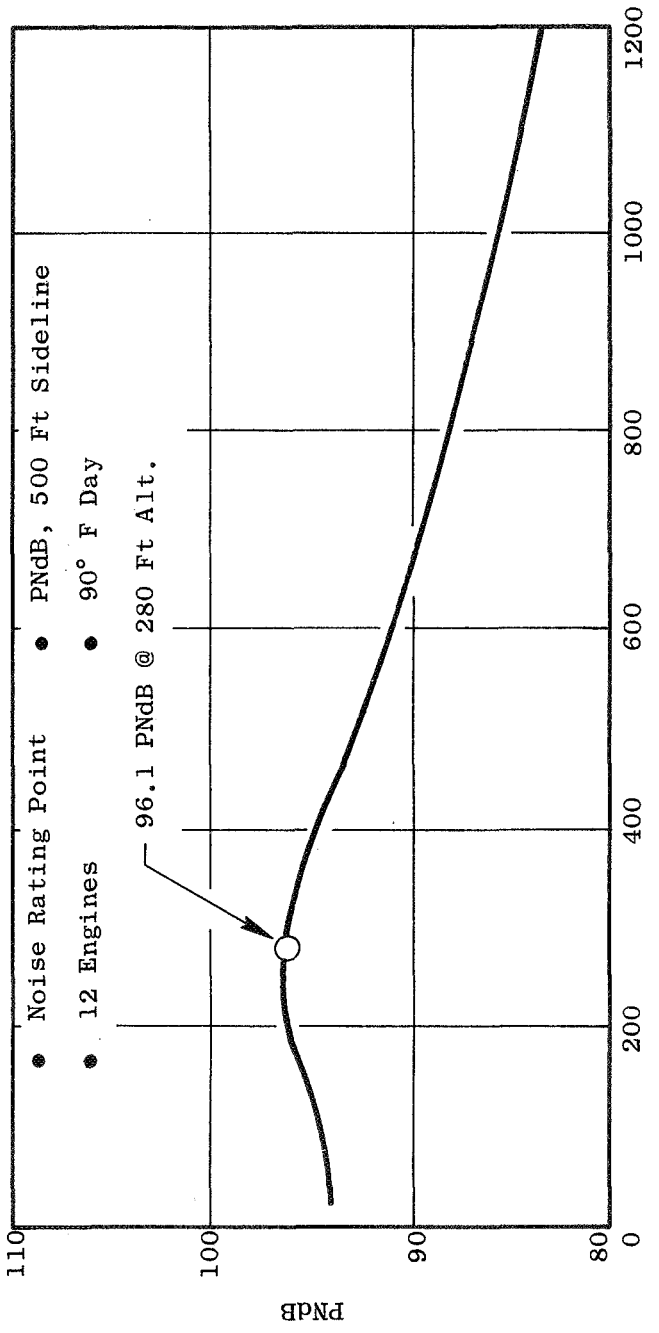

Figure 107. ILF1A1 Vertical Takeoff Noise (1.25 P/P).

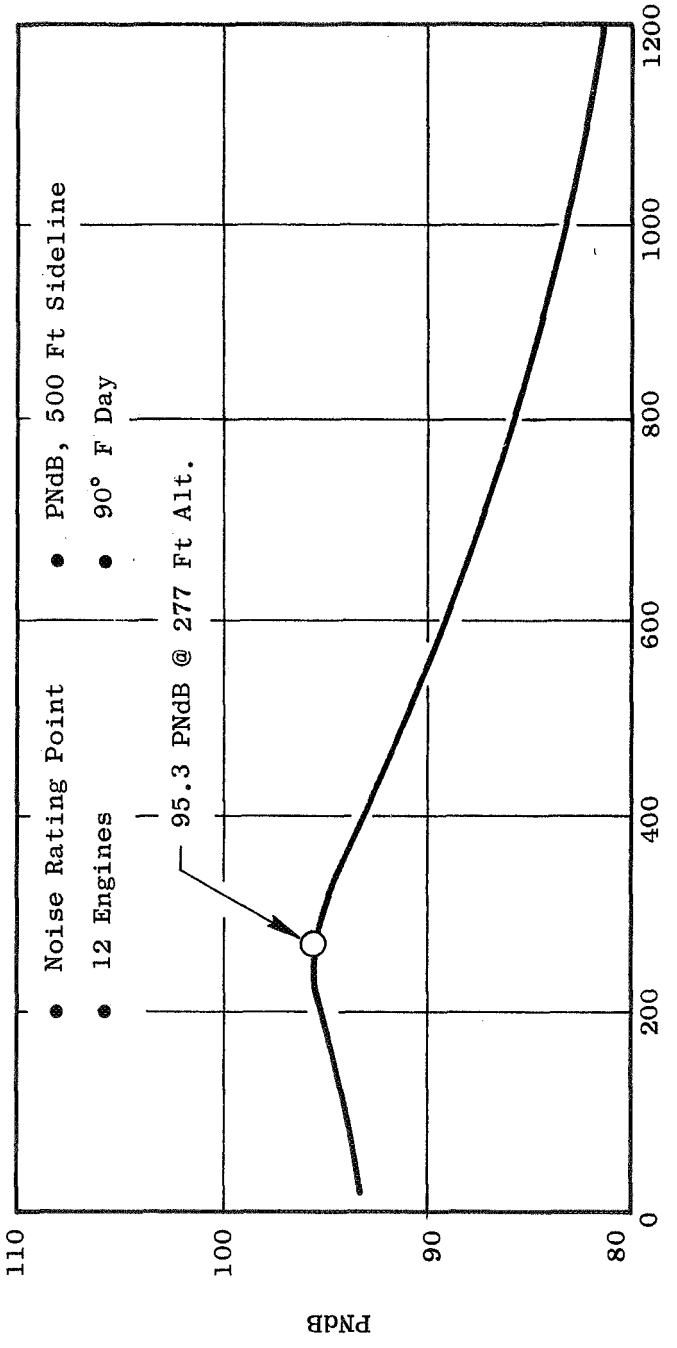

Figure 108. ILF2A1 Vertical Takeoff Noise (1.20 P/P).

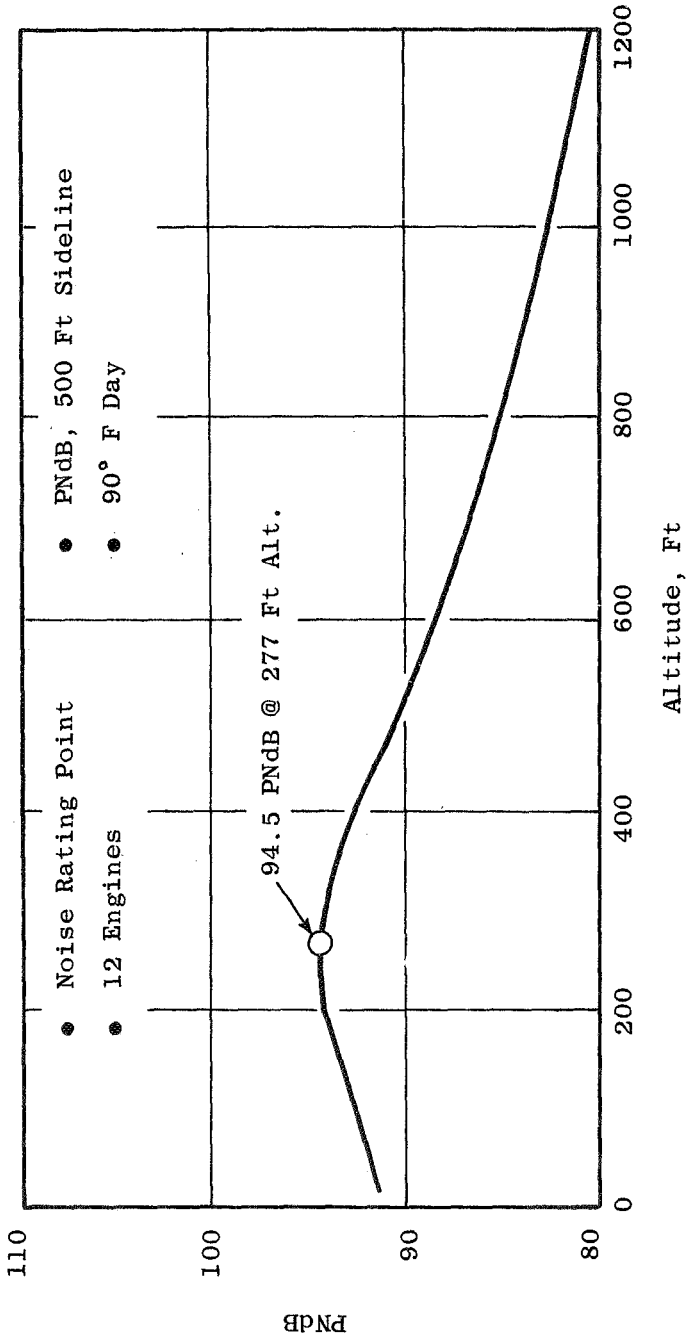

Figure 109. ILF2A2 Vertical Takeoff Noise (1.20 P/P).

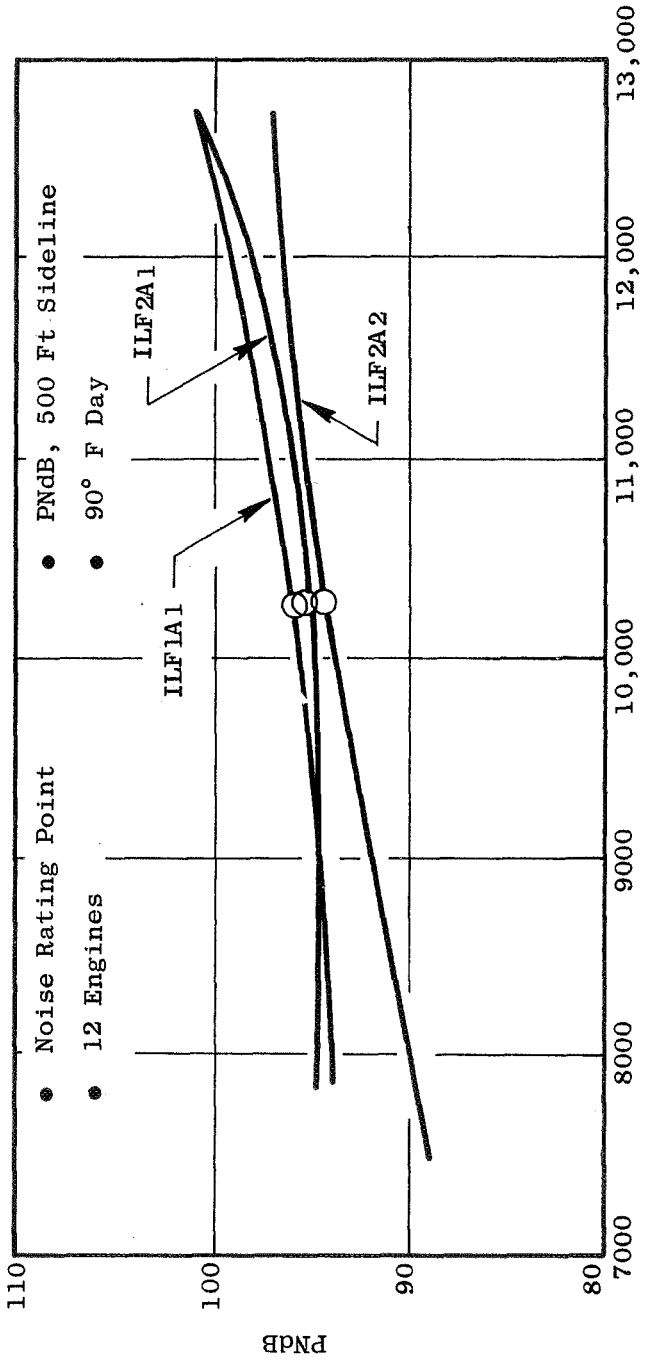

Figure 110. Vertical Takeoff Integral Lift Fans.

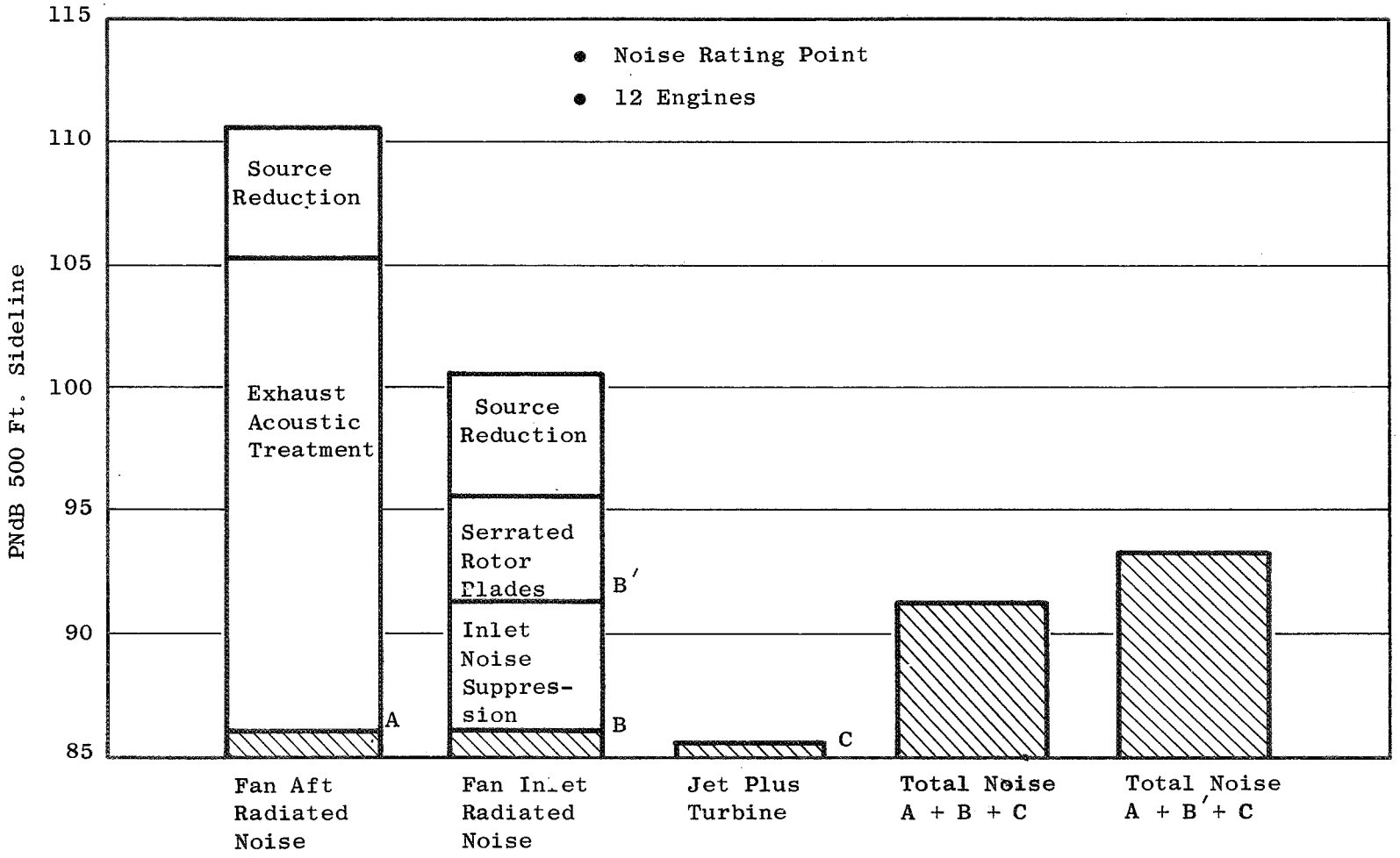

Figure 111. Fan Suppression - ILF1A1.

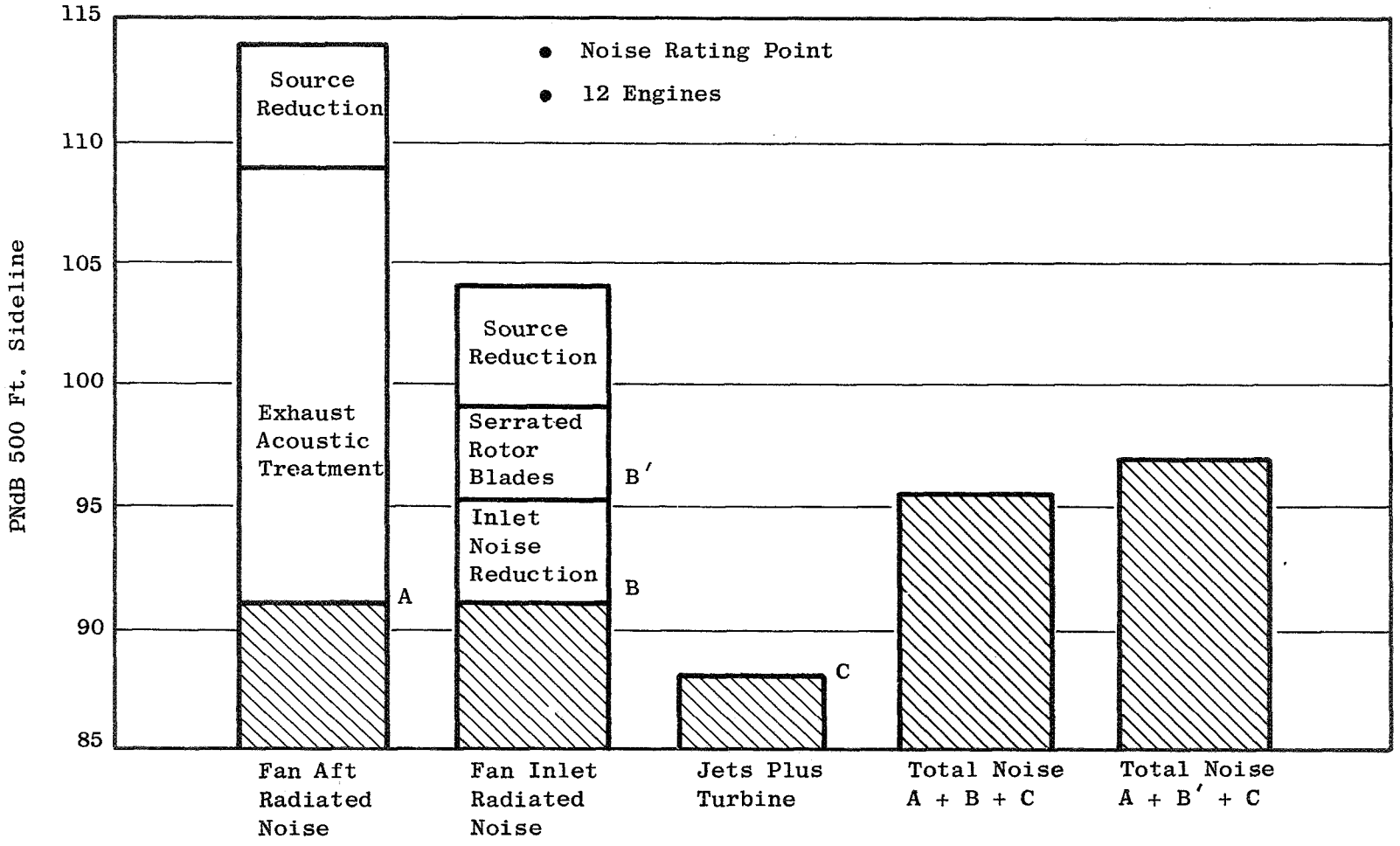

Figure 112. Fan Suppression - ILF2A1.

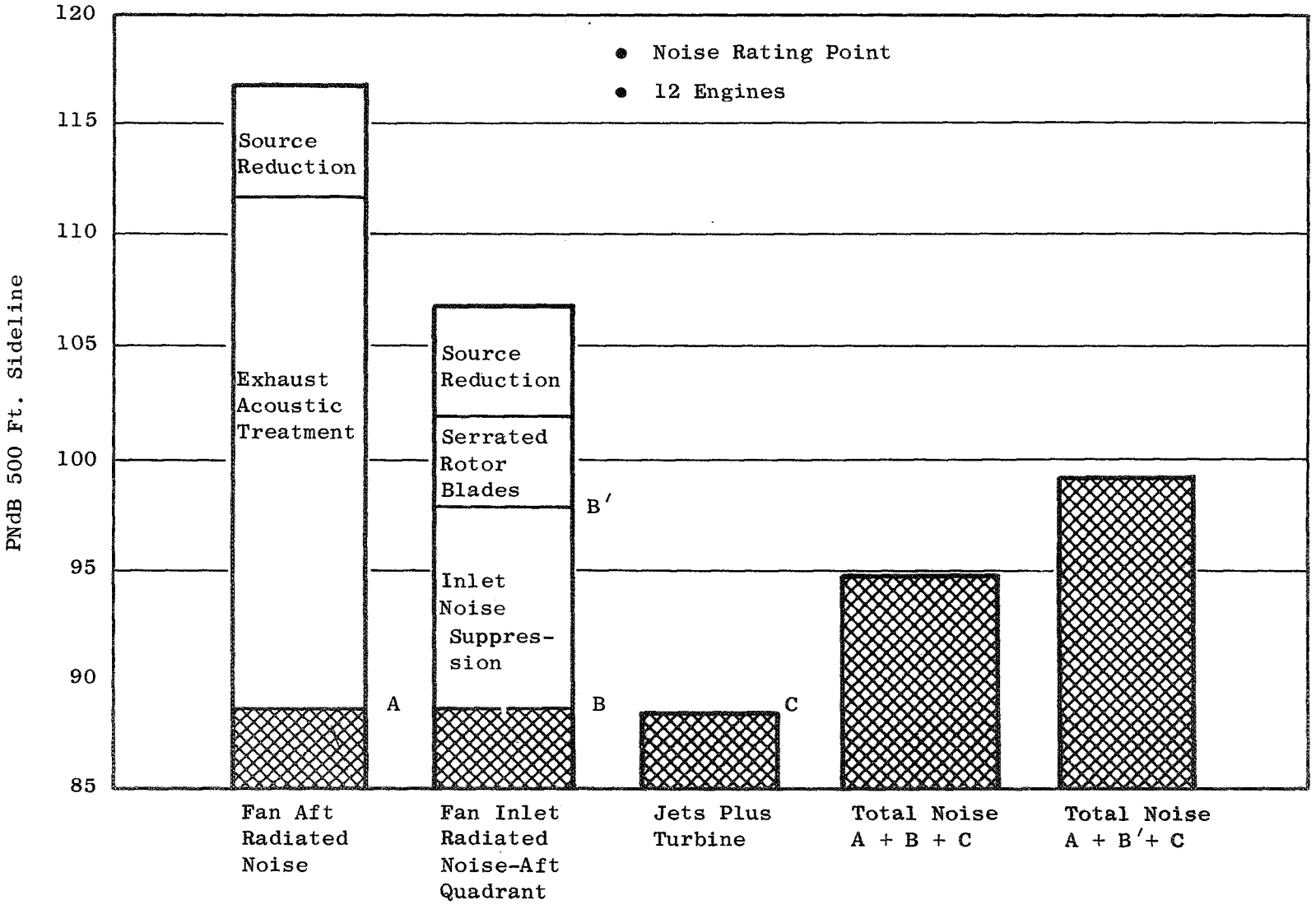

Figure 113. Fan Suppression - ILF2A2.

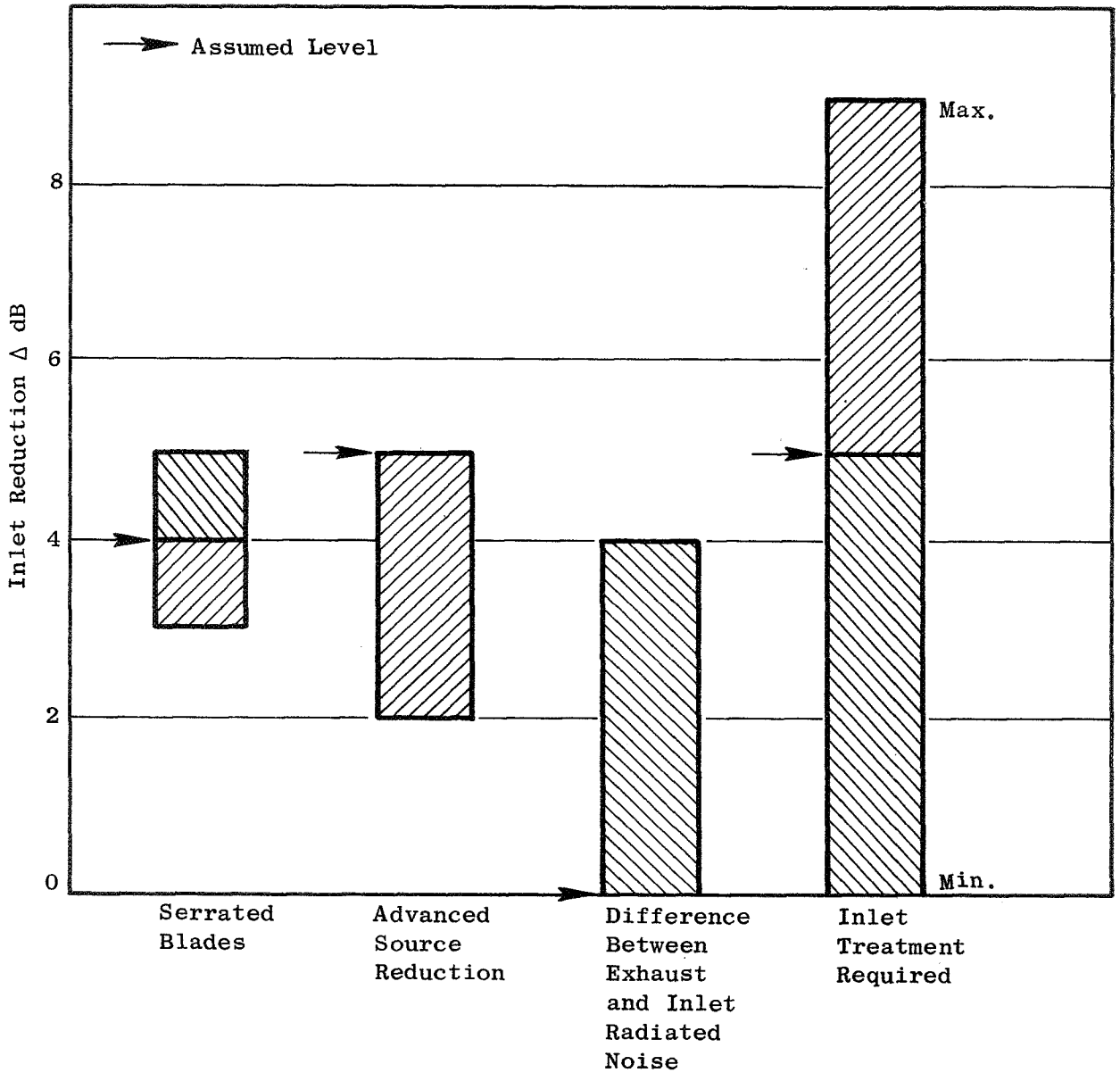

(0 Represents Assumed -10 dB Difference)

Figure 114. Inlet Noise Reduction Assumptions.

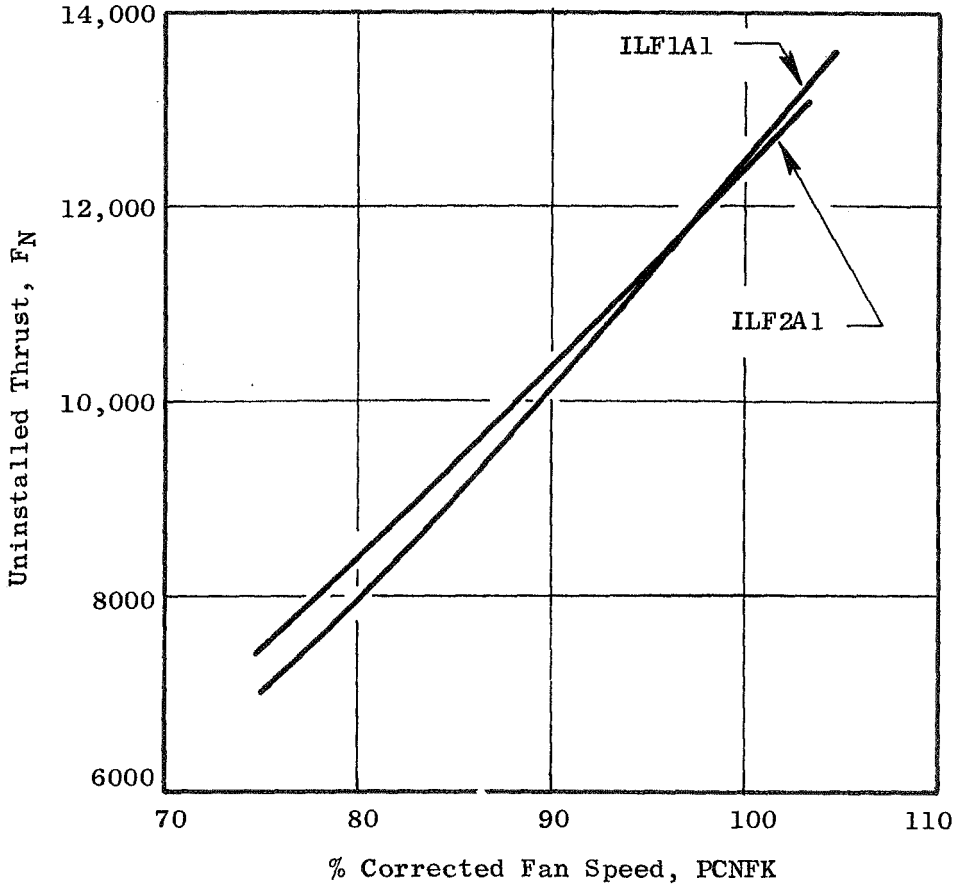

Figure 115. Uninstalled Performance - Sea Level Static, 90° Day.

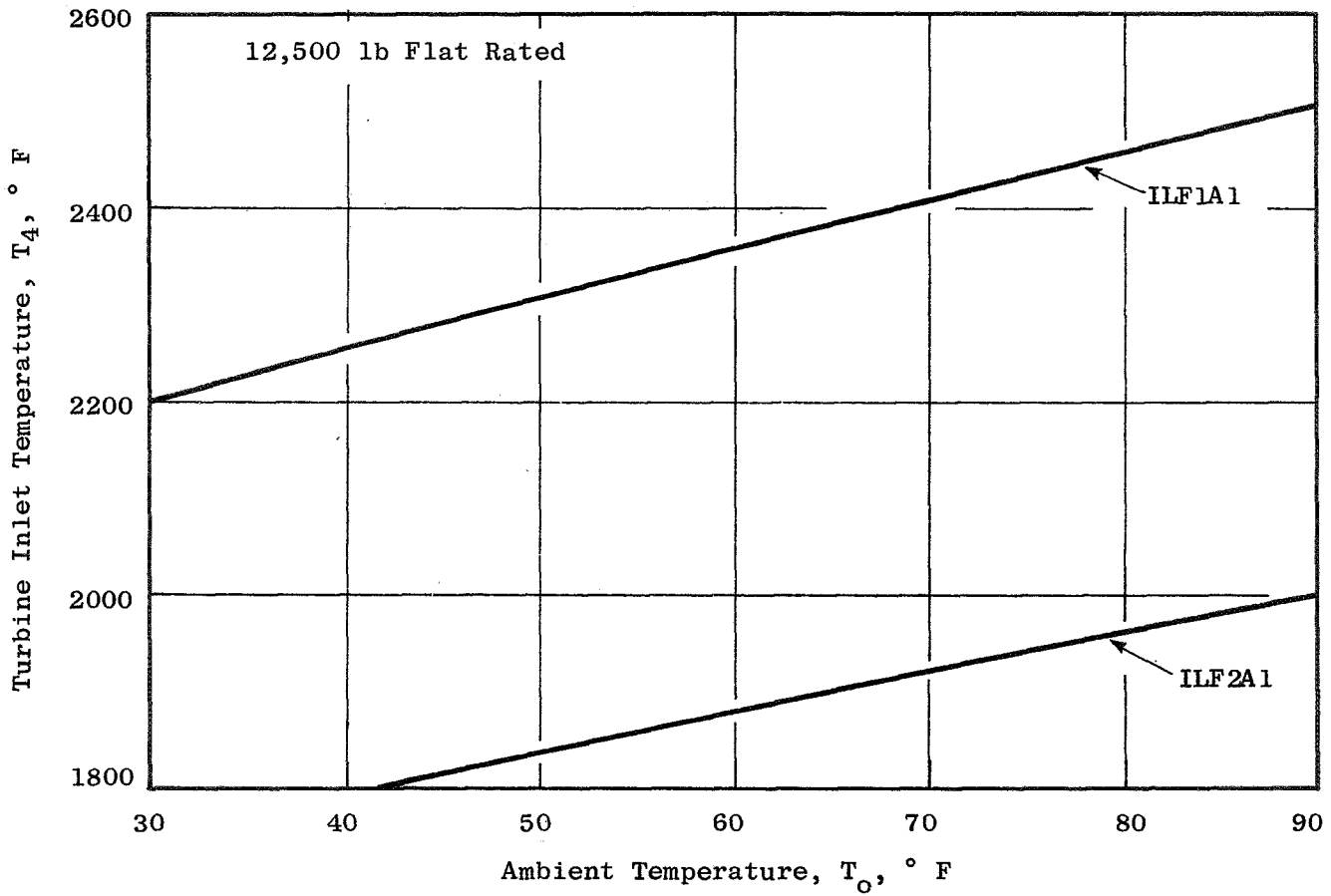

Figure 116. Uninstalled Performance - Sea Level Static, Standard Day.

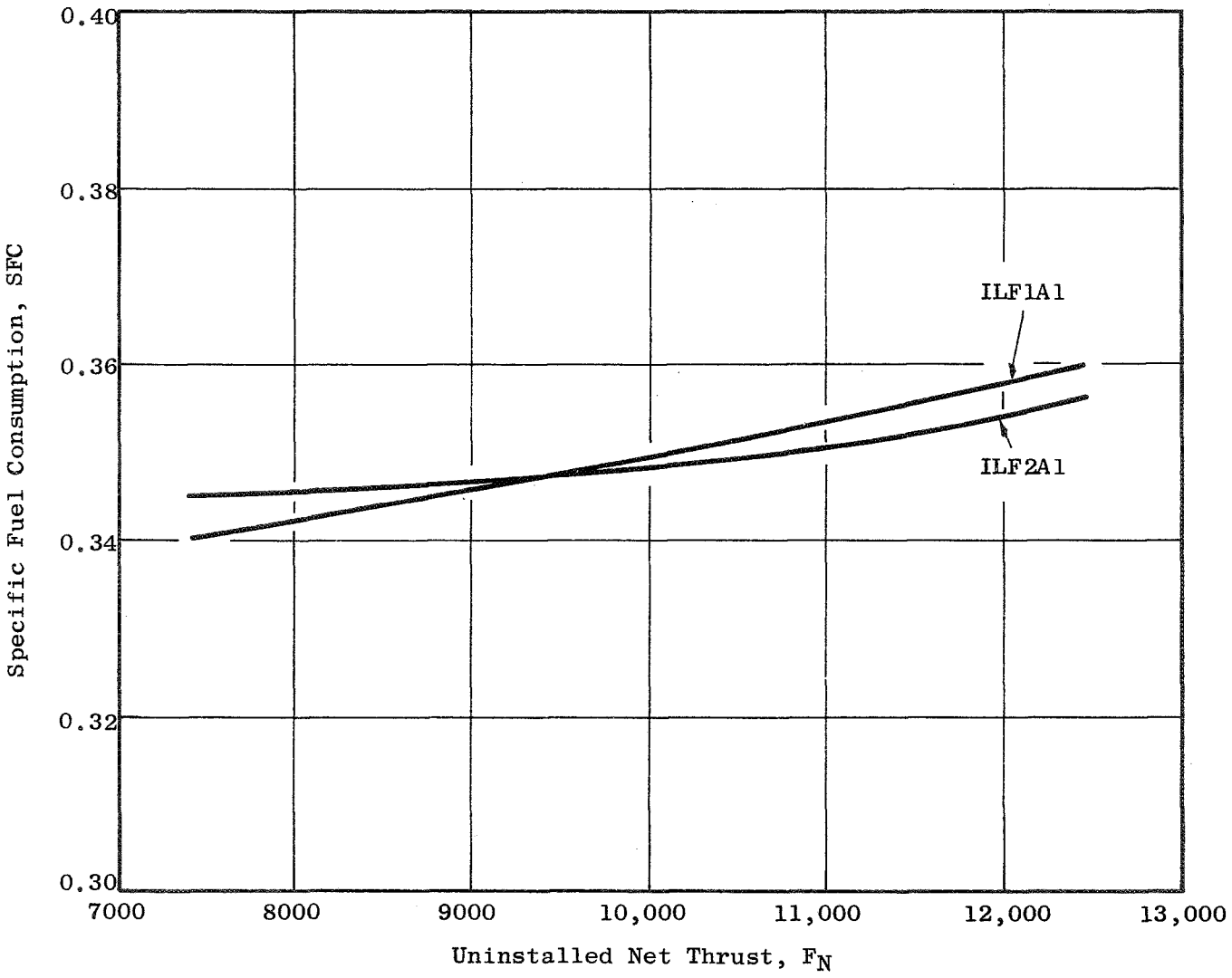

Figure 117. Uninstalled Performance - Sea Level Static, 90° Day.

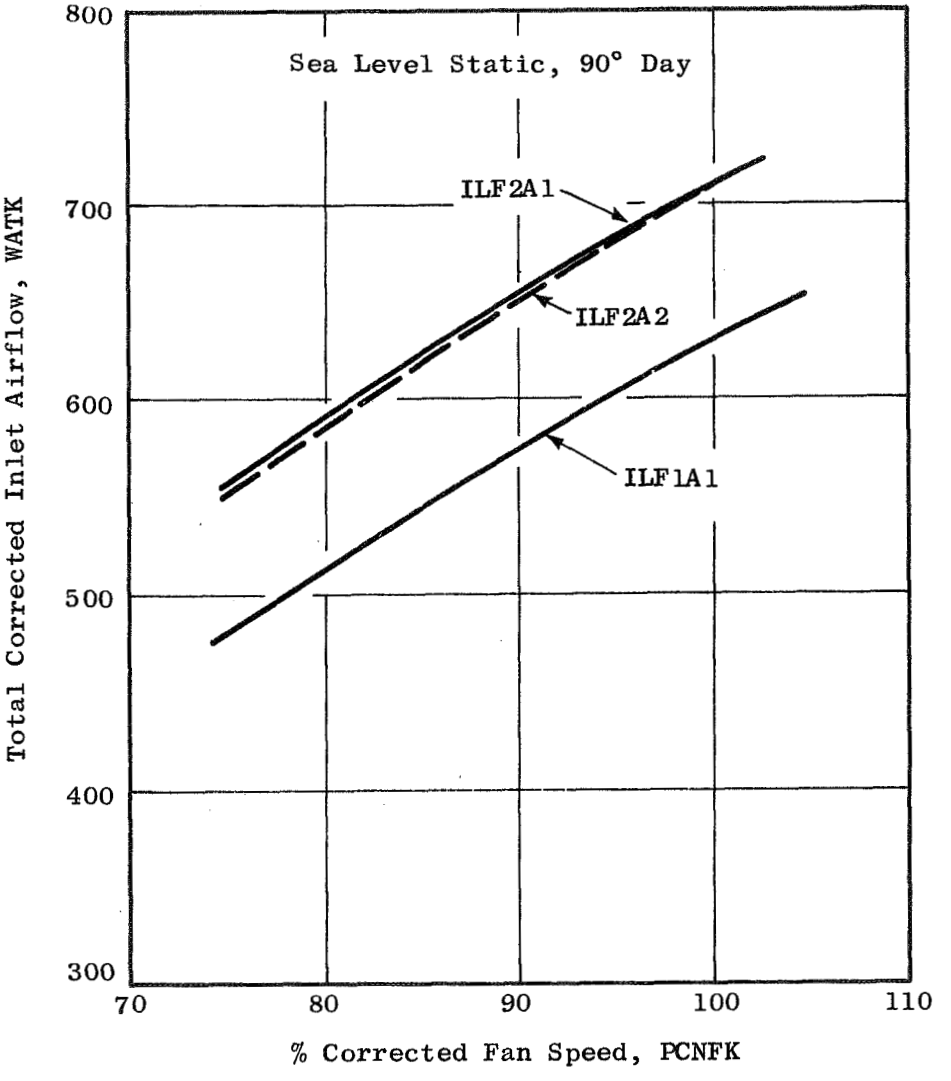

Figure 118. Integral Lift Fan Characteristics.

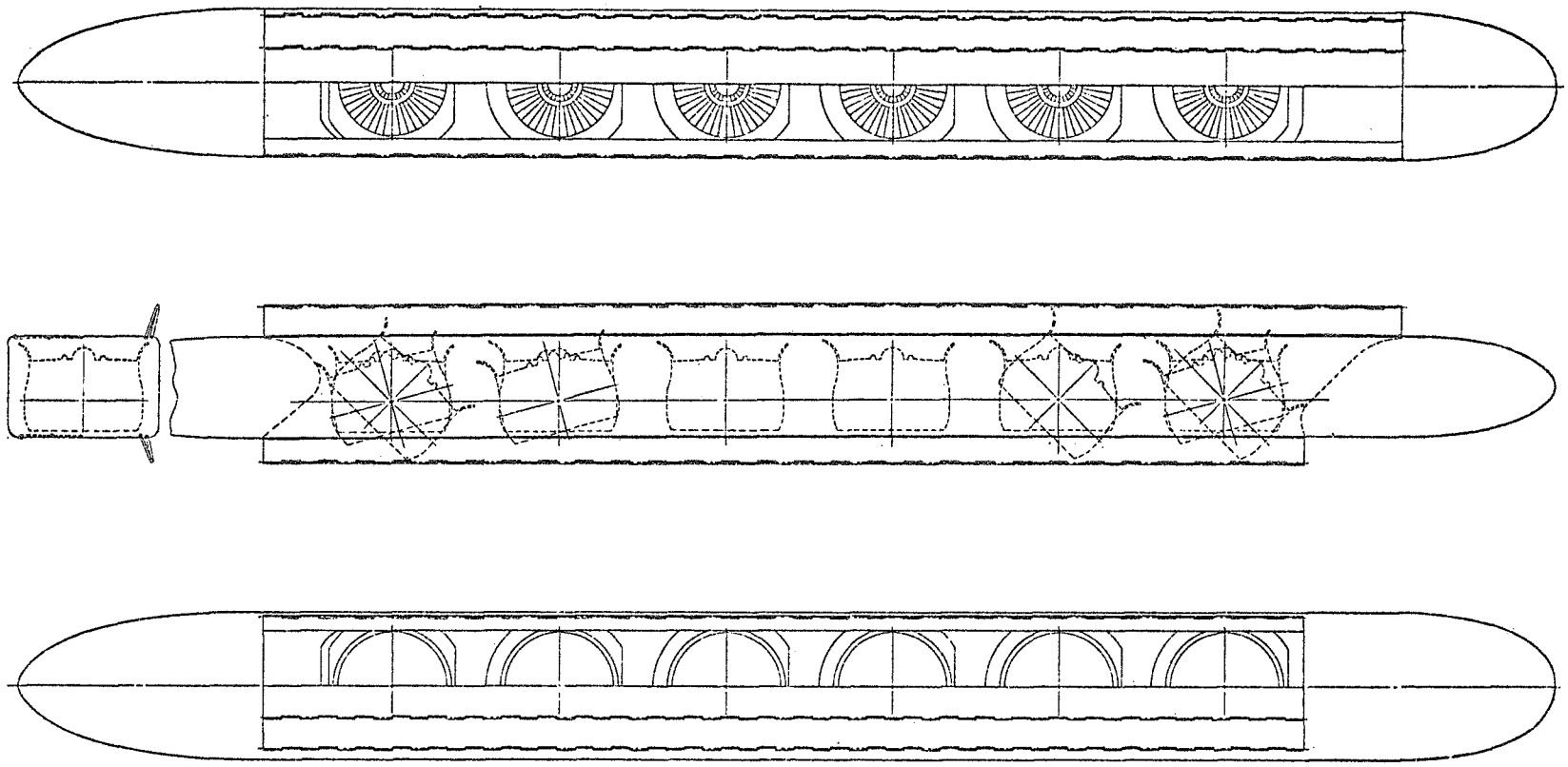

Figure 119. Pod and Vectoring System Arrangement.

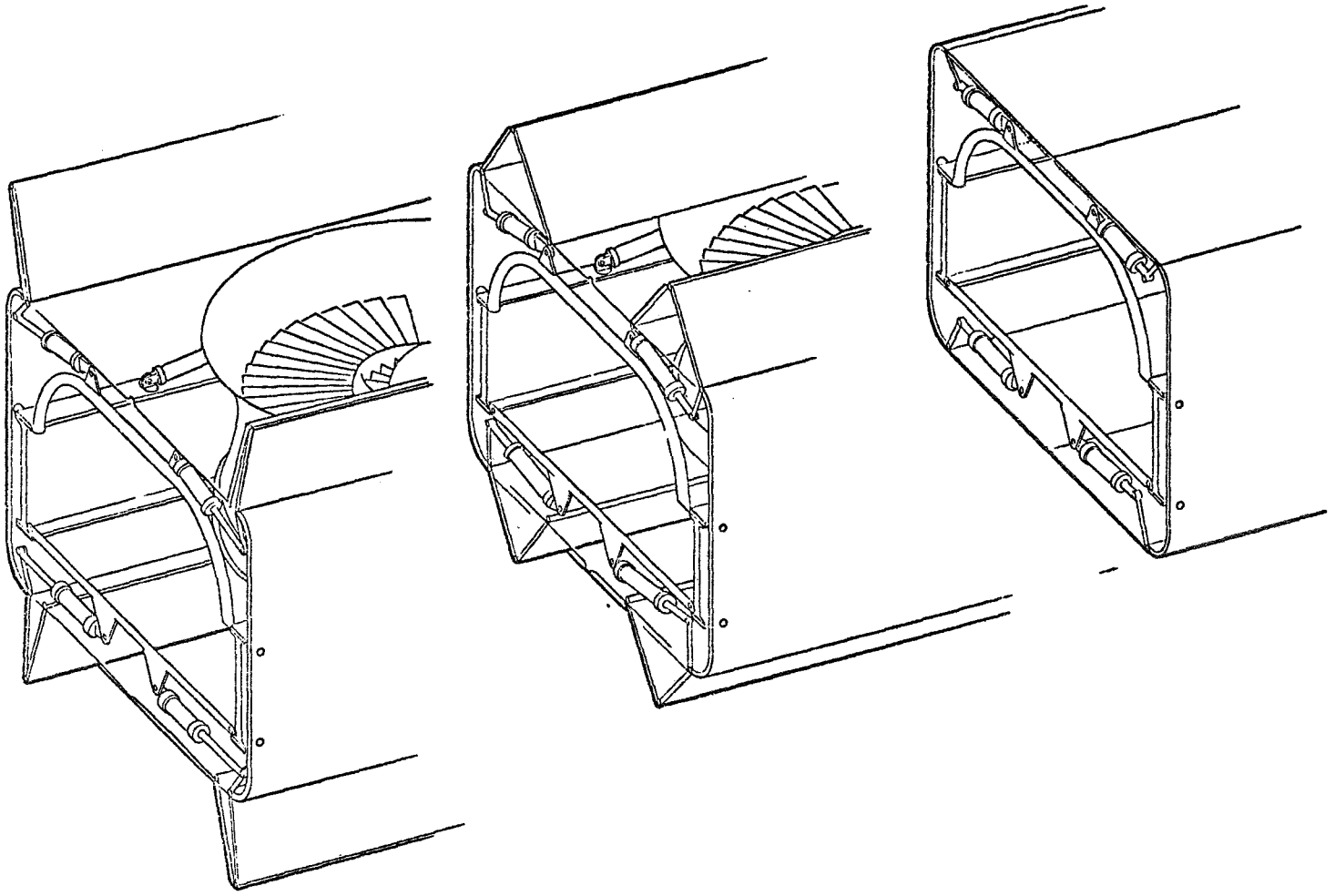

Figure 120. Inlet and Exhaust Door Schematic.

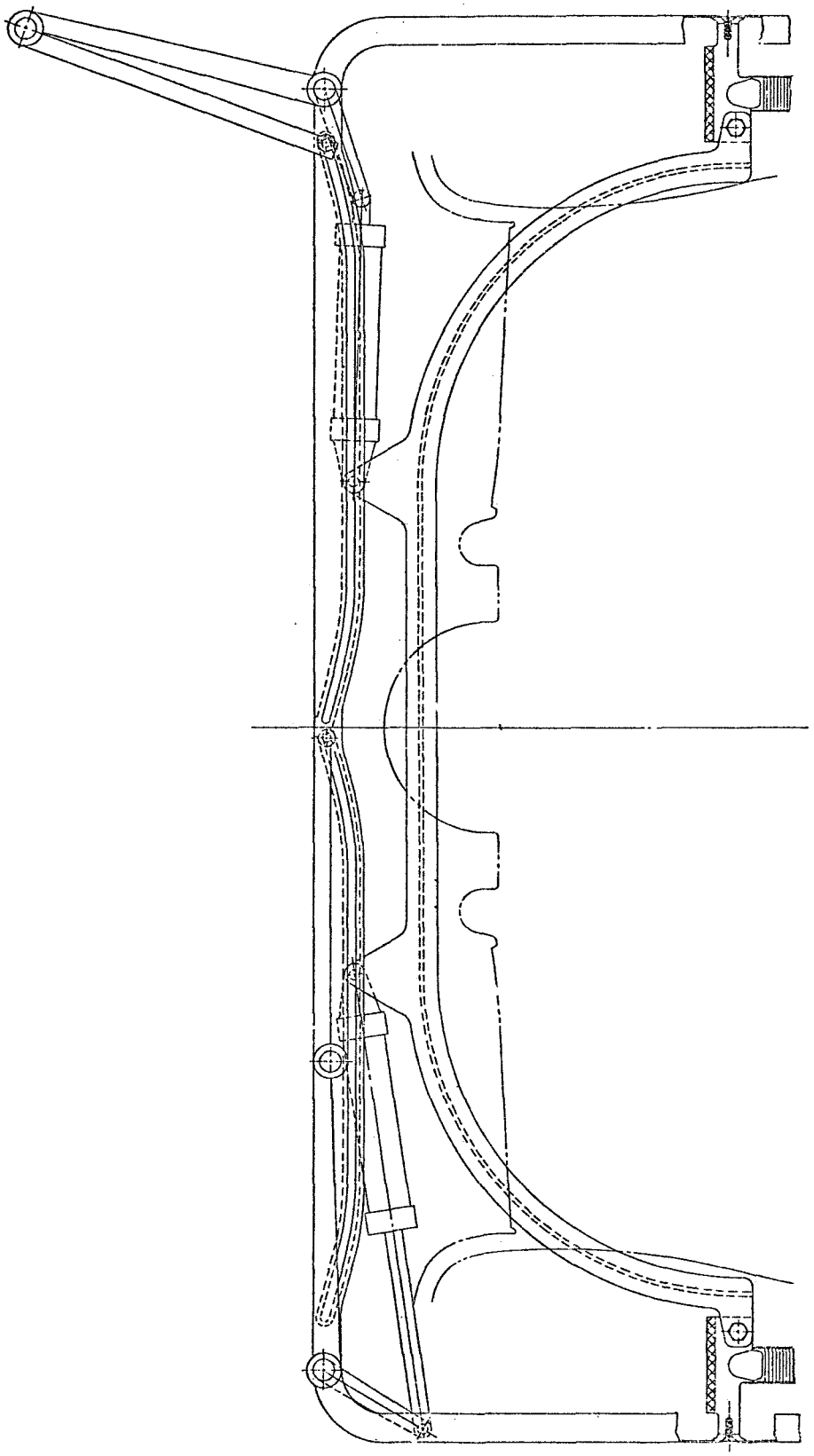

Figure 121. Inlet Door Cross Section.

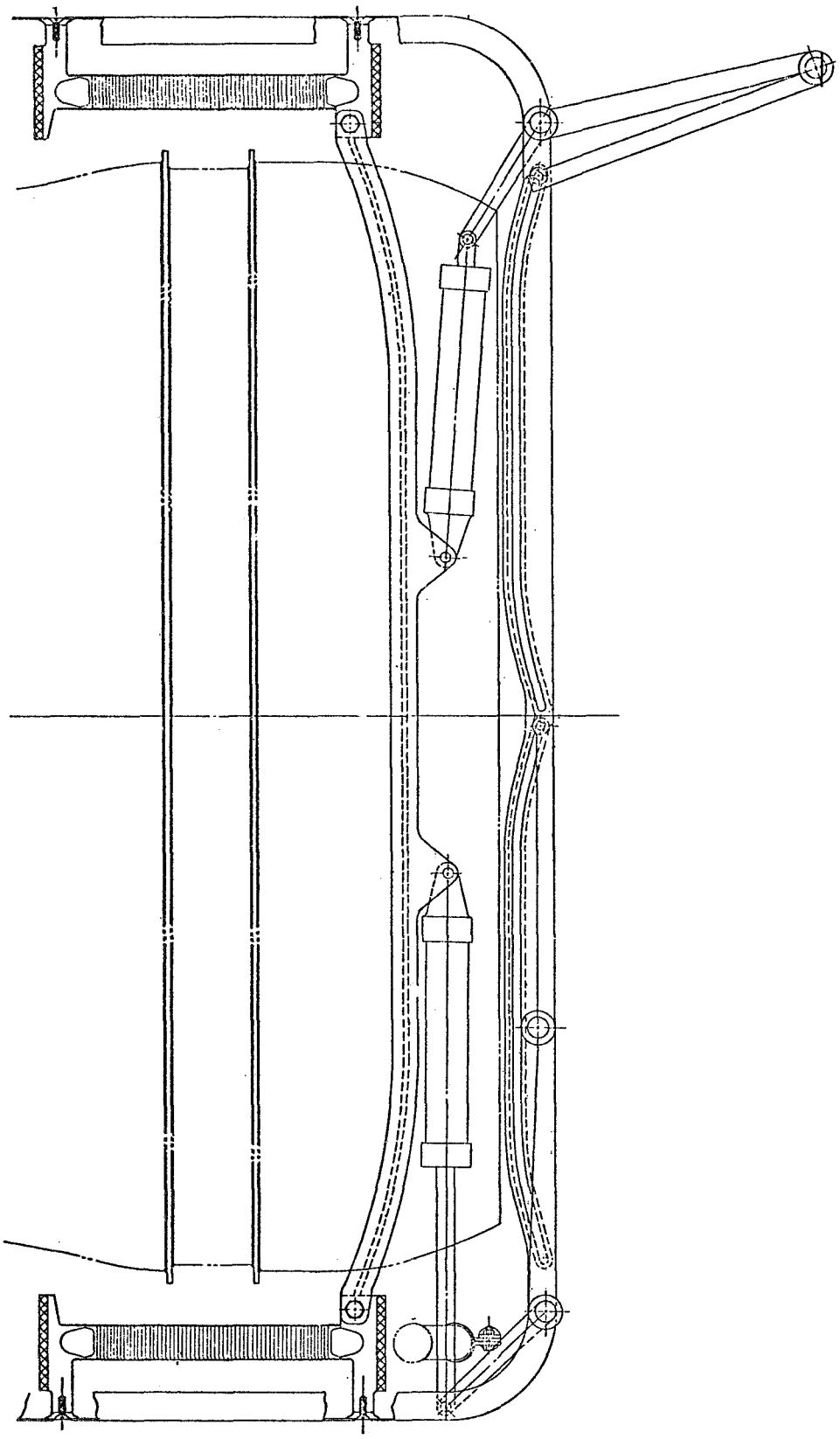

Figure 122. Exhaust Door Cross Section.

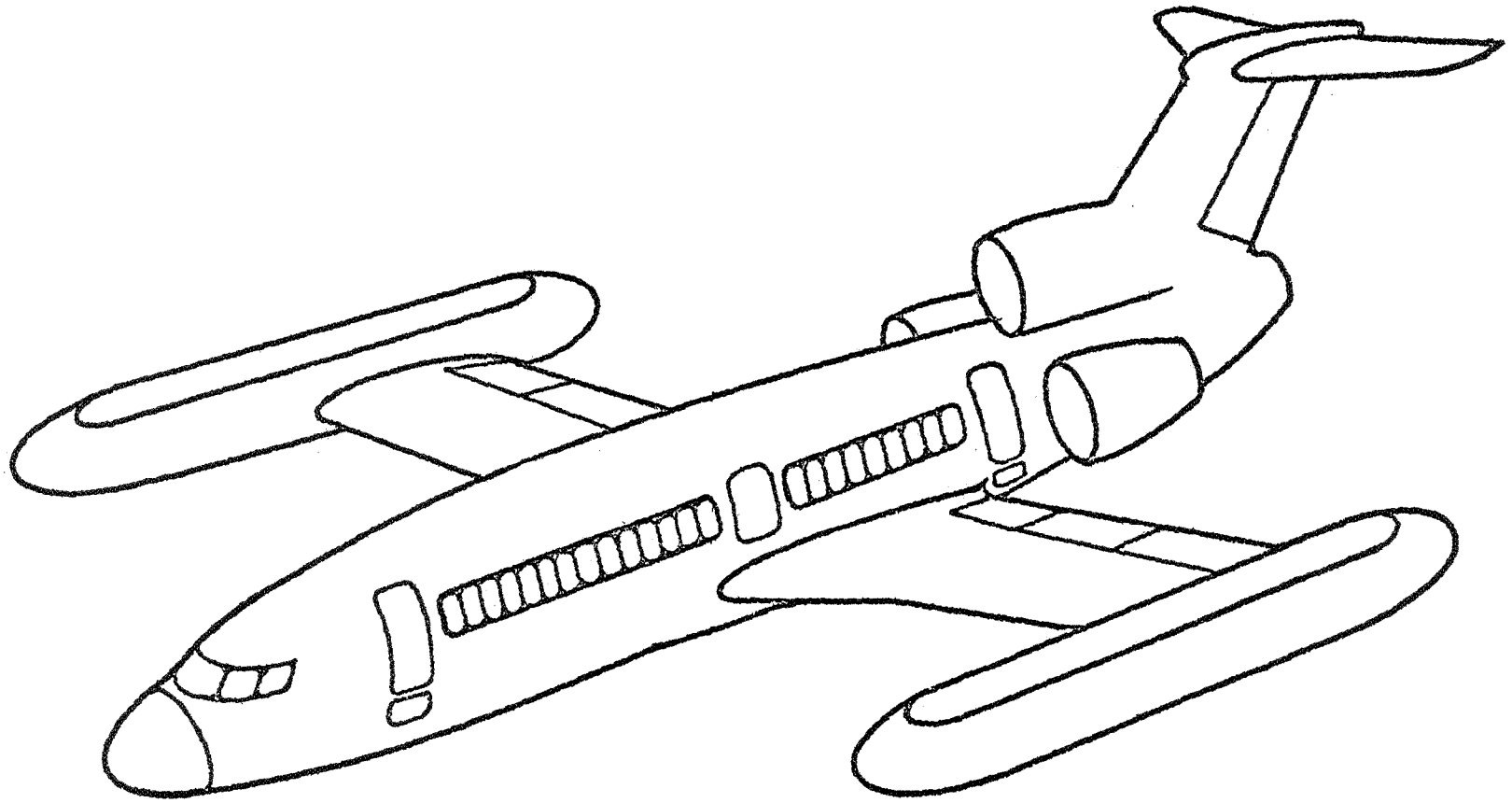

Figure 123. Typical VTOL Transport.

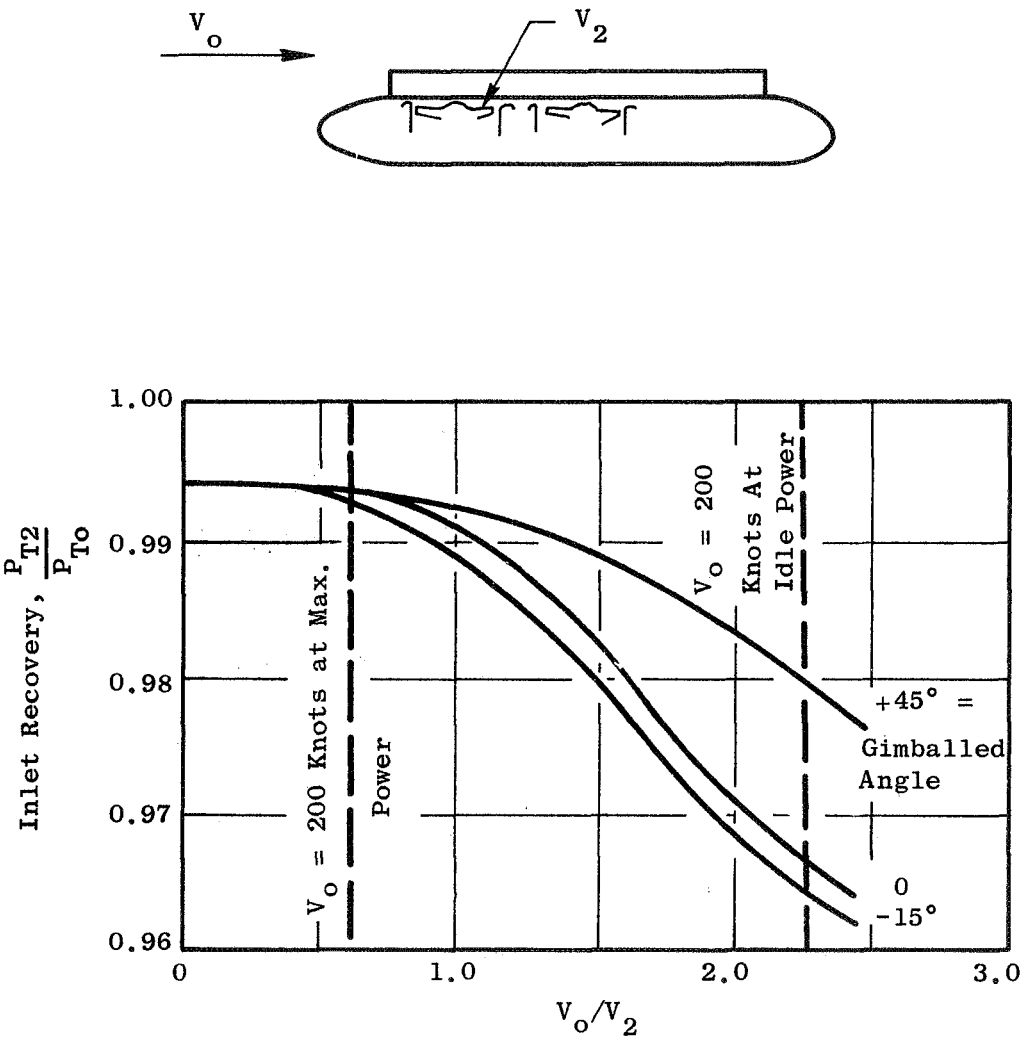

Figure 124. Objective - Recovery of Assumed Inlet Design

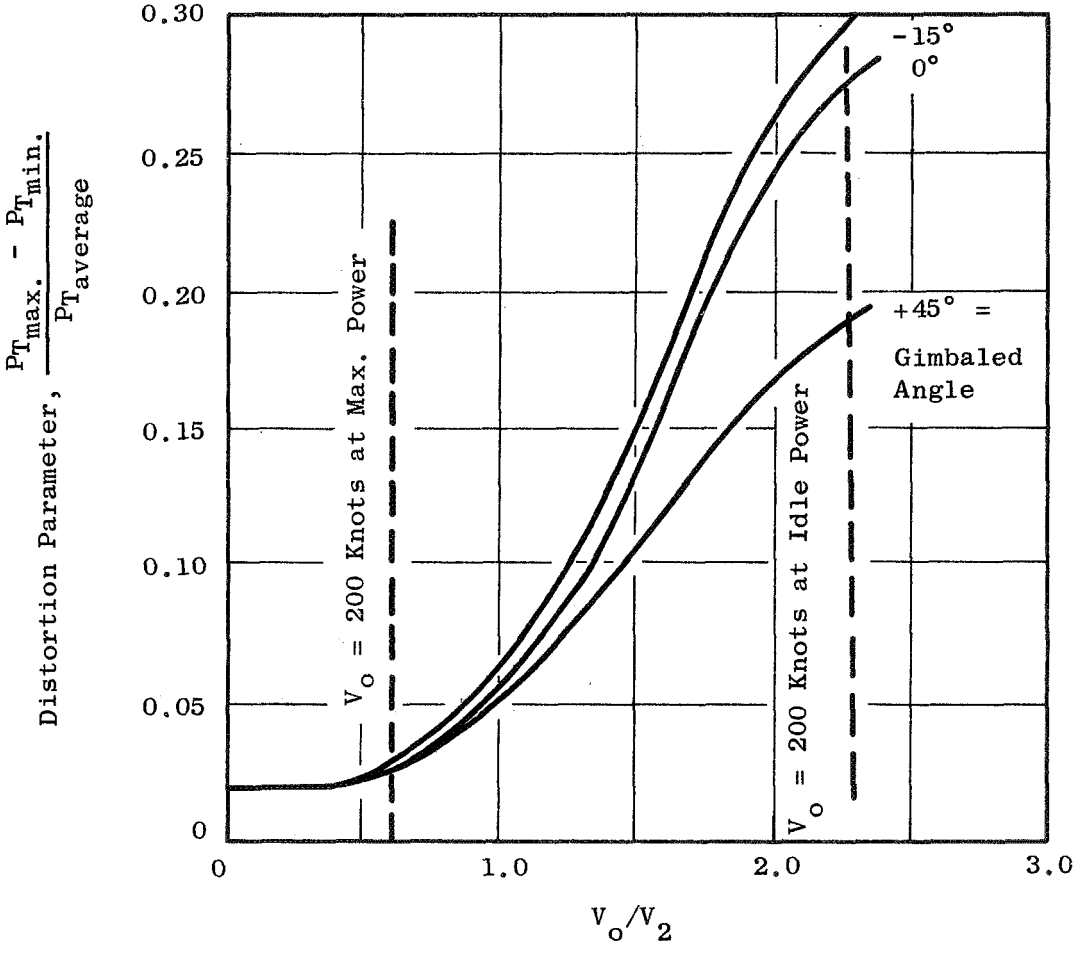

Figure 125. Objective Distortion Parameter of Assumed Inlet Design.

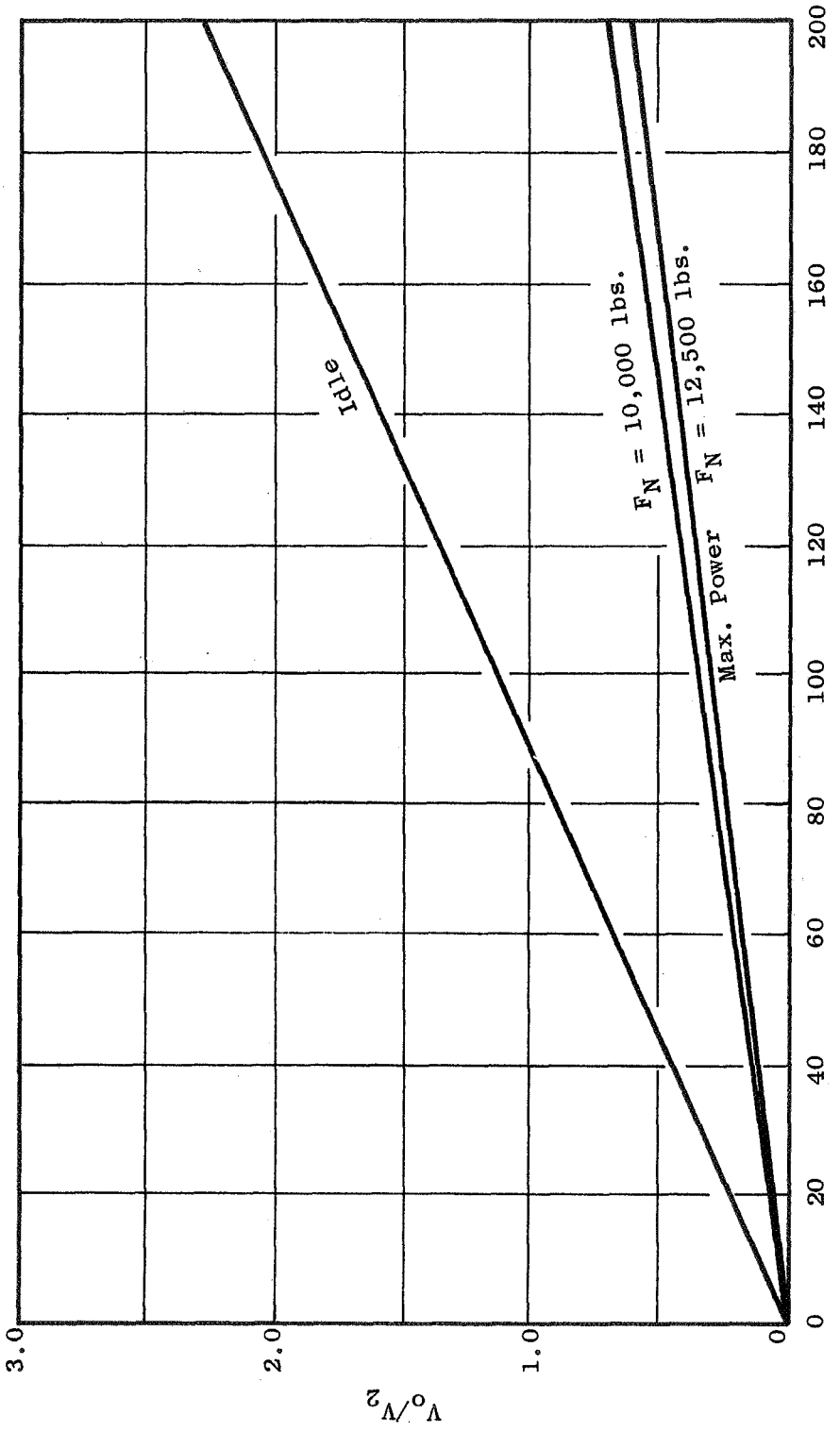

Figure 126. Crossflow Velocity Ratio as a Function of Power Setting.

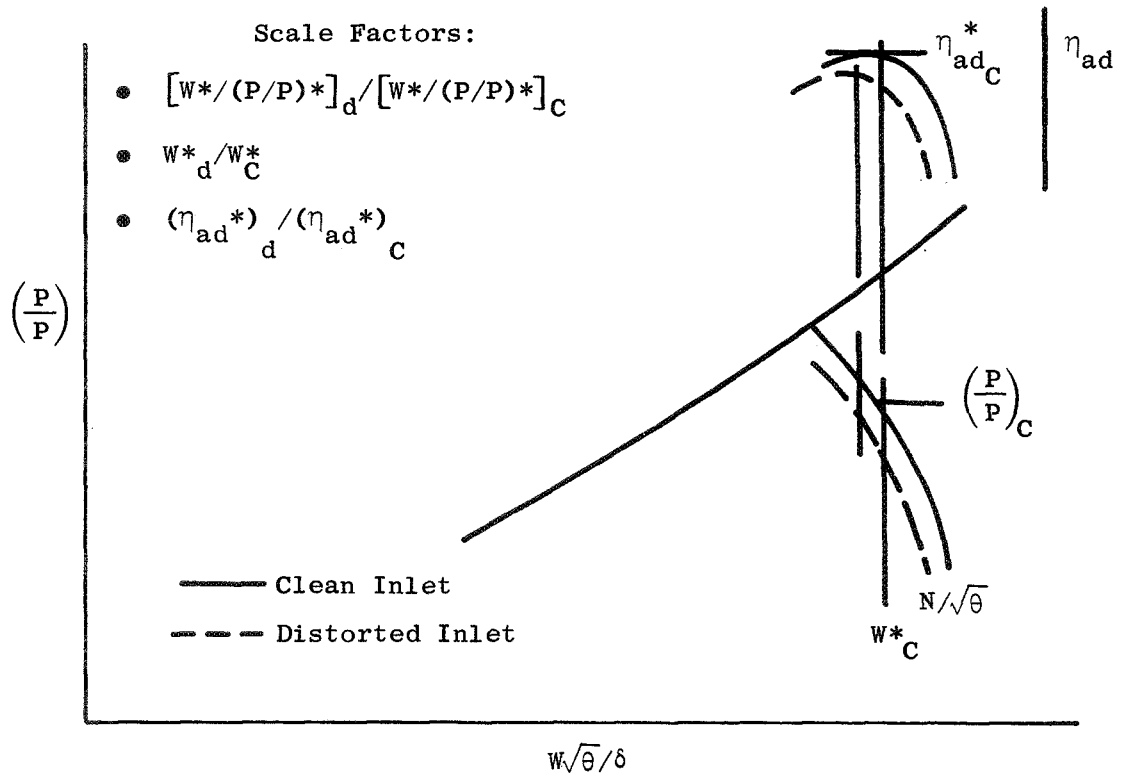

Figure 127. Procedure for Estimating Inlet Distortion Effects on Performance.

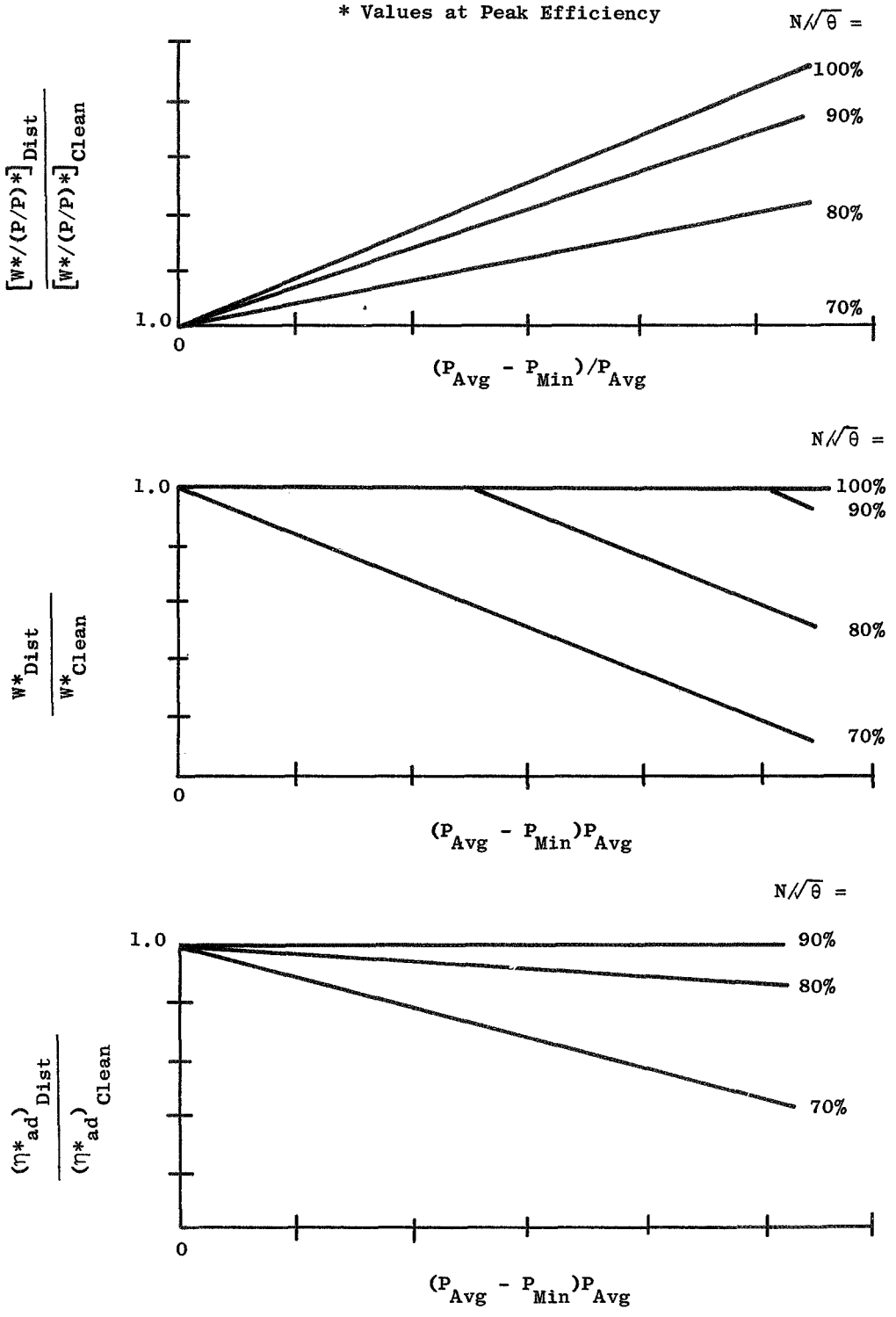

Figure 128. Crosswind Distortion Effects on Compressor Performance.

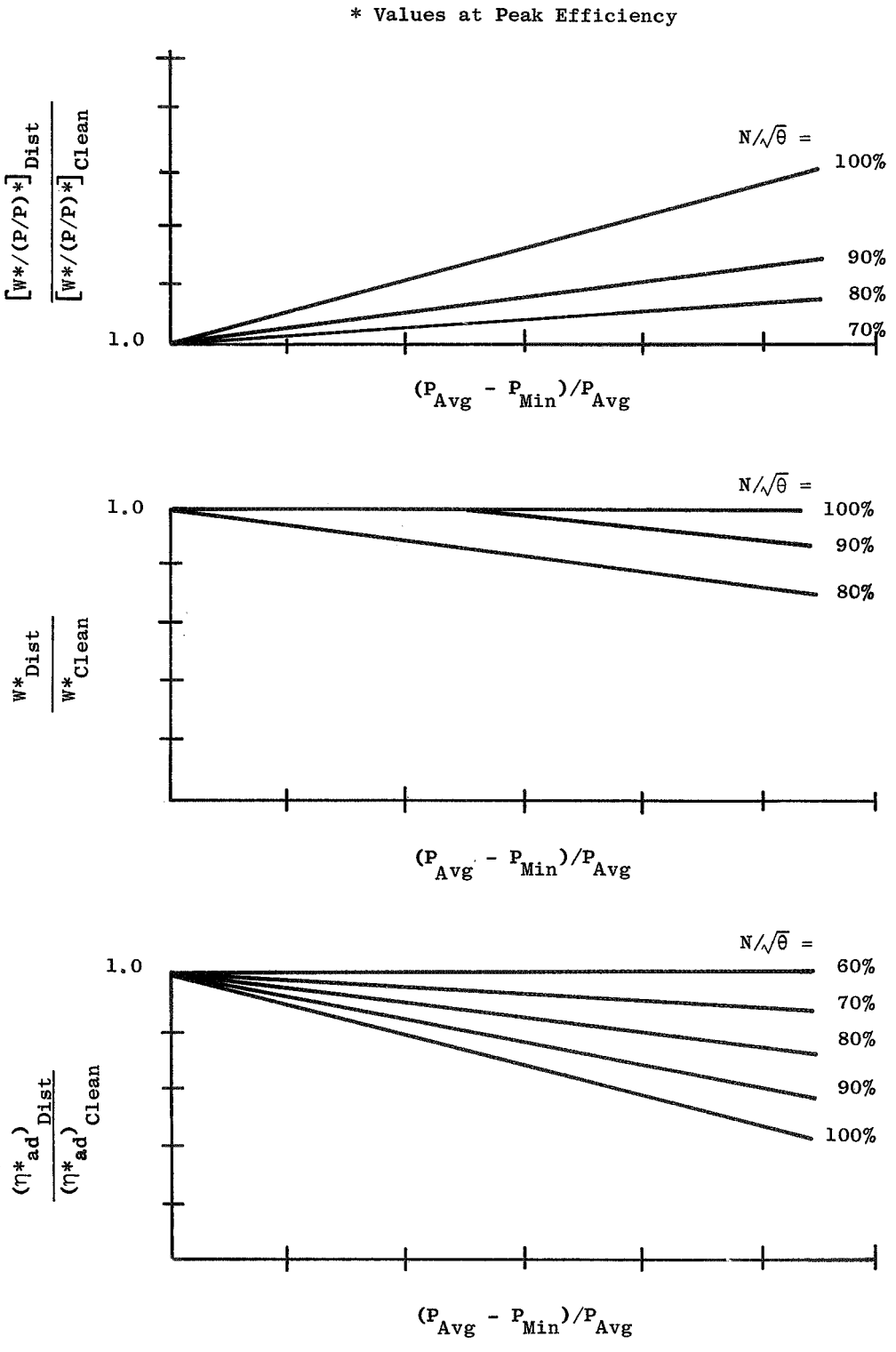

Figure 129. Crosswind Distortion Effects on Fan Performance.

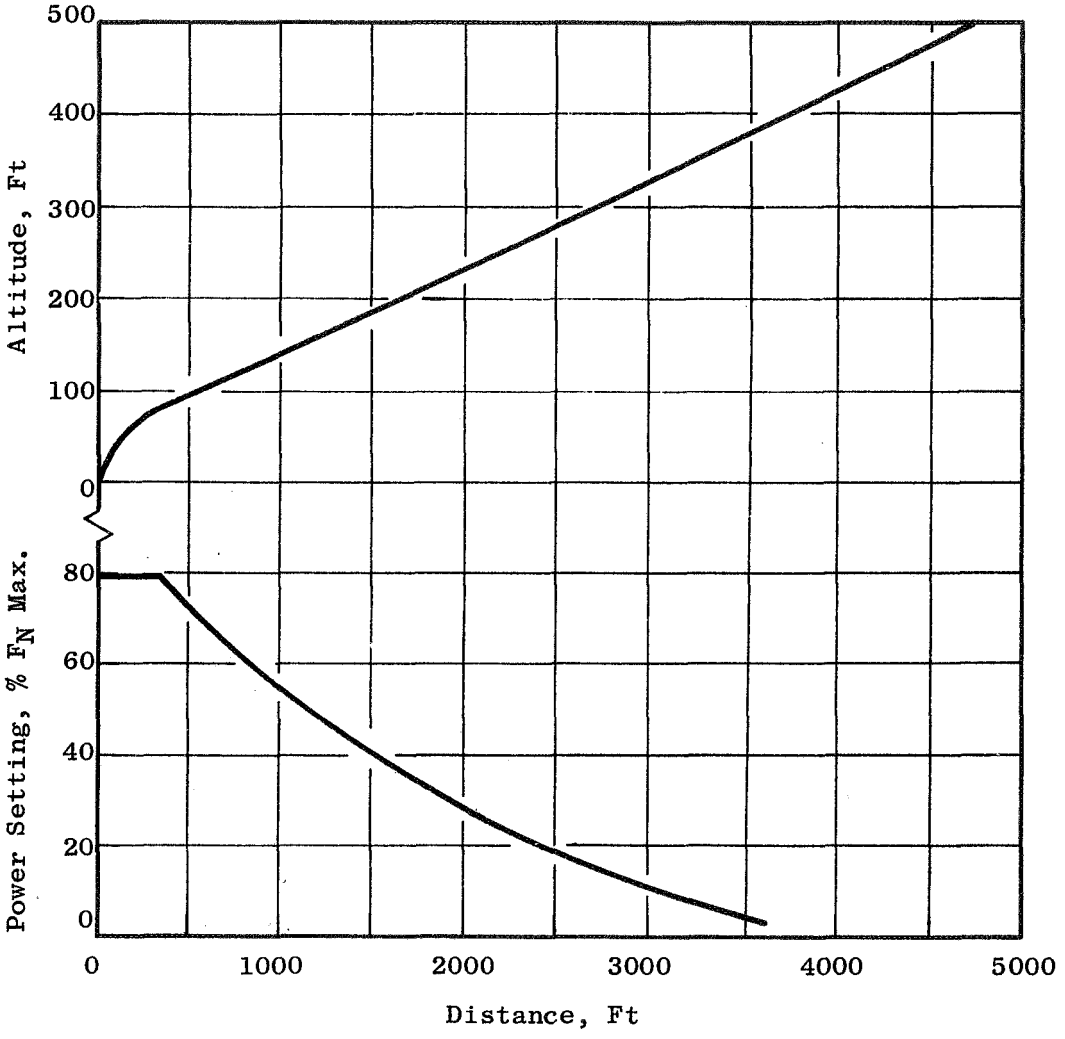

Figure 130. Typical Takeoff Trajectory.

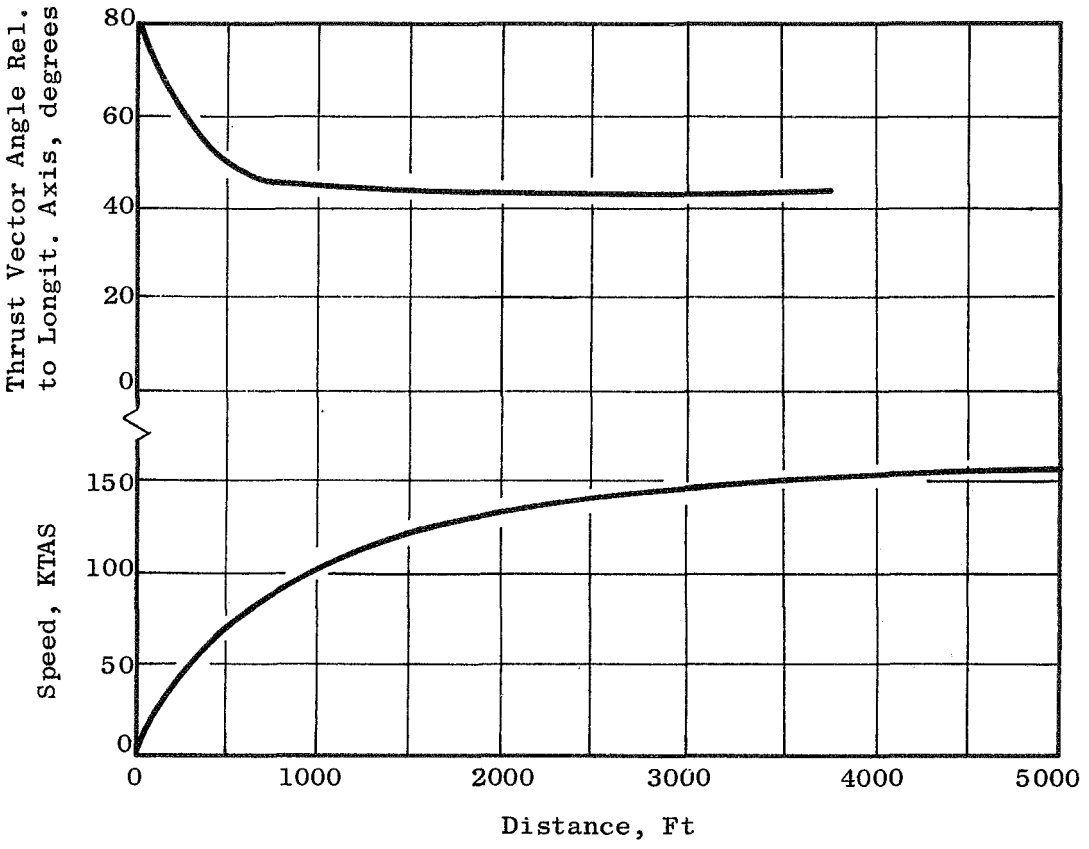

Figure 131. Typical Takeoff Trajectory.

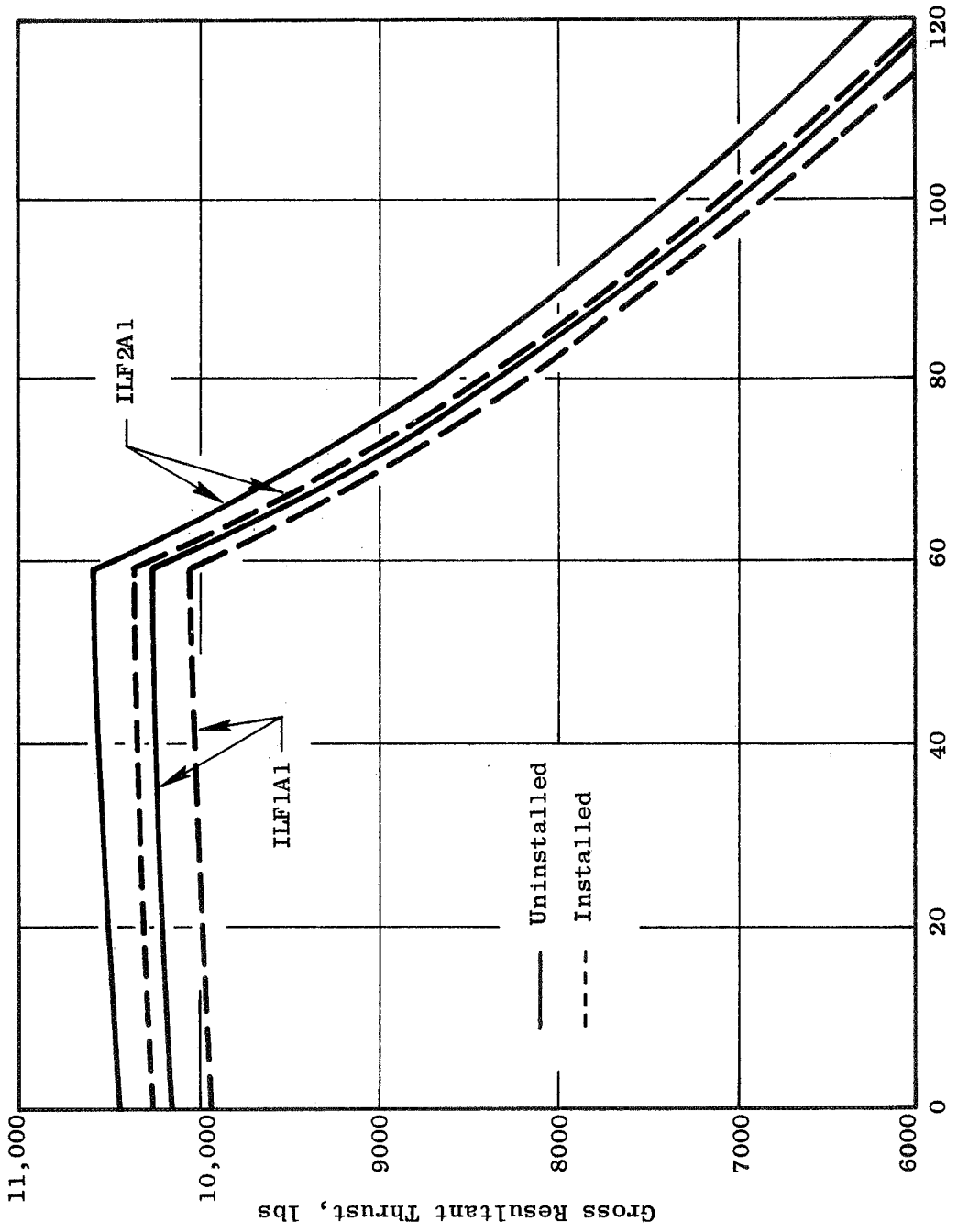

Figure 132. Effect of Installation for Typical Trajectory Points.

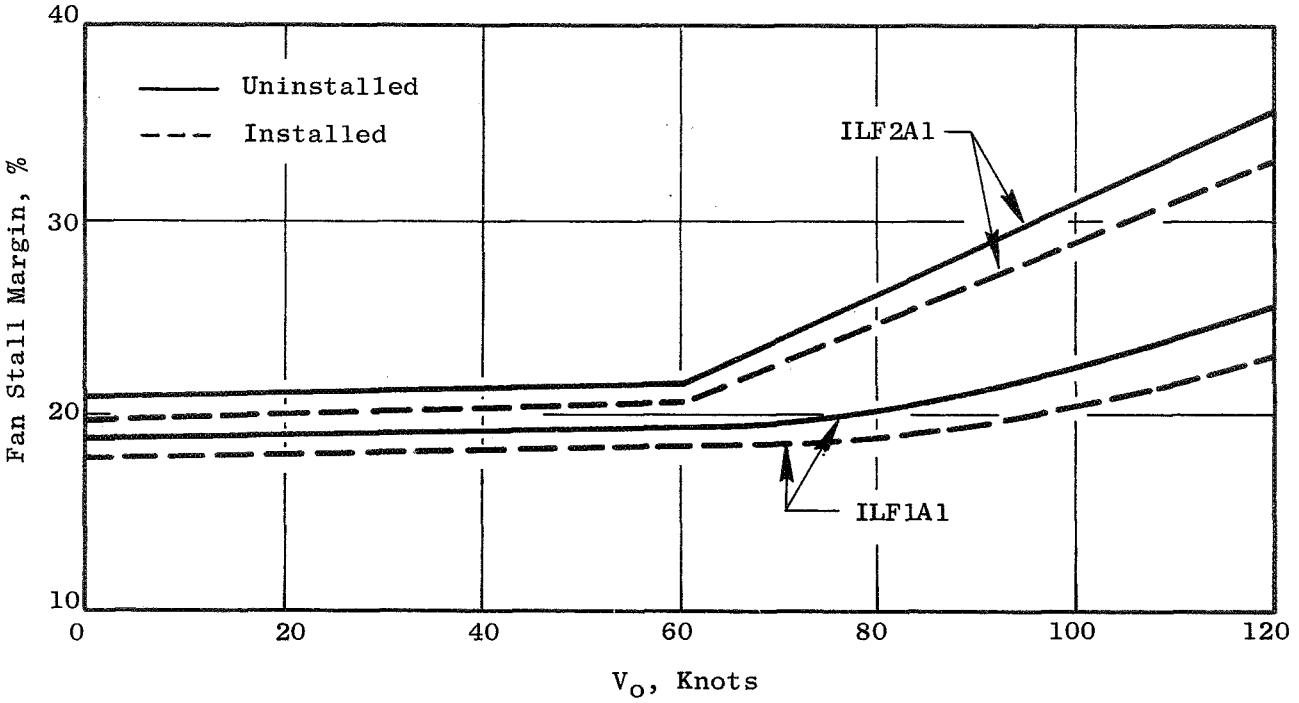

Figure 133. Effect of Installation for Typical Trajectory Points.

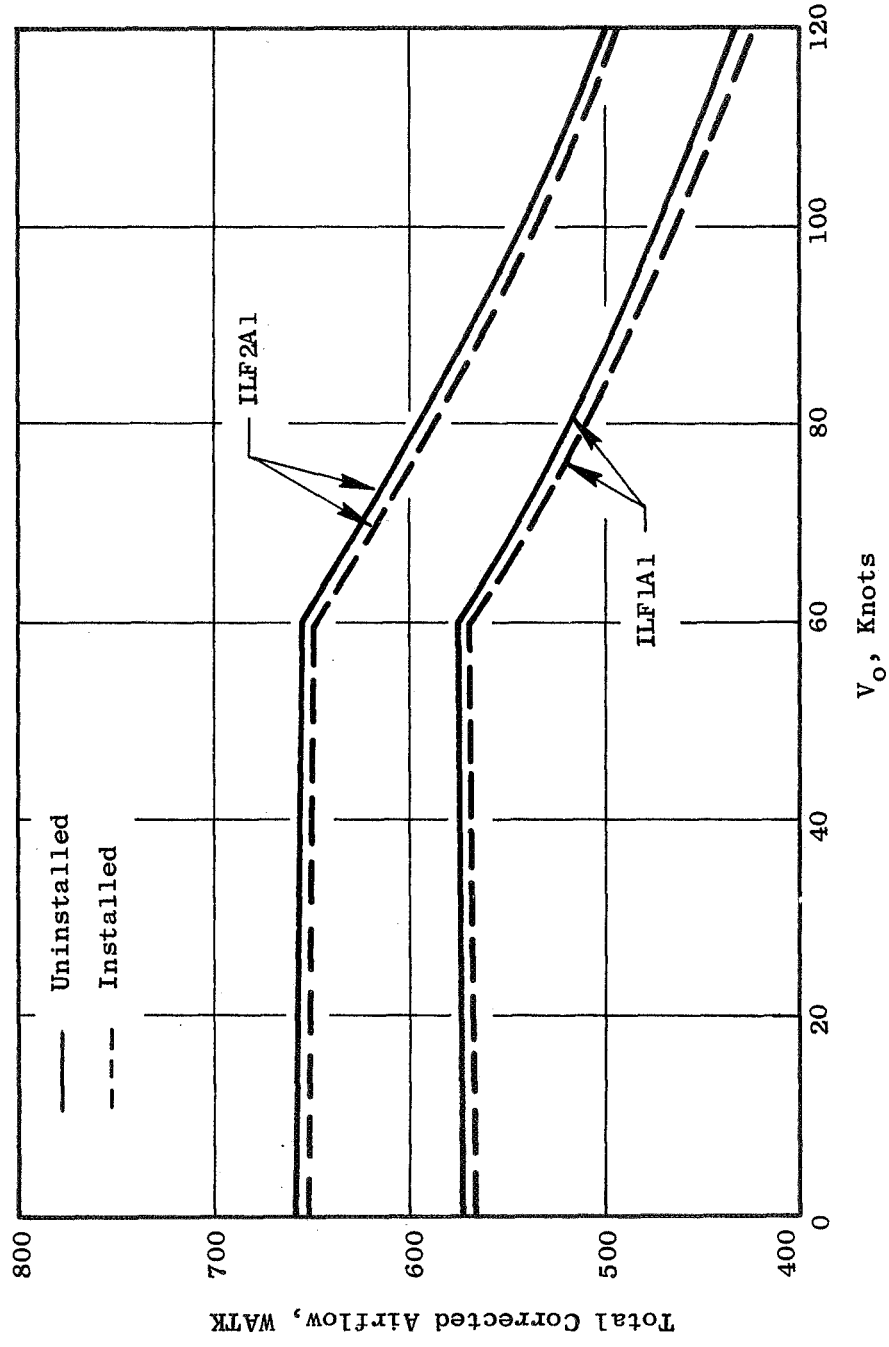

Figure 134. Effect of Installation for Typical Trajectory Results.